ONR GRANT N00014-95-1-0539
A DoD Multidisciplinary Research Program
of the University Research Initiative (M-URI)

YEAR 3 REVIEW

INTEGRATED DIAGNOSTICS

March 1, 1997 - May 31, 1998

FOR
Office of Naval Research
800 N. Quincy Street
Arlington, VA 22217-5660

PREPARED BY
Richard S. Cowan, Program Manager
Ward O. Winer, Principal Investigator
Georgia Institute of Technology
MULTIUNIVERSITY CENTER FOR INTEGRATED DIAGNOSTICS
Woodruff School of Mechanical Engineering
Atlanta, GA 30332-0405
Ph: 404-894-3200

SUBGRANTEES
Northwestern University
Jan D. Achenbach, Director
Center for Quality Engineering and Failure Prevention
Ph: 847-491-5527

University of Minnesota
Dennis Polla, Professor
Department of Electrical Engineering
Ph: 612-624-8005
S. Ramalingam, Professor
Department of Mechanical Engineering
Ph: 612-625-4017

Georgia Institute of Technology
The George W. Woodruff School of Mechanical Engineering

June 3, 1998

P. Peter Schmidt
Office of Naval Research
Ballston Tower One
800 N. Quincy Street
Arlington, VA 22217-5660

Director
Naval Research Laboratory
Attn: Code 2627
Washington, DC 20375

Administrative Grants Officer
Office of Naval Research
Regional Office, Suite 2805
101 Marietta Street
Atlanta, GA 30323-0008

Defense Technical Information Center
Building 5
Alexandria, VA 22304-6145

Enclosed is a technical report "Integrated Diagnostics," summarizing basic research activity for the third year of M-URI research grant N00014-95-1-0539.

Should you have any questions or comments about this submission, do not hesitate to contact Principal Investigator Ward Winer of Georgia Tech at 404-894-3200.

Sincerely,
CENTER FOR INTEGRATED DIAGNOSTICS

Richard S. Cowan
Program Manager

Atlanta, Georgia 30332-0405 U.S.A.
Administration Office 404•894•3200
Finance Office 404•894•7400
Graduate Program 404•894•3204
Undergraduate Office 404•894•3203
Fax 404•894•8336 or
web site: http://www.me.gatech.edu/

ONR GRANT N00014-95-1-0539
A DoD Multidisciplinary Research Program
of the University Research Initiative (M-URI)

YEAR 3 REVIEW

INTEGRATED DIAGNOSTICS

March 1, 1997 - May 31, 1998

FOR
Office of Naval Research
800 N. Quincy Street
Arlington, VA 22217-5660

PREPARED BY
Richard S. Cowan, Program Manager
Ward O. Winer, Principal Investigator
Georgia Institute of Technology
MULTIUNIVERSITY CENTER FOR INTEGRATED DIAGNOSTICS
Woodruff School of Mechanical Engineering
Atlanta, GA 30332-0405
Ph: 404-894-3200

SUBGRANTEES
Northwestern University
Jan D. Achenbach, Director
Center for Quality Engineering and Failure Prevention
Ph: 847-491-5527

University of Minnesota
Dennis Polla, Professor
Department of Electrical Engineering
Ph: 612-624-8005
S. Ramalingam, Professor
Department of Mechanical Engineering
Ph: 612-625-4017

INTRODUCTION

Office of Naval Research (ONR) Grant N00014-95-1-0539, *Integrated Diagnostics*, was initiated on March 1, 1995, following approval of a research proposal submitted to the Department of Defense Multidisciplinary Research Program of the University Research Initiative (M-URI). To accomplish the objectives set forth by the M-URI program, the MULTIUNIVERSITY CENTER FOR INTEGRATED DIAGNOSTICS was formed, supported by faculty and staff from the Georgia Institute of Technology, University of Minnesota, and Northwestern University.

PROGRAM OBJECTIVE

America's military machines (e.g., ships, aircraft, and land vehicles) are growing old. Many of the systems that are confidently relied upon today were designed and built twenty and thirty years ago. Given the present economic climate, replacement with next generation equipment can no longer be taken for granted. As a result, an expectation of keeping aging machines in service well into the next century has emerged, which has elevated concern that poor performance, inadequate safety, and increasingly expensive maintenance will result.

To respond to this technological challenge, pending failures must be identified before disastrous consequences occur. Incipient failures, however, are hard to locate, and current maintenance systems have limited capabilities to do so. Today's systems rely mainly on time-based inspection, which requires that parts be inspected at specified intervals, and be replaced when deemed unfit for service. A potentially more effective and efficient alternative to time-based inspection is to continuously monitor critical components. This necessitates an understanding of *Integrated Diagnostics*, a term associated with the technologies and methodologies used to determine how mechanical failures occur, and how they can be detected, predicted, and diagnosed in real-time.

As shown in Fig. 1, a systematic approach has been implemented to enable innovative ideas to be developed and mature with respect to mechanical system diagnostics and prognostics. Provided funding through the Department of Defense M-URI for a basic period of three years with a potential for two additional years, a technical organization has been built to facilitate and combine the various disciplines required to generate the payoff of a system capable of being used on a commercial or defense service vehicle. Researchers, representing a variety of engineering disciplines at the Georgia Institute of Technology, Northwestern University, and the University of Minnesota have been assembled, offering expertise with respect to material fatigue, fracture, nondestructive testing, sensors, and signal processing. To gain first-hand knowledge of the problems that maintenance personnel face, engineering support has been obtained through the CHERRY POINT NAVAL AVIATION DEPOT. Additional experience has been made available through industrial partnerships.

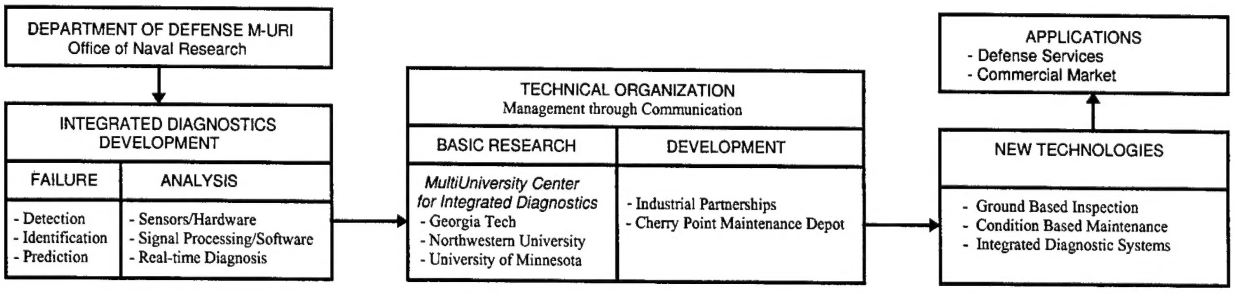

Figure 1. Technology Delivery

The MULTIUNIVERSITY CENTER FOR INTEGRATED DIAGNOSTICS is committed to perform studies associated with three major Integrated Diagnostic needs: the need to monitor the condition of a component or mechanical system in real-time, the need to reliably predict the occurrence of failures, and the need to detect and identify incipient failures. Organizationally, this has led to the formation of three research thrust areas, the objectives of which are defined below.

I. **Mechanical System Health Monitoring** (Direct Sensing, Analysis, Real-time Diagnosis)
perform studies with respect to the responses of signals early in fault inception, including research on sensors that can be placed at critical sites on mechanical systems for responses to change in variables of state or vibration.

II. **Failure Characterization and Prediction Methodology**
perform studies pertaining to the methodology for failure prediction in real-time, including modeling fault initiation and failure signatures, and observing the propagation and fracture phases of fatigue-based failure.

III. **Nondestructive Evaluation** (Failure Detection and Identification)
perform studies pertaining to deterioration mechanisms and techniques for detecting the initiation of fractures or other failures.

PROGRAM ORGANIZATION

A technical organization has been formed to facilitate and combine the various disciplines required to develop the needed scientific and engineering foundation outlined above. The participating faculty and staff, representing the Georgia Institute of Technology, Northwestern University, and the University of Minnesota, are recognized for their significant contributions with respect to structural fatigue, fracture, nondestructive testing, acoustics, ultrasonics, sensors, and signal processing. Integrated Diagnostics research is being carried out by nineteen (19) faculty associated with four schools from the Georgia Tech College of Engineering, four (4) faculty from Northwestern University, and eleven (11) from the University of Minnesota. In addition, the program has accommodated ten (10) post-doctoral researchers, thirty-five (35) graduate students, and seven (7) advanced undergraduate students.

ONR PROGRAM REVIEW

In this third year of M-URI funding, studies continue with respect to understanding the mechanisms of failure (through detection, identification, and prediction) and the means to detect, identify and analyze them (through sensors/hardware, signal processing/software, and real-time diagnosis). To facilitate an OFFICE OF NAVAL RESEARCH Program Review of these activities, this two-section publication was created.

- Section 1 provides a synopsis of each sponsored research project.
- Section 2 provides a copy of the viewgraph materials used at the ONR Arlington, VA review meeting of 20 January, 1998.

MULTIUNIVERSITY CENTER FOR INTEGRATED DIAGNOSTICS

INTEGRATED DIAGNOSTICS

Section 1

Project Summaries ♦

M-URI PROJECT SUMMARIES
Table of Contents

1.0 M-URI Thrust I
MECHANICAL SYSTEM HEALTH MONITORING (Direct Sensing, Analysis, Real-time Diagnosis)

1.1 Detection of the Precursor to Mechanical Seal Failure in Turbomachinery 1
1.2 Real-time Monitoring & Controlling of Mechanical Face Seal Dynamic Behavior 3
1.3 Dynamic Metrology as a Bearing Wear Diagnostic 5
1.4 Integrated Microsensors for Aircraft Fatigue and Failure Warning 9
1.4.1 Piezoelectric Materials 9
1.4.2 Wideband Acoustic Emission Microsensors 12
1.4.3 Signal Processing 14
1.4.4 Sensor Interface Circuits and Telemetry 17

2.0 M-URI Thrust II
FAILURE CHARACTERIZATION AND PREDICTION

2. 1 Structural Fatigue Investigation 21
2.1.1 Stress and Flaw Analysis of Components 22
2.1.2 Characterization and Modeling of Fatigue Damage
2.1.2.1 Modeling of Small Fatigue Crack Growth under Multiaxial Loading 24
2.1.2.2 Small Crack Behavior in Ti-6Al-4V 27
2.1.2.3 Fretting Fatigue and Small Crack Growth 29
2.1.3 Remaining Life Prediction 32
2.2 Failure Prediction Methodology/Fatigue Reliability 35
2.3 Acoustic Emission Modeling for Integrated Diagnostics 38
2.4 Study of Acoustic Emission and Transmission from Incipient Fatigue Failure 40

3.0 M-URI Thrust III
NONDESTRUCTIVE EVALUATION (Failure Detection and Identification)

3.1 Crack Detection in Annular Structures by Ultrasonic Guided Waves 43
3.2 Laser-Based Ultrasonics for Integrated Diagnostics 46
3.3 Eddy Current Microsensors for Integrated Diagnostics 49

1.1 DETECTION OF THE PRECURSOR TO MECHANICAL SEAL FAILURE IN TURBOMACHINERY

Co-Principal Investigators: Richard F.Salant and Jacek Jarzynski (Georgia Tech)
Graduate Research Assistant: William Anderson
M-URI Funding Allocation: 6.7%

DoD NEED

The U.S. Navy uses a large number of mechanical seals in such turbomachines as centrifugal pumps, compressors, turbines, turbopumps, propeller shaft assemblies, and gas turbine engines. Two specific examples of naval mechanical seal applications are the compressors in water chillers for air conditioning in submarines and surface vessels, and refrigeration compressors for ships' stores. Mechanical seal failure is one of the principal causes of breakdown of these machines. The use of a monitor to detect a precursor to seal failure will allow preventive action to be taken to avoid failure. Such a monitor will eliminate the need for scheduled preventive maintenance, thereby reducing costs, and will minimize the possibilities of catastrophic failure and the disruption of naval operations due to seal failure.

PROJECT MISSION

Mechanical seals generally fail as the result of the collapse of the lubricating film between the two seal faces. The goal of the present project is to develop a real-time monitoring system that will detect the collapse of the lubricating film before mechanical and thermal damage to the seal is sustained.

RESEARCH ACCOMPLISHMENTS

In the work done so far, a monitoring system has been built, analyzed, and successfully tested on a seal in a laboratory environment, under controlled steady-state conditions. The monitoring system utilizes actively generated ultrasonic waves to determine if the two seal faces make contact and, if so, the degree of contact. A piezoelectric transducer is placed behind one of the seal faces and is used as a source, generating a train of ultrasonic wave packets that propagate toward the interface between the seal faces. A second piezoelectric transducer is placed behind the other seal face, and is used to detect the waves that are transmitted across the interface. On the basis of theoretical work and work by other investigators [1-3], it had been expected that the transmitted signal would be virtually zero when the film is intact and nonzero when the film has collapsed, with an amplitude indicative of the degree of contact between the seal faces.

The monitoring system has been installed on the double mechanical seal shown in Fig. 1. This seal, originally designed for a turbopump, seals air and is electronically controlled so that the separation between the seal faces can be varied at will. A large number of steady-state tests have been run, in which the spacing between the seal faces was varied. Typical results are shown in Fig. 2. The transmitted signal strength, at the driving frequency, is plotted against the leakage rate. The latter is a measure of the spacing between the seal faces. As the leakage rate is reduced from approximately 12.4 l/min to about 1.7 l/min (by reducing the spacing), the signal strength remains substantially constant at the noise level (0.25 V). The leakage rate of 1.7 l/min corresponds to the seal faces making contact (there is leakage bypassing the

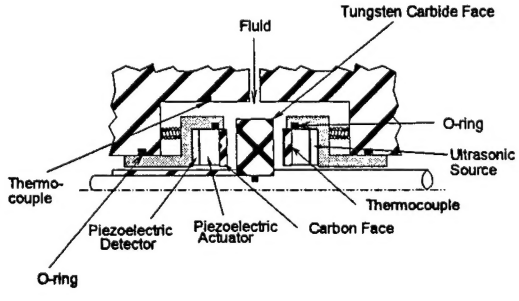

Figure 1. Apparatus

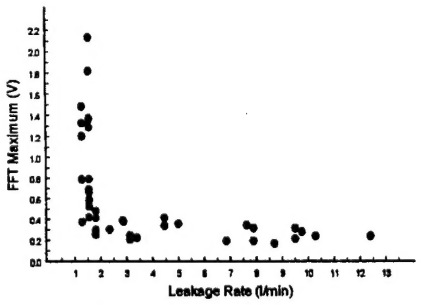

Figure 2. Transmitted Signal Strength

seal). At this contacting condition, the signal strength takes on values ranging from the noise level to approximately nine times the noise level.

To interpret these results, two series of bench tests were performed. In the first series, the shaft with the rotating tungsten carbide face and the two floating carbon face assemblies were placed in a jig, with the same relative positions as in the seal tester. The film thicknesses between the tungsten carbide and carbon faces were set using Mylar spacers of known thickness. Ultrasonic waves were generated and detected as in the seal tester. These tests showed that for all non-zero film thicknesses, the transmitted signal is essentially zero; it is non-zero only when there is mechanical contact between the faces, in agreement with the results of our analytic model. In the second series of bench tests, the seal components were stacked vertically, and ultrasonic measurements were made with various weights placed on the assembly to vary the contact pressure between the faces. These tests showed that as the contact pressure is increased, the transmitted signal strength increases. This is due to an increase in the real area of contact, and is in agreement with the work of other investigators [1-3].

It is therefore clear, from Fig. 2, that the strength of the transmitted signal indicates whether or not face contact occurs. If the signal strength is equal to the noise level, there is no contact. If the signal strength is greater than the noise level, there is contact, and the magnitude of the signal strength is a measure of the contact pressure between the faces. This is a very favorable characteristic for a seal monitor, because it allows assessment of the severity of the contact.

Efforts are currently underway to make ultrasonic measurements on the seal under transient conditions. These, as well as destructive tests to failure, will be completed prior to the end of year 3. During years 4 and 5, it is proposed to install a similar monitoring system on a seal used in an actual Navy application, which will be tested in the laboratory. Three candidate applications have been identified: i. the seal on the York T-86 centrifugal compressor, used on water chillers for air-conditioning on submarines and surface vessels, ii. the John Crane T-2 seal for the York R reciprocating compressor, used for refrigeration of naval stores, iii. The John Crane seal for the York F reciprocating compressor, used for refrigeration of naval stores. The choice will depend on seal availability and Navy interest.

References:

[1] Drinkwater, B. W., Dwyer-Joyce, R. S. and Cawley, P., 1995, "A Study of the Transmission of Ultrasound Across Real Rough Solid-Solid Interfaces," *Rev. Prog. Quantitative Non Destructive Evaluation*, Vol. 14, Plenum, New York.

[2] Drinkwater, B. W., Dwyer-Joyce, R. S. and Cawley, P., 1996a, "A Study of the Interaction Between Ultrasound and a Partially Contacting Solid-Solid Interface," *Proc., Royal Society of London A*, Vol. 452, pp. 2613-2628.

[3] Drinkwater, B. W., Dwyer-Joyce, R. S. and Cawley, P., 1996b, "The Interaction of Ultrasound with a Partially Contacting Solid-Solid Interface in the Low Frequency Regime," *Review of Progress in Quantitative Non Destructive Testing* Vol. 15, Plenum, New York.

M-URI PUBLICATIONS

Anderson, W. B., Salant, R. F. and Jarzynski, J., 1997, "Detection of Lubricating Film Breakdown in Mechanical Seals," ASME Public. TRIB-7, *Emerging Technologies for Machinery Health Monitoring and Prognosis*, R. Cowan, ed., 1997 ASME Mechanical Engineering Congress and Exposition, Dallas, November 16-21, 1997.

Anderson, W. B., 1997, "Detection of Lubricating Film Breakdown in Mechanical Seals," M. S. Thesis, Georgia Institute of Technology.

Jarzynski, J., Salant, R. F., Anderson, W. B., "Condition Monitor for a Mechanical Seal," U.S. Provisional Patent Application, # 60/048,960, June 6, 1997.

Jarzynski, J., Salant, R. F., Anderson, W. B., "Improved Condition Monitor for a Mechanical Seal," U.S. Provisional Patent Application, Serial no. to be issued, November 7, 1997.

1.2 REAL-TIME MONITORING & CONTROLLING OF MECHANICAL FACE SEAL DYNAMIC BEHAVIOR

Co-Principal Investigator: Itzhak Green (Georgia Tech)
Graduate Research Assistant: Min Zou
M-URI Funding Allocation: 6.1%

DoD NEED

Mechanical face seals are mainly used in centrifugal pumps, compressors, and powered vessels where a rotating shaft passes through two regions containing different fluids, and there is a need to keep the regions sealed. Unpredictable seal lives and random failures are very common in mechanical seals. In critical applications, seal failure may have severe implications. Maintenance costs, attributed to mechanical face seal failures, is much higher than just the cost of the seal itself when down time is taken into account. Contact and wear of the seal faces is believed to be the major cause of seal failure. Therefore, there is a need to monitor, detect and control undesired contact between seal faces during seal operation. The techniques of monitoring, detection, and control developed in this research can be applied to water seals in Naval chillers to increase their reliability and to reduce maintenance cost. This technology can also be applied to any rotating machinery that has a mechanical seal that critically needs to be monitored.

PROJECT MISSION

The objective of this research is to develop a system that can monitor seal dynamic response in real-time, detect seal face contact, and control the seal at close proximity and yet prevent the seal from contacting. A test rig featuring a flexibly mounted rotor (FMR) noncontacting mechanical face seal is used for the current study. The instantaneous dynamic response of the rotor is measured using Eddy current proximity probes. Decisions are being made based on geometrical contact criteria, rotor angular response in an orbit analysis, and/or spectrum analysis of the proximity probes signals to detect detrimental higher harmonic oscillations (HHO). These methods of contact detection are implemented in real-time. Such a monitoring system has been constructed and demonstrated to detect seal contact and monitor the dynamic behavior of mechanical face seal [1]. Based on data from the proximity probes active control of the seal clearance has also been achieved [2].

RESEARCH ACCOMPLISHMENTS

The following has been accomplished:

1. Numerous design modifications to the FMR noncontacting mechanical seal test rig have been made. The most significant are:
    - Replaced the manual air pressure regulator with an electropneumetic transducer that can convert voltage signal to pressure. This allows for automatic (computerized) control of the seal clearance by adjusting air pressure in the rotor chamber.
    - Designed and implemented a new support system for the rotor to include two springs compressed at both ends of the rotor. This design better balances the applied forces and moments acting upon the rotor. This design is more efficient in restricting the rotor angular response than a single spring support.
2. The DAS16 data acquisition board has been replaced with a dSPACE DS1102 board, along with the corresponding software (TRI and TRACE), and a dedicated Texas Instrument C compiler which compiles and links C code generated from Matlab's SIMULINK models. The computer environment has been properly set for the dSPACE software tools, along with wiring.
3. We calibrated the motor speed controller using TRACE software from dSPACE Inc., to enable the determination of the motor speed on-line.
4. We estimated seal clearance from leakage measurement using a leakage analysis and a flow meter capable of measuring minute flows with A/D capabilities for sampling and real-time processing.

5. We conducted experiments and successfully reproduced higher harmonic oscillations (HHO) using the operating parameters that previously produced HHO.
6. We integrated the control setup in the test rig system. The strategy was to use proximity probes and flow meter as sensors for the rotordynamic responses, use electropneumatic transducer as an actuator, use Mathworks software Matlab and corresponding tool boxes to perform signal processing and controller design, and use the dSPACE DS1102 controller board for data acquisition and controller realization.
7. We obtained the relationship between the seal clearance and the air pressure in the rotor chamber based on a force balance. This relationship is helpful in determining the air pressure in the rotor chamber for clearance control.
8. We constructed a real-time monitoring system that calculates the seal clearance, rotor angular misalignment, stator misalignment and relative misalignment between the rotor and stator based on the proximity probes signals.
9. We developed an algorithm to display the orbit of the rotor angular misalignment in real-time [1].
10. We implemented real-time fast fourier transformation (FFT) to process the proximity probe signals and display power spectrum densities (PSD) [1].
11. We used contact criteria to detect contact in real-time.
12. We performed system identification using experimental data. We determined the seal axial dynamic model by measuring the seal response to a step excitation of air pressure in the rotor chamber.
13. We designed and implemented a controller to the test rig system. The controlled system can maintain a pre-selected seal clearance to be independent of operation disturbance in speed and/or sealed pressure. The controlled system can also follow set-point changes in seal clearance [2].
14. We performed experiments to test the control system upon seal performance [2].
15. Work is underway to design a controller for the reduction and, if possible, elimination of HHO, once detected during seal operation.

Since the sealed fluid in the test rig is water, the monitoring, detection and control techniques developed in this research can be applied to the water seals used in Naval chillers.

Future Work:

1. Continue to work on the design and implementation of the controller in point 15 above.
2. Force analysis has shown that direct variation of the sealing dam coning has a more dramatic effect on the fluid film stiffness and damping coefficients than through variation of the closing force. Hence, through an on-line change of the coning it will be possible to control the opening force and the fluid film moments in the sealing dam more easily due to the greater sensitivity to coning. The closing force will be utilized here for either generating or controlling HHO. The dynamics of intermittent face contact and impact will also be analyzed. This stage is necessary for a thorough understanding of the mechanical and physical processes that generate and constitute HHO.
3. The test rig we work on has been purposely designed to detect seal failure only. It is unclear when signals from a seal indicate seal failure or whether failure occurred in other system components, such as bearings, gears, shaft, etc. We will investigate how failure (or failure onset) in another system component (e.g., cracked shaft) may effect the seal behavior, and how such failure can be detected through the sensors that monitor the seal dynamic behavior.

M-URI PUBLICATIONS (REFERENCES)

[1] Zou, M., and Green, I., 1997, "Real-time Condition Monitoring of Mechanical Face Seal," Proc. the 24th Leeds-Lyon Symposium on Tribology, London, Sept. 4-6, 1997.
[2] Zou, M., and Green, I., "Clearance Control of Mechanical Face Seal," Submitted to STLE Annual Meeting, 1998.
[3] Zou, M., and Green, I., "Real-time Detection of Contact in Mechanical Face Seal," In preparation for Vibration, Noise & Structural Dynamics 1999.

1.3 DYNAMIC METROLOGY AS A BEARING WEAR DIAGNOSTIC

Co-Principal Investigators: Thomas Kurfess, Steven Liang, Steven Danyluk
Graduate Research Assistants: Scott Billington, Yawei Li, Xavier Ribadeneira
M-URI Funding Allocation: 6.9%

DoD NEED

A large portion of catastrophic failures in complex mechanical systems such as helicopters are the direct result of bearing failure. Such failures can yield damaging and cataclysmic results, and are increasing in probability as the average age of the helicopter fleet in the Navy continues to rise. Thus, real-time, on-line techniques to determine the current health of bearings typically found on helicopters must be developed. Such techniques are critical in the maintenance of the helicopter fleet. The techniques are also applicable to a wide range of other systems that employ bearings. Furthermore, these diagnostic techniques are the foundation of prognostic efforts that may be used to predict the useful life of critical components such as bearings.

PROJECT MISSION

To fully utilize the latest sensors available today in an intelligent fashion, this project targets the development and implementation of real-time and on-line methods for bearing wear and failure detection. The ultimate objective of the project is to develop a compact self-contained processing package that can be attached to an array of sensors used to monitor bearing health during the operation of a rotary winged aircraft. To accomplish this a number of sensors will be employed, including: contact potential difference probes (CPD), eddy current, accelerometer, and acoustic emission sensors. In order to successfully meet project objectives, these individual sensors must be calibrated and integrated into a single diagnostic package. By using a multiple sensor approach, it is anticipated that a number of wear and failure modes will be detectable in real-time. Furthermore, the use of multiple sensors will improve the confidence interval on the estimation of the bearing's condition.

RESEARCH ACCOMPLISHMENTS

This section briefly presents some of the more critical results generated during the project period. During the course of the project, the bearing test bed has been developed to perform thermal, load and speed calibrations as well as sophisticated diagnostics using multiple sensors. Insight into the roller bearing set-up was further enhanced by data from both The Timken Company and the Torrington Company, who aided in this research. Successful diagnostic tests were also conducted on large scale (40,000 cfm) turbo-pumps and high speed (150,000 rpm) spindles. Based on the diagnostic tools developed, some work in the area of prognostics has been initiated. The initial results of the prognostic work are presented in this report as well.

With respect to the diagnostics, Fig.1 shows a plot of accelerometer RMS vs. rotational speed and radial load. A stud mounted triaxial accelerometer was used to generate these results. Both axial and radial acceleration measurements are in good agreement in these tests. The experiments demonstrate that the use of multiple sensors and sensor types is critical for any bearing diagnostic system. For example Fig. 1 shows a counterintuitive relationship between load and speed. For all speeds tested, higher radial loads produced lower acceleration levels. These higher load levels basically reduce the amount of vibration in the overall system. When the data presented in Fig. 1 are considered in conjunction with similar acoustic emission data, the load relationship is clear. Similar results were obtained for band-passed RMS levels as well as the peak indicators for defect frequency and the maximum FFT at 4-6 kHz resonance. Peak indicators (*e.g.*, peak in envelope spectrum and the maximum FFT amplitude) also increase. This phenomena is not explained by the same reason as the RMS increase. The amplitude spectrum FFT used in this research assigns signal amplitude to a frequency. Therefore, the race impact magnitude also increases with increasing speed. Figure 2 shows the defect frequency peak in the enveloped spectrum with a band-pass filter of 4000-6000 Hz.

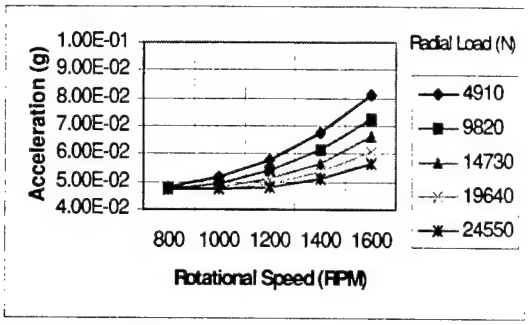

Fig. 1. Z RMS Acceleration, Housing Above Bearing.

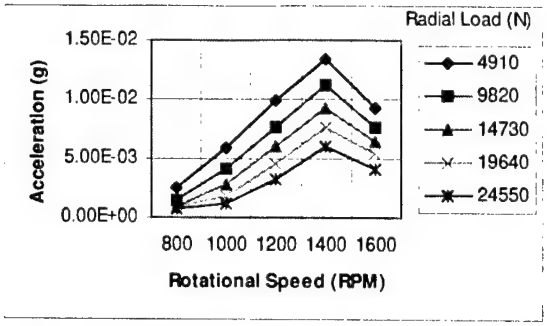

Fig. 2. 4-6 kHz Envelope Spectrum Peak, Z Accelerometer, Housing Top.

It is interesting to note that at speeds above 1400 rpm, there is a decrease in the accelerometer signal strength (see Fig. 2). This is a result of defect impulses decaying vibration (as shown by the time constant) overlapping with the onset of the next defect impulse. The second harmonic of the defect frequency also modulates the housing resonant frequency. This second harmonic cancels part of the signal from the primary defect frequency via destructive interference. At 1600 RPM, this cancellation is the last part of the pulse signal that occurs before the next impulse. As a result, the impulse decay appears faster than the decay time constant of the impulse generated during defect impact. Figure 3 shows the impulse shape (due to defect impact) for various rotational speed. As can be seen, when the impacts occur in close temporal proximity, part of their signal energy is camouflaged by the subsequent defect impact signal. This demonstrates a heretofore undefined fundamental limitation to the HFRT (High Frequency Resonance Technique).

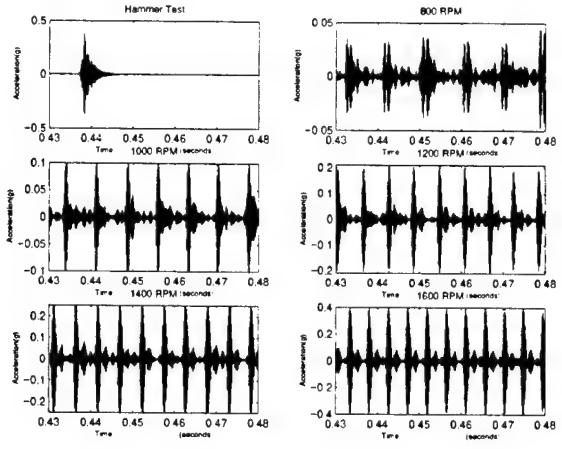

Fig. 3. Effects of Speed on Impulse Shape, 14730 N Radial Load

After determining that load-speed relationships are repeatable, it is possible to model changes in nominal signal level by a linear relationship over regions of the load-speed response. Figure 4 shows five replications of response values for all combinations of 4 speed and 4 load levels with a smaller level increment than the previous investigations. A plane is fitted to this region. This linear relationship is useful in diagnostic models that allow calibrated measurements in a range of varying conditions. Figure 5 shows three planes that are fitted to a region of signal response similar to that shown in Fig. 4. Clearly, the fitted planes do not have the same slope, but the precision of the linearized approximation is adequate, given the data variation shown, over regions such as that shown in Fig. 5.

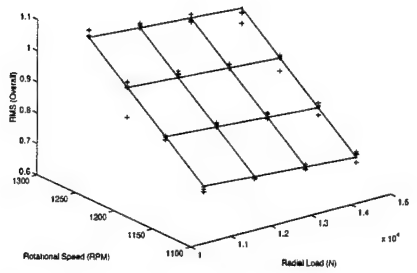

Fig. 4. Load-Speed Relationship in a Small Region.

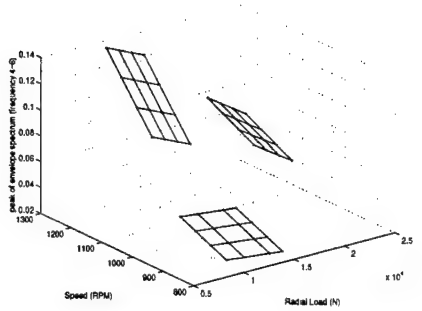

Fig. 5. Different Linearized Regions of Load-Speed.

Results from the preliminary prognostic work are shown in Fig. 6 and Fig. 7. The estimated data in both figures are predicted solely from the mechanistic model using apriori information. These initial results indicate that the model and prediction methods will provide a solid foundation from which to continue the prognostic work.

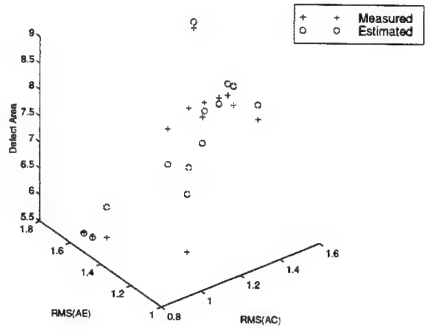

Fig. 6. Defect Area Estimated using Multiple Sensors.

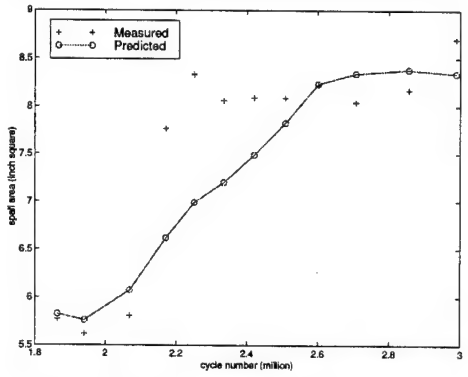

Fig. 7. Estimated Spall Area for a Bearing Life Test.

Human Resource Development:

The following masters' students have completed their theses: Jason Shiroishi, Scott Billington. Currently, Xavier Ribadeneira is supported as a masters candidate and Yawei Li is supported as a Ph.D. candidate.

Conclusions:

The results of this years work have demonstrated a significant understanding of the methodology behind integrating multiple sensor signals to perform diagnostics on roller bearing systems. Tests using the diagnostic models have been run on a variety of systems including the bearing test stand at Georgia Tech as well as large turbo-blowers and high speed spindles with tangible results on all systems. Linearization of diagnostic results about nominal operating conditions permits the direct determination of defect severity as a function of a number of operating parameters such as load and speed.

Furthermore, the models developed and enhanced by the diagnostic program have been successfully integrated into a model based prognostic system. Preliminary results of the prognostic system indicate that the models and techniques proposed will yield meaningful and useful results with respect to prediction of bearing damage levels well before failure.

Future Work:

Future work in this area will further explore the non-linear response of signals to operating conditions, as well as their interaction with bearing damage level and type. Additionally, non-linear approximations and heuristic modeling approaches to address operating condition effects will be investigated as a practical addition to current diagnostic and prognostic methods. A new probe, the contact potential difference (CPD) probe, will be integrated into the system. Recent experiments with a CPD probe mounted in the outside race of a roller bearing have demonstrated its utility in identifying roller damage in real-time.

Furthermore, with support for the Air Force and the Torrington Company, the test stand will be modified to operate at higher speeds under larger loading conditions. The system will also be modified to permit the analysis of ball bearings. Finally, a spray lubrication system will be added to the system to better simulate a number of operational helicopter systems.

M-URI PUBLICATIONS

Shiroishi, J., Li, Y., Liang, S., Kurfess, T., Danyluk, S., "Bearing Condition Diagnostics Via Multiple Sensors," *Mechanical Systems and Signal Processing*, Vol. 11, No. 5, pp. 693-705, September, 1997.

Shiroishi, J.W. , Li, Y., Liang, S., Danyluk, S., and Kurfess, T.R., "Vibration Signal Analysis for Bearing Race Damage Diagnostics," Keynote paper for the *7th International Conference on Dynamic Problems in Mechanics*, Brazil, pp. 187-190, March 1997.

"Bearing Fault Detection via High Frequency Resonance Technique with Adaptive Line Enhancer," Li, Y., Shiroishi, J.W., Kurfess, T.R., Liang, S., and Danyluk, S., accepted by the *12th Biennial Conference on Reliability, Stress Analysis, & Failure Prevention*, 1997, Virginia Beach, VA, April 15-17.

"Roller Bearing Defect Detection with Multiple Sensors," Billington, S.A., Li, Y., Kurfess, T.R., Liang, S.Y., Danyluk, S., *Emerging Technologies for Machinery Health Monitoring and Prognosis*, TRIB-Vol. 7, R. Cowan, ed., pp. 31-36, ASME IMEC&E, Dallas, TX, November 1997.

1.4 INTEGRATED MICROSENSORS FOR AIRCRAFT FATIGUE AND FAILURE WARNING

Project Coordinator: Dennis L. Polla (University of Minnesota)
M-URI Funding Allocation: 36.8%

PROJECT OVERVIEW

Four principal activities have taken place with the goal of developing miniature structural health monitoring systems using microelectromechanical systems (MEMS) technology. These include 1) piezoelectric materials, 2) acoustic emission and vibration microsensors, 3) signal processing, and 4) sensor interface circuits and telemetry.

The main accomplishments for each of these activities are briefly summarized below:

- Piezoelectric sensor materials have been developed for both acoustic emission sensing and vibration monitoring. The sensor manufacturing methods are compatible with standard 2-μm CMOS integrated circuit processing methods and MEMS surface-micromachining processes.
- Acoustic emission sensors and signal conditioning electronics have been tested in laboratory fatigue experiments. Analysis of the voltage versus time response and time-frequency energy spectrum have been directly correlated with crack propagation
- AE signal detection, pre-filtering, and deconvolution algorithms have been devised. Analysis of AE transient parameters such as time-of-arrival, duration, energy, average frequency, and time-frequency energy has been successfully applied to classify fracture and noise signals.
- A general MEMS interface circuit approach has been developed to allow MEMS sensors to communicate by wireless telemetry to a central receiving station.

1.4.1 PIEZOELECTRIC MATERIALS

Co-Principal Investigators: L. F. Francis (lead), W. W. Gerberich, W. P. Robbins, D. L. Polla
Students: D. Bahr, C. R. Cho, D. Drinkwater, J. Plummer, A. Schmidt, J. S. Wright

DoD NEED

Microsensors for integrated diagnostics (acoustic emission sensing of crack propagation and vibration sensing) rely on a piezoelectric ceramic thin film integrated with Si-based circuits for amplification, signal processing, and telemetry. Acoustic emission from crack propagation in a material leads to sound waves which deform the piezoelectric ceramic in the microsensor and create an electrical signal. For vibration sensors, the piezoelectric film is on top of a cantilever beam which defects with vibration; deflection in the beam deforms the ceramic and generates an electrical response. The operation of these sensors requires a high quality piezoelectric thin film which in turn demands research aimed at gaining a full understanding of processing-structure-property relationships for the thin film and other materials needed for integration (e.g., electrodes, barrier layers).

PROJECT MISSION

The primary objective of this project is to fabricate and characterize integrated piezoelectric thin films in order to improve properties and performance for integrated acoustic emission and vibration sensors. To meet this objective, we explore the important effects of processing on the development of crystal structure, microstructure and the resulting elastic, dielectric, ferroelectric, and piezoelectric properties of the piezoelectric thin films. A related goal is to fabricate and characterize other materials needed in the integrated structure, including electrodes, layers to promote bonding and barrier layers to prevent interdiffusion during processing.

RESEARCH ACCOMPLISHMENTS

The main accomplishments of the last three years are: (i) development of solution deposition-based processing routes for the fabrication of integrated piezoelectric thin films, (ii) characterization of the structures and properties of piezoelectric thin films (including the construction of a laser interferometer to characterize piezoelectric response) and other materials needed for integration, and (iii) fabrication of an integrated acoustic emission sensor and testing of sensor response. These three areas of accomplishment are described below.

Solution deposition-based processing routes for piezoelectric ceramic thin films were developed. The piezoelectric that we have most intensively studied is lead zirconate titanate, $Pb(Zr_{0.53}Ti_{0.47})O_3$ (PZT). The solution deposition process involves the synthesis of a metal organic solution, deposition by spin coating, and heating to crystallize a ceramic film. We developed a processing route for PZT that involves preparing a metalorganic solution from Ti isopropoxide, Zr acetylacetonate, and Pb acetate trihydrate (referred to here as the MOD route). The complex chemistry of this route leads to continued changes in chemical structure with time; however, we explored these effects completely and control them through a combination of accelerated aging followed by freezing the solution. These frozen solutions can then be used as needed with reproducible results, creating a convenient system. We have also prepared PZT films using solution processing routes reported in the literature and refined them to improve results. One of these routes is based on a combination of alkoxides and acetates in a 2-methoxyethanol solvent (referred to here as the MOE route) and has also proven to provide excellent results.

Processing-structure-property relationships for PZT thin films were established and this understanding led to the PZT thin films with good properties for acoustic emission sensing. The main processing variables explored were solution processing conditions and heating schedules. Under optimized conditions, the desired perovskite crystal structure, a dense microstructure and good electrical properties were obtained. The perovskite structure is necessary to develop the dielectric, ferroelectric and piezoelectric properties. The microstructure, as shown in Fig. 1 for the MOD route, is dense and consists of submicron grains of PZT; similar results were achieved for the MOE route. The dielectric and ferroelectric properties of MOD films (dielectric constant ~1000, loss tangent ~0.04, remnant polarization ~ 25 $\mu C/cm^2$ and coercive field of 50 kV/cm) are similar to those of bulk PZT and comparable to those achieved in PZT thin films by others working in this field. The piezoelectric performance (d_{33} piezoelectric constant) was determined using a laser interferometer built for this project. The results show a d_{33} of ~80 pm/V with DC bias of 4V; this value is less than that of bulk PZT ceramics, but is consistent with the results of others. The lower response of the thin film is believed to be due to the substrate constraint as well as the restriction on the reorientation of ferroelectric domains. In order to understand the piezoelectric properties more fully, we are studying the effect of crystallographic orientation and poling (application of an electric field to align domains) on the piezoelectric response. For example, we have found that films with predominately (100) orientation have better piezoelectric response (d_{33} ~ 85 pm/V) relative to films with predominately (111) orientation (d_{33} ~ ~60 pm/V).

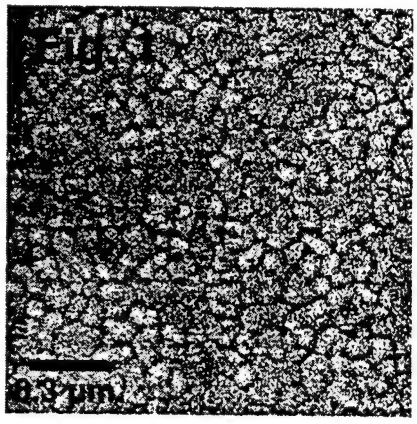

The elastic moduli and hardnesses of PZT thin films and other materials used for integration were characterized by nanoindentation methods. To facilitate preparation of AE sensors and cantilever-based vibration sensors, electrodes (Pt), bonding layers (Ti, poly-Si), barrier layers (TiO_2, SiO_2) and structural materials are used (Si_XN_Y). The table shows the average elastic moduli. The only unexpected results are the high elastic moduli of

Pt and PZT. The former may be due to residual stress in the film and the latter to nonlinear elastic deformation.

Material	Thickness (nm)	Elastic Modulus (GPa)
Poly-Si	1000	172
Si_xN_y	1000	267
SiO_2	526	78
TiO_2	1000	185
Ti	1700	113
Pt	1600	237
PZT	600	150

Acoustic emission tests were carried out on PZT thin films in a variety of amplifier/package conditions. For example, Fig. 3 compares the response of a commercial sensor with that of a thin film microsensor (without packaging) to the impact of a tweezers on a piece of metal. The sensors were mounted on the metal, equidistant from the impact. The fast response and lack of ringing are the interesting features of the microsensor response. While the addition of packaging affects the response, these data show the potential of piezoelectric thin film microsensors. The test chip shown in Fig. 2 was designed to be used with an integrated CMOS amplifier (fabricated on separate Si chips and bonded on the test chip above or to the right of the array of sensors and connected via wirebonds). This type of chip will be used to determine the effects of electrode area on the sensor/amplifier response to different AE events. In addition, this new test structure will allow us to investigate the effects of piezoelectric material composition, thickness, and crystallographic orientation on the electromechanical properties and sensor response. Some interesting results may also be possible with a different materials system (lead scandium niobate titanate) and with the use of a conducting oxide electrode ($LaNiO_3$) which preliminary results show as effective in controlling crystallographic orientation.

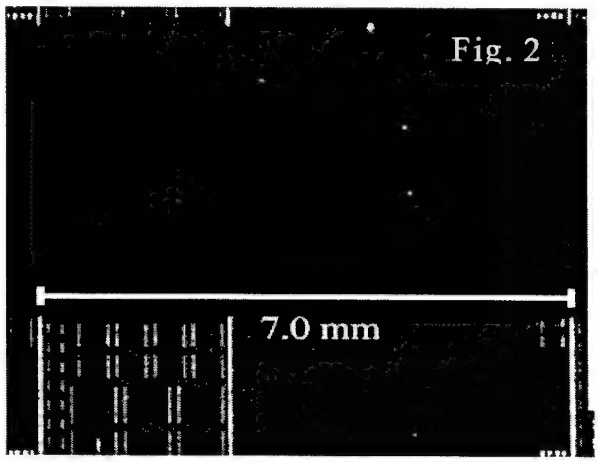

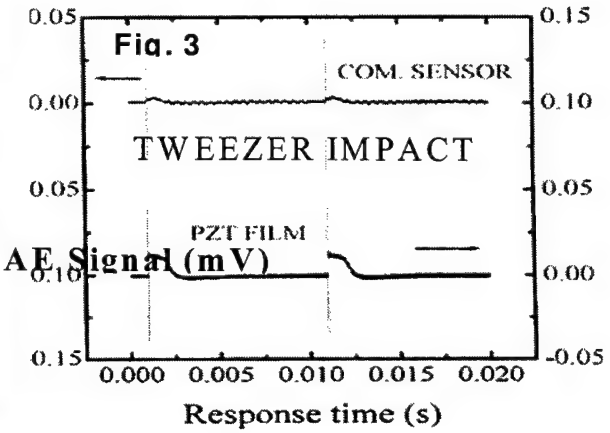

M-URI PUBLICATIONS

J. S. Wright and L. F. Francis, "Processing and Electrical Properties of a Water Soluble Hybrid MOD Route to PZT Thin Films," submitted to *Journal of Electroceramics*

C. R. Cho, D. E. Drinkwater, L. F. Francis and D. L. Polla, "Enhancement of Electrical Properties of Nb-Doped Lead Scandium Niobate Titanate Thin Films," submitted to *Applied Physics Letters* (1997).

D. L. Polla and L. F. Francis, "Processing and Characterization of Piezoelectric Materials and Integration into Microelectromechanical Systems," submitted to *Annual Reviews of Materials Science* (1997).

D. F Bahr, J. S. Wright, L. F. Francis, N. R Moody, and W. W. Gerberich, "Mechanical Behavior of a MEMS Acoustic Emission Sensor " *Mat. Res. Soc. Symp. Proc.,* **444** 209-214 (1997).

1.4.2 WIDEBAND ACOUSTIC EMISSION MICROSENSORS

Co-Principal Investigators: W. P. Robbins (lead), R. Harjani, D. L. Polla
Students: A. Schmidt, J. Plummer, K. Nair, K. Rho, T. Ma, A. Drexler

DoD NEED

As mechanical components in systems (planes, helicopters, etc.) become heavily fatigued, microcracks develop and grow in the component, ultimately leading to failure. The development of microcracks is accompanied by the release of transient broadband acoustic emissions that can be detected by appropriately-placed acoustic emission (AE) sensors. If AE sensors were permanently mounted on critical components in a system, continuous monitoring for microcrack development could be carried out while the component is in service. The system would be taken out of service only when the development of microcracks reached a predetermined threshold and maintenance time and expense would be minimized. This would maximize the availability of the system for mission assignments and reduce the number of routine inspections.

Unfortunately currently available AE sensors are too large, expensive, and fragile, to permanently mount on critical mechanical components. In addition most AE sensors lack sufficient bandwidth and also require ancillary electronic amplification of the detected signal. Hence the current time-consuming and expensive method of periodic inspection, which includes system disassembly to access the critical components, is the only alternative for minimizing catastrophic failures. This procedure severely limits the availability of systems for mission assignments.

PROJECT MISSION

The goal of this project is to develop small, rugged, and wideband acoustic emission sensors that can be mounted on failure-prone mechanical components for continuous in-service monitoring for the development of microcracks. The AE events picked up by the sensors would be directed to appropriate electronics for recording, analysis, and if appropriate, issuance of warnings to system operators (e.g. the pilot of the plane or helicopter) and maintenance personnel. The specific goals for the AE sensor are:

1. Approximate size: 8-10 mm diameter and 5-7 mm thick.
2. Bandwidth: 50 kHz to 10 MHz.
3. Sensitivity: 10^6 [V/unit strain] (prior to post-sensor amplification)
4. Minimum detectable strain: 10^{-10}
5. Power requirements (for on-board charge amplifier): 5 V at 1 mA
6. Two-wire interconnect (ground and combined dc power-signal line)
7. Temperature range: -50 to +100 °C

RESEARCH ACCOMPLISHMENTS

Three generations of hybrid AE sensors have been fabricated and tested. The term hybrid refers to the on-board charge amplifier being fabricated with discrete surface mount components and positioned on a circuit board. The current version of the AE sensor is shown in Fig. 4. The PZT sensor is 5 mm in diameter and 0.2 mm thick. The charge amplifier uses a single 18 volt dc supply and draws approximately 15 mA. The charge amplifier bandwidth is 30 kHz to 10 MHz. The sensitivity of the sensor is approximately 10^6 [V/unit strain]. Initial tests indicate that the sensor responds to incident ultrasonic energy well into the MHz range. Testing is currently underway to characterize the sensitivity and frequency response of the sensors.

A first generation integrated circuit containing the op amp building block for an eventual integrated circuit charge amplifier has been designed and fabricated. The preliminary testing indicates that the op amps are functional and meet specifications (5 V at 200 mA and 100 MHz unity gain cross-over frequency). A second generation design which implements the complete charge amplifier will be

carried out during Year 4 of this project. When functional chips of the second generation design are available, the size of the AE sensor will be considerably smaller than the present 14 mm diameter by 9 mm thick hybrid AE sensor.

Fatigue testing of the acoustic emission microsensors was carried out using devices and amplifiers fabricated at the University of Minnesota and controlled steel specimen cyclic loading at Georgia Institute of Technology. Multiple fatigue experiments were carried out to material failure. Figure 5 shows an AE sensor response to crack-generating strain. While these experiments are still continuing at the time of this writing, additional work in Year 4 will identify issues of 1) sensor placement, 2) crack location determination based on triangulation and analysis of sensor rise-time, 3) time-frequency energy analysis, and 4) sensor fusion.

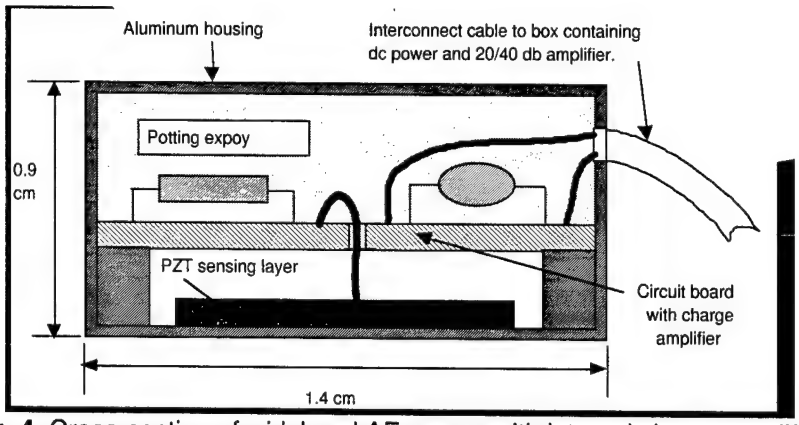

Fig. 4. Cross-section of wideband AE sensor with integral charge amplifier.

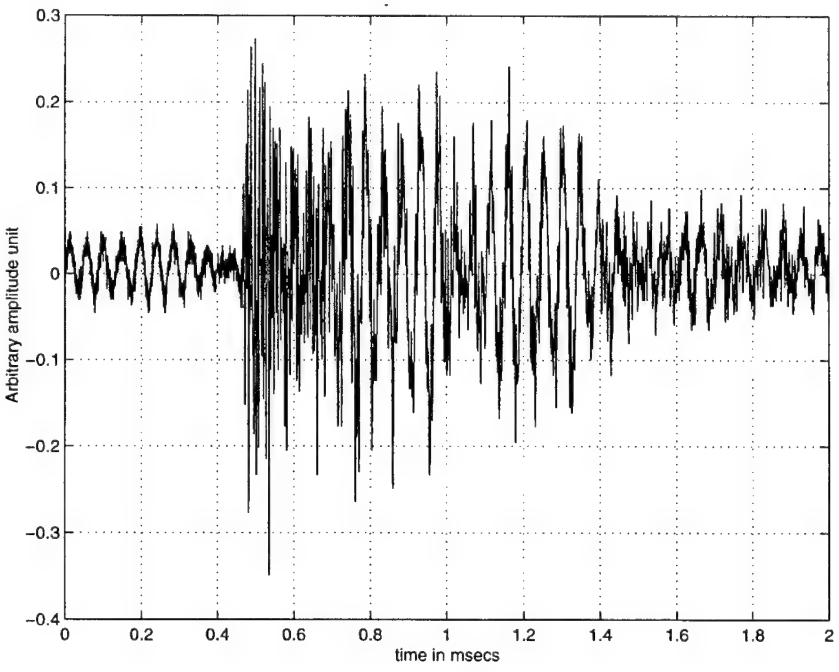

Fig. 5 University of Minnesota AE Sensor Response

1.4.3 SIGNAL PROCESSING

Co-Principal Investigators: M. Kaveh (lead), A. H. Tewfik, and K. M. Buckley
Students: D. West, D. Zhang, and G. Venkatesan

DoD NEED

Intelligent systems which monitor machinery and detect the onset of potentially catastrophic faults have great economic and life-saving value to the Navy. Acoustic Emissions (AEs) are informative signals which are generated by the initiation and growth of cracks. Hence, a monitoring system based on the detection and localization of AEs is a passive, nondestructive method, which may provide the means of circumventing expensive and time-consuming periodic maintenance procedures that require substantial down time. Signal processing techniques which are, at once, based on realistic models of signal, interference and measurement mechanisms, but robust to physical and operational variations are needed.

PROJECT MISSION

The primary objective of the signal processing effort is the design and evaluation of algorithms and measurement strategies which can lead to reliable detection of acoustic emission (AE) signals generated by potentially catastrophic cracks, during the operation of a machinery. The application of particular interest is the monitoring of the condition of a helicopter rotor shaft during flight. As a result, this detector must, not only recover the legitimate crack-initiated AE transient signals from noise, but must also differentiate these from other transients with similar spectral content generated by electromagnetic sources and other mechanisms such as mechanical fretting. The interference-rich situation encountered in this application sets this work apart from most other research involving AEs, which have primarily operated on data measured in laboratory environments, where the in-band noise is small enough to be neglected. A secondary objective of this work is the localization of the location of the crack.

RESEARCH ACCOMPLISHMENTS

Noise and Signal Measurements/Analysis. We have made two visits to the St. Paul Airport and three visits to the Cherry Point Marine Air Station for acquiring noise vibration data from helicopters. The vibration data collected from these measurements have enabled us to gain a better understanding of the noise characteristics that we can expect in an in-flight situation. Conclusions drawn herewith were confirmed by the Boeing test-bed data provided to us by Honeywell. A variety of acoustic emission (AE) data were obtained from experiments performed at the University of Minnesota facilities by Prof. Gerberich and his students, at Georgia Tech, and at Northwestern University. Our analysis of the above data has provided us with information on the range of crack-initiated and crack fretting AE characteristics. These measurements also provided us with a general idea about the propagation characteristics of the AEs.

Signal+Noise Model. With information derived from studying various noise and signal data, we have proposed a model for the in-flight scenario. The time series measured at a sensor after prefiltering will consist of (see [3] for details), 1) crack formation/propagation signal transients (if any), 2) fretting noise transients, 3) electromagnetic transients, 4) other transient signals, 5) background noise, and, 6) measurement/quantization noise. We believe that differentiating between the first four components is the major challenge in providing reliable fault diagnostics using AEs.

Signal Modeling and Detection. We have modeled the transients as a combination of decaying sinusoidal waveforms. In specific cases, however, depending on the material geometry and characteristics, it might be possible to predict the range of decay rates as well as the range of frequencies

exhibited by the crack AE transient. This assumption has initiated our work on eigenfilter banks that span the above space of decay rates/frequencies in some optimal sense. Filtering the measured data with these optimal filter banks and thresholding the output of these filters in some suitable way provides a robust technique for the detection of signals in noise[3](see Fig. 6). Other related detectors, using composite detection techniques are also being developed.

Channel/Source Characterization and Source Localization. Blind deconvolution techniques can be used in our fault diagnostic context to not only estimate the unknown source (crack) waveform but to also obtain as estimate of the propagation channel characteristics. This channel characterization can possibly aid in localizing the source. However, blind deconvolution techniques in the context of our AE diagnostics scenario are fundamentally different from typical digital communication situations (see [4][5] for a detailed discussion). The differences preclude efficient use of standard blind deconvolution algorithms for the AE problem. Hence, it has been necessary to not only modify existing algorithms but to also devise new solutions that will be more effective for this problem. In this context, we have provided generalizations of the blind multichannel-FIR identification schemes, and we have introduced solutions for blind multichannel-IIR identification for both the finite-length and persistent source cases[4][5].

Parameter Extraction and Multisensor Data Fusion using Neural Networks. Parameters such as relative times-of-arrival, duration, energy, average frequency, etc. of the transients received by multiple sensors can be valuable for the determination of the approximate location of the signal source, and the distinction between different types of transients. Parameter vectors are extracted using, amongst other schemes, the detection and deconvolution techniques outlined above for every cycle of data at different sensors. Using such parameter vectors, derived from representative data, we have obtained preliminary results on the training of neural networks that provide reliable classification of the transients. A block diagram summary of the proposed system is shown in Fig. 7.

M-URI PUBLICATIONS (REFERENCES)

[1] K. M. Buckley, G. T. Venkatesan, D. West and M. Kaveh, "Detection and Characterization of Cracks for Failure Monitoring and Diagnostics," *IEEE Conference on Acoustics, Speech and Signal Processing*, Atlanta, May 1996.

[2] D. West, G. T. Venkatesan, A. H. Tewfik, K. M. Buckley and M. Kaveh, "Detection and Modeling of Acoustic Emissions for Fault Diagnostics," *IEEE Statistical Signal and Array Processing Workshop*, Corfu, Greece, 1996.

[3] G. T. Venkatesan, D. West, K. M. Buckley, A. H. Tewfik and M. Kaveh, "Automatic Fault Monitoring using Acoustic Emissions," *IEEE Conference on Acoustics, Speech and Signal Processing*, Munich, 1997.

[4] G. T. Venkatesan, M. Kaveh, A. H. Tewfik and K. M. Buckley, "Blind Identification of Single-Input Multiple-Output Pole-Zero Systems," submitted *to IEEE Conference on Acoustics, Speech and Signal Processing*, Seattle, 1998.

[5] G. T. Venkatesan, M. Kaveh, A. H. Tewfik and K. M. Buckley, "Blind Identification of Single-Input Multiple-Output Pole-Zero Systems," submitted to *IEEE Transactions on Signal Processing.*

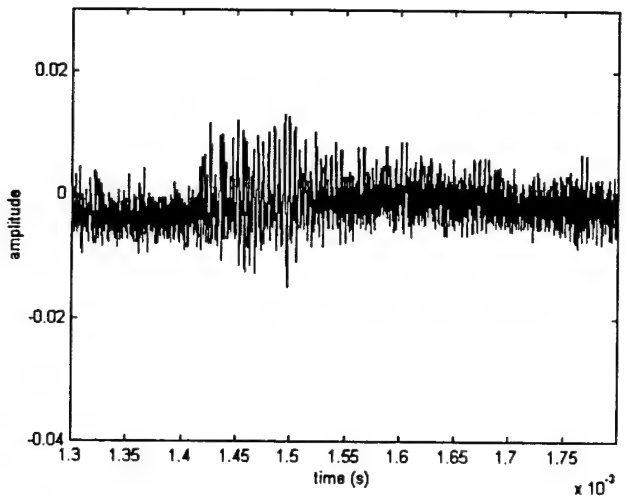

Figure 6(a) : Input to Eigenfilter Bank

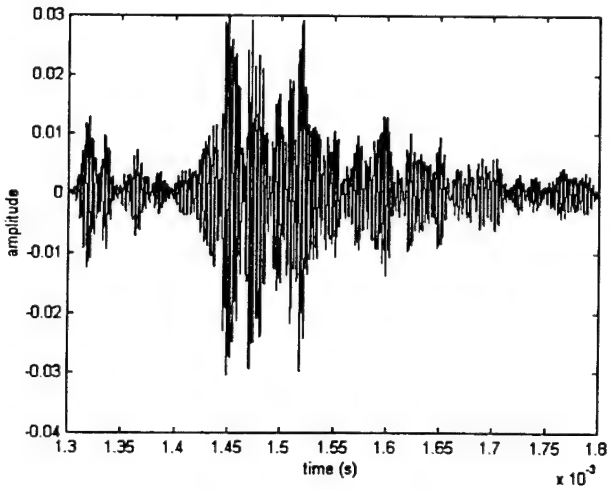

Figure 6(b) : Output of one channel of filter bank

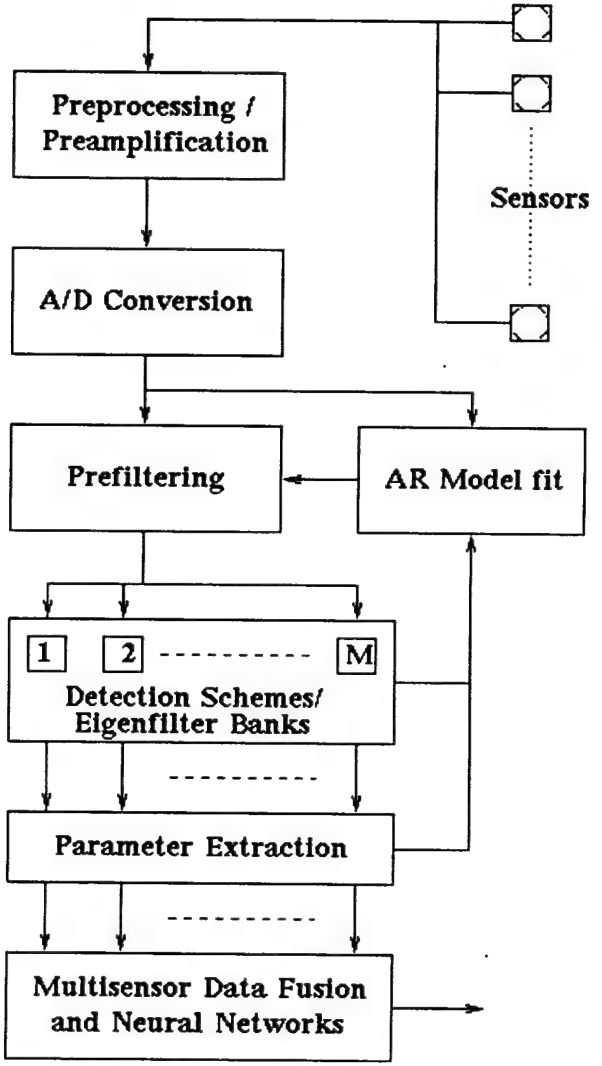

Figure 7 : Block Diagram of Proposed System

1.4.4 SENSOR INTERFACE CIRCUITS AND TELEMETRY

Co-Principal Investigator: R. Harjani (lead)
Students: J. Kim, K. Nair, C. Zillmer

DoD NEED

The goal of this activity is to develop sensor interface circuits and telemetry. The overall microelectronic sensor circuitry and telemetry is shown in Fig. 8. Acoustic waves and temperature are the inputs to the acoustic emission sensor and the temperature sensor respectively. The analog outputs from these sensors is then converted into digital using the analog-to-digital converter. The telemetry is RF circuitry which sends this information to a remote base station. _Jonghae Kim is working on the telemetry part of the system.

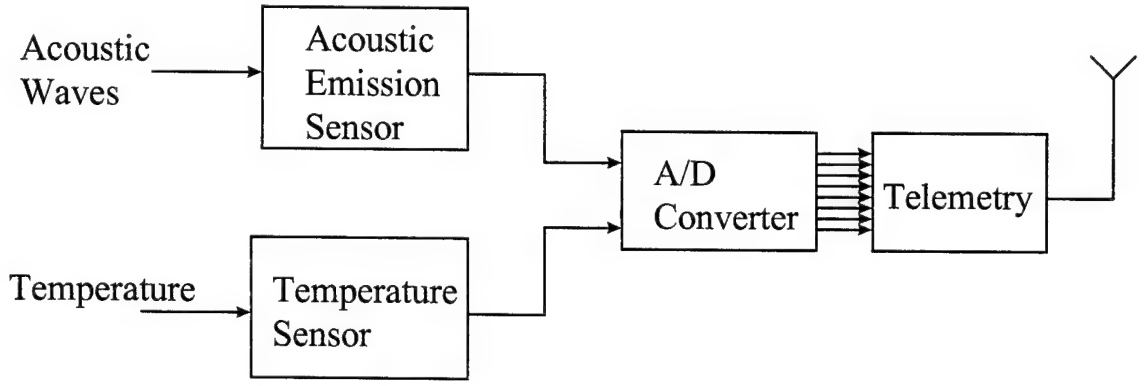

Fig. 8. Telemetry architecture.

PROJECT MISSION

The acoustic emission sensor system is made up of three main blocks namely, the piezoelectric sensor, the charge amplifier and the analog to digital converter as shown in Fig. 9. The sensor is a thin film piezoelectric which is being designed by the material science group at the University of Minnesota. The charge amplifier is used to convert this charge into appropriate voltage. The analog-to-digital converter converts this analog signal into a digital signal which can transmitted by the RF circuitry.

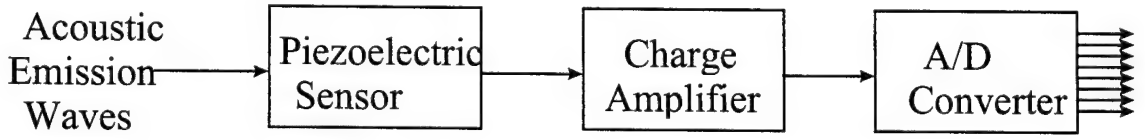

Fig. 9. Acoustic Emission Sensor System Block Diagram

CMOS-based telemetry circuits have been designed to local structural health information to a central receiving station such as in the cockpit of a helicopter. A block diagram for the telemetry system is shown in Fig. 10.

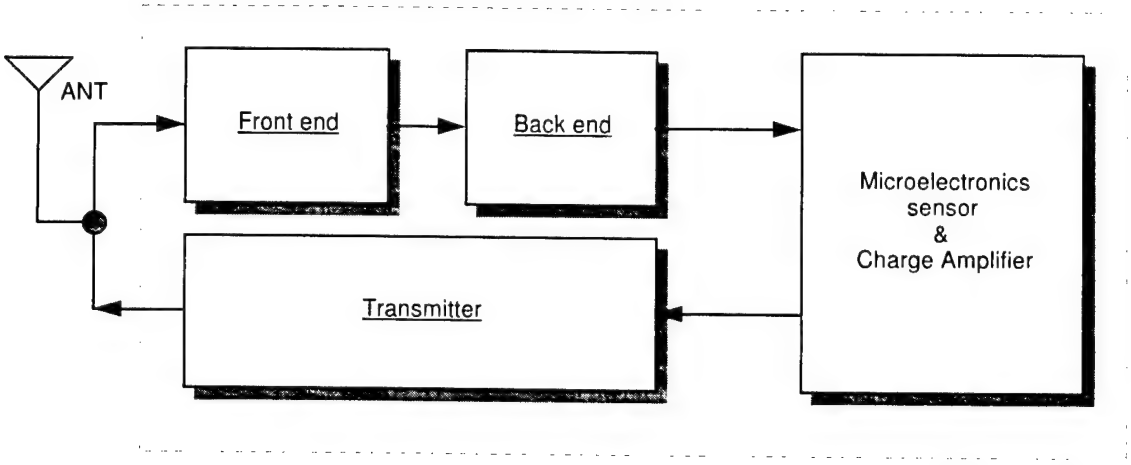

Fig. 10. Telemetry system block diagram.

RESEARCH ACCOMPLISHMENTS

The charge amplifier has been designed, implemented and fabricated in the 0.5u CMOS process. The charge amplifier was designed to have a bandwidth of 1.5 MHz and sensor capacitance of up to 25 pF. The charge amplifier has been tested and it gives satisfactory results. The analog-to-digital amplifier is currently being designed. The two requirements for this A/D converter is speed and resolution. Other important considerations are low power and minimal area.

A block diagram of the temperature sensor circuitry is shown in Fig. 11. The system consists of a temperature sensor, voltage reference, signal conditioning, and A/D conversion. The temperature sensor, voltage reference and signal conditioning circuits have been designed, fabricated, and tested individually. The A/D converter is currently being designed, and will be fabricated in April of 1998. After the A/D converter has been tested, the individual circuit blocks will be incorporated into the system shown in Fig 11. All of the described circuits are being fabricated in a CMOS 2μm process. Each cell is designed to occupy a small area while consuming very little power. The final output will be a digital 8-bit word which will correspond to the on-chip temperature.

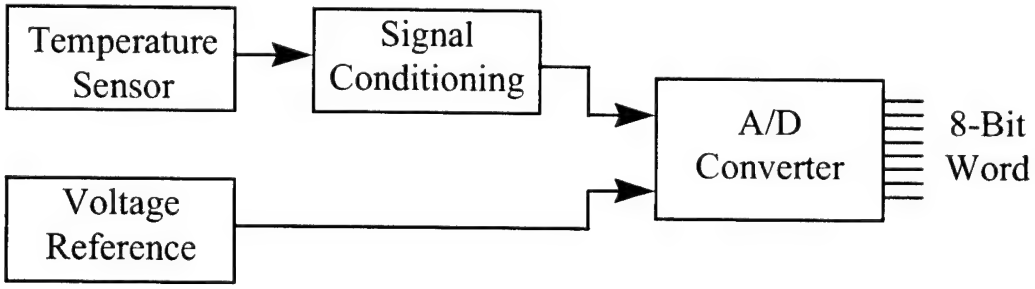

Fig. 11. Temperature Sensor System Block Diagram

An analog-to-digital converter has been designed and is currently in fabrication. The goal of this activity is to integrate the sensor, charge amplifier and the analog-to-digital converter into a single chip which will occupy small area and dissipate less power. Finally this system will have to be integrated with the temperature sensor and the telemetry system.

The telemetry portion is composed of three parts which are front end, back end and transmitter. It was fabricated by 0.5 um CMOS process and tested. The ASK (Amplitude Shift Keying) modulation scheme is used to both RX (Receiving path) and TX (Transmitting path) and it is connected to the microelectronics sensor and circuitry to carry detecting data to a base station. This system is able to communicate for distance's within 100 m.

The LNA has 25 dB gain at 950 MHz with off-chip inductor and its power consumption is 3 mW. The mixer works as a frequency down-converter with RX input signal and local oscillator. The AGC (Automatic Gain Control) works at 40 dB dynamic range. The transmitter portion works as an amplifier but we need more efficiency and gain.

M-URI PUBLICATIONS

K. Nair and R. Harjani, "An Ultra Low Power Transconductance Cell", ISCAS 1996.

Oyvind Birkeness "CMOS Circuits for Wireless Communication", Masters Thesis, University of Minnesota, July 1997.

K. Nair, C. Zillmer, R. Harjani, and D. Polla, "Data Acquisition and Conversion", Encyclopedia of Electrical and Electronics Engineering, John Wiley & Sons Inc.

2.1 *STRUCTURAL FATIGUE INVESTIGATION*

Project Coordinator: David L.McDowell (Georgia Tech)
M-URI Funding Allocation: 15.6%

PROJECT OVERVIEW

The mission of the Structural Fatigue Investigation project is to develop analysis and visualization tools to characterize the 3-D stress state in components, develop robust modeling approaches for growth of small cracks at hot spots in structures, conduct supporting studies to interrogate microstructure-property relations, to model growth of long, 3-D cracks in components, and to develop algorithms suitable for estimation of component remaining life. The class of applications relates to integrated prognostics for transport vehicles such as ships, helicopters, and machinery. To date, we have used helicopter rotor hubs as a means of technology demonstration.

The first three years of this project address the technology gaps that exist in the modeling of small cracks interacting with material microstructure, small cracks growing from notches and regions of contact (fretting), improved methods for visualization of 3-D stress states in components to identify "hot spots," calculation of crack driving forces for 3-D cracks, and characterization of the influence of material microstructure on physical fatigue processes (deformation and damage) for smooth specimens and cracked bodies are various scales, ranging from tens ofnanometers to hundreds of microns to component analyses.

Materials considered in the experimental programs included 4340 and PH 13-8 Mo SS, Ti-6Al-4V and 1045 and 304 SS. It is emphasized that the concept of integrated diagnostics/prognostics implies that given information regarding crack position and crack length, with a specified degree of certainty, the rate of growth of the crack(s) can be estimated at a level of accuracy suitable for ensuring that catastrophic failure will not occur before a maintenance decision can be made - all predominantly during active operation of the system. Mechanistically-based models are necessary to satisfy this objective. Addressing these basic science and engineering issues enables the technology necessary to conduct remaining life estimation based on sensor outputs. Basic research will continue in selected technology-enabling areas to assure technical feasibility of modeling various fatigue damage mechanism and characterization of fatigue damage at various length scales. In years 4-5, increasing attention will be devoted to the connection of progressive fatigue processes and sensor signals through experimental collaboration with NDI/NDE efforts within the MURI, as well as development of algorithm concepts that are suited for sensing and life prediction of components.

In the following sections, we highlight accomplishments to date according to tasks as listed below:

- Task I: Analysis and visualization of components.
- Task II: Characterization and modeling of fatigue damage.
- Task III: Algorithms for real-time prognostics.

2.1.1 STRESS AND FLAW ANALYSIS OF COMPONENTS

Co-Principal Investigator: Jianmin Qu
Graduate Student: Brian Gardner

DoD NEED

The stress analysis can provide detailed stress distribution on critical components in naval structures. Knowledge of the stress distribution is critical to identify "hot" spots on those components where failure is most likely to occur. The fracture mechanics studies can provide a predictive tool to estimate the crack growth rate which is essential to estimate the remaining life of such components.

PROJECT MISSION

I. Stress analysis of critical components
II. Fracture mechanics analysis of 3-D crack growth under complex loading conditions
III. Computer Simulation and Visualization of stress distribution and crack growth.

RESEARCH ACCOMPLISHMENTS

Three major objectives have been achieved. (1) Using the H-46 rotor hub as a case study, a finite element model was developed for stress analysis, see Fig. 1. Based on this calculations, "hot" spots in the rotor hub under normal flying conditions are identified. These predicted failure sites agree well with those observed at Cherry Point as indicated in Fig. 2. (2) A computer visualization program was developed for easy display of the stress distribution in complex components. As a demonstration, a video was made from this program to visualize the stress distribution in the interior of the H-46 rotor hub under various loading conditions. (3) A new algorithm is developed to calculate the individual stress intensity factors at a kinked-crack tip. The algorithm is based on the path-independent integrals of Eshelby. The methodology provides an easy and accurate method to predict the kinking direction and the mixed mode stress intensity factors at the kinked crack tip, which, in turn, will be used as a driving force in the crack growth calculation for remaining life estimation.

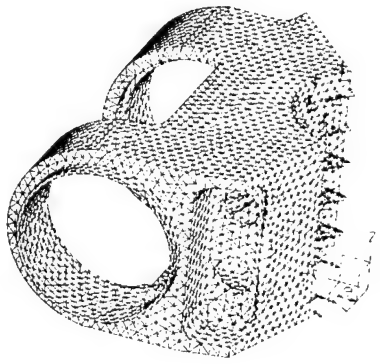

Fig. 1 FEM mesh of the H-46 rotor hub

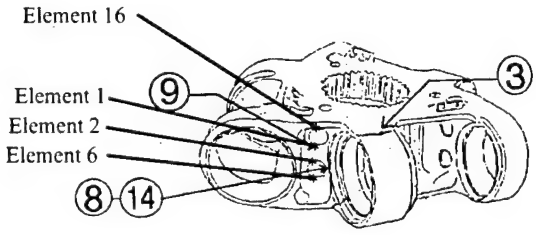

Fig. 2 Predicted and observed failure sites coincide

Research to date has shown that fatigue cracks do not grow self-similarly. They tend to become non-planar due to complex geometry and loading conditions. Therefore, in order to provide accurate information on fracture driving force for remaining life estimation, efficient computational algorithm is needed for 3-D non-planar cracks. Currently, no numerical method can do this. To meet this need, the superposition technique developed early in this project for kinking cracks will be extended to 3-D non-planar cracks in years 4 - 5. Major tasks to be carried out include

(1) Integrating this new algorithm into a commercially available finite element code (ABAQUS). Such integration will greatly speed up the technology transfer to the Navy.

(2) Crack growth under fretting fatigue will be used as a test vehicle to validate the computation algorithm.

(3) Making use of the crack-tip parameters calculated from this new algorithm, various available fracture criteria (maximum energy release rate, maximum mode I stress intensity factor, etc) will be compared and evaluated against experimental measurements.

Since this project is an integral party of the Structural Fatigue Investigation, the research will be closely coupled with other projects in the group. For example, numerical algorithms being developed here will be validated by experiments conducted by other co-PIs in the structural fatigue group. Crack driving forces calculated from this research provide the critical crack-growth information to remaining life estimation. Calculation of the driving force for crack growth also plays important supporting roles for other projects within the CID, such as the projects on statistical reliability analysis and AE monitoring of crack growth. As needs for interaction arise, other issues may also become important. It is expected that the numerical algorithms developed here will also add to the understanding of crack arrest, rogue flaws, multi-site cracking, etc.

In summary, the computational algorithms developed here will be one of the critical tools to be developed at the CID that enables the application of fracture mechanics to real-time diagnostics and prognostics of engineering structures and components.

M-URI PUBLICATIONS

McDowell, D.L., Neu, R.W., Qu, J. and Saxena, A., "Prognostic Tools for Small Cracks in Structures," submitted to ASME.

Gardner, B. and Qu, J., "A Numerical Technique to Calculate the Stress Intensity Factors for Cracks with Multiple Kinks," submitted to ASTM.

2.1.2.1 MODELING OF SMALL FATIGUE CRACK GROWTH UNDER MULTIAXIAL LOADING

Co-Principal Investigator: D.L.McDowell
Graduate Research Assistant: V. Bennett
Undergraduate research students: M.Kamel, T. Edwards, A. Bell

DoD NEED

To support prognostics for estimation of remaining life for cracks monitored at hot spots in components by (i) developing robust engineering models for microstructurally to physically small fatigue crack growth as a function of applied stress state and amplitude and (ii) understanding the influence of microstructure heterogeneity on the driving force and distribution of fatigue damage in metals.

PROJECT MISSION

Project objectives focus on supporting integrated prognostics by

- developing a framework for estimating remaining life to a given crack length that includes mixed mode growth, microstructure-crack interactions, diminishing influence of microstructure, and transition to physically small growth behavior with less microstructure influence;
- performing computational micromechanics studies of microstructurally small cracks to investigate stress state dependence on the cyclic microplastic strain distribution, free surface effects on constraint, and mixed mode crack opening displacement behavior;
- conducting combined axial-torsional experiments to validate prediction of amplitude and stress state sequence effects in alloys well-characterized under constant amplitude multiaxial loading conditions and to characterize behavior of 4340 steel & PH 13-8 Mo stainless steel; and
- coordinating the overall effort in the Structural Fatigue Investigation project of the ONR M-URI on *Integrated Diagnostics*, including interactions with sensor groups to make connections between evolution of signals in component hot spot locations and physics of accumulation of fatigue damage.

RESEARCH ACCOMPLISHMENTS

- Developed computationally efficient three stage model for small crack propagation based on a CTOD/CTSD extension of critical plane Stage I growth theory, including amplitude and stress state sequence effects, and applied it to small crack behavior of 1045 steel (publications: Int. J. Fract., Int. J. Fatigue, Fat.Fract. Engng. Mater. Struct.)
- Implemented crystal plasticity code implemented in ABAQUS UMAT and began work on novel micromechanical calculations involving distribution of microplastic strain and microstructure dependence of crack opening/sliding displacements as a function of crack length, forming the basis of the doctoral research of Ms. V. Bennett.
- Established an experimental protocol to conduct axial-torsional experiments to study naturally occurring small crack behavior in 1045 steel, 304 SS, 4340 steel and PH 13-8 Mo SS; conducted stress state sequence experiments on 1045 steel and 304 SS and initiated interactions with AE sensor groups on fatigue damage in smooth specimens.
- Guest-edited special issue of *Int. J. Fracture* on high cycle fatigue which appeared early in 1997; invited to lecture on modeling small crack multiaxial fatigue growth at Engineering Foundation Conference (Sept. 1996) and Engineering Against Fatigue in Sheffield, UK (March 1997); authored chapter on Multiaxial Fatigue in ASM Handbook in Dec. 1996; authored or co-authored four refereed journal articles, three conference articles, and one book chapter; presented two papers summarizing overall MURI effort and the Structural Fatigue Investigation mission, presented program objectives and accomplishments at the ASME IMEC&E Symp. on Quantitative Nondestructive Evaluation in Integrated Diagnostics held in Dallas in November 1997.

MODELING: 2-D Crystal Plasticity

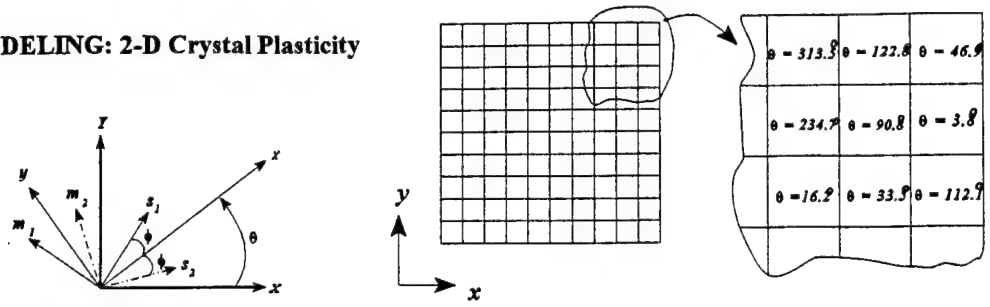

Configuration of the two slip systems (left) and 100 grain representation of the polycrystal (right).

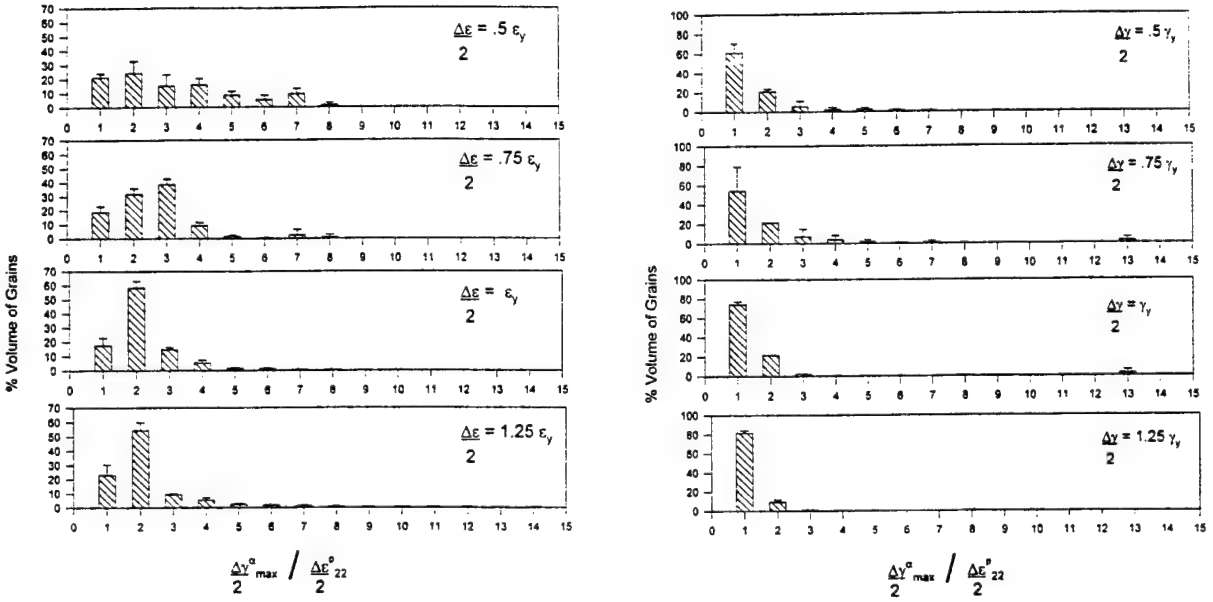

Distribution of cyclic microplastic shear strain among grains for tension (left) and torsion (right)

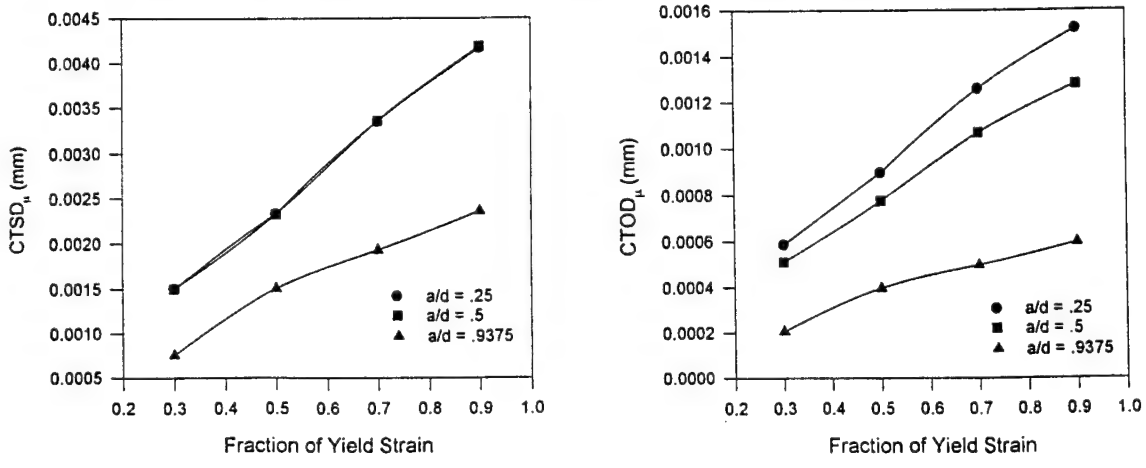

Crack tip sliding displacement (left) and crack tip opening displacment (right) as a function of applied polycrystal strain for Stage I crack in shear as a function of crack length over grain size

Three Stage Model - I (less than one obstacle spacing), II (from one to 3-10 spacings), III (physically long cracks)

$$\left(\frac{da}{dN}\right)_I = D_{aN}\psi A\psi^B\left(1 - \frac{a}{d}\right)$$

$$\left(\frac{da}{dN}\right)_{II} = D_{aN}\psi\left\langle\psi^r\left(\frac{a}{kd}\right) - D\right\rangle$$

$$\left(\frac{da}{dN}\right)_{III} = D_{aN}\psi\left\langle\psi^r\left(\frac{a}{kd}\right) - D\left(\frac{a}{kd}\right)^{1-Mr}\right\rangle$$

Generalization of Hobson-Brown framework based on fatigue limit due to grain boundary/obstacle blockage, where ψ is the driving force parameter from the critical plane multiaxial crack opening displacement approach of McDowell & Berard (1990, 1992), i.e.

$$\Psi_p = (1 + \mu\rho)\left(\beta_p(R_n)R_n + 1\right)\left(\frac{\Delta\tau_n}{2}\frac{\Delta\gamma^p_{max}}{2}\right)$$

Prediction of "anomalous" small crack behavior for 1045 steel in da/dN versus ΔK

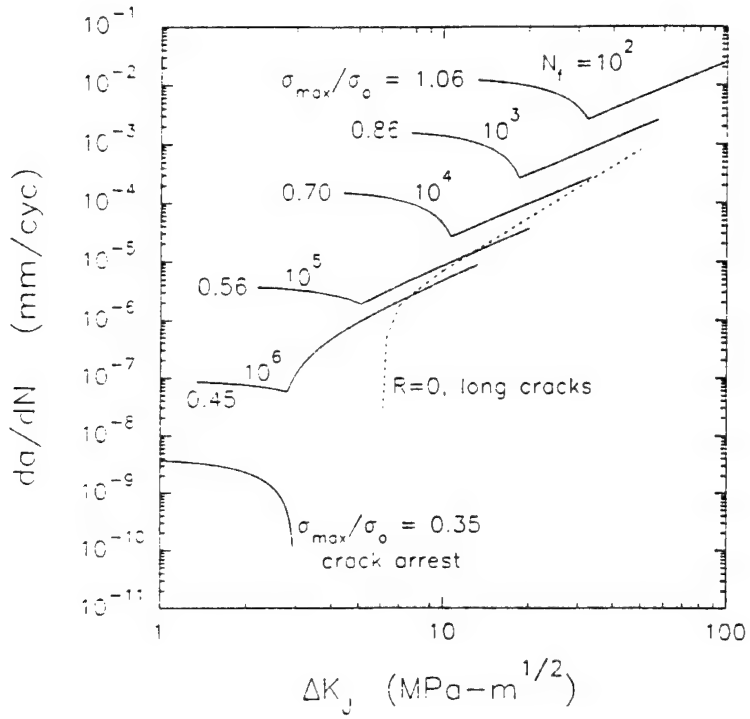

Year 4-5 plans: Computational micromechanics of small cracks will be pursued, along with embedding results into improved crack growth laws with material length scale dependence. Multiaxial fatigue experiments will be conducted on 4340 steel and PH 13-8 Mo stainless steel. Prognostic algorithms for real-time or near-real time applications will be pursued, including uncertainties of loading, inspection/monitoring and material behavior.

M-URI PUBLICATIONS

1. McDowell, D.L. and Bennett, V.P., "A Microcrack Growth Law for Multiaxial Fatigue," Fat. Fract. Engng. Mater. Struct., Vol. 19, No. 7, 1996, pp. 821-837.
2. McDowell, D.L., "Multiaxial Fatigue Strength," ASM Handbook, Vol. 19 on Fatigue and Fracture, ASM International, 1996.
3. McDowell, D.L., "Basic Issues in the Mechanics of High Cycle Metal Fatigue," International Journal of Fracture, Vol. 80, 1996, pp. 103-145.
4. McDowell, D.L., "An Engineering Model for Propagation of Small Cracks in Fatigue," Engineering Fracture Mechanics, Vol. 56, No. 3, 1997, pp. 357-377.
5. McDowell, D.L., "Mechanics of Small Fatigue Crack Growth in Metals," to appear in Int. J. Fatigue, 1997.
6. McDowell, D.L., "A Model for Multiaxial Small Fatigue Crack Growth," submitted for publication in Proc. of Engineering Against Fatigue, 17-21 March, 1997, revised April 1997.
7. McDowell, D.L. and Bennett, V., "Micromechanical Aspects of Small Multiaxial Fatigue Cracks," Proc. 5th Int. Conf. On Biaxial/Multiaxial Fatigue & Fracture, Cracow, Poland, 8-12 Sept., 1997.
8. McDowell, D.L, Neu, R.W., Qu, J. and Saxena, A., "Prognostic Tools for Small Cracks in Structures," Emerging Technologies for Machinery Health Monitoring and Prognosis, TRIB-Vol. 7, R. Cowan, Ed., ASME, 1997, pp. 1-12.

2.1.2.2 SMALL CRACK BEHAVIOR IN TI-6AL-4V

Co-Principal Investigator: W. Steven Johnson
Graduate Student: Richard Hamm

DoD NEED

Small-crack research has expanded from basic studies to aiding in the design of various types of structures and components because fracture mechanics methods have become widely accepted in damage-tolerant assessment procedures. In order to make structures durable and thus more cost efficient, very small cracks must be assumed in the analysis. This is especially true for aging aircraft, which are now expected to surpass their predicted service lives. In order to apply fracture mechanics to a design, all stages of crack growth must be known. Using fracture mechanics predictions is seen as a more deterministic approach than traditional S-N approaches, especially in relation to design evaluations. In addition, an emphasis must be placed on the small-crack regime because most cracks spend 70-90% of their fatigue lives as "small cracks". By investigating the behavior of small cracks in Ti-6Al-4V, more accurate predictions of service lives can be made for aircraft like the CH-53 helicopter, which uses Ti-6Al-4V for structural components in the engine housing.

PROJECT MISSION

The focus of the current research is to determine the behavior of small cracks under constant amplitude loading and under load interactions. In addition, a multi-regime small crack growth model comparison is being performed to determine which model gives the best overall constant amplitude fatigue life predictions up to a critical crack length defined by NDE crack size thresholds. Two of the models are based on microstructural formulations, two are continuum based and one model is empirical. An important part of the model comparison is to determine a characteristic microstructural length for input into the microstructural models. Determining this length is more difficult in Ti-6Al-4V than in most other engineering materials since Ti-6Al-4V has a two phase microstructure, whereas most engineering materials have only a single phase microstructure.

RESEARCH ACCOMPLISHMENTS

To this point, the small crack constant amplitude test matrix has been completed. The test matrix included four maximum stresses; 249, 263, 277 and 305 MPa at a stress ratio of .4. In order to determine the small crack behavior in Ti-6Al-4V in relation to the large crack behavior, two large crack tests have been performed. The results are shown in terms of the stress intensity factor range vs. crack growth rates in Figure 1 on the next page. In addition to this, constant amplitude small crack data has been obtained through AGARD at stress ratios of 0 and -1, with three different maximum stresses at each stress ratio.

Investigations into the microstructure have revealed bands of alpha and beta rich material. the bands have atypical width between 50-100 microns. Post mortem observations of etched crack surfaces has revealed that these bands roughly correspond to the points where the cracks have changed their direction of growth. This change in direction is referred to as the transition between Stage I and Stage II type growth and is usually associated with crack growth through the first 5-10 grains. Crack surface observations have shown that the transition in this Ti-6Al-4V is associated with the material bands and not with single grains.

The data gathered on the material microstructure and its interaction with crack growth was particularly useful for the modeling portion of the investigation. Specifically, the band widths found in the microstructure were input into the models as the characteristic microstructural length. The results from this can be seen in Fig. 2.

Because all but one of the models were formulated for the small crack regime, the models become invalid once the crack becomes "large". To overcome this, a modification is being proposed that can unify small crack models with large crack models. The modification will be implemented on one of the microstructural models in the comparison to gage its usefulness.

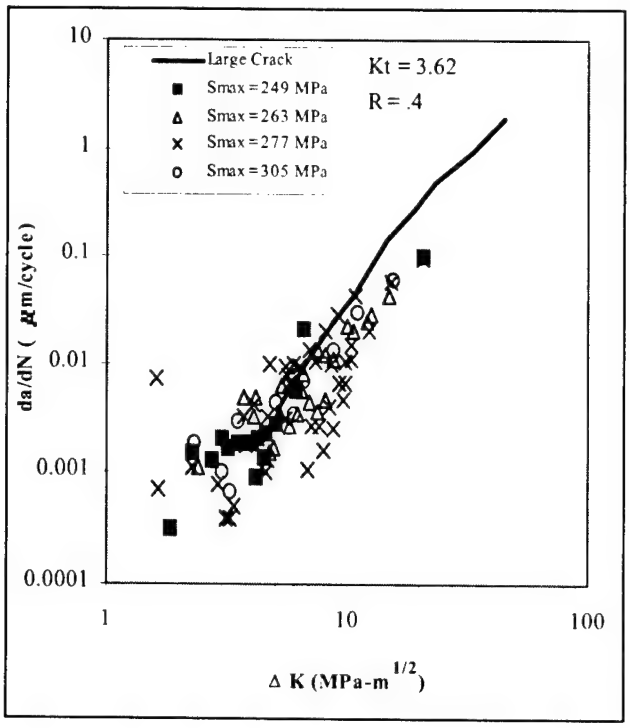

Fig. 1: Small crack behavior in Ti-6Al-4V.

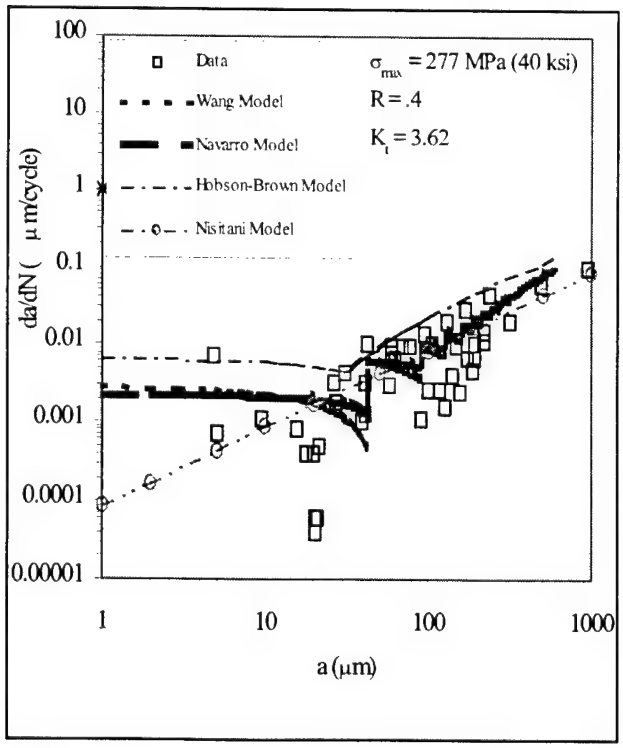

Fig. 2 A representative plot of model predictions.

2.1.2.3 FRETTING FATIGUE AND SMALL CRACK GROWTH

Co-Principal Investigator: Richard W. Neu
Graduate Students: A.M. Patel, (9/95 - 5/97); J.A. Pape, GRA (6/97 -)

DoD NEED

Fretting fatigue is a widespread phenomenon that occurs in a vast number of engineering components where two bodies are in contact and undergo a small oscillatory slip and at least one of the bodies is experiencing a bulk cyclic loading. Fretting fatigue is a widespread problem in navel structural components and is often the root cause of fatigue crack nucleation. Some examples include fasteners such as bolted, riveted, and clamped joints; press-fit components; keyways, splines, and dovetails; steel ropes and springs. Since it is often not feasible to eliminate fretting fatigue as a failure mode, the use of sensors at critical locations ("hot spots") where fretting fatigue cracks will grow is a viable option. However, to interpret the sensor signals under these conditions requires a better fundamental understanding of the stages of fretting fatigue and how they relate the sensor signals. A model that describes this damage evolution which includes crack nucleation and the growth of small cracks is needed for prognostics.

PROJECT MISSION

Fretting fatigue crack nucleation and early crack growth is characterized using both destructive and non-destructive methods to determine the stages of the fretting fatigue process. This research involves understanding the growth of small cracks under both plain (i.e., absence of fretting) and fretting fatigue conditions. These well-controlled tests are used as a test bed for emerging sensor technologies in both determining minimum damage size that can be detected as well as separation of damage from fretting and plain fatigue. This information is used to develop the next generation life prediction models for fretting fatigue crack nucleation and early crack growth. The materials under investigation include PH 13-8 Mo stainless steel and 4340 steel used in critical aerospace components (as in CH-46 helicopter).

RESEARCH ACCOMPLISHMENTS

Literature Survey - Prognostic Modeling for Fretting Fatigue:

An extensive literature survey of modeling methodologies that can be used to predict fretting fatigue crack nucleation and crack growth was conducted to determine the state of the art and directions for the next generation in modeling. Nucleation involves all the processes leading to the formation of a crack, typically of the order of 10 μm. The crack growth process describes the additional crack driving forces under fretting fatigue. The Fretting Fatigue Damage Parameter (Ruiz and Chen, 1986) is currently the most widely used model to predict fretting fatigue crack nucleation. It is an empirical model that has been shown to accurately predict the location of fretting fatigue cracks along a contact interface, but cannot account for differences in fretting fatigue behavior for different materials because of its lack of a physical basis. Next generation nucleation models may be based on multiaxial fatigue criteria, such as a critical plane approach (Socie, 1993), which can predict the direction of early crack growth as well as the nucleation location. These critical plane approaches can potentially bridge nucleation and fracture mechanics approaches. Detailed discussion is given in McDowell et al. (1997) and Pape (1997).

Small Crack Growth in PH 13-8 Mo Stainless Steel:

Before investigating combined fretting and fatigue loading, some basic studies of the fatigue crack growth behavior was needed as a baseline, especially on the PH 13-8 Mo stainless steel, which does not have an extensive published fatigue database. This included determining the fatigue crack growth behavior when subjected to high cycle fatigue at different mean stress. Most of this task focused on the small crack growth to determine the limit of the applicability of conventional fracture mechanics which is often used in remaining life prediction methodologies. Constants for long crack growth models

were also determined for this material. In addition, two fatigue crack growth models (Newman, 1981; Wang, 1996) for predicting the growth of small cracks were evaluated. The details are given in Patel (1997).

Fretting Fatigue of PH 13-8 Mo Stainless Steel:

A preliminary study of the fretting fatigue behavior of PH 13-8 Mo stainless steel was conducted. The design and implementation of a fretting fatigue testing apparatus proved quite successful in nucleating and propagating fretting fatigue cracks. The fretting fatigue testing apparatus developed for this investigation is unique in that it addresses the needs of both life prediction modeling and integrated diagnostics. The fretting fatigue test set-up is ideally suited for evaluating sensors and other crack growth monitoring techniques, due to the large area on the fatigue specimen where sensors can be attached. Many parameters which influence fretting fatigue behavior can be controlled, including the fatigue stress amplitude, mean fatigue stress, nominal relative slip amplitude, contact pressure distribution, normal contact load, and frequency of oscillation. Thus, this test set-up provides all of the experimental information required to evaluate current state of the art life prediction methods for crack nucleation and propagation under fretting fatigue.

The fretting fatigue tests performed at stress levels of 40% to 50% of the fatigue limit exhibited extremely short lives. Many interesting and significant observations have been made during this preliminary work (Pape, 1997) which will stimulate further research in years 4 and 5. For example, the evolution of the frictional force was monitored throughout the fretting fatigue tests. The general trend of a relatively quick increase during the first few hundred cycles (bedding-in), followed by a gradual decrease throughout the remainder of the test, was seen in most of the tests (Fig. 1). Furthermore, a sharp drop in the range of frictional force was observed near the end of the test. This drop has been correlated with the presence of a major fatigue crack in the specimen. It seems to be possible, based on the observations made, to use the frictional force evolution as a measure of the size of the fatigue cracks.

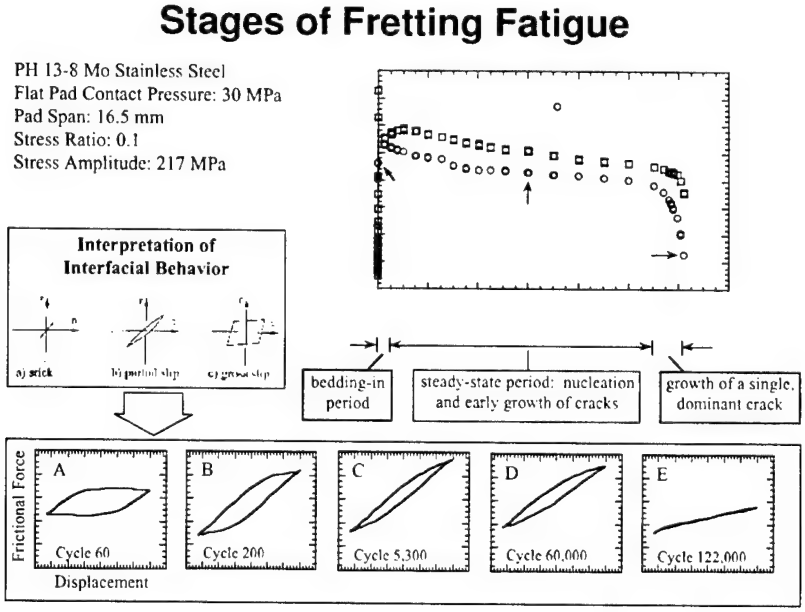

Fig. 1 Stages of fretting fatigue.

A great deal can be learned by monitoring the progression of fretting damage with sensors. Due to the extensive plastic deformation and numerous crack nuclei generated in the early stages of fretting fatigue, it may be difficult to detect the growth of very small cracks with sensors. Fortunately, the

evolutionary nature of the fretting fatigue damage may be more easily detected than cracks initiating naturally under plain fatigue. A preliminary comparison of the evolution of frictional force/displacement hysteresis with the frequency of acoustic emission events suggests it is possible to detect the characteristic changes during this evolution even when the fretting fatigue damage is not very extensive such as during the early stages of fretting fatigue damage accumulation

References:

Newman, J.C., 1981, "A Crack Closure Model for Predicting Fatigue Crack Growth Under Aircraft Spectrum Loading," *Methods and Models for Predicting Fatigue Crack Growth Under Random Loading*, ASTM STP 748, pp. 53-84.

Ruiz, C. and Chen, K.C., 1986, "Life Assessment of Dovetail Joints Between Blades and Disks in Aero-Engines," *Proc. Int. Conf. on Fatigue and Structures*, I. Mech. Eng., London.

Socie, D.F., 1993, "Critical Plane Approaches for Multiaxial Fatigue Damage Assessment," *Advances in Multiaxial Fatigue*, ASTM STP 1191, D.L. McDowell and R. Ellis, eds., pp. 7-36.

Wang, C.H., 1996, "Effect of Stress Ratio on Short Fatigue Crack Growth," *Journal of Engineering Materials and Technology*, Vol. 118, pp. 362-366.

M-URI PUBLICATIONS

Patel, A.M., "Growth of Small Fatigue Cracks in PH 13-8 Mo Stainless Steel," M.S. Thesis, Georgia Institute of Technology, May 1997.

Pape, J.A., "Design and Implementation of an Apparatus to Investigate the Fretting Fatigue of PH 13-8 Mo Stainless Steel," M.S. Thesis, Georgia Institute of Technology, December 1997.

McDowell, D.L., Neu, R.W., Qu, J., and Saxena, A., "Prognostic Tools for Small Cracks in Structures," *Emerging Technologies for Machinery Health Monitoring and Prognosis*, TRIB-Vol. 7, R. Cowan, Ed., ASME, 1997, pp. 1-12.

2.1.3 REMAINING LIFE PREDICTION

Co-Principal Investigators: A.Saxena and D.L.McDowell
Researcher: Fan Yang (Grad Student 3/95-6/96 and Post-doc 7/96-9/97)
Graduate Student: Laurent Cretegny (9/97-)

DoD NEED

The purpose of this task is to understand the damage modes and crack growth mechanisms in helicopter parts which are subjected to fatigue loading during normal service. The understanding developed will be used as an input for developing models for predicting the evolution of fatigue damage in 4340 steel used in the components of helicopter rotors. Such models are needed to predict the remaining life of components.

PROJECT MISSION

Over the past three years our efforts have focussed on (a) characterizing damage in a retired rotor hub (b) defining the technological requirements for a methodology for predicting the remaining life of helicopter parts subjected to fatigue loading (c) acquiring, heat-treating and characterizing the helicopter rotor material (d) conducting basic fatigue crack growth tests on the heat-treated material (e) exploring the nanoindentation and Atomic Force Microscopy (AFM) techniques for studying the fatigue damage evolution in 4340 steel.

RESEARCH ACCOMPLISHMENTS

From a detailed microstructural analysis of a retired helicopter rotor hub, it was determined that the depth of the fatigue cracks responsible for the retirement of the hub were limited to the protective chromium coating on the inner surface of the pin holes. Thus, the hub may have been retired prematurely.

Fatigue crack growth and initiation tests were conducted on 4340 steel in the quenched and tempered and in the annealed conditions. Large differences were found between the fatigue crack growth resistance of the annealed and quenched and tempered steels with the former micrstructure displaying significantly higher resistance to fatigue crack growth. In the annealed microstucture consisting of pearlite and ferrite colonies, the fatigue crack preferred to pass through the boundaries between the pearlite colonies when such boundaries were aligned normal to the loading direction (Fig.1a). Elsewhere, the crack grew at the cementite/ferrite interface. In the quenched and tempered steels, the fatigue cracks grew normal to the loading direction, even at the microscopic levels (Fig.1b). A microstructure consisting of a hard exterior shell to enhance fatigue crack initiation and a pearlite/ferrite interior may be able to enhance the fatigue lives of the rotor hubs. This should be explored in the future years 4 and 5.

It was shown that the nanoindentation technique potentially provides an effective means of characaterizing in-situ deformation properties of the constituents in the microstructure (Fig. 2). This should be of considerable benefit in understanding the relationship between fatigue crack initiation and growth resistance and the microstructure. In years 4 and 5, this technique will be developed further by varying the indent size according to the length scales of the constituents within the microstructure.

It was shown that Atomic Force Microscopy (AFM) is a powerful tool for examining and analyzing surface topography of fatigued specimens. It was successfully applied to quantitatively study the evolution of plastic slip bands during fatigue of 4340 steel. A direct correlation was established between surface roughness measured by AFM and the fraction of fatigue life expended (Fig. 3). These studies are very useful in studying the formation of small fatigue cracks and their interactions with microstructures, including cracks growing under fretting conditions. These aspects will be explored in years 4 and 5.

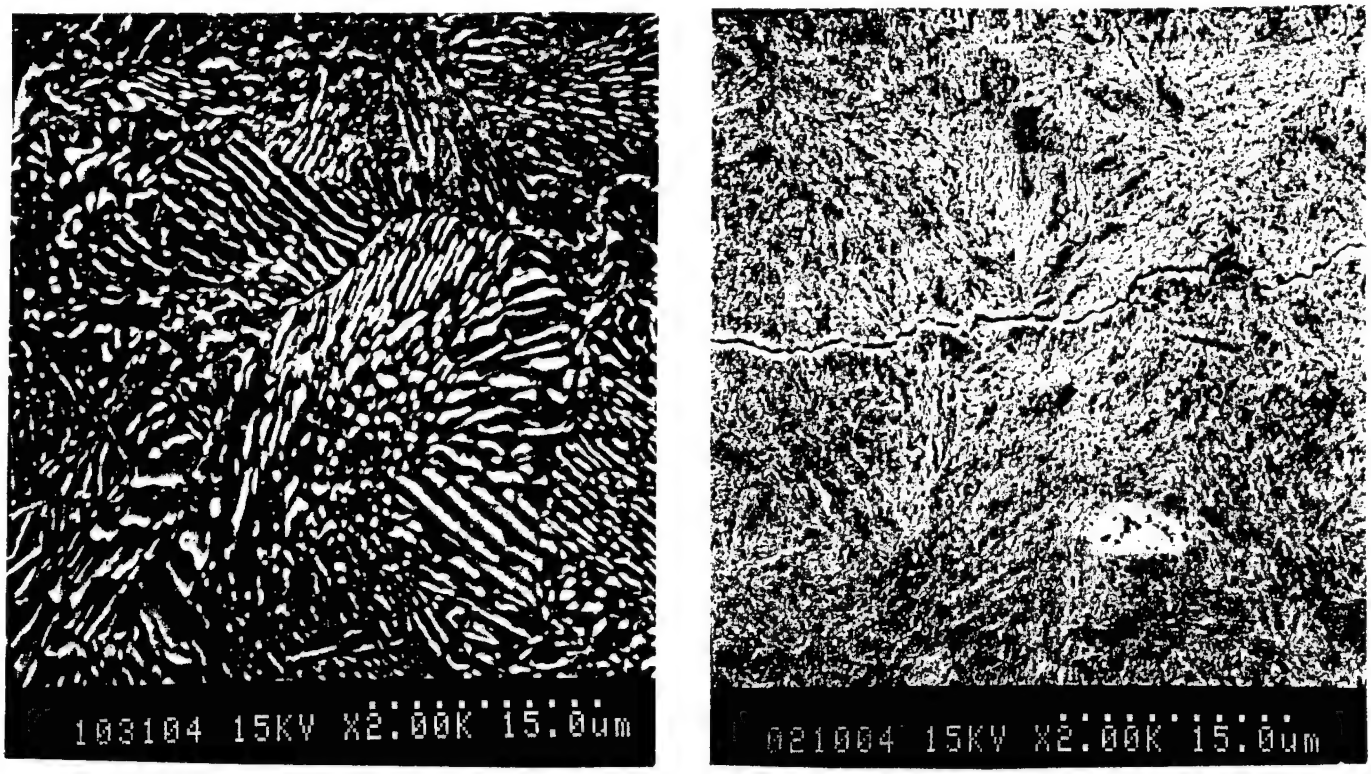

Fig.1 - Microstructure/fatigue crack growth path interactions in 4340 steel
(a) in annealed and (b) in quenched and tempered conditions.

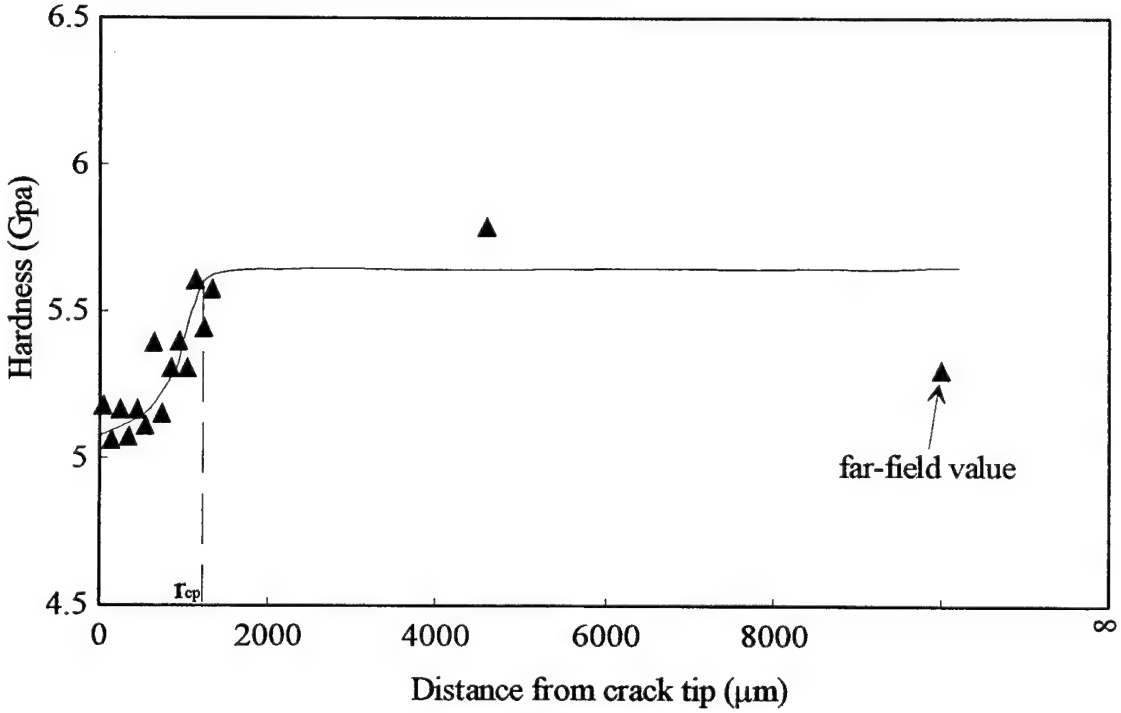

Fig. 2 - Nanoindentation hardness as a function of distance from the crack tip for a tested quenched and tempered 4340 steel fatigue crack growth specimen,
clearly resolving the cyclically softened region at the crack tip.

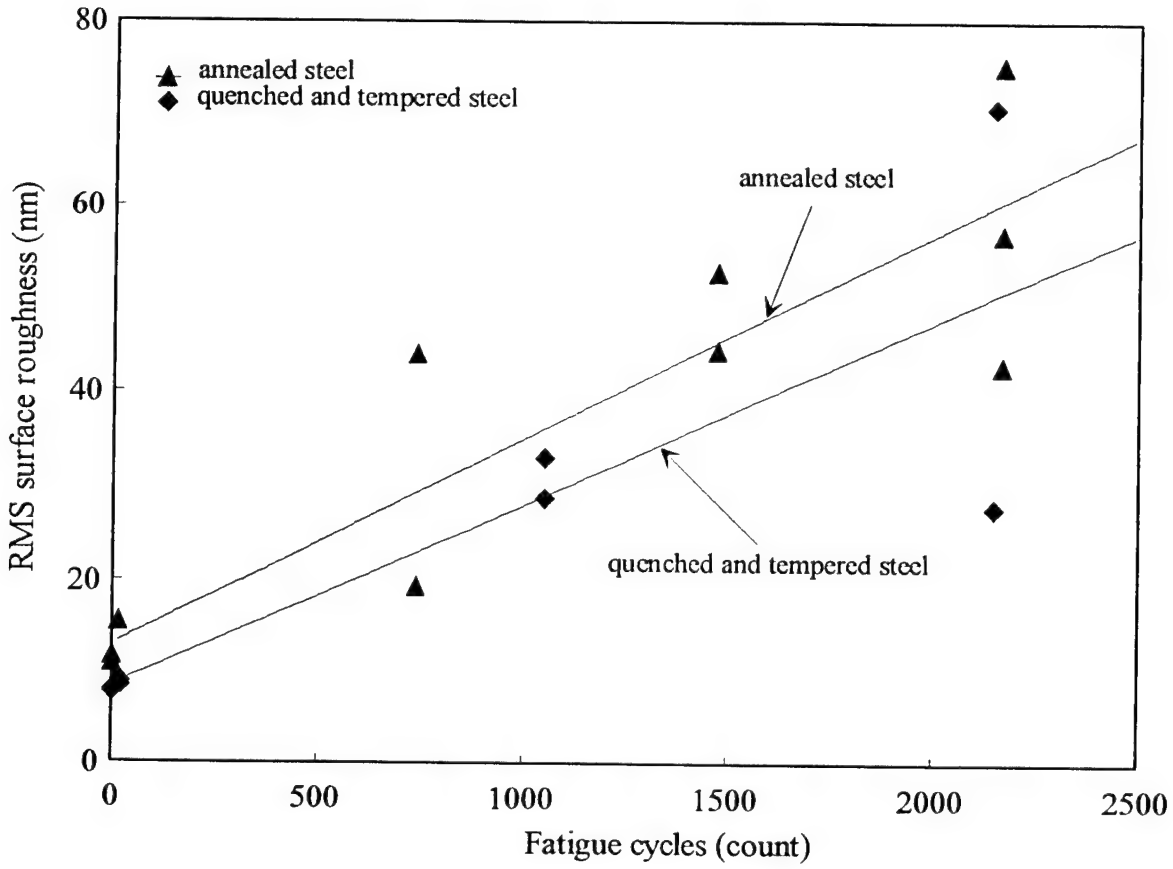

Fig. 3- Correlation between RMS surface roughness measured using the atomic force microscope (AFM) and the number of fatigue cycles at a total strain range of 1.5 %.

M-URI PUBLICATIONS

A.Saxena and C. Muhlstein, " Fatigue Crack Growth and Testing Applications", *Fatigue and Fracture*, ASM Handbook, Vol. 19, ASM International, Metals Park, Ohio, 1996, pp 168-184.

A.Saxena, "Fatigue Crack Growth in Elevated Temperature Power-Plant Materials and Components", *Proc.. of the Sixth International Conference on Fatigue*, Berlin, May 1996, Elsevier, pp729-740.

Fan Yang, A.Saxena and L. Riester, "Use of Nanoindentation Technique for Studying Microstructure/Crack Interactions in Fatigue of 4340 Steels", submitted to *Materials and Metallurgical Transactions*, Sept 1997.

Fan Yang and A.Saxena, " Use of Atomic Force Microscopy for Studying Fatigue Crack Initiation in 4340 Steel", Manuscript under preparation (90 % complete).

2.2 *FAILURE PREDICTION METHODOLOGY/FATIGUE RELIABILITY*

Co-Principal Investigator: Professor Brian Moran (Northwestern University)
Research Professor: Dr. Yonglin Xu
Graduate Student: Ali Zulfiqar
M-URI Funding Allocation: 2.8%

DoD NEED

There is a need for the development of computational tools for the simulation of complex aspects of structural reliability as an integral part of engineering life cycle design and, in particular,the design of fatigue critical components in ships, helicopters and rotating machinery.

PROJECT MISSION

To develop robust and accurate computational tools for structural reliability and for the modeling of crack growth in complex three-dimensional components.

RESEARCH ACCOMPLISHMENTS

Accomplishments in the two thrust areas of I) probabilistic fracture mechanics for fatigue reliability and II) computational simulation of fracture in three-dimensions are presented.

Methodology for Fatigue Reliability:

A new method, termed the Limit State Surface Element (LSSE) method, for problems in structural reliability has been developed. The first order reliability method (FORM) is a popular method for problems in fatigue reliability because the number of realizations or trials of the problem being simulated is vastly reduced over traditional Monte Carlo methods for example. This is especially true for cases where each trial involves computationally intensive simulations in three dimensions such as fatigue crack growth in complex components. A limitation of the method, however, is that it is inaccurate when the curvature of the limit state surface is large and this is often the case in fatigue reliability problems. In contrast, the LSSE method, which is based on the discretization of the limit state surface into a number of elements in the vicinity of the most probable failure point, allows for a better representation of the limit state surface in regions of high curvature. In Table 1, the results obtained using the LSSE method are compared with the exact solution and with those obtained by FORM for the case of a circular safe domain. As can be seen from the table, the LSSE method is extremely accurate for all radii considered. Accuracy in the FORM is poor when curvature is high (small radius). In Fig. 1, the results for elliptical safe domains of different aspect ratios (with one axis fixed at b=1) are shown. Results obtained using the LSSE method exhibit, as expected, a gradual increase in reliability as the length, a, of the remaining axis is increased. In contrast, the FORM gives only a constant value of 0.6826 corresponding to an infinite value of a. Additional applications of the method, including to problems in probabilistic fracture mechanics can be found in (Moran and Xu, 1997).

Table 1 Reliability for Circular Safe Domain (120 elements)

a	$1-P_{f_1}$(FORM)	$1-\hat{P}_f$(LSSE)	$1-P_f$(Exact)
0.5	0.6914	0.1175	0.1175
1.0	0.8413	0.3934	0.3934
1.5	0.9332	0.6752	0.6753
2.0	0.9772	0.8645	0.8646
2.5	0.9938	0.9560	0.9560
3.0	0.9987	0.9889	0.9889

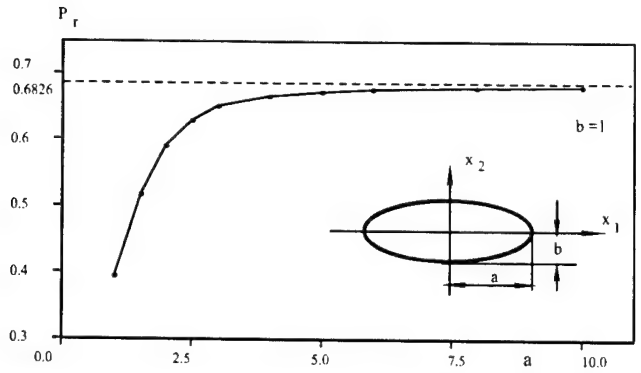

Figure 1 Reliability for an elliptical safe domain using the LSSE

Stress Intensity Factor Evaluation Along Curved, Non-Planar Crack Fronts:

New domain integrals for extracting mixed-mode stress intensity factors along non-planar cracks in three-dimensions have been developed. Domain integrals are used to represent J-integrals and other interaction energy type integrals for the evaluation of crack tip parameters in three-dimensional crack problems. Interaction energy integrals for extraction of mixed-mode stress intensity factors require the use of auxiliary fields based on the asymptotic crack tip solutions for the two-dimensional problem. Their use in three-dimensions introduces additional terms associated with the curvature (both in-plane and out of plane) of the crack front. We have formulated new domain integrals which account for these additional terms and have developed computational techniques for implementing them in finite element codes. An example problem is shown in Fig. 2 below. As can be seen from the finite element mesh, the crack is curved out of plane. Energy release rate and mixed-mode stress intensity factor results are shown in the table. As can be seen from the first column, the accuracy of the finite element (FEM) result for the energy release rate is very good. We have also solved problems consisting planar curvilinear crack fronts in 3-D and a spherical cap shaped crack surface in 3-D. For irregular crack surfaces, unstructured meshes are required. The domain integral method is currently being modified to account for unstructured tetrahedral meshes and for general representations of crack front curvature. This work is being prepared for publication.

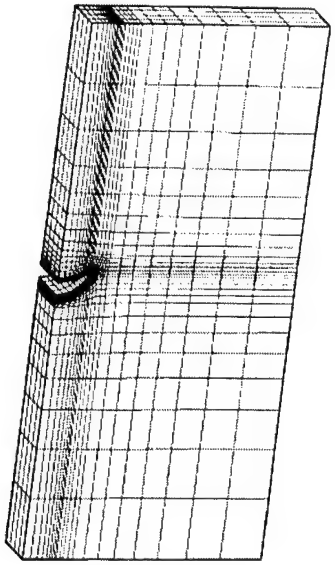

$\frac{G^{FEM}}{G^{analytical}}$	$\frac{K_I^{FEM}}{\sigma\sqrt{(\pi R\alpha)}}$	$\frac{K_{II}^{FEM}}{\sigma\sqrt{(\pi R\alpha)}}$	$\frac{G^{FEM}}{\frac{1-\upsilon^2}{E}\left(K_I^2+K_{II}^2\right)}$
0.998	0.53	0.59	0.996

Figure 2 Example problem

Future Work:

The limit state surface element method will be further developed as a robust computational tool for fatigue reliability. The domain integral method will be implemented for general out of plane cracks and will be applied to the simulation of mixed mode fatigue crack growth in three-dimensions. This will permit the evaluation of various proposed criteria for growth of cracks in both the small and large scale regimes and will provide a foundation for computational simulation of crack growth in life-cycle engineering design.

M-URI PUBLICATIONS

Achenbach, J., Moran, B., and Zulfiqar, A., 1997, "Techniques and instrumentation for structural diagnostics," in *Proc.of the International Workshop on Structural Health Monitoring*, Fu-Kuo Chang, ed., pp.179-190.

Moran, B. and Xu, Y., 1997, "Limit State Surface Element Method for Reliability Analysis," submitted for publication.

Moran, B. and Zulfiqar, A., and Sukumar, N., 1996, "On the Direct Integration Method for Fatigue Reliability Calculations," Technical Report to MultiUniversity Center for Integrated Diagnostics, Georgia Tech, July, 1996.

2.3 *ACOUSTIC EMISSION MODELING FOR INTEGRATED DIAGNOSTICS*

Co-Principal Investigator: Isaac M. Daniel (Northwestern University)
Post-docs: H.-J. Chun, C. G. Sifniotopoulos
Research Assistant: J.-J. Luo
M-URI Funding Allocation: 2.8%

DoD NEED

This project addresses the need to monitor in real time the condition of key components of naval systems, to detect and characterize critical flaws, monitor damage growth and provide input to life prediction modeling.

PROJECT MISSION

The objective of this project is to investigate and develop/adapt acoustic emission methods for detection and characterization of fatigue damage growth in metallic components.

RESEARCH ACCOMPLISHMENTS

Techniques were developed for monitoring acoustic emission (AE) activity during cyclic loading of notched metallic specimens. Spatial filtering techniques were implemented to suppress extraneous noise. Crack growth and AE activity were monitored independently and concurrently during fatigue loading.

Crack growth versus normalized fatigue cycles is independent of fatigue load amplitude, i.e., fatigue lifetime. Whereas crack growth increases smoothly with fatigue cycles, AE output shows jumps near the middle of the fatigue lifetime.

The phase of the loading cycle was identified as an important parameter in analyzing AE data. The AE output can be separated into three groups or regions according to the phase of the loading cycle in which it occurs (Fig. 1). AE signals in group A, corresponding to the end of the unloading cycle, are primarily associated with noise. AE activity in group B, occurring during the loading part of the cycles, takes the form of jumps and corresponds to crack opening and crack propagation. AE signals in group C, occurring near the end of the fatigue lifetime near the peak of the loading cycle, correspond to rapid crack propagation in the final stage.

In addition to analysis based on AE parameters, actual waveform data are being used to provide a more comprehensive approach to signal processing amenable to Neural Network analysis.

The pattern of AE activity, its waveform characteristics, and its loading phase distribution could provide a valuable indicator of "age" of a component and help prevent catastrophic failures. Future research will be directed towards quantitative correlation of AE and physical damage, assessment of "age" or condition and life prediction.

M-URI PUBLICATIONS

I. M. Daniel, J.-J. Luo, C. G. Sifniotopoulos and H.-J. Chun, "Acoustic Emission Monitoring of Fatigue Damage in Metals," *Review of Progress in Quantitative Nondestructive Evaluation,* vol. 16, ed. by D. O. Thompson and D. E. Chimenti, Plenum Press, New York, 1997, pp. 451-458.

I. M. Daniel, J.-J. Luo, C. G. Sifniotopoulos and H.-J. Chun, "Acoustic Emission Monitoring of Fatigue Damage in Metals," *Nondestr. Test Eval.,* 1997, pp. 1 - 15.

I. M. Daniel, C. G. Sifniotopoulos and J.-J. Luo, "Analysis of Acoustic Emission Output from Propagating Crack," to be published in *Review of QNDE*, vol. 17, ed. by D. O. Thompson and D. E. Chimenti, Plenum Press, New York, 1998.

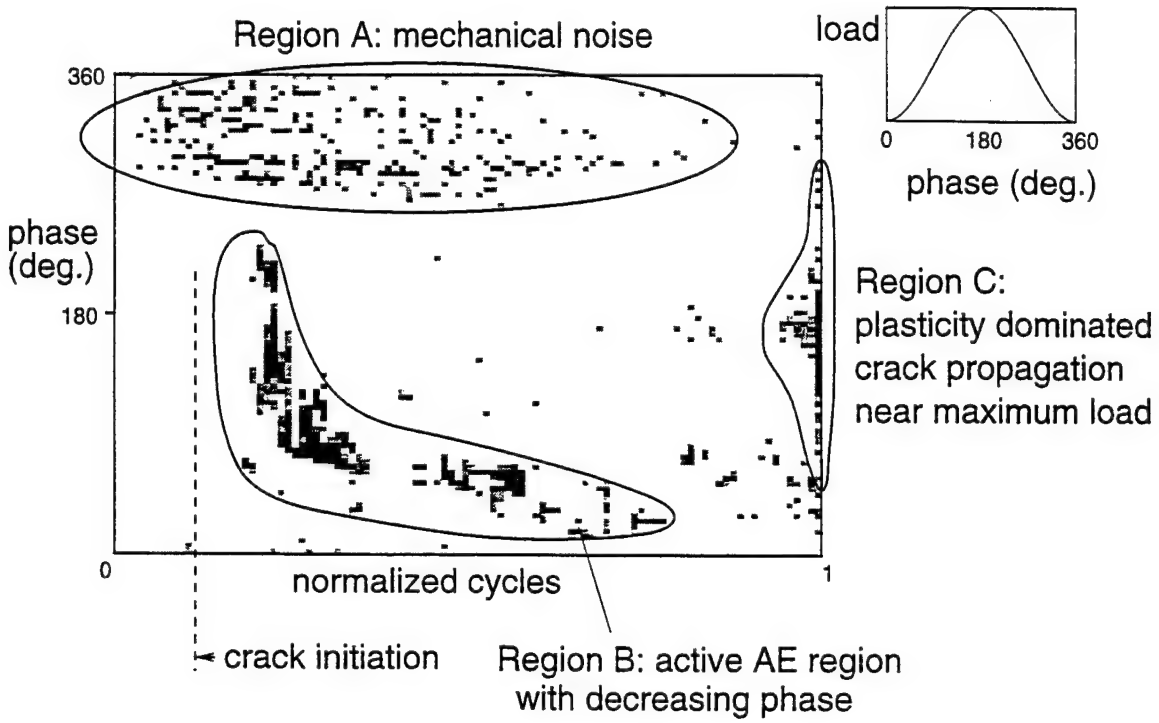

Figure 1 Loading Phase Distribution and Grouping of AE Activity
(4340 Steel; Compact tension specimen)

2.4 *STUDY OF ACOUSTIC EMISSION AND TRANSMISSION FROM INCIPIENT FATIGUE FAILURE*

Co-Principal Investigators: Laurence Jacobs, Jacek Jarzynski, Scott Bair (Georgia Tech)
Graduate students: Zhiqiang Shi, Maxim Koutsak and Brad Beadle
M-URI Funding Allocation: 4.5%

DoD NEED

(a) Catastrophic failure of an in-service, structural component can be prevented if small cracks can be identified and arrested before they propagate into large cracks. As a result, it is necessary to develop a technique that can accurately detect and characterize any small cracks that may exist in complex, in-service components; such an ability is a critical step towards developing a methodology for quantitatively predicting remaining service life.

(b) Successful implementation of the detection technique described in (a) requires the development of ultrasonic sensors (for acoustic emission and transmission) which are capable of improved discrimination against environmental noise and reverberation.

PROJECT MISSION

The goals of this research are to:

(a) develop passive, acoustic emission (AE), and active, ultrasonic transmission, techniques that can quantitatively locate and characterize small cracks in complex engineering components.

(b) develop two new ultrasonic receiving transducer designs: (1) an array of piezoactive ceramic (PZT) elements, and (2) an optical fiber sensor designed to measure tangential (in-plane) surface strains.

RESEARCH ACCOMPLISHMENTS

This research is working to develop quantitative, waveform based, acoustic techniques that can identify small cracks in complex engineering components. This work has realized an understanding of the acoustic source characteristics of a crack propagation event, successfully discriminating these source signals from ambient environmental noise. This work uses a combination of: an understanding of the mechanics of a crack propagation event, consideration of the physics of wave propagation in a complex component, and the application of innovative sensors, to accomplish this task. A unique feature of this investigation is the ability to experimentally capture and characterize complete acoustic waveforms, in real time.

Experiments have been performed to quantitatively determine and characterize the waveform characteristics of acoustic emission signals from a variety of fracture sources. These fracture sources include fatigue crack growth events (Mode I, II and mixed mode) as well as other sources of micro-damage. This work uses a four channel data acquisition system that captures and digitizes the entire acoustic emission waveform. Laboratory specimens examined include a notched tension specimen as well as a circular torsion fatigue specimen. The measured acoustic emission waveform characteristics (such as amplitude and frequency spectrum) are correlated with the observed crack growth.

The first set of experiments monitors crack growth, acoustic emission signals from a tension-tension fatigue specimen; the source of these signals is mode I crack propagation, emanating from a starter notch. Next, this procedure is repeated with a tension specimen that has fretting pads which cause acoustic signals (similar to a "crack source") from the interaction of the fretting pads with the specimen. An advantage of this configuration is that crack propagation signals are generated at later stages of the loading history, enabling comparison with the fretting signals observed in the initial loading stages. The third set of experiments monitors acoustic emission signals during a torsion fatigue experiment. By conducting these three distinct sets of experiments, each of which generates acoustic emission signals from a variety of different damage mechanisms, it is possible to isolate and identify the source that created a particular, experimentally measured acoustic emission waveform.

As a specific example of the correlation between acoustic measurements and fracture phenomena, the torsion fatigue tests show three distinctive regimes of crack growth: uniform growth (and

distribution) of small, sub-grain sized cracks; growth of these micro-cracks across grain boundaries; and finally coalescence of these cracks into localized cracks. The experimentally measured acoustic results match extremely well with the fracture phenomena observed, also showing three distinct regimes of both frequency of acoustic emission waveforms observed (number of acoustic events) and waveform type (waveform characteristics such as frequency content), which exactly correspond to the three regimes of crack growth.

Additional failure characterization work completed includes the development of transfer functions that remove extraneous geometric effects from a measured acoustic emission signal, and as a result, can help to isolate and identify the contribution from a damage source. Other work involved field measurements on a ground based helicopter platform (rotors revolving, but not engaged) to determine the influence of environmental noise under operating conditions. A final set of measurements used active acoustic transmission techniques (and the same set of "passive" sensors) to quantify localized crack distribution in the torsion specimen present in the final stages of fatigue. These active measurements are being extended to examine distributed micro-crack damage present in the first stages of loading.

Ongoing research is working to correlate specific waveform characteristics with the exact fracture feature which caused it; this is the next step in developing a prognostic technique. As an aid to this correlation, theoretical point source models are being used to predict frequency content of measured acoustic emission waveforms, to enable a more accurate comparison. Other research efforts can examine these fracture phenomena in more complex structural components as a more realistic test of the robustness of the proposed technique.

As part of the new sensor development, two transducer arrays have been assembled. A commercial array with PZT-plastic composite elements, from Material Systems, and an array with miniature (2mm x 2mm) PZT elements, were assembled in-house and testing of the above arrays is underway. The advantage of the array sensor is that it can be phased to respond to signals from a specific source direction, and reduce the response to reverberation due to echoes from various boundaries. Both arrays are broadband, operating over a frequency range of 100 kHz to 4 MHz.

A new design for an optical fiber sensor has been developed. This sensor has been assembled and tested, and the initial results are very promising. This new sensor is designed to measure in-plane surface strains and, therefore, discriminates against environmental noise which produces mainly out-of-plane surface vibrations. The optical fiber sensor is narrowband. It can be designed for a frequency in the range 200 – 700 kHz. The minimum displacement which can be detected with this sensor is estimated to be ~ 5 x 10-14 meters. An additional advantage of this sensor is freedom from electromagnetic pickup.

The next stage of research for the array sensors are tests and optimization of performance on a complex machinery component, such as the rotor assembly of a helicopter. The next stage of research for the optical fiber sensor is the development of a robust design which can be used in-situ on complex machinery. This design could be tested in the field, for example on the bulkhead of a helicopter.

M-URI PUBLICATIONS

Hurlebaus, S., Jacobs, L.J. and Jarzynski, J., "Laser Techniques to Characterize the Effect of Geometry on Acoustic Emission Signals," *Nondestructive Testing and Evaluation*, accepted for publication, 1997.

Hurlebaus, S., Jacobs, L.J. and Jarzynski, J., "Optical Techniques to Develop Transfer Functions to Remove Geometric Features in Acoustic Emission Signals," *Review of Progress in Quantitative Nondestructive Evaluation*, Vol. 16A, pp. 421-426, 1997.

Shi, Zhiqiang, Koutsak, M., Bair, S., Jarzynski, J. and Jacobs, L.J., "Characterization of Acoustic Emission Signals from Fracture Events," *Review of Progress in Quantitative Nondestructive Evaluation*, to appear in Vol. 17.

3.1 CRACK DETECTION BY ULTRASONIC GUIDED WAVES

Co-Principal Investigators: Yves Berthelot, Laurence Jacobs, Jianmin Qu (Georgia Tech)
Post-doc: G. Liu
Graduate Students: Z. Li, C. Valle
M-URI Funding Allocation: 6.8%

DoD NEED

A recurring problem in many mechanical systems is the failure of annular components, such as collars, caused by radial cracks on their inner walls. Unfortunately, it is often impossible to detect these cracks by either standard ultrasonic inspection techniques or by visual inspection; this shortcoming is a critical missing link in determining remaining life and structural integrity of a mechanical system. As a specific example, there are a number of critical annular components in Navy helicopters (e.g., CH-46) such as the pitch shaft and rotor hub. Radial cracks tend to initiate at the inner wall of the shaft-bearing assembly. The guided wave technique developed here will assist the early detection of such radial cracks.

PROJECT MISSION

The goal is to develop a robust nondestructive method using ultrasonic guided waves to detect and localize radial cracks in annular components of mechanical structures.

RESEARCH ACCOMPLISHMENTS

The major focus for the past three years has been to lay the ground work for developing ultrasonic guided wave techniques to detect cracks in mechanical structures. Using annular components as examples, both experimental and analytical studies were conducted to understand how ultrasonic guided waves propagate and interact with structural defects (e.g., cracks) in such annular components.

Analytical and numerical studies based on the mode expansion method and the finite element method have identified some unique characteristics of the guided circumferential waves in an annulus. These include the dispersion relationships, the displacement profiles across the wall thickness and the transient response of the scattered fields. These findings are significant in several ways. First, they enable us to interpret the measurement results to identify the crack and its location. Secondly, they provide guidelines for designing the sensors and for selecting sensor locations strategically for optimal crack detection. Thirdly, and more importantly, they could help us develop predictive models for remaining life estimation, which will be the main goal for the next two years.

Experiments have been performed on (a) ideal rings with and without EDM notches of various sizes, and (b) on the pitch-shaft of the H-46 helicopter with and without cracks. It has been demonstrated that guided ultrasonic waves can be used to detect inner radial cracks either in a pitch-catch arrangement (two transducers) or in the pulse-echo mode (one transducer). Cracks of 1 mm in length have been detected with a 2.25 MHz transducer. A key element in the successful detection and localization of the defects is the implementation of a new methodology based on integrating the magnitude of the wavelet transform of the signal over both a sliding time window and the finite bandwidth of the transducer. (See Fig. 1).

In summary, three objectives have been accomplished: (1) it has been demonstrated that ultrasonic guided wave is a viable technique to detect cracks, (2) a methodology to design the detection system based on this guided wave concept has been developed, (3) a prototype of such detection system has been constructed for laboratory use.

Obviously, we need to further improve the current system both in terms of hardware and software so that the technology can be extended one step closer to field applications. The software improvement will be primarily based on finite element analysis of more complex crack and component geometries. The hardware improvement will include optimization of the sensors (types, position, coupling to the structure, etc.).

Typical fatigue crack growth consists of several distinctive stages as shown in Fig. 2. Generally speaking, the detection system described above is able to identify the size and location of the crack. However, for prognostics purposes, one needs to specify at what stage the crack growth is and what the remaining life might be. This will be one of our major focuses for the next two year. It is driven by the ultimate goal of providing information on remaining life through nondestructive evaluations. As shown in Fig. 3, fatigue crack faces typically are rough with crack face contacts. The crack tips are usually accompanied by either a small plastic zone or a zone of micro-cracks. Because of the small feature size in comparison with the wavelength used in practical applications, linear ultrasonic is unable to discriminate the different features of the fatigue crack. However, nonlinearity in the scattered wave fields is generated by the geometrical (partial contact) and material (plasticity) nonlinearity. By measuring the magnitude of the nonlinear parameter (e.g., higher order harmonics) in the scattered fields, one can then associate such nonlinear parameters with the different features of the fatigue cracks. This will allow identification of the crack growth stage and provide information on the remaining life of the component.

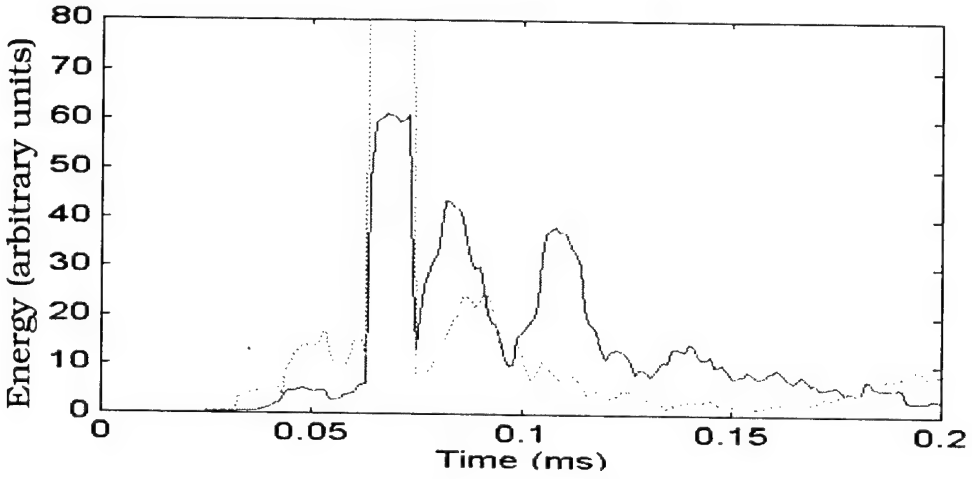

Figure 1a. The signal energy in frequency band of 2.0 to 2.5 MHz and time duration of 0.01 ms(solid line: with 3.0mm crack, dotted line: without crack).

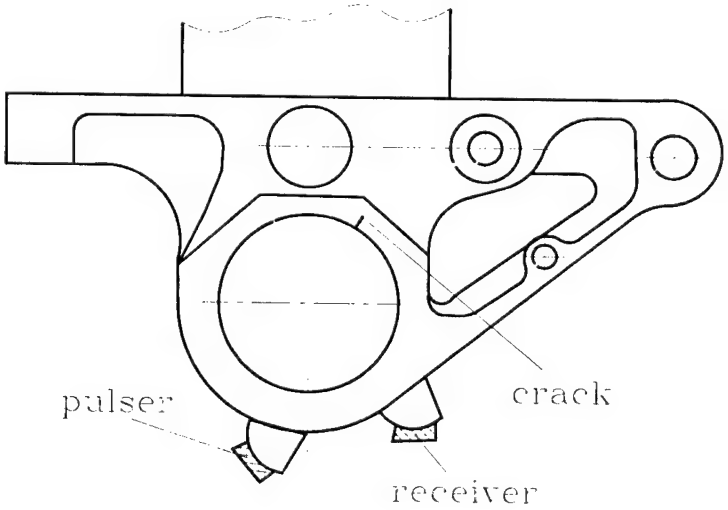

Figure 1b. Geometry of the pitch shaft and experimental setup of the pitch-catch testing.

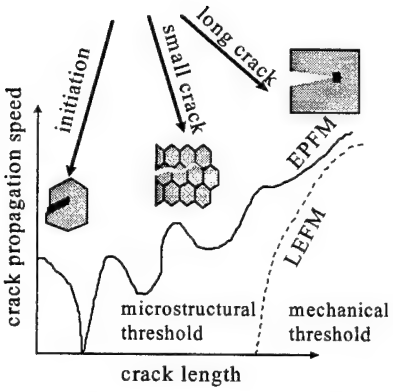

Fig. 2 Stages of crack growth

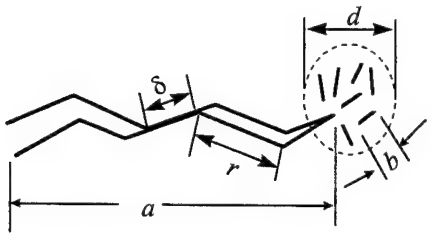

Fig. 3. A Typical fatigue crack

M-URI PUBLICATIONS

Liu, G. and Qu, J., "Guided Circumferential Waves in a Circular Annulus," *J. Appl. Mech.*, to appear.

Liu, G. and Qu, J., "Transient Wave Propagation in a Circular Annulus Subjected To Impulse Excitation on Its Outer Surface," *J. Acoust. Soc. Am.*, submitted.

Moser, F., Valle, C., Jacobs, L.J., and Qu, J., "Modeling of Guided Waves in Annular Components," *Review of Progress in Quantitative NDE, Review of Progress in Quantitative NDE*, to appear.

Moser, F., Jacobs, L.J. and Qu, J, "Application of Finite Element Methods to Study Wave Propagation in Wave Guides," *NDT & E Int.*, submitted

Liu, G. and Qu, J., "Guided Wave Propagation in Annulus Components," *Review of Progress in Quantitative NDE, Review of Progress in Quantitative NDE*, to appear.

Qu, J. and Liu, G., "Effect of Residual Stress on Guided Waves in Layered Media," *Review of Progress in Quantitative NDE, Review of Progress in Quantitative NDE*, to appear.

Qu, J., Berthelot, Y., and Li, Z., "Dispersion of Guided Circumferential Waves in a Circular Annulus," *Review of Progress in Quantitative NDE, Review of Progress in Quantitative NDE*, Vol. 15, p. 169-176, 1996.

Z. Li and Y. Berthelot, "Mode Control of Ultrasonic Guided Waves for Crack Detection in Thick Cylinders," 131st Meeting of The Acoustical Society of America, Indianapolis, IN, 13-17, May, 1996.

Z. Li and Y. Berthelot, " An Experimental Study of Crack Detection in Annular Component by Ultrasonic Guided Waves," *Review of Progress in Quantitative NDE, Review of Progress in Quantitative NDE*, to appear.

3.2 *LASER-BASED ULTRASONICS FOR INTEGRATED DIAGNOSTICS*

Co-investigators: J. D. Achenbach, A. Kromine, P. Fomitchov, S. Krishnaswamy (Northwestern)
M-URI Funding Allocation: 5.1%

DoD NEED

Naval helicopter structures may suffer cracks or other defects at locations that are not accessible for in-service visual inspections. In this work ultrasonic waves are used to detect such flaws without disassembly. One particularly attractive method of generating and detecting ultrasonic signals is by the use of laser-based techniques. Laser-based ultrasonics (LBU) methods provide a number of advantages over conventional ultrasonic techniques (non-contact, higher spatial resolution, curved surfaces applications, hard-to-access areas, ability to generate both narrowband and broadband ultrasound, scanning ease, ability to operate at high temperature and in a hostile environment). Fiber delivery is the most attractive feature of LBU for practical use. Fiber delivery allows access even to internal components, requiring only enough space for the passage of optical cables (i.e. a few millimeters in diameter).

PROJECT MISSION

The objectives of this study are:
- to develop an ultrasonic technique for the in-situ detection and characterization of flaws in components of complicated structures without disassembling or physically touching the component.
- to design portable, reliable and completely fiberized non-contact ultrasonic devices for field applications.

RESEARCH ACCOMPLISHMENTS

The experiments carried out in the first two years have demonstrated the advantages of laser generation of ultrasonic waves. Both narrowband and broadband generation were performed in laboratory conditions using a Q-switched Nd:YAG laser with both conventional optical elements (free-space generation) and a fiber delivery system. For comparison a piezo-electric transducer (PZT) was also employed as the ultrasonic detection unit. Non-contact detection of ultrasound using various types of interferometers was also investigated. A fiberized Sagnac interferometer having significant advantages in terms of flexibility, small size, relative simplicity and low cost was chosen as the prototype for the detection part.

A compact laser system for ultrasound generation with a flexible fiber delivery based on a Big Sky Laser was designed, manufactured and tested (see Figure 1). This Nd:YAG laser system is portable (18" x 3.6" x 3.7" head, 18" x 12" x 10" electronics/cooling system, 55 lbs total weight), has a low power consumption, can provide better beam quality than a previously used laser and does not require an external cooling source.

Several variants of the fiber delivery bundle and the focusing output head were designed and investigated. A single line thermoelastic source was used for generation of bulk ultrasonic waves. A fiberized Sagnac interferometer was used for the detection of ultrasound. It was found that the Sagnac interferometer can detect body waves which can be used to search for internal flaws and nonuniformities in solid bodies. A single thermoelastic line source was also used for generation of guided ultrasonic waves to check their use for crack detection in annular components (in co-operation with Georgia Tech Professor Berthelot's group). It was shown that it is possible to detect a reflection from artificial notches of 1.5 mm depth on the inner surface of 0.5" thick ring using only the outer surface to generate (by laser) and detect (by PZT) ultrasound. The possibility of using the fiberized Sagnac interferometer for detection of guided waves was also investigated, but further work in this direction will be required.

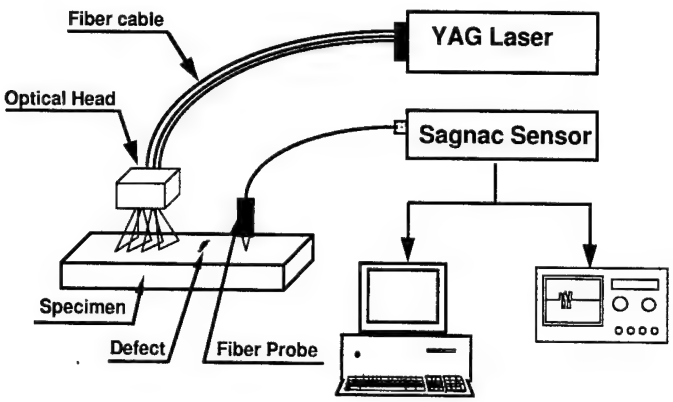

Figure 1. Optical setup of the fiber array laser-based ultrasonic generation and detection system. Only three fibers are shown here though the actual generating array consists of 10 fibers.

A single line source operated in the ablative regime was used to characterize two AE microsensors (University of Minnesota team). Bulk broadband ultrasonic waves were generated in an 1" thick aluminum specimen, and the sensors' responses were obtained and processed.

A new focusing system for ultrasound generation having significantly smaller dimensions compared with the previous versions was designed and tested using the fiberized Sagnac interferometer as the detector. The output head provided eight thermoelastic source lines at an energy of 1-2 mJ per line. The magnification of the double-cylindrical lens system can be adjusted from 0.7 to 1.8 in order to change the spacing and consequently the center frequency of generation. It was found that this system can provide narrow band ultrasonic generation at frequencies from about 4 to 6 MHz. The bandwidth of the generated ultrasound was from 1 to 1.5 MHz about the center frequency.

Narrow-band laser generation of ultrasonic waves was carried out on aluminum specimens having various thicknesses (from 0.5 mm to 25 mm). The main goal of this experiment was to assess the ability of laser-based ultrasonics to detect surface defects in plates, while having access only to the surface opposite to the one containing the defect. It was established that the efficiency of ultrasonic generation depends on the plate thickness. It was found that laser thermoelastic generation can be used to detect 5 mm long notches of width about 0.5 mm and depth from 0.2 to 1 mm on the opposite side of a rough aluminum plate of 0.5 - 1 mm thickness. Using appropriate filtering procedures it was possible to detect a 1.5 mm deep notch in a 2 mm plate while having access only to the opposite side of the specimen. The distance between the interferometer probe and defect should not exceed 12-15 mm to avoid signal attenuation.

It is expected that a portable system consisting of combined laser generation and detection systems will be finalized for field tests during years 4 and 5. Development of a fiber time-delay array for ultrasound generation will be initiated. The possibility of a time-delay array will be explored to steer beams for inspection of the interior of components. Signal analysis by use of measurement models and neural network techniques for signal classification will also be investigated.

M-URI PUBLICATIONS

L.S. Wang, J.S.Steckenrider and J.D.Achenbach. "A Fiber-Based Laser Ultrasonic System for Remote Inspection of Limited Access Components", in *Review of Progress in Quantitative Nondestructive Evaluation*. (D.O.Thompson and D.E.Chimenti edition), Vol. 16A, 507-514 (1996).

P.Fomitchov, S.Krishnaswamy and J.D.Achenbach. "Sagnac Interferometer for Ultrasound Detection on Rough Surfaces", in *Proceedings of 8th Int. Symposium on Nondestructive Characterization of Materials*, Boulder, CO, June 15-20, 1997.

L.S. Wang, P.Fomitchov, A.Kromine, S.Krishnaswamy and J.D.Achenbach. "A Portable Laser-Based Ultrasonic System for the Inspection of Aging Aircraft Structures", in *Proceedings of the 1st DOD/FAA/NASA Joint Conference on Aging Aircraft*, Ogden, UT, July 8-10, 1997.

P.Fomitchov, A.Kromine, S.Krishnaswamy and J.D.Achenbach. "Characterization of Laser Ultrasonic Source using a Sagnac Interferometer", in *Proceedings of QNDE'97 Conference*, San Diego, CA, July 28 - August 1, 1997.

J.D.Achenbach, B.Moran and A.Zulfiqar, "Techniques and Instrumentation In Structural Diagnostics", in *Structural Health Monitoring: Current Status and Perspectives,* edited by F.-K. Chang, Technomic Publishing Co., Inc., pp. 179-190, 1997.

3.3 EDDY CURRENT MICRO SENSORS FOR INTEGRATED DIAGNOSTICS

Co-Principal Investigator: S. Ramalingam (University of Minnesota)
Research Assistants: Jianhua Xue and Zheng Shi
M-URI Funding Allocation: 5.9%

DoD NEED

Critical components of fixed and rotary wing flight system now in use are prone to flaw initiation and growth which eventually attains a critical flaw size when catastrophic failure occurs. In the absence of on-board sensors to detect flaw initiation and to monitor flaw growth in real-time, components prone to failure are disassembled and systematically inspected off-line. Propagating flaws, typically several mm in size (or more), are readily detected and repaired. However, a major part of critical component life is in its flaw initiation phase where flaw dimensions are small and characteristic transverse dimensions are in the 25 to 100 μm range. Detection of initiation flaws is a skill and time-intensive process requiring highly trained operators. Flaws of this dimension are below the limit of detectability of the present generation eddy current inspection systems. Developing and implementing low cost EC sensors compatible with eddy current imaging and automation of this inspection process can substantially lower the man-power requirements and cost of off-line inspection of highly stressed, critical components.

PROJECT MISSION

One major goal of this project is to develop and implement eddy current micro sensors, (below 1 mm in lateral dimensions) so that the spatial resolution for defect flaw detection is substantially improved and extended to the flaw initiation phase of a critical component's life. Spatial resolution for flaw detection sought is 100 μm and less in transverse dimension. The second goal is to make EC inspection objective in order to reduce the skill/training requirements for EC flaw detection, i.e., to eliminate subjective flaw identification.. Eddy current imaging methods are also sought so that unambiguous EC inspection/imaging can eventually be fully automated.

Following 100 μm resolution flaw imaging demonstration with disposable eddy current micro sensors at the beginning of the 3rd year, the Project Monitor and the Project PI have suggested progress towards the development of a pencil probe (incorporating EC micro sensors) compatible with fully automated EC imaging to facilitate multi-axis CNC or robotic inspection using motion control derived from the CAD database of the component. This activity is now in progress.

RESEARCH ACCOMPLISHMENTS

Since the flux available to detect the perturbation in the AC magnetic field due to the presence of flaw in a test object decreases with the decrease in sensor dimensions, and since the excitation coil current can directly add to the sensor signals to adversely affect the signal-to-noise ratio, flux focusing methods had to be developed both to shield and to enhance the flaw signals sensed by the EC micro sensor. Starting with manually wound macro sensors, the flux focusing concepts were first verified (Year 1 effort). Using the same sensor, digital flaw imaging methods were also developed to demonstrate the transition from flaw detection to 3-dimensional flaw imaging. This required the development and use of a computer-driven X-Y Table for automated data acquisition and display of signals acquired for objective flaw imaging. Model flaws, created with EDM and drilling (cylindrical holes, slots and keyhole defects) were used. Wound core (macro) sensors are compatible with flaw imaging but the flaw resolution required, as anticipated, could not be achieved.

Photo lithographic techniques were then used to construct single element and 4 x 4 eddy current micro sensors in Silicon. Single element sensors, 1300 μm x 1300 μm in size, implemented in Silicon were used to construct flux-focusing probes for eddy current inspection and imaging. Automated scanning of test objects containing model flaws in the computer-driven X-Y table demonstrated that a flaw resolution of 100 μm is feasible (through-the-thickness 5 mm long flaw created by wire EDM using a 0.004" diameter brass wire). Spatial resolution of 100 μm has been achieved. Three dimensional images of the flaw have been obtained. Following this single element and array sensors were

implemented in a flexible (Kapton) substrate to realize low cost or disposable sensors. Sensing elements are disposed in Kapton such that micro sensor damage in routine use is unlikely.

The Si sensors made in Year 2 were 1300 μm x 1300 μm in size. Scaled down Kapton sensors (350 μm x 350 μm), smaller than those implemented in Si have been made and are now in use. Functionality of the Kapton micro-sensors has been verified in the computer driven X-Y table. It has been shown that it is possible to resolve 100 μm EDM slot resolved with 1067 μm x 1067 μm sensors.

To facilitate automated EC inspection, a ruggedized "Pencil Probe" has been developed using a 320 μm x 320 μm EC micro sensor. A model keyhole flaw (2 mm drilled hole extended with a 5 mm long EDM slot created with 0.004" diameter brass wire) created in a test object has been scanned (scanning time of ~ 15 minutes). Resolution limit of 100 μm has been achieved.

Work in progress focuses on automated inspection using the ruggedized pencil probe equipped with the 320 μm x320 μm sensor and a 3-axis CNC machine. Three axis system now in use is sensitive to changes stand-off distance and local normality (sensor orientation normal to surface under inspection). This can be overcome by using the pencil probe in a robotic inspection system with an end effector having two degrees of freedom. It is anticipated that this approach can be evaluated in year 3 so that the 4th and 5th year effort can focus on totally automated inspection. Path control for automated inspection is to be derived from the CAD database of the part geometry. Pro-E software will be used for CAD representation and the automated derivation of sensor path geometry. Down loading this to the automated inspection system will facilitate untended inspection of critical components whenever they are disassembled for off-line inspection.

Square loop magnetic cores offer one means of rendering stand-off distance variation less significant during automated inspection. Fluxset probes are made with an excitation and a concentric sensor coil. A Metglass core is then placed within the concentric solenoidal coils. AC excitation of the primary (outer) coil leads to saturation of the square loop magnetic core. Field flipping of the core is sensed by the inner solenoid (sensor) coil. In the presence of a magnetic field, if the AC excitation current is maintained constant, the sensor coil voltage signal is time-shifted in saturation (forward saturation occurs sooner and reverse saturation is retarded). Measuring the time-shift with respect to a reference excitation current, say the current maximum, enables measurement of applied fields with high precision. Stand off distances as large as 5 mm are sufficient to sense partially-through-the-thickness ED flaws in non-magnetic materials. It is anticipated that the Fluxset probe technique can be evaluated and perfected in the Year 4 & 5 effort to demonstrate automated EC inspection with less sensitivity to variations in stand-off distance. A less expensive CNC or robotic system may then be used for automated inspection at an even lower total cost.

M-URI PUBLICATIONS:

L. Zheng, J. Xue and S. Ramalingam, "Eddy-Current Micro-Sensors For Flaw Imaging: Numerical Simulation And Experimental Evaluation", ASME/STLE Joint Conference, October 1996, San Francisco, CA.

J. Xue, S. Ramalingam and Z. Shi, "Modeling Eddy Current Imaging with Thin Film Micro-Sensors, International Mechanical Engineering Congress, November 1997, Dallas, TX.

J. Xue, S. Ramalingam and Z. Shi, "Eddy Current Flaw Imaging using Micro-Sensor Arrays", *Emerging Technologies for Machinery Health Monitoring and Prognosis*, TRIB-Vol. 7, R. Cowan, ed., ASME, 1997, pp. 13-18.

MULTIUNIVERSITY CENTER FOR INTEGRATED DIAGNOSTICS

INTEGRATED DIAGNOSTICS

Section 2

Viewgraph Materials ♦

Integrated Diagnostics

M-URI Program Review

Ward O. Winer, Principal Investigator
Richard S. Cowan, Program Manager

Office of Naval Research
Arlington, VA

P. Peter Schmidt, Program Officer
ONR GRANT N00014-95-1-0539

Department of Defense Needs

- To understand deterioration mechanisms and identify means to detect the initiation of flaws and other potential failure sites.
- To develop methodology for failure prediction in real-time, including modeling fault initiation and failure signatures, and observing the propagation and fracture phases of fatigue-based failure.
- To identify responses to signals generated early in fault inception, including designing sensors that can be placed at critical sites on mechanical systems for response to changes of variables of state or vibration.

Program Mission

To provide a systematic approach
for providing basic and applied research,
needed in developing technologies and methodologies
of use in determining how mechanical failures occur,
and how they can be detected, predicted, and diagnosed
in real-time.

Program Participants

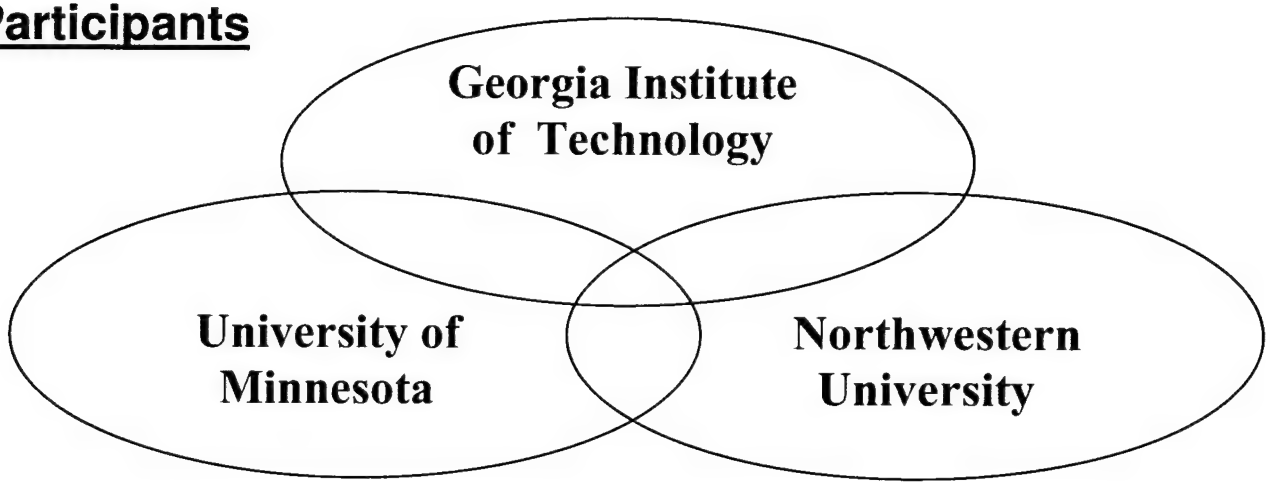

21 Faculty Co-PI's
13 Support Faculty
10 Post-Doctoral Researchers
35 Graduate Students
7 Undergraduate Students

Representing the disciplines of
Mechanical Engineering, Materials Science & Engineering,
Electrical & Computer Engineering, and Civil Engineering.

M-URI FUNDING - PARTICIPATING INSTITUTES

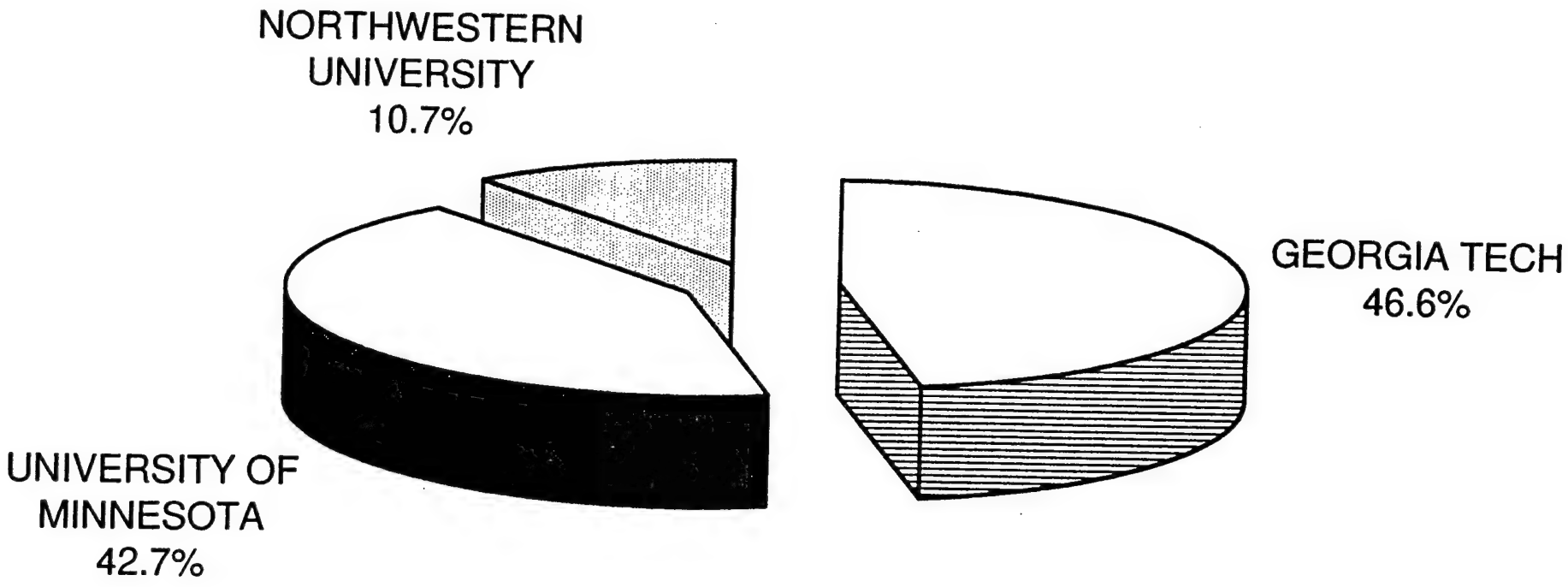

Program Elements

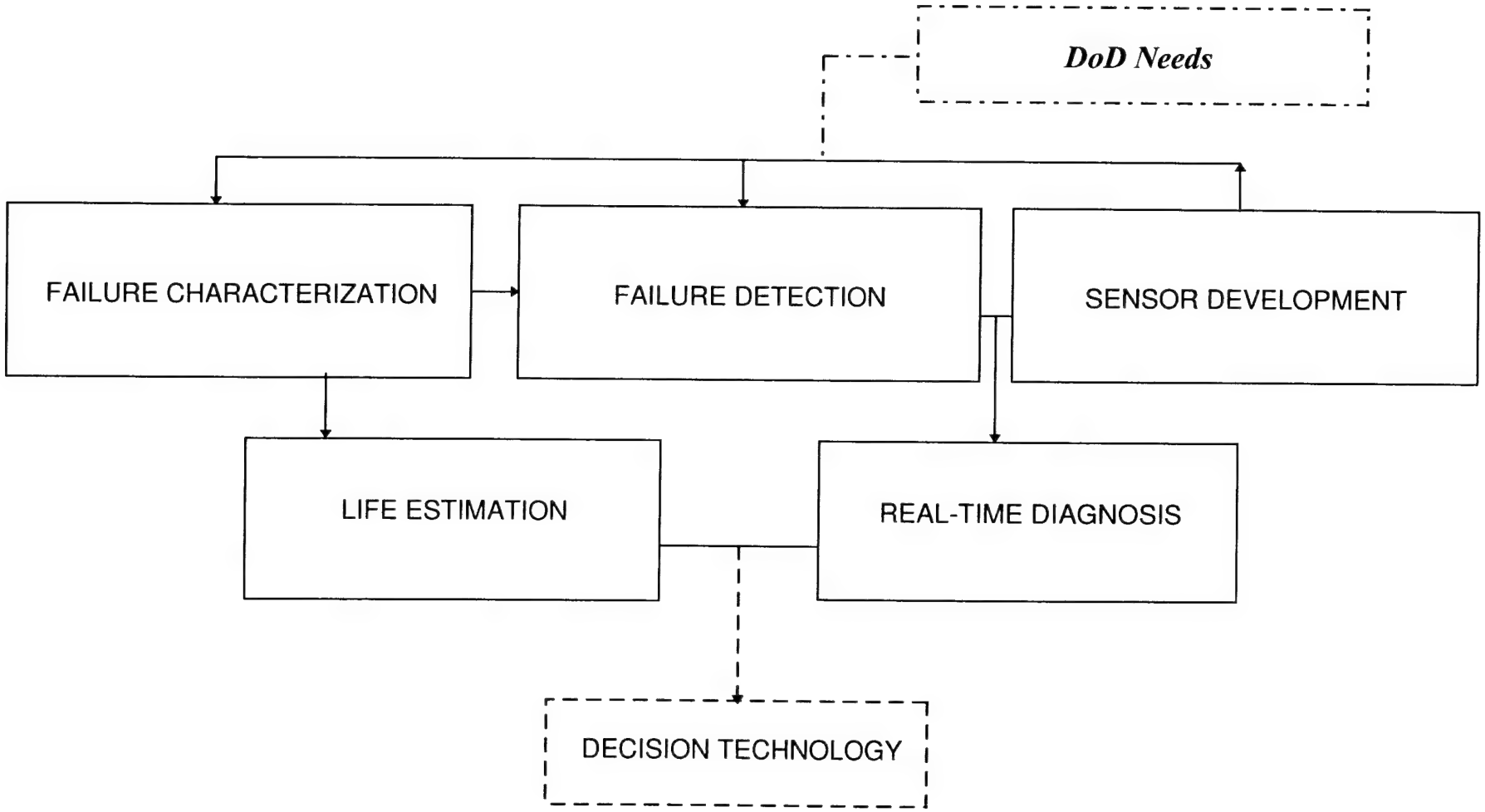

M-URI FUNDING - RESEARCH FOCUS

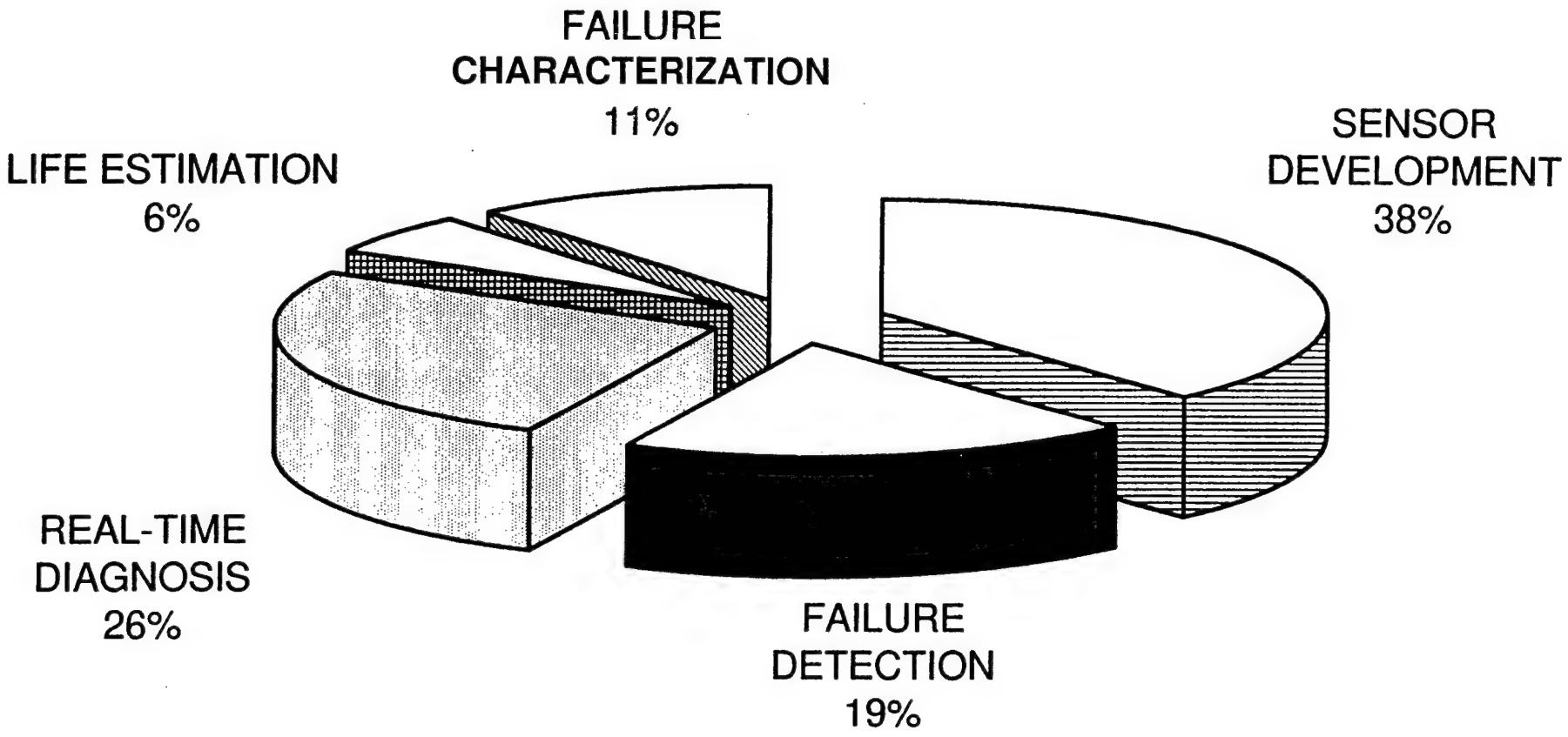

Technology Delivery

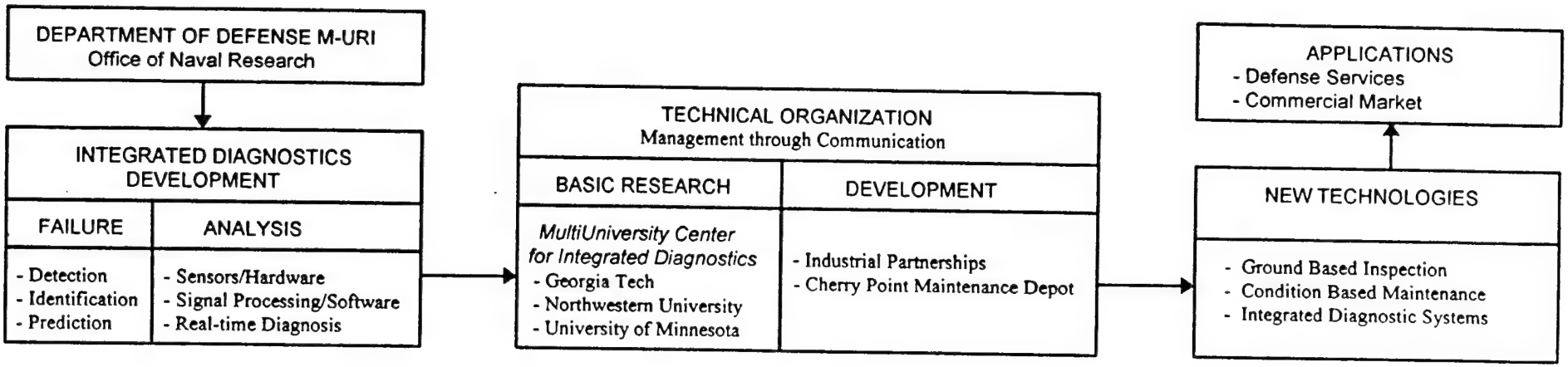

Technology Transfer (M-URI Year 3)

- Publications
  - Refereed Journals (9)
  - Non-refereed Journals (16)
- Presentations (29)
- Books (and sections thereof) (8)
- Patents Filed (1)
- Partnerships
  - Cherry Point Naval Aviation Depot, Cherry Point, NC
  - Honeywell Technology Center, Minneapolis, MN
  - Timken Company, Canton, OH
  - Torrington Co., Norcross, GA

Technology Transfer (M-URI Year 3)

- Graduates (9)

Bill Anderson, MS (12/97) - Mechanical Engrg.	Georgia Tech
Davis Bahr, Ph.D. (5/97) -Electrical Engrg.	U. of Minnesota
Scott Billington, MS (12/97) - Mechanical Engrg.	Georgia Tech
Angela Drexler, BS (5/97) - Electrical Engrg.	U. of Minnesota
John Pape, MS (12/97) - Mechanical Engrg.	Georgia Tech
Akshay Patel, MS (5/97) - Mechanical Engrg.	Georgia Tech
Aaron Schmidt, MS (7/97) - Electrical Engrg.	U. of Minnesota
Lei Wang, Ph.D. (8/97) - Electrical Engrg.	U. of Minnesota
J. S. Wright, Ph.D. (5/97) - Materials Science	U. of Minnesota

- Monthly Progress Reports

- Information Highway - World Wide Web
  http://www.me.gatech.edu/Diagnostics

Organization

Thrust I:

Mechanical System Health Monitoring

- Sensor Development
- Real-time Diagnosis

Thrust II:

Failure Characterization and Prediction Methodology

- Failure Mechanisms
- Life Estimation

Thrust III:

Nondestructive Evaluation

- Failure Detection
- Failure Identification

Thrust I

Mechanical System Health Monitoring

Direct Sensing, Analysis, Real-time Diagnosis

Perform studies with respect to the responses of signals early in fault inception, including research on sensors that can be placed at critical sites on mechanical systems for responses to change in variables of state or vibration.

Thrust I Projects

Mechanical System Health Monitoring

Direct Sensing, Analysis, Real-time Diagnosis

- Detection of the Precursor to Mechanical Seal Failure
  Salant-Jarzynski (Georgia Tech)

- Real-time Monitoring & Controlling of
  Mechanical Face Seal Dynamic Behavior
  Green (Georgia Tech)

- Dynamic Metrology as a Bearing Wear Diagnostic
  Kurfess-Liang-Danyluk (Georgia Tech)

- Integrated Microsensors for Aircraft Failure Warning
  Polla-Francis-Robbins-Harjani-Kaveh (University of Minnesota)

Thrust II

Failure Characterization and Prediction Methodology

Perform studies pertaining to the methodology for failure prediction in real-time, including modeling fault initiation and failure signatures, and observing the propagation and fracture phases of fatigue-based failure.

Thrust II Projects

Failure Characterization and Prediction Methodology

- Structural Fatigue Investigation
  McDowell-Neu-Qu-Johnson-Saxena (Georgia Tech)

- Failure Prediction Methodology - Fatigue Reliability
  Moran (Northwestern University)

- Acoustic Emission Modeling for Integrated Diagnostics
  Daniel (Northwestern University)

- Study of Acoustic Emission and Transmission from Incipient Fatigue Failure
  Jarzynski-Jacobs-Bair (Georgia Tech)

Thrust III

Nondestructive Evaluation

Failure Detection and Identification

Perform studies pertaining to deterioration mechanisms and techniques for detecting the initiation of fractures or other failures.

Thrust III Projects

Nondestructive Evaluation

Failure Detection and Identification

- Crack Detection in Annular Structures by Guided Waves
  Berthelot-Jacobs-Qu (Georgia Tech)

- Laser-Based Ultrasonics for Integrated Diagnostics
  Achenbach-Kromine (Northwestern University)

- Eddy Current Microsensors for Integrated Diagnostics
  Ramalingam (University of Minnesota)

MULTIUNIVERSITY CENTER FOR INTEGRATED DIAGNOSTICS

Mechanical System Health Monitoring

Direct Sensing, Analysis, Real-time Diagnosis

Detection of the Precursor to Mechanical Seal Failure in Turbomachinery

Richard F. Salant, Jacek Jarzynski, Bill Anderson

Goal: Develop a system to detect the collapse of the lubricating film in a mechanical seal before mechanical and thermal damage to the seal is sustained.

Approach: Use active ultrasonic wave transmission as indicator of film breakdown.

Schematic of Apparatus

NASA turbopump seal

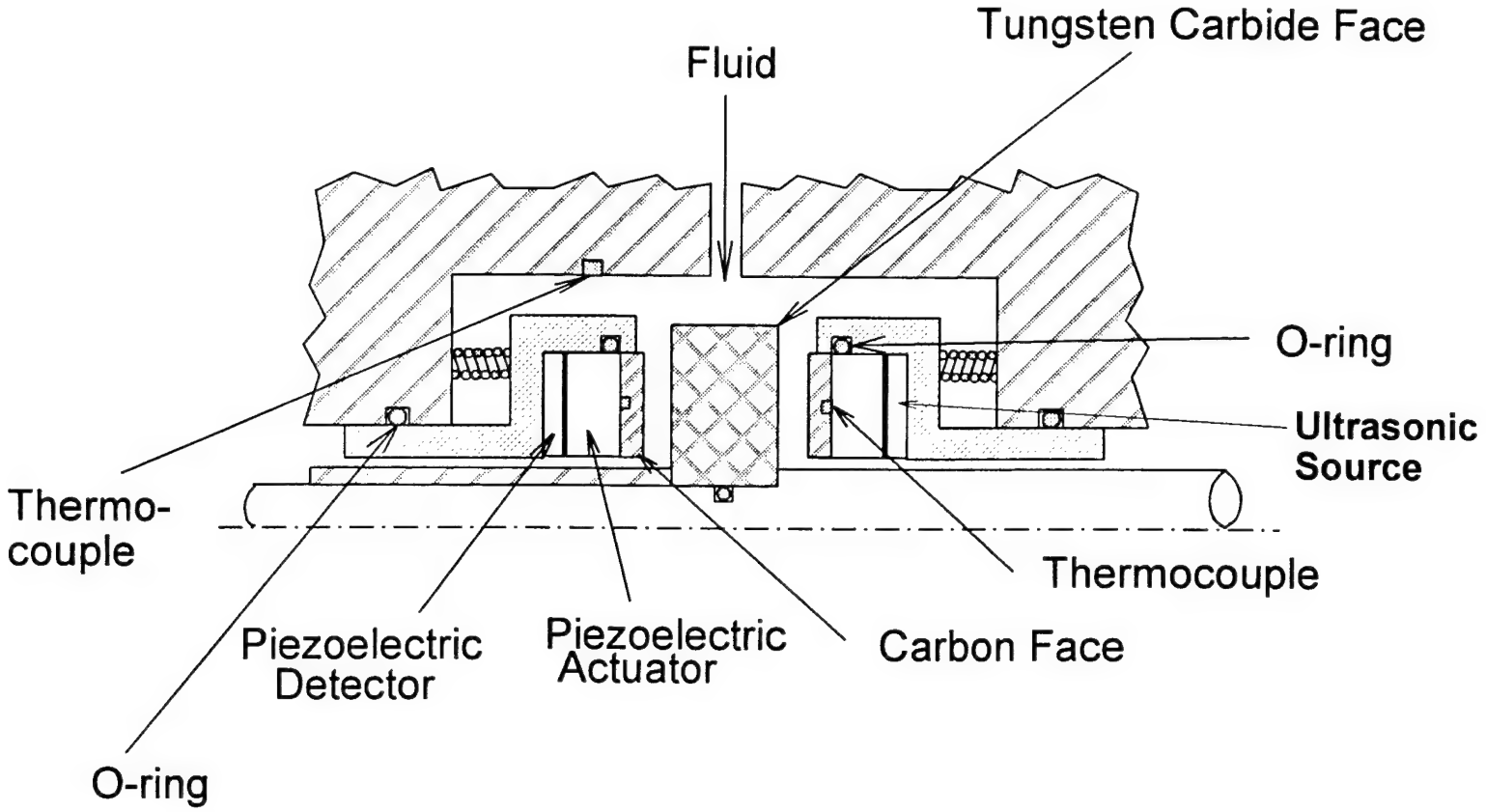

Bench Test Results I

Effect of varying film thickness

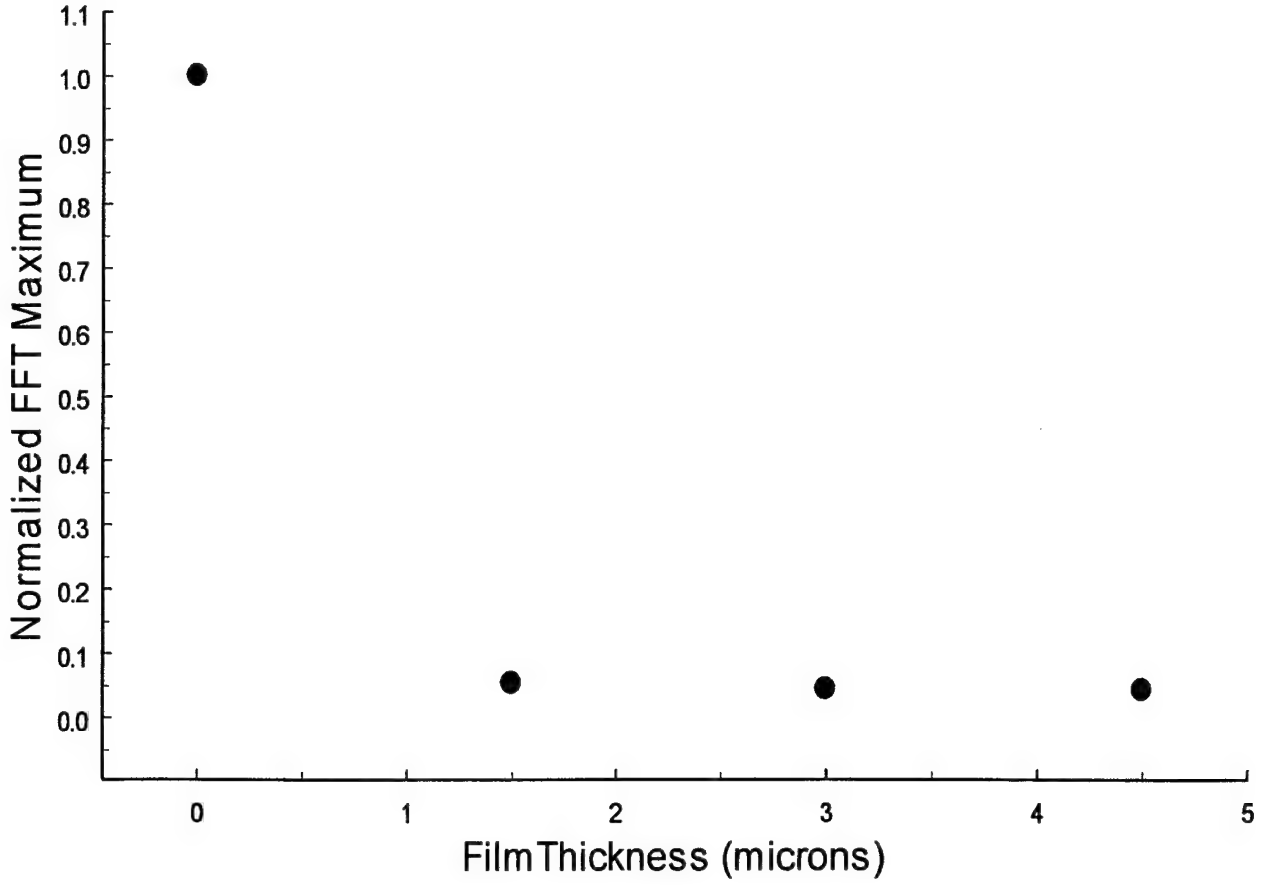

Bench Test Results II

Effect of varying contact pressure

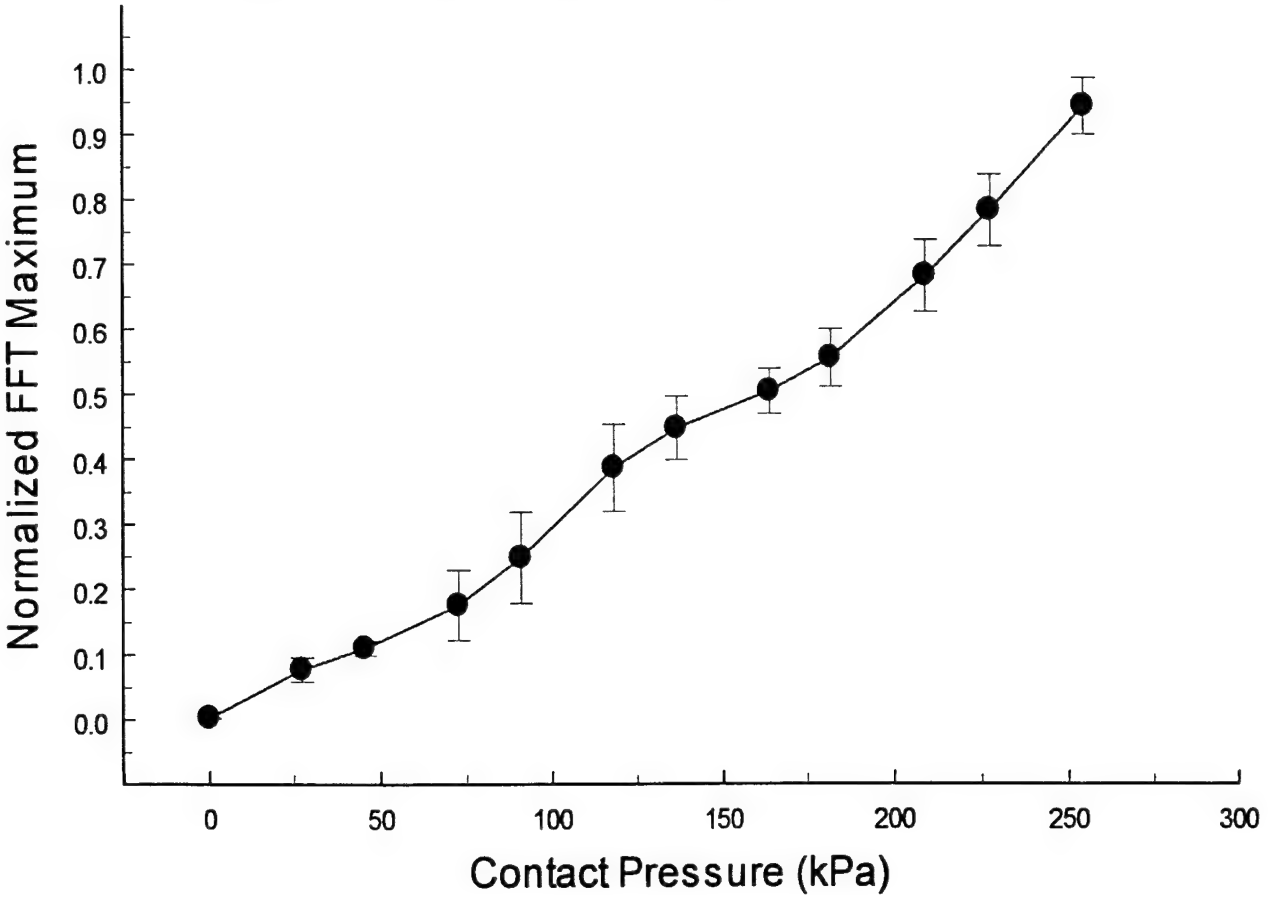

Steady State Test Results I

689 kPa, 565 rad/sec

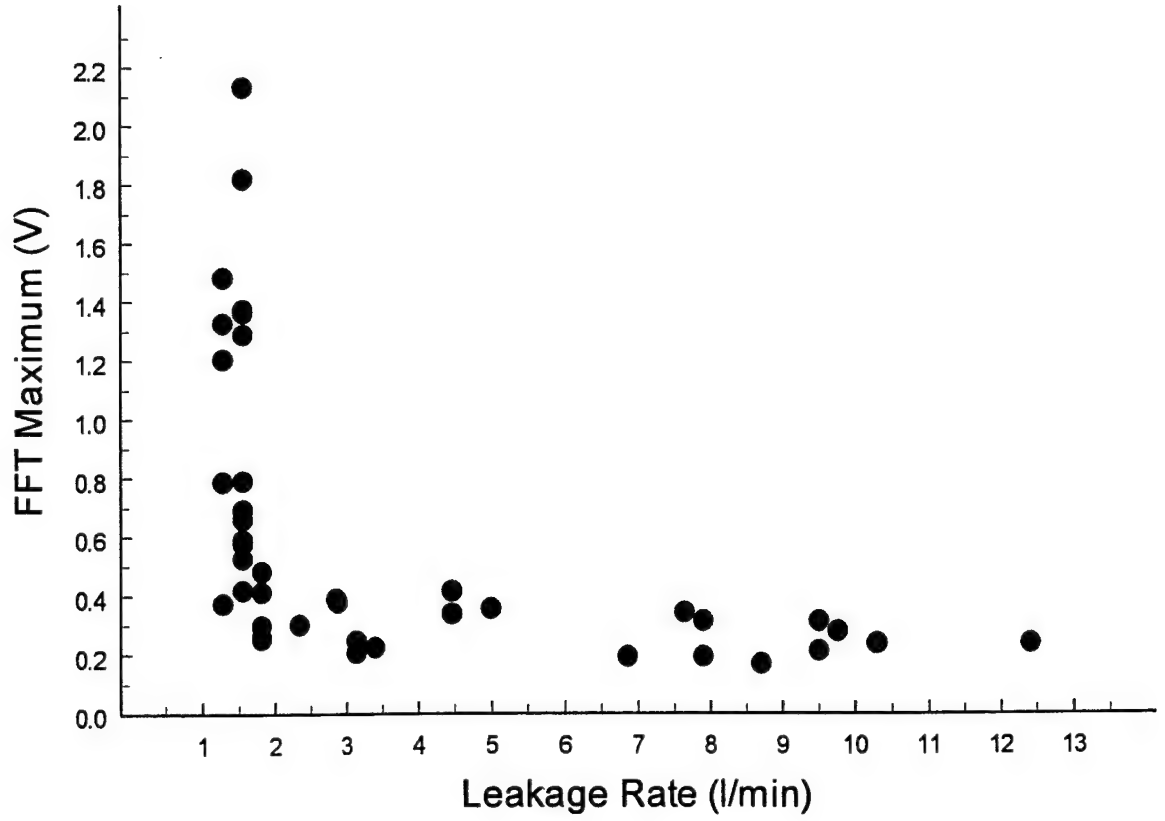

Steady State Test Results II

1.38 Mpa, 754 rad/sec

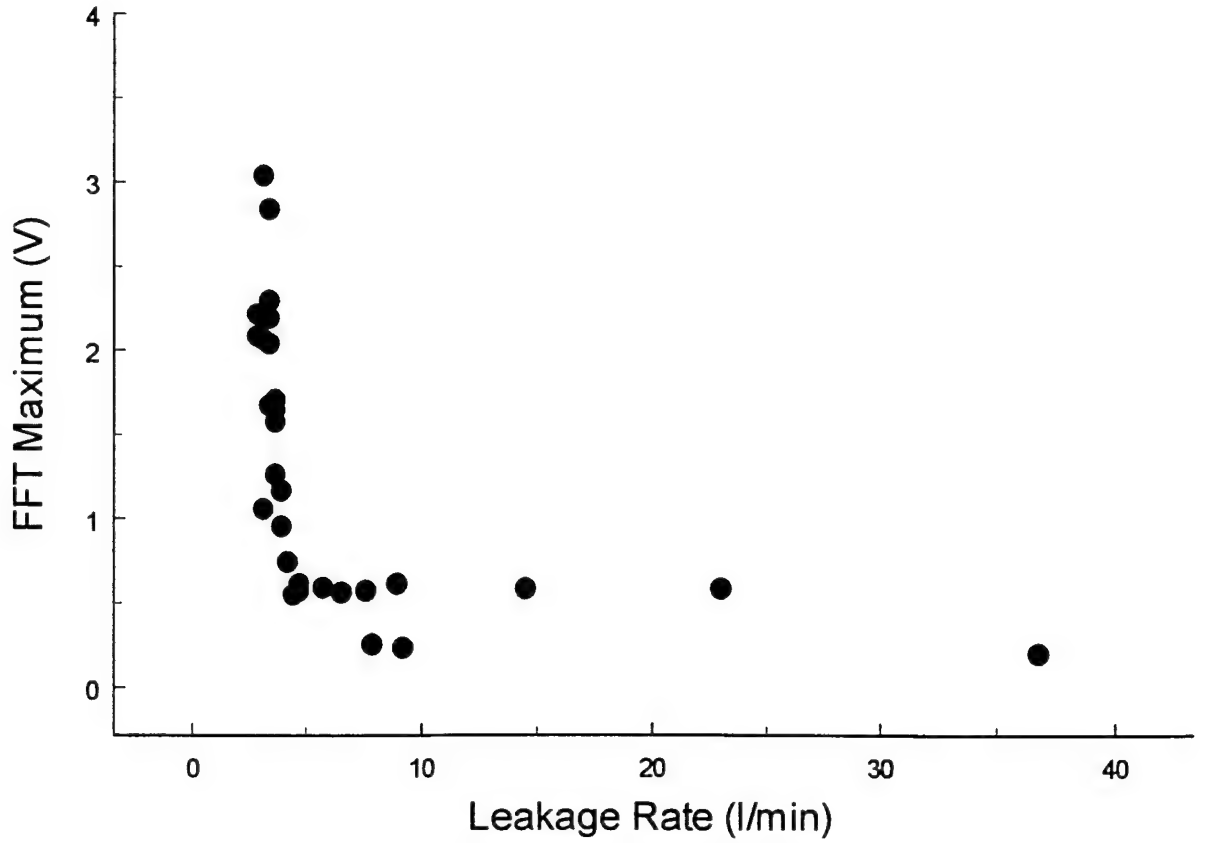

Detection of the Precursor to Mechanical Seal Failure in Turbomachinery

Remainder of Year 3

- Transient tests
- Destructive tests to failure

Detection of the Precursor to Mechanical Seal Failure in Turbomachinery

Plans for Years 4 & 5

- Active ultrasonic monitoring system installed on seal used in Navy application.
- Candidate seals:
  - York T-86 compressor - chiller for submarines/surface vessels
  - York R compressor - refrigeration unit for naval stores
  - York F compressor - refrigeration unit for naval stores
- Tests performed in a laboratory tester

York T-86 Centrifugal Compressor

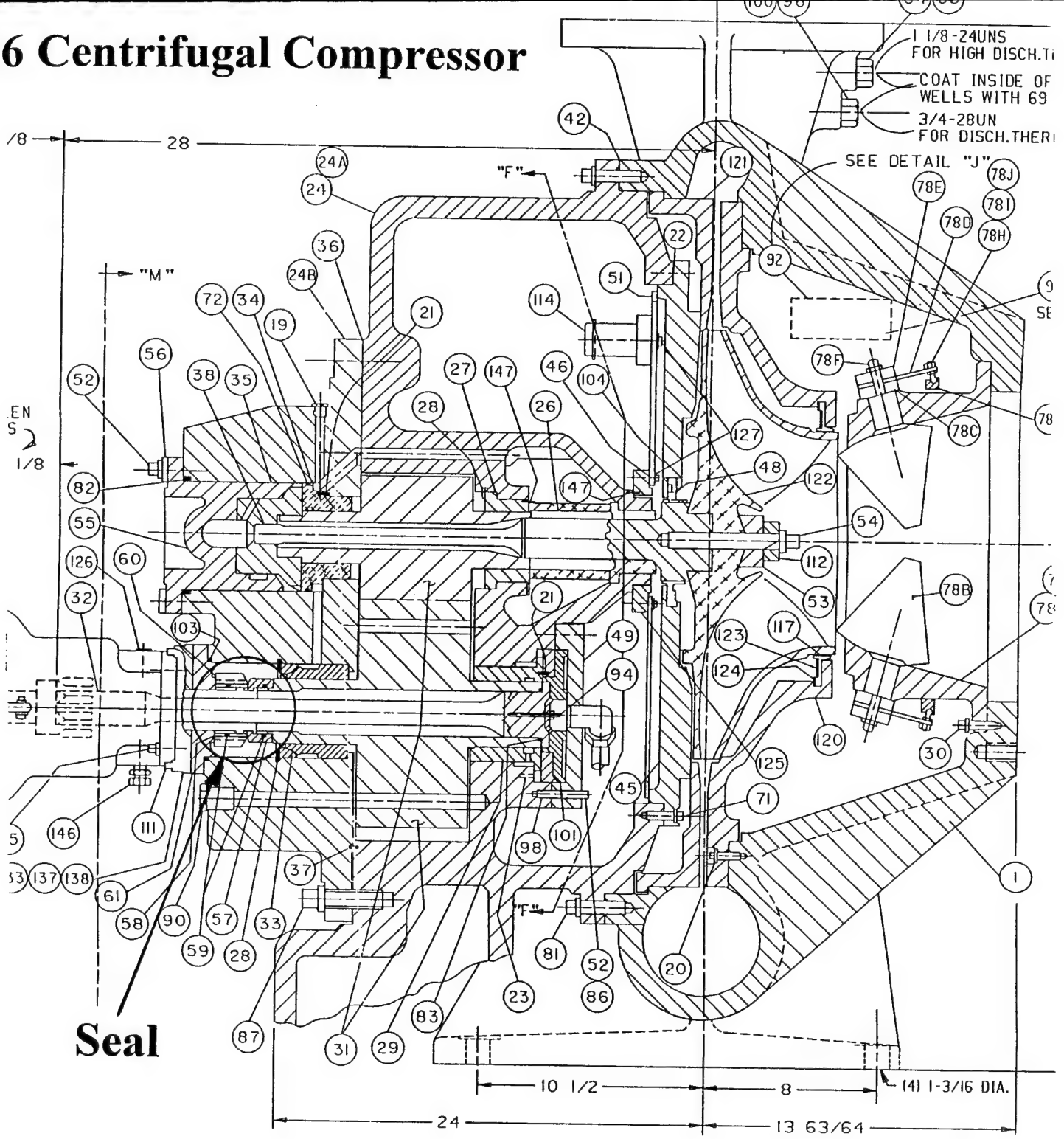

York R Compressor Seal

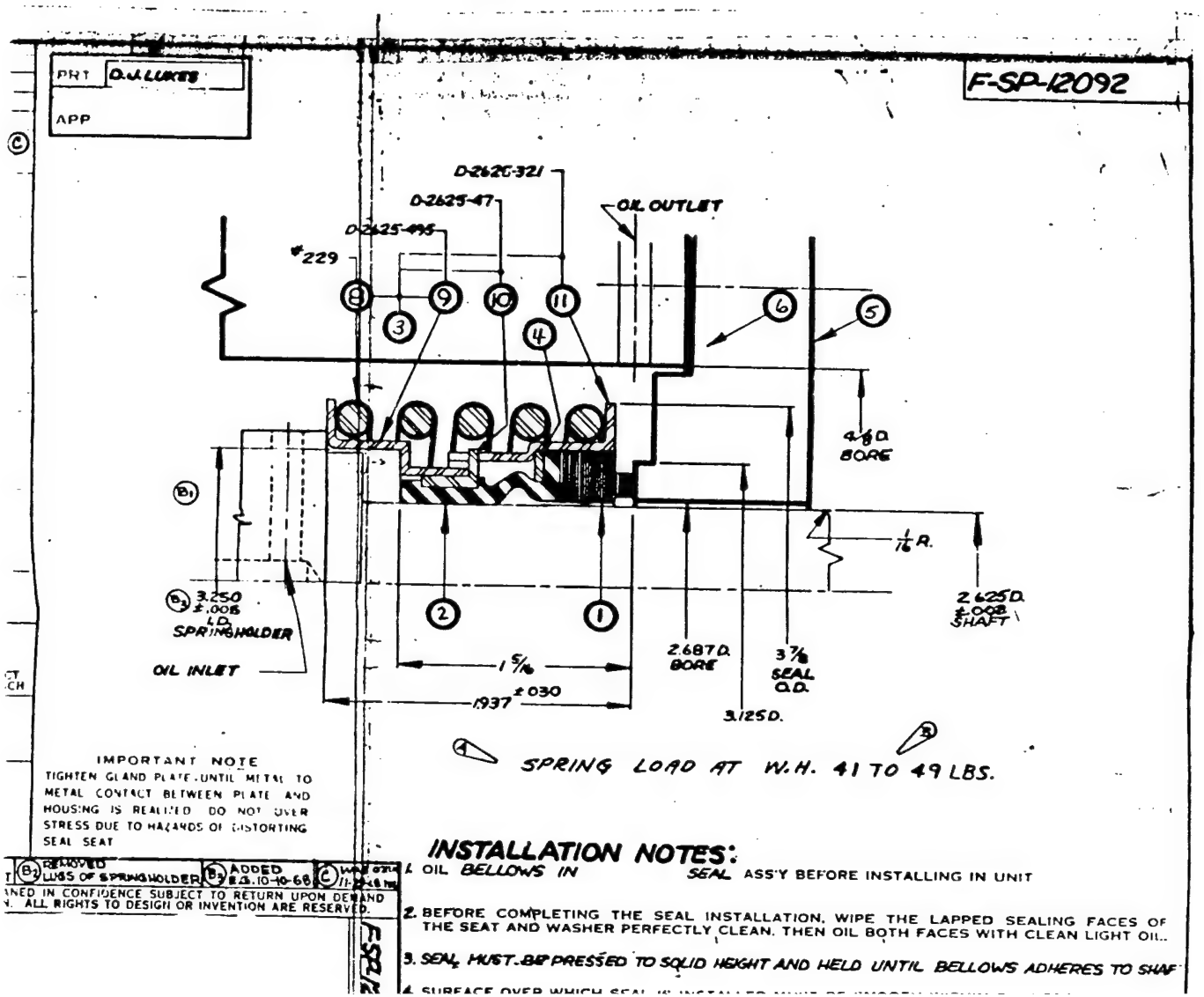

QUANTITY PER UNIT	PART NO.	ITEM	DESCRIPTION

York F Compressor Seal

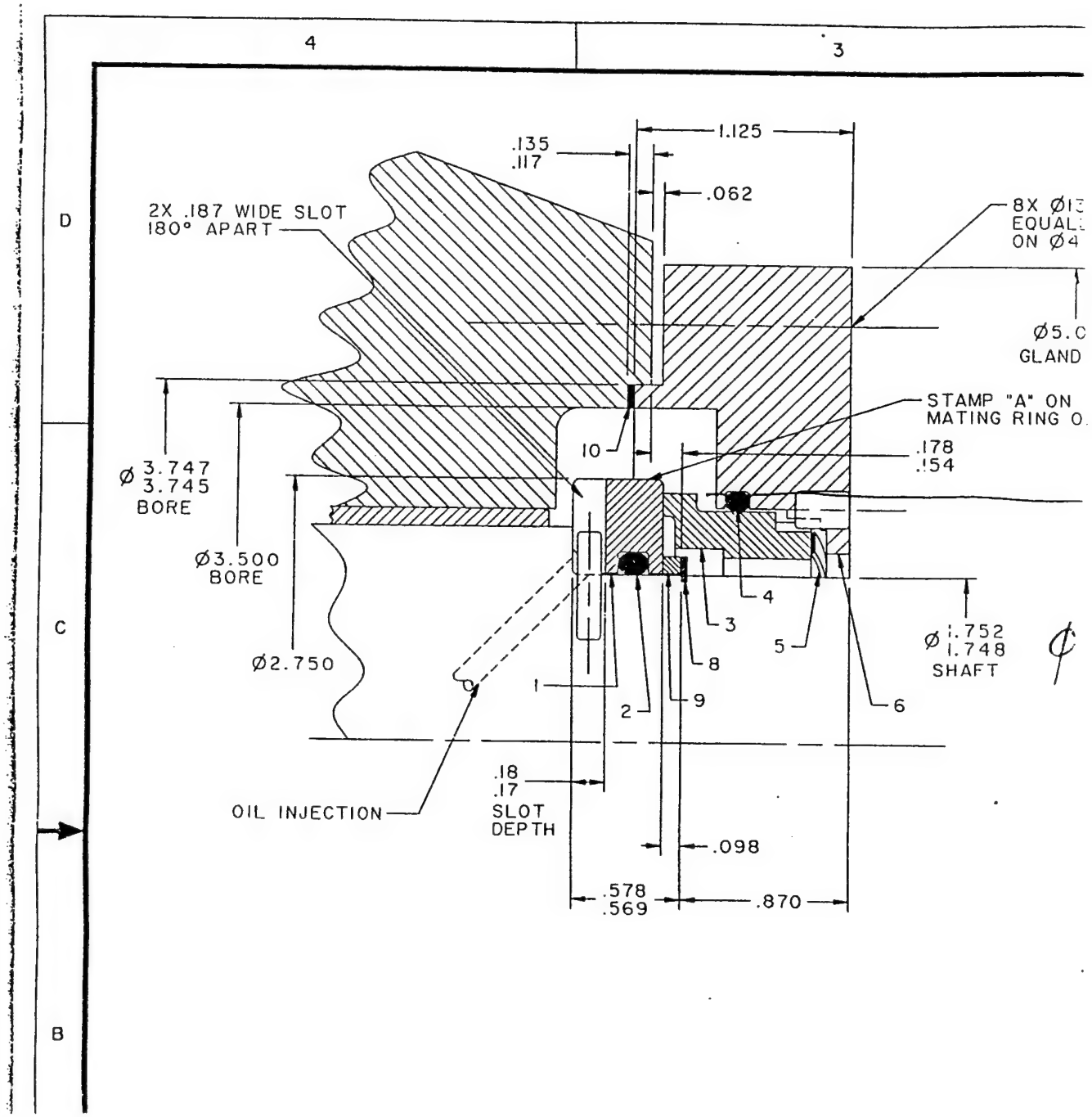

MULTIUNIVERSITY CENTER FOR INTEGRATED DIAGNOSTICS

REAL-TIME MONITORING AND CONTROLLING OF THE DYNAMIC BEHAVIOR OF MECHANICAL FACE SEALS

Itzhak Green

Min Zou

Woodruff School of Mechanical Engineering
GEORGIA INSTITUTE OF TECHNOLOGY

Mission

To develop techniques in real-time for monitoring seal dynamic response, detecting seal face contact, and controlling seal faces at close proximity so as to avoid contact.

Approach

- Use a flexibly mounted rotor (FMR) noncontacting mechanical face seal test rig. Reproduce higher harmonic oscillations (HHO) in the seal test rig.
- Use eddy current proximity probes to measure seal dynamic response.
- Develop algorithms and integrate a computerized environment for real-time monitoring of seal dynamic response and detection of face contact.
- Design a control system to adjust the closing force (on rotor) for maximum reduction of rubbing contact (HHO).

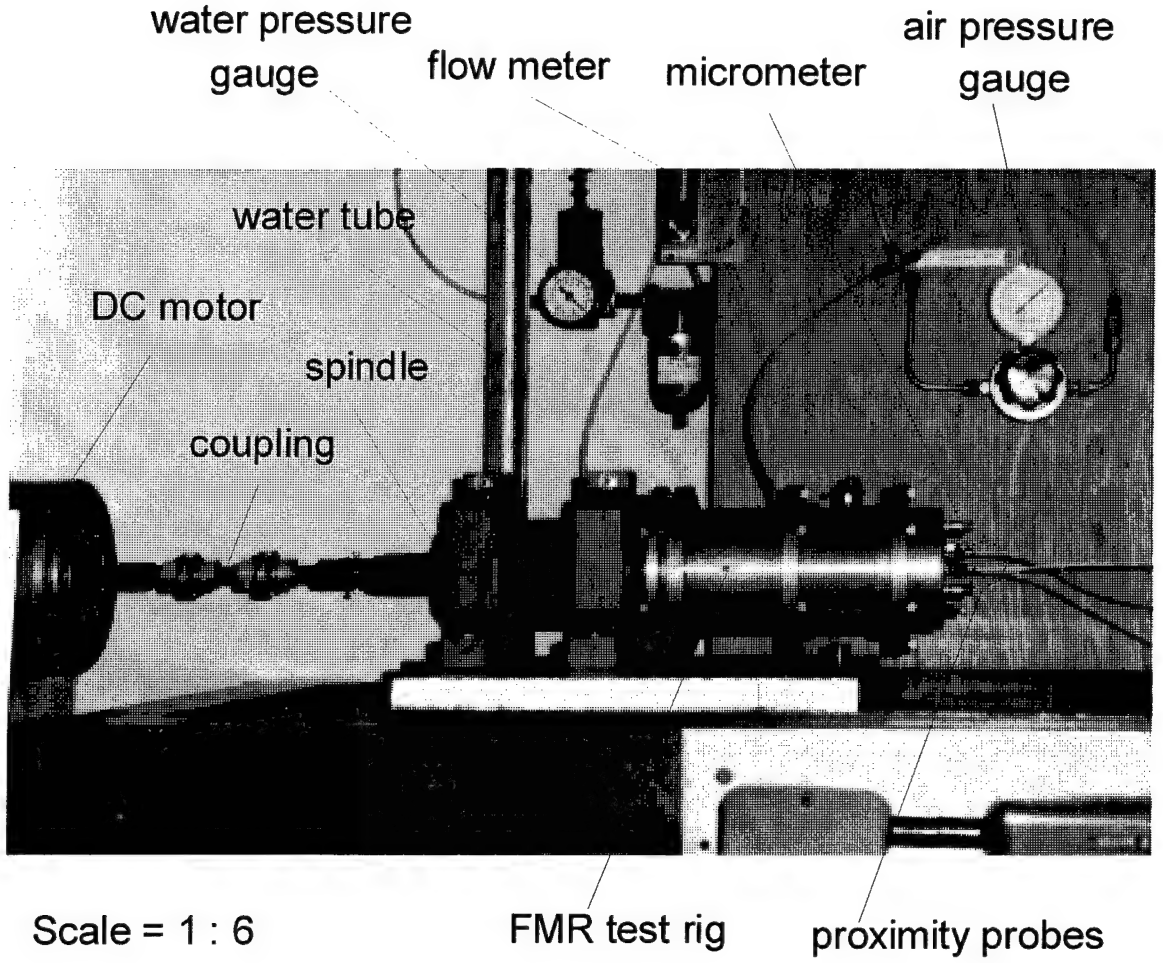

FMR Mechanical Face Seal Test Rig (Photograph)

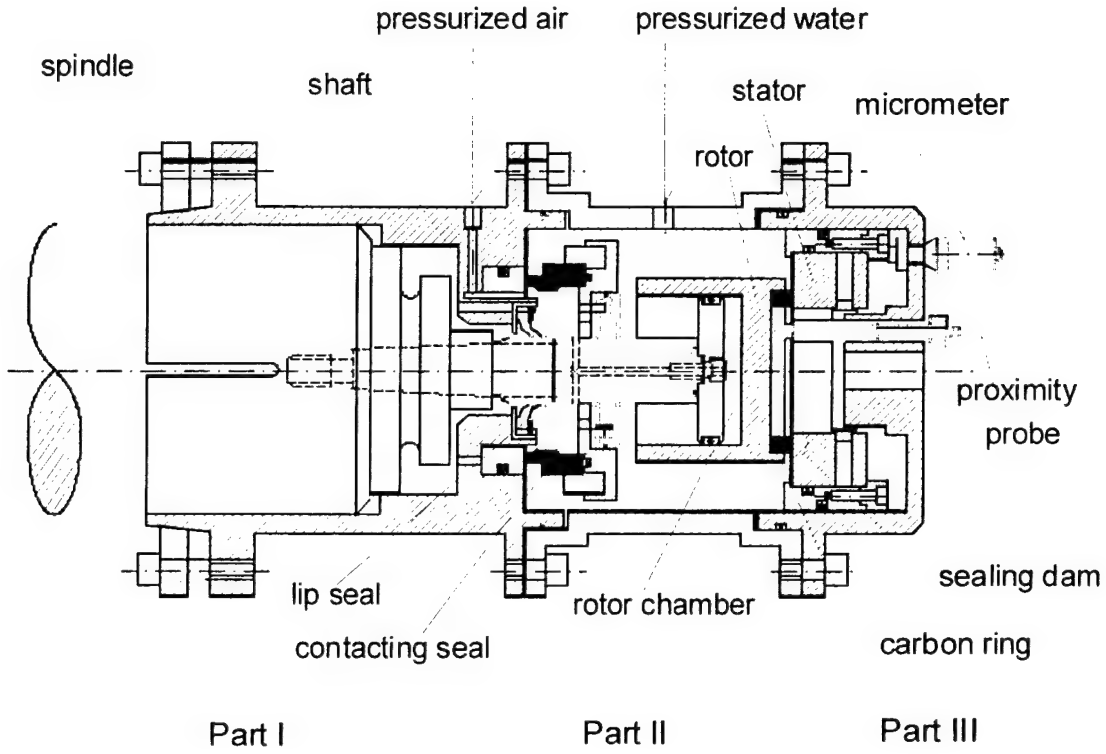

FMR Mechanical Face Seal Test Rig (Schematic)

Results

REAL-TIME MONITORING OF MECHANICAL SEAL DYNAMIC RESPONSE

- Measured rotor dynamic response using proximity probes.
- Determined seal clearance, stator misalignment and stator angle, rotor misalignment and precession angle, and relative misalignment between rotor and stator in real-time.

ON-LINE DETECTION OF SEAL CONTACT

- Based upon relative misalignment between the rotor and the stator (developed from seal motion and geometry).
- Based upon the orbit (plot) of the rotor angular response.
- Based upon spectrum analysis of the proximity probe signals.

SEAL CLEARANCE CONTROL

- Determined seal axial dynamic model experimentally.
- Designed a seal clearance controller based on experimental model.

Proximity Probe Signals

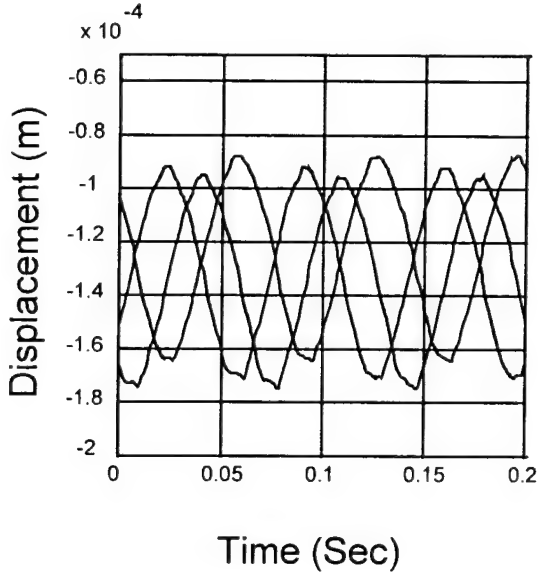

Power Spectral Density (Probe Signals)

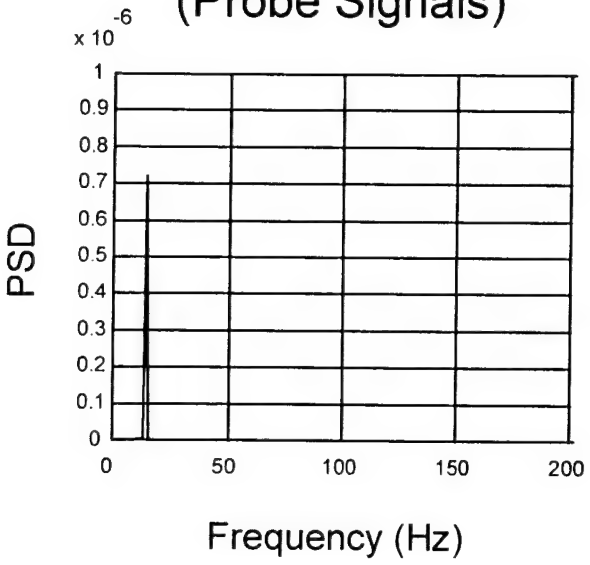

Rotor Angular Response Orbit

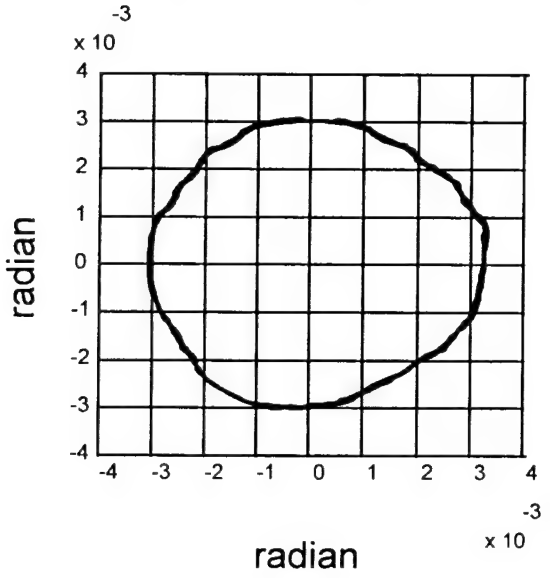

Rotor Dynamic Response (noncontacting operation)

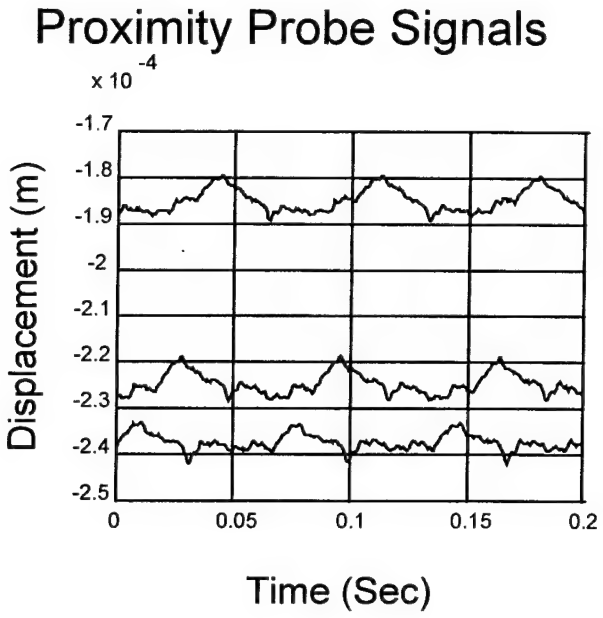

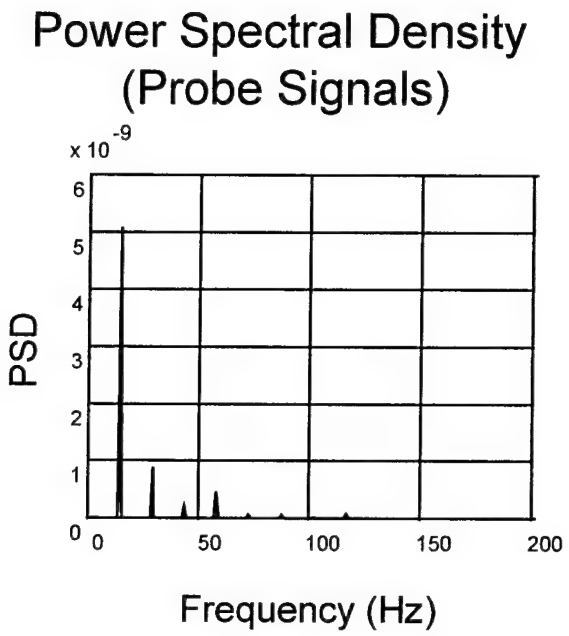

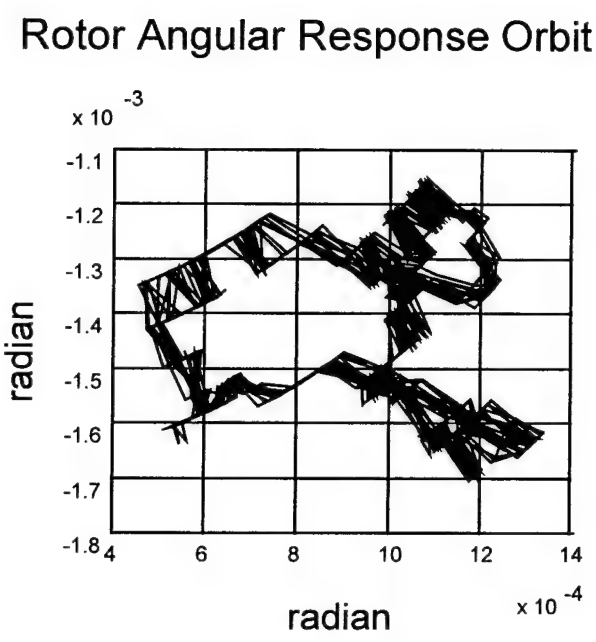

Rotor Dynamic Response (contacting operation)

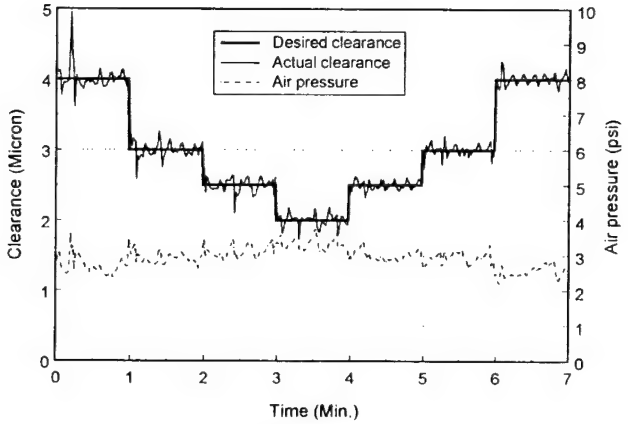

Set-point change trace results (small steps and range)

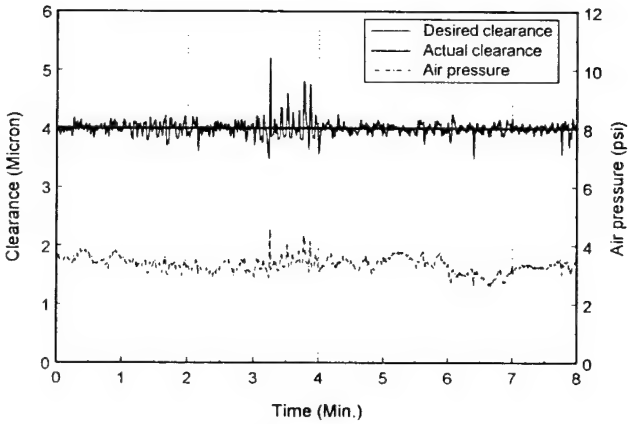

Transient results (without set-point change)

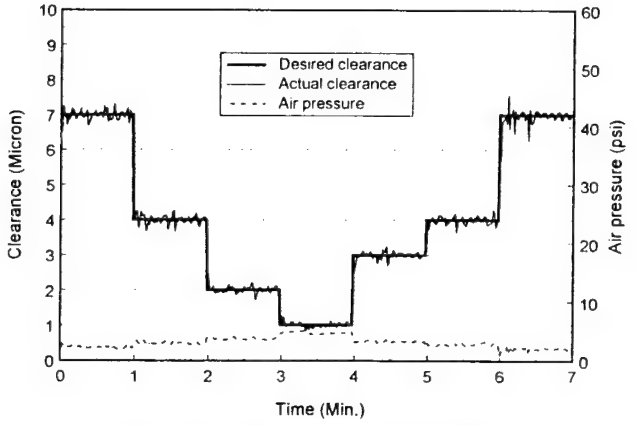

Set-point change trace results (larger steps and range)

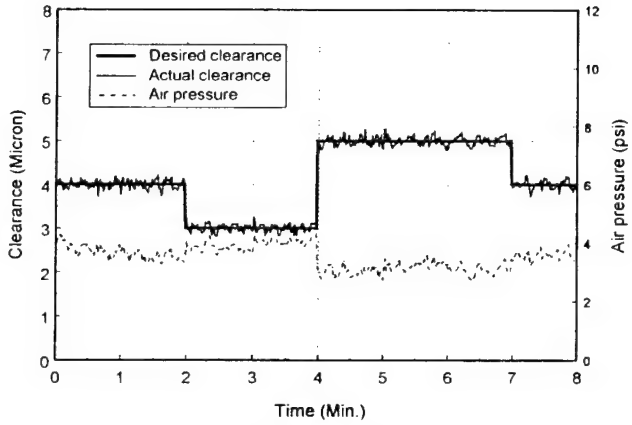

Transient results (with set-point changes)

Seal Clearance Control Results

Immediate Plans

Objective:

Reduce or eliminate face contact (HHO) by adjusting air pressure in the rotor chamber.

Methodology:

Experimentally determine the correspondence between air pressure (in rotor chamber) and rotor angular response.

Generate an angular mode model based upon the angular dynamic response, and integrate a controller into the test rig.

Plans for Years 4-5

- Use an opening force (instead of the closing force) as the controlling mechanism for reducing and eliminating HHO.
- Analyze the dynamics of intermittent contact and impact; correlate with experimental data.
- Investigate how failure (or failure onset) in other system components (e.g., cracked shaft) may affect the seal behavior, and how such failure can be detected through the sensors that monitor the seal dynamic behavior.

Summary

- Real-time monitoring of the dynamic behavior of a mechanical seal with clearance control has been accomplished by using eddy current proximity probes.
- The robustness of the diagnostic/control system should be associated with how critical an application is.
  For very critical applications - three probes are necessary;
  (it is more involved but the investment may be worthwhile).
  For less critical applications - need one or two probes;
  (orbit plots cannot be generated).
- When contact (HHO) has been detected:
  Option 1: Immediately shut down for maintenance.
  Option 2: Eliminate/reduce the damaging behavior.
  (i.e., use active control until maintenance can be done).
- Work is underway for the reduction/elimination of HHO.

Dynamic Metrology as a Bearing Wear Diagnostic

Personnel

Steven Danyluk (ME Faculty)
Thomas Kurfess (ME Faculty)
Steven Liang (ME Faculty)
Scott Billington (Master's Student)
Yawei Li (Ph. D. Student)
Xavier Ribadeneira (Ph. D. Student)

Publications

Shiroishi, J., Li, Y., Liang, S., Kurfess, T., Danyluk, S., "Bearing Condition Diagnostics Via Multiple Sensors," *Mechanical Systems and Signal Processing*, Vol. 11, No. 5, pp. 693-705, September, 1997.

Shiroishi, J.W. , Li, Y., Liang, S., Danyluk, S., and Kurfess, T.R., "Vibration Signal Analysis for Bearing Race Damage Diagnostics," Keynote paper for the *7th International Conference on Dynamic Problems in Mechanics*, Brazil, pp. 187-190, March 1997.

"Bearing Fault Detection via High Frequency Resonance Technique with Adaptive Line Enhancer," Li, Y., Shiroishi, J.W., Kurfess, T.R., Liang, S., and Danyluk, S., *12th Biennial Conference on Reliability, Stress Analysis, & Failure Prevention*, 1997, Virginia Beach, VA, April 15-17.

"Roller Bearing Defect Detection with Multiple Sensors," Billington, S.A., Li, Y., Kurfess, T.R., Liang, S.Y., Danyluk, S., *1997 International Mechanical Engineering Congress and Exposition*, Dallas, TX, TRIB- Vol. 7, R. Cowan, ed. pp. 31-36, November 1997.

Background

Need:

- real-time, on-line techniques to determine the current health of rolling-element bearings.
- diagnostic techniques (the foundation of prognostic efforts) that may be used to predict the useful life of bearings.

Mission:

- to fully utilize and integrate sensors in an intelligent fashion.
- to develop a compact self-contained processing package that can be attached to an array of sensors for use in monitoring bearing health.

Experimental Diagram

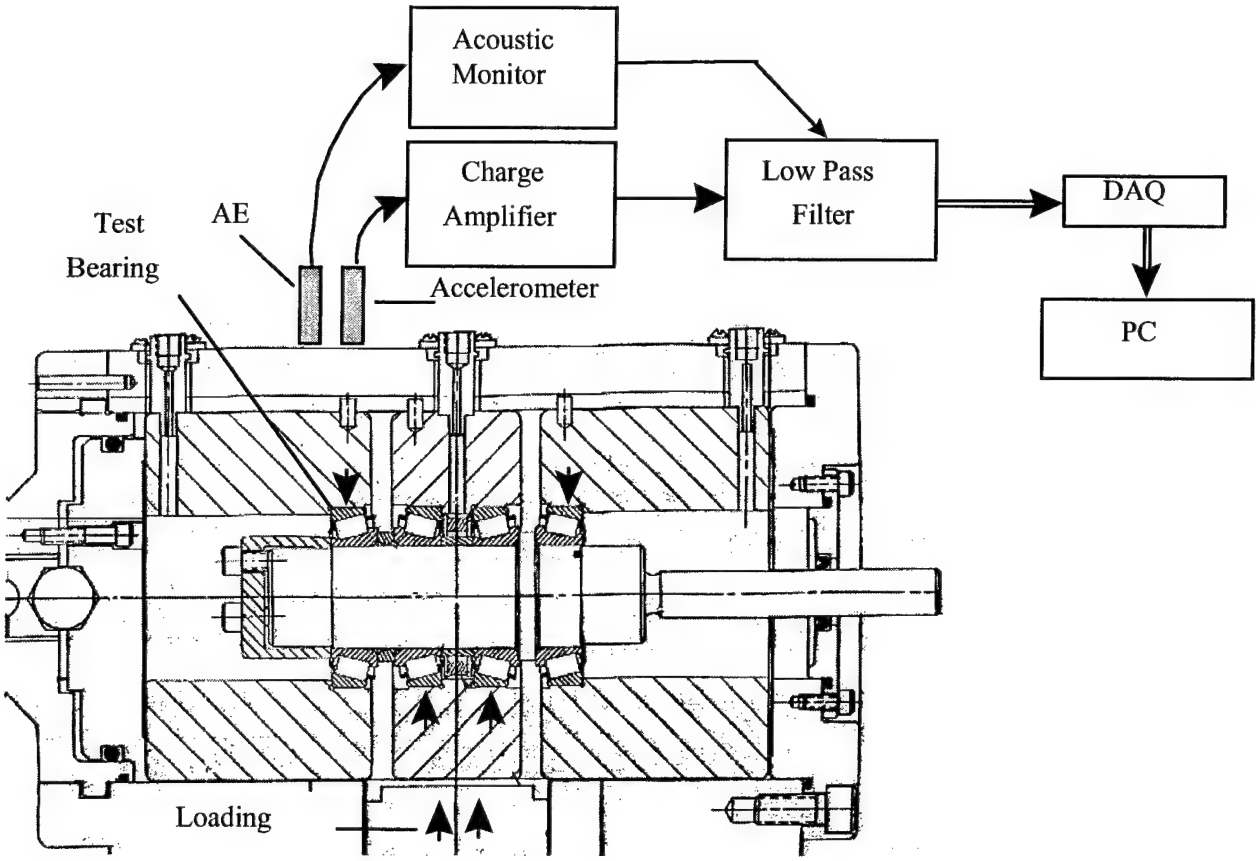

Sensor Placement

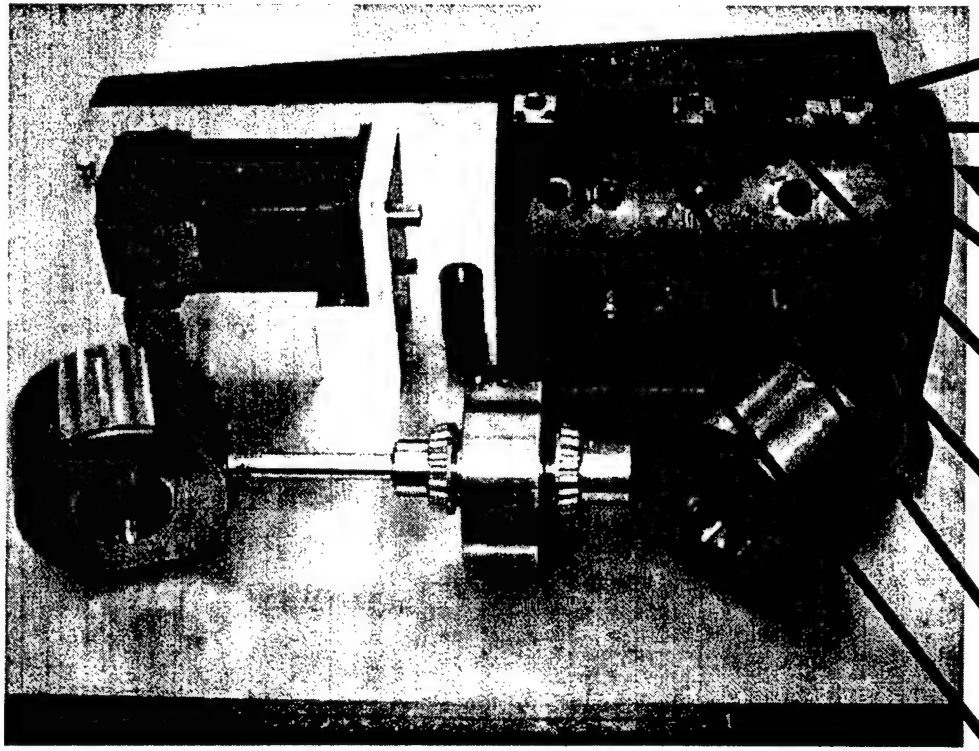

Signal Processing

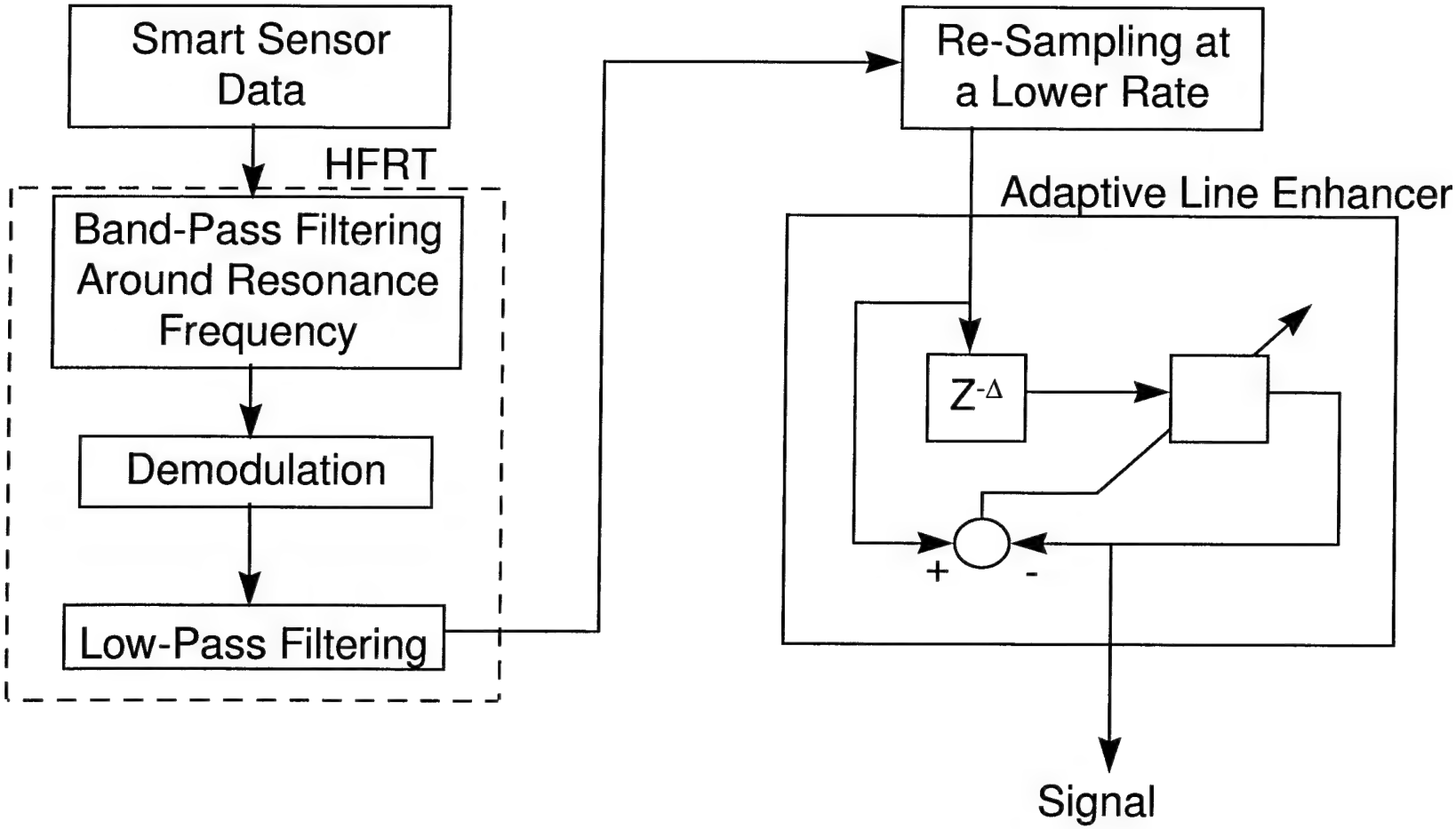

Speed-Load Effects

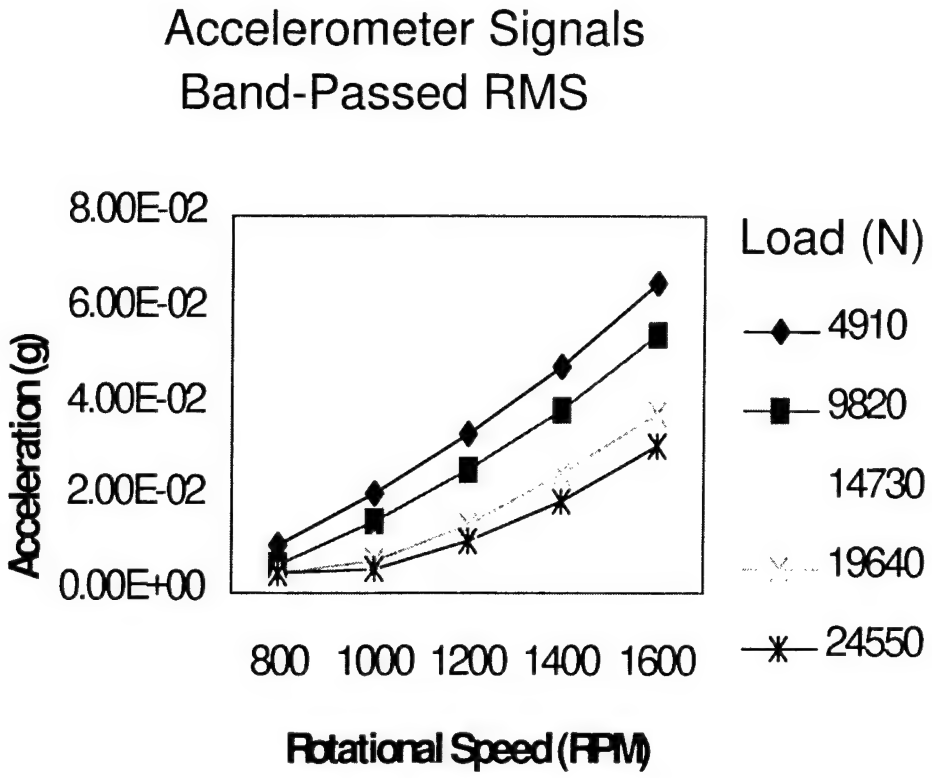

Increasing Speed, Increasing RMS

- Linear increase in number of Outer Race impacts.
- Similar increase over all loads.

Increasing Load, Decreasing RMS

- Increasing load reduces signal levels of statistical indicators.
- ~50% error in diagnostic metric.

Accelerometer positioned directly over the bearing on the housing.

Speed-Load Effects

Accelerometer Signals
Band Passed RMS

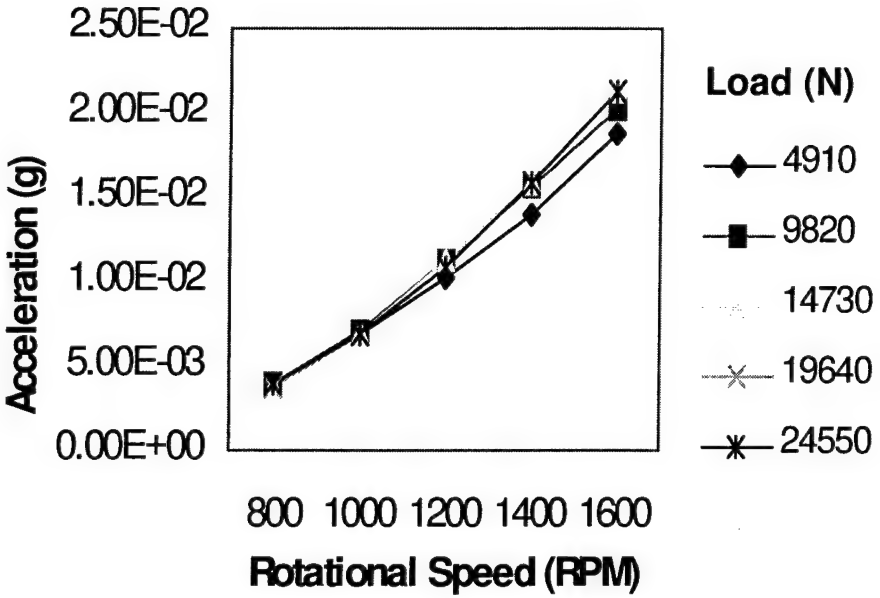

Acoustic Emission
RMS

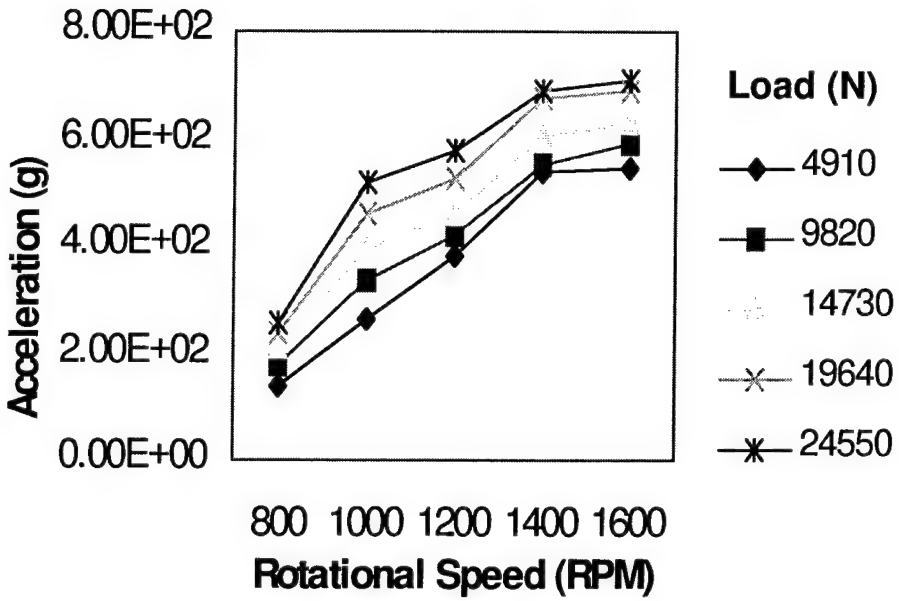

Accelerometer location in unloaded zone of housing.

Relationship is explained by dynamic model.

Acoustic emission sensor directly over bearing on housing.

Contact-area sensitive.

System Response is Piecewise Linear

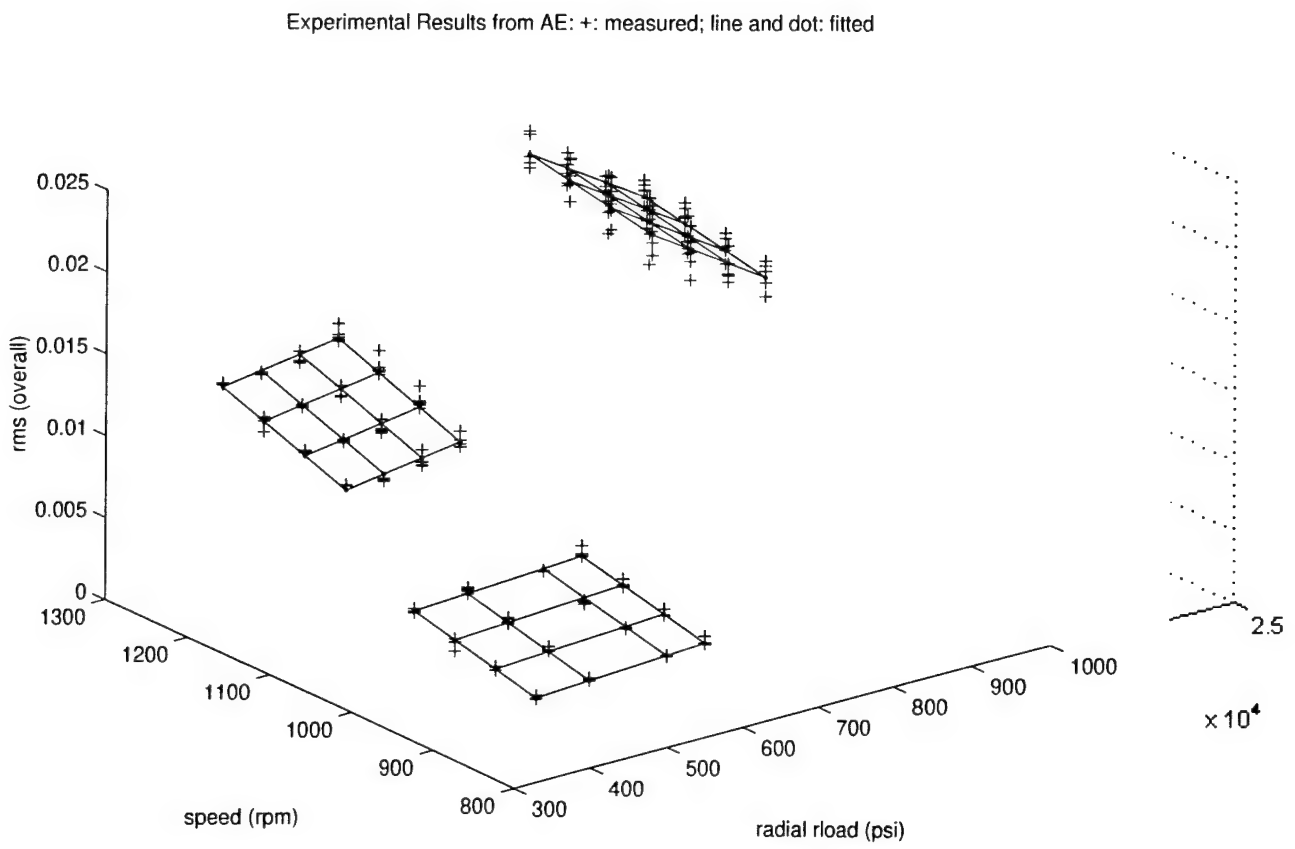

Condition Estimation

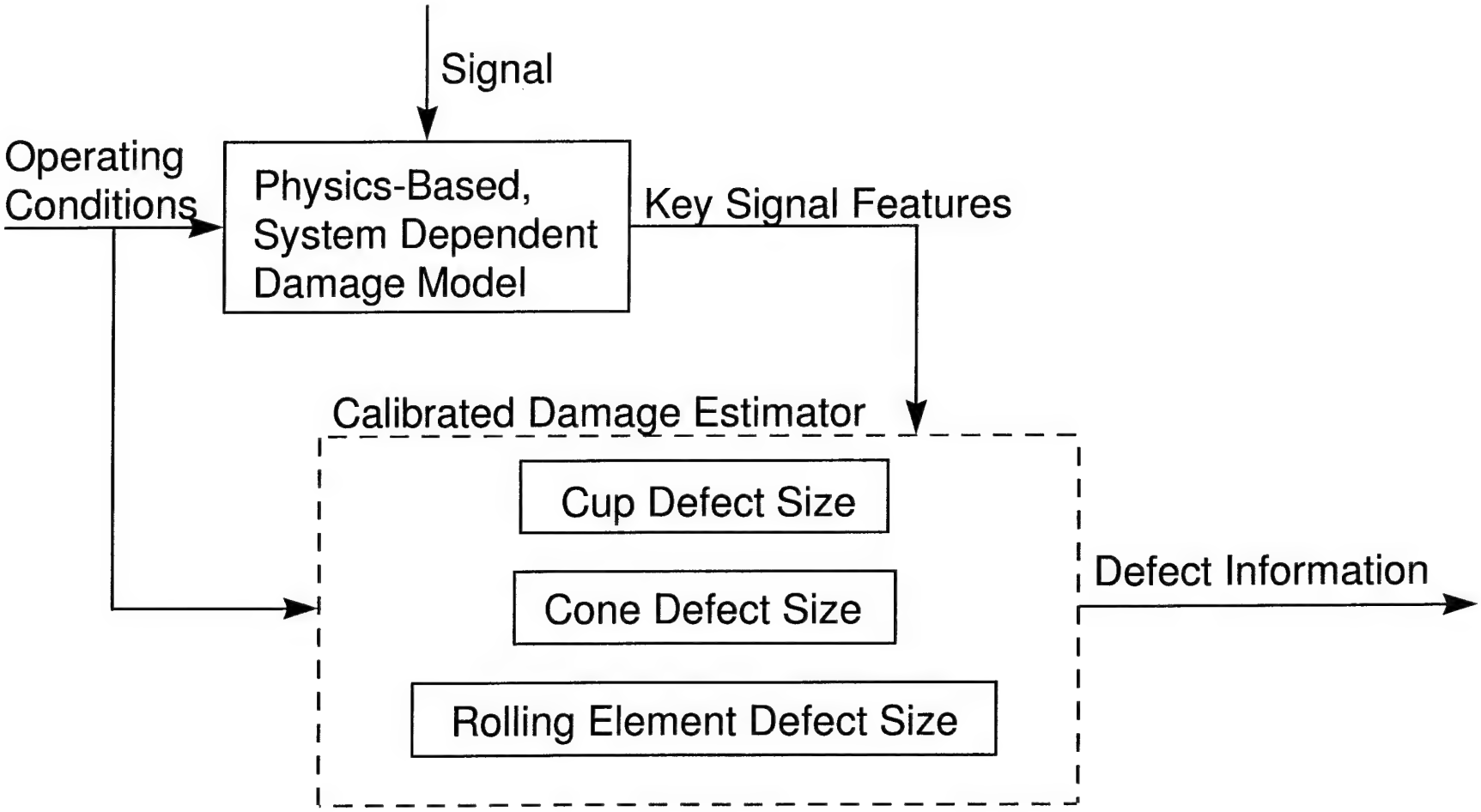

Evolution of Diagnostics to Prognostics

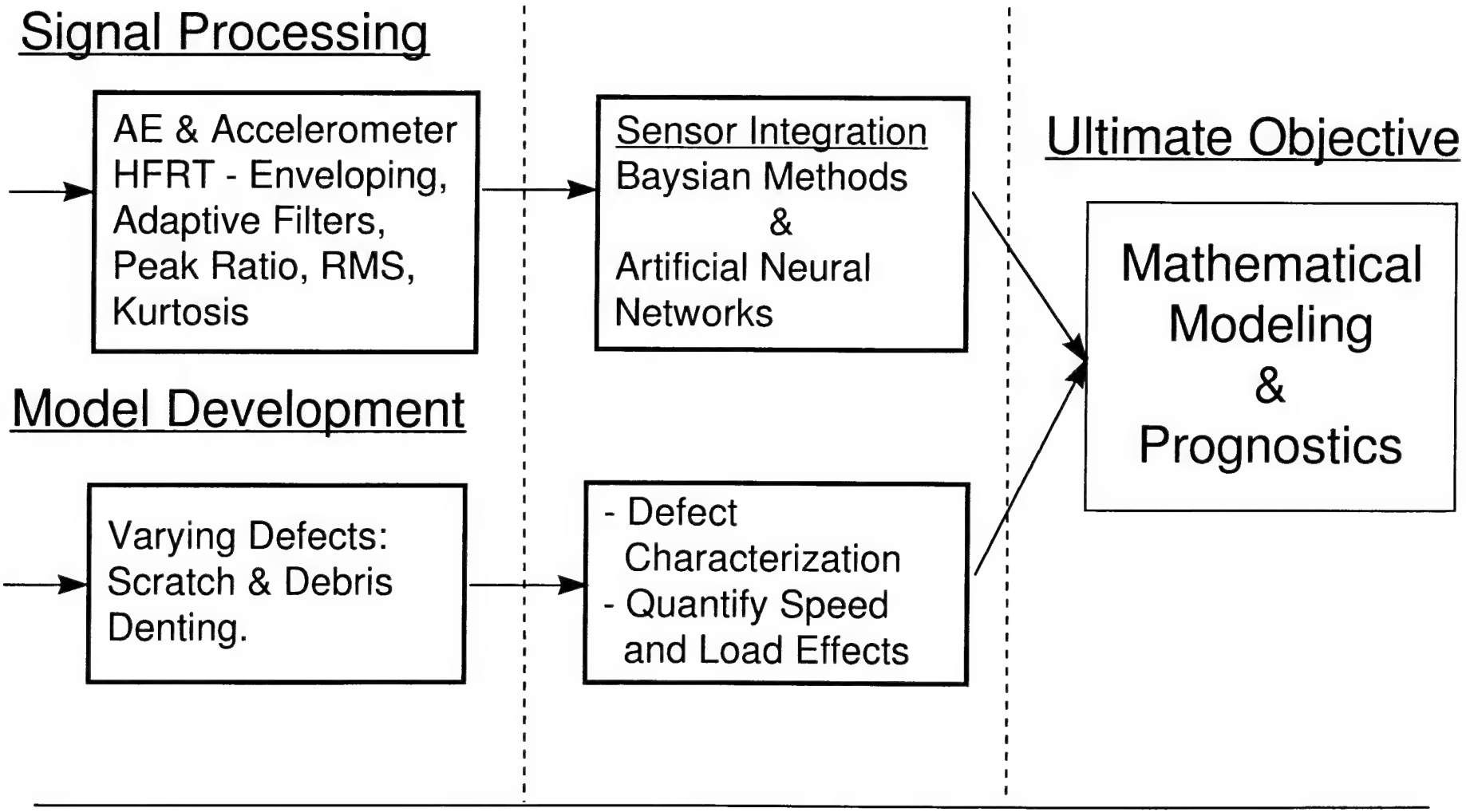

Initial Prediction Results

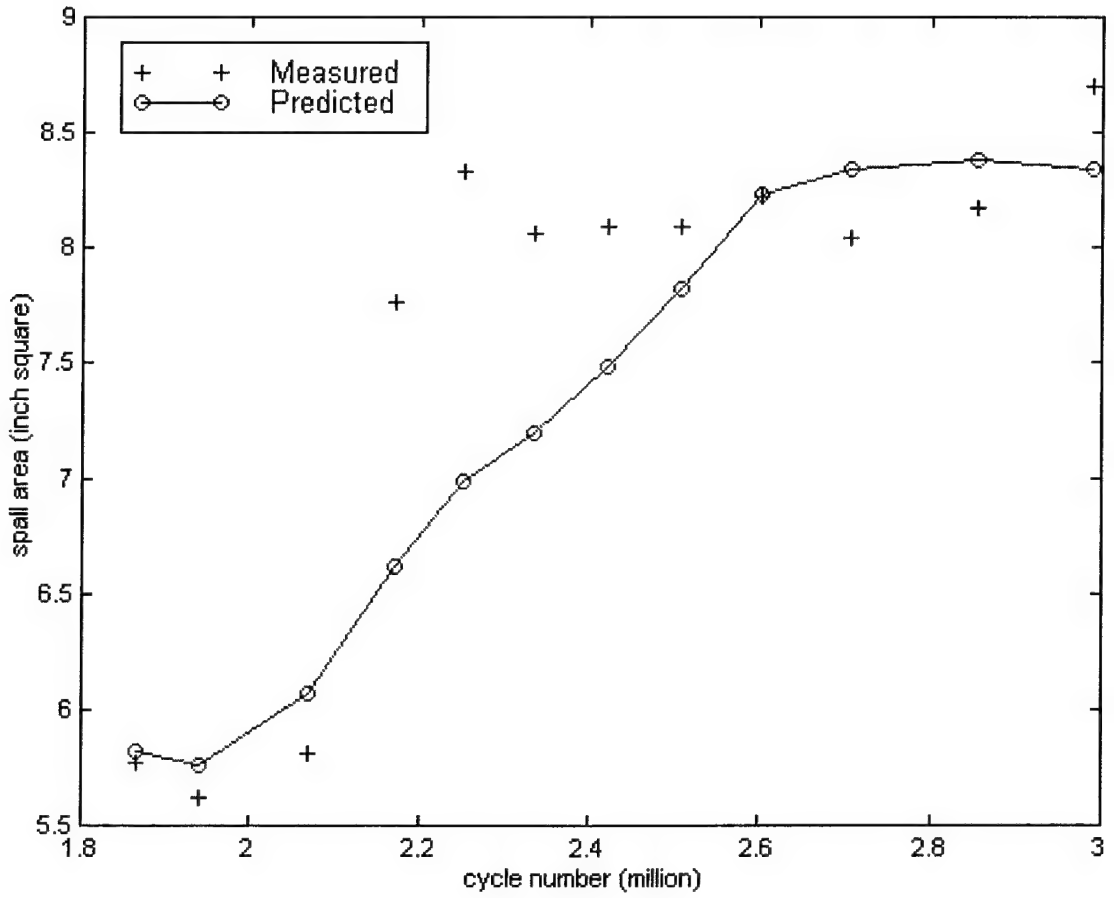

Adaptive Prognostics

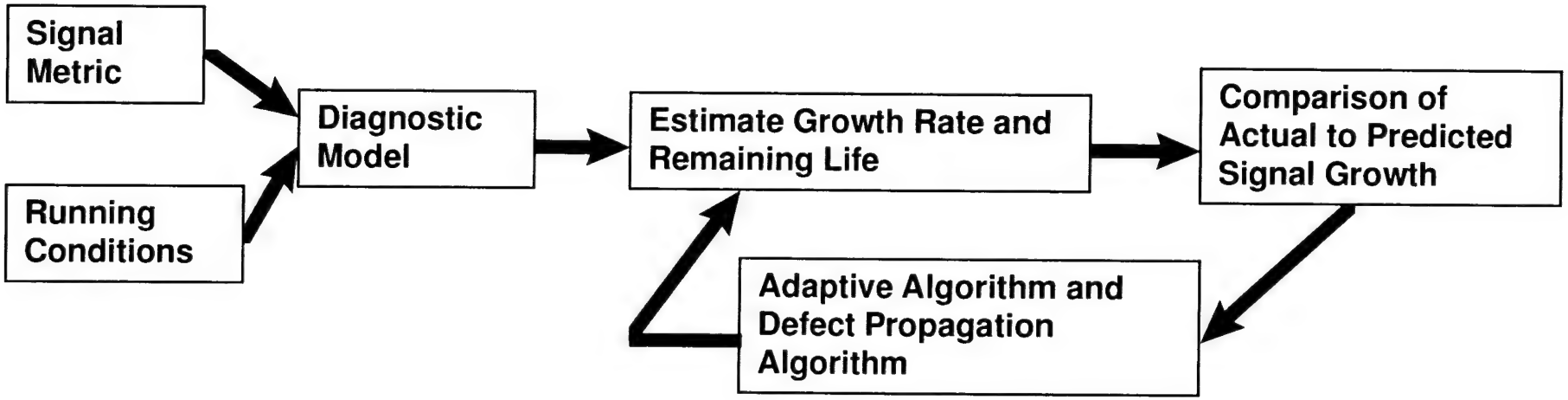

Estimates damage level with diagnostic model.

Estimates bearing damage growth according to signal growth rate.

Conclusions

- Sensor placement and type yields drastically different effects for changes in rotational speed and load.

- Speed and load relationships can be explained by dynamic models.

- Signal processing techniques are affected differently by changes in rotational speed and load.

- A piecewise linear model can be used to relate speed and load effects.

- Adaptive prognostics are calibrated on signal growth rate.

Integrated Microsensors for Aircraft Fatigue and Failure Warning

Dennis Polla, Mostafa Kaveh, Ahmed Tewfik, Ramesh Harjani, William Robbins, William Gerberich, Lorraine Francis, Susan Mantell, and Kevin Buckley

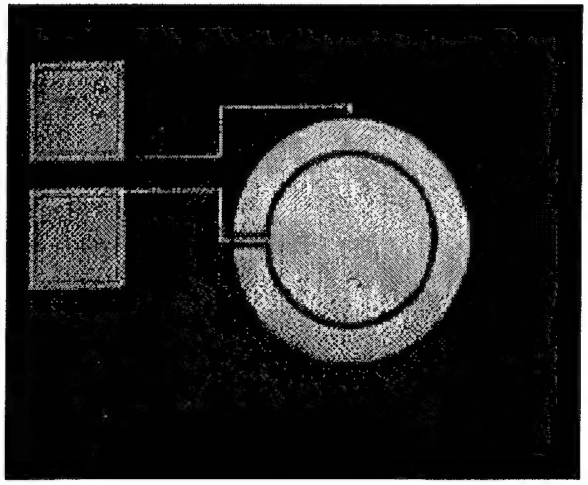

Center for Integrated Diagnostics

Georgia Institute of Technology, University of Minnesota,and Northwestern University

Office of Naval Research

MEMS, Signal Processing, and Integrated Circuits

- **Project A**
  - ***MEMS***

    Dennis Polla (ECE), William Robbins (ECE), Lorraine Francis (Mat Sci), Susan Mantell (ME)

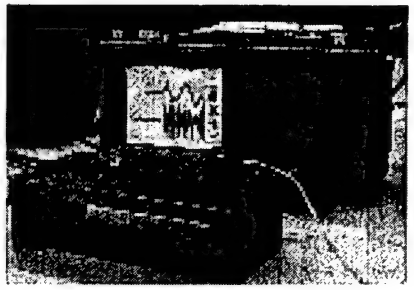

- **Project B**
  - ***Signal Processing***

    Mostafa Kaveh (ECE) , Ahmed Tewfik (ECE), Kevin Buckley (ECE), William Gerberich (Mat Sci)

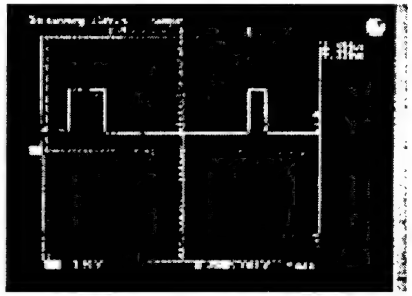

- **Project C**
  - ***Telemetry and Sensor Interface Electronics***

    Ramesh Harjani (ECE)

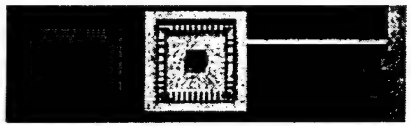

Year 3 Accomplishments

- Piezoelectric materials technology has been developed for both AE sensors and vibration monitors.
- CMOS signal processing electronics have been developed as AE microsensor interfaces.
- AE microsensors have been tested in laboratory fatigue experiments.
- AE signal detection, pre-filtering, and deconvolution algorithms have been developed.
- AE microsensors and signal processing algorithms have been demonstrated with crack propagation due to fatigue.
- A general-purpose MEMS telemetry microchip technology has been developed and tested.

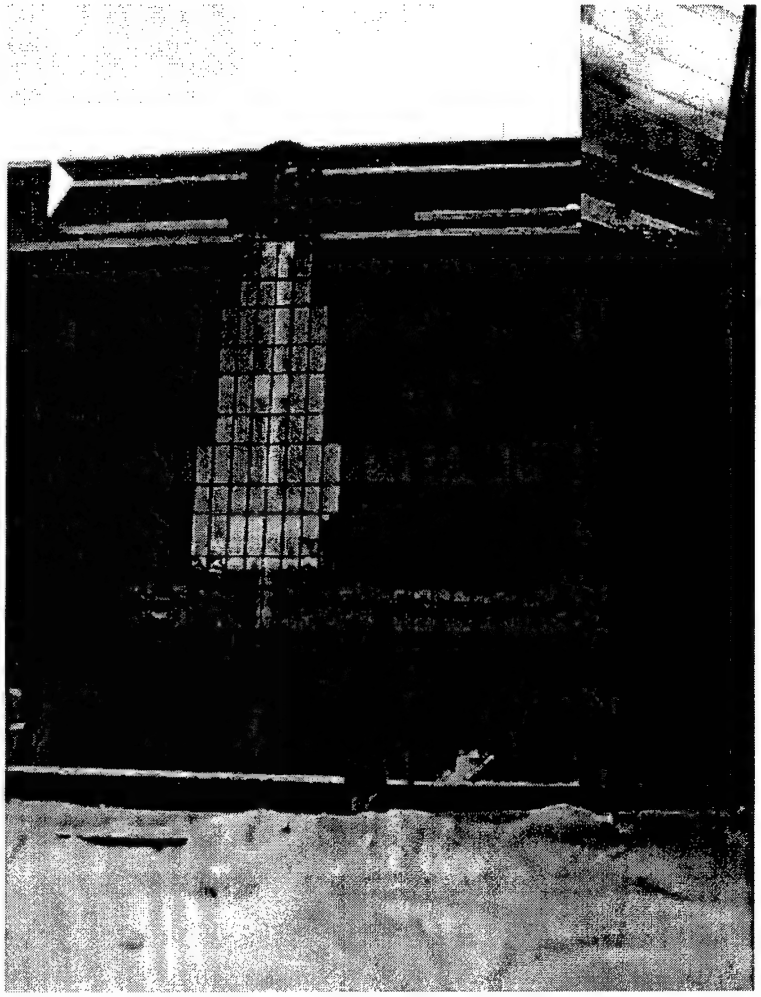

Integrated Microsensors for Aircraft Fatigue and Failure Warning

Objective

Develop solid-state microsensors and associated signal processing methods for direct sensing, analysis, and real-time diagnosis of critical aircraft components.

Approach

Develop integrated systems with multi-functional sensors and signal processing electronics.

MEMS-Based Sensors

- Piezoelectric Acoustic Microsensors
- Cantilever Microbeam Vibration Monitors
- Strain Sensors
- Temperature Sensors

Integrated Circuits

- High-Frequency Charge Amplifiers
- Telemetry Circuits

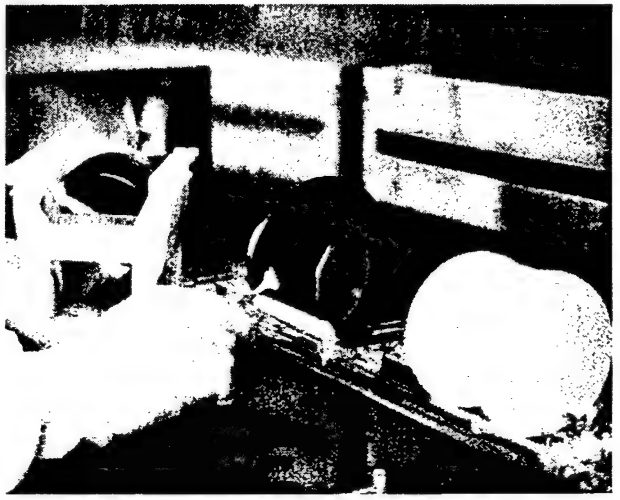

Structural-Health Monitoring Coupon

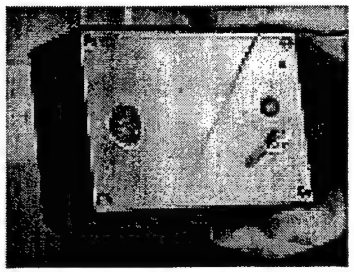

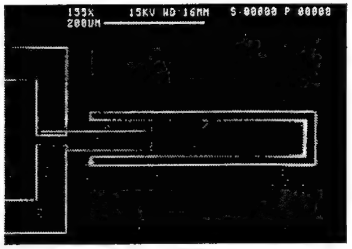

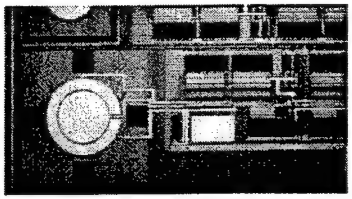

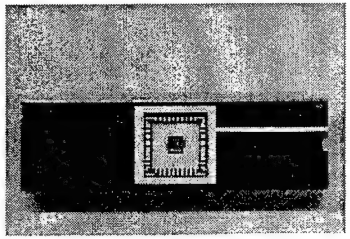

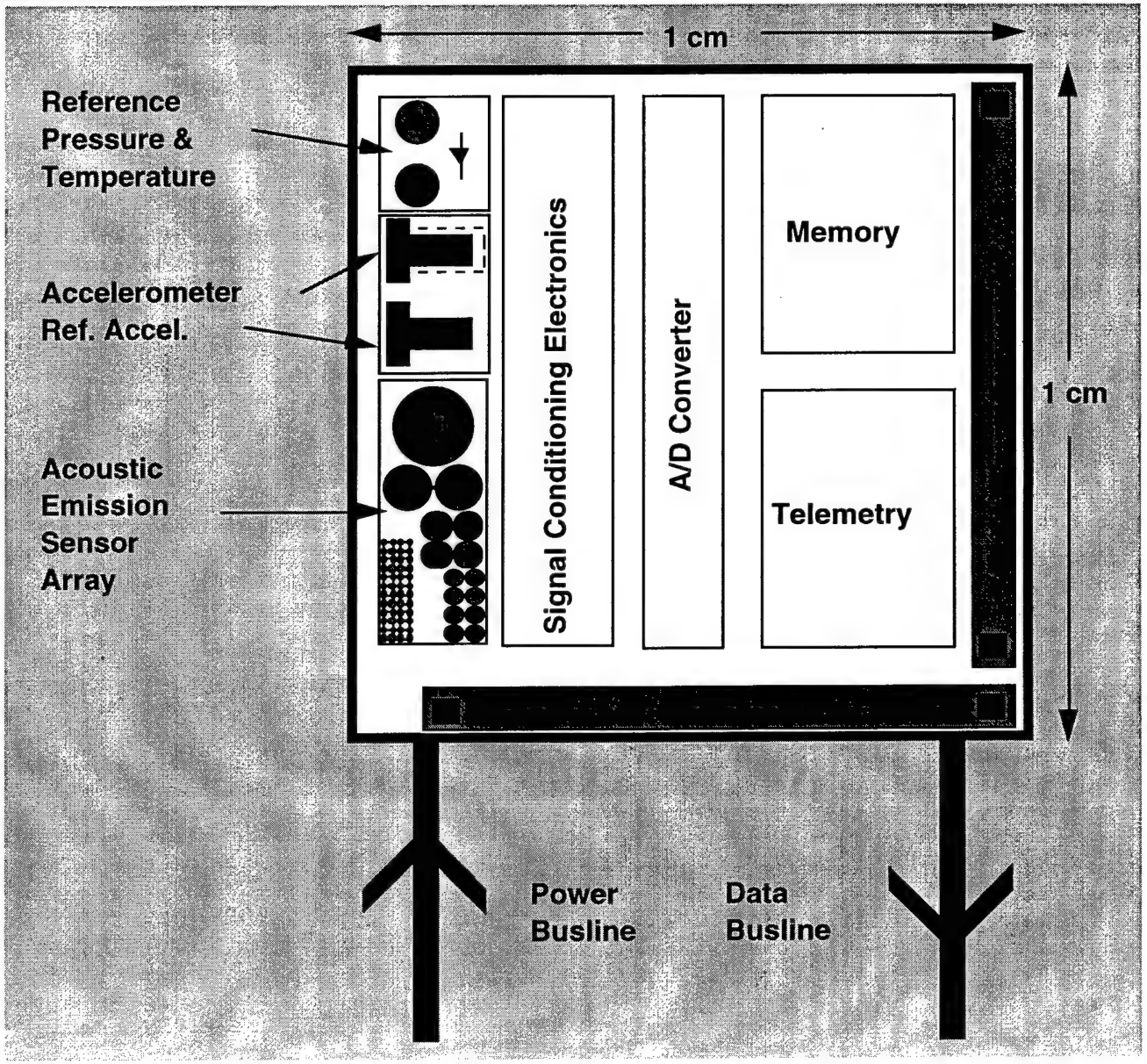

Project Overview

Microcrack Physics

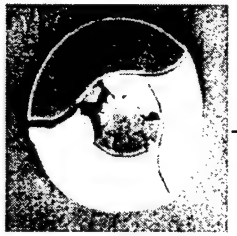

Signal Analysis

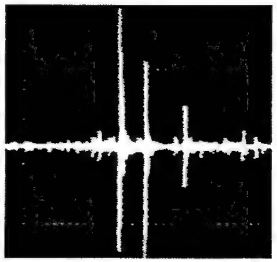

Microsensor Design

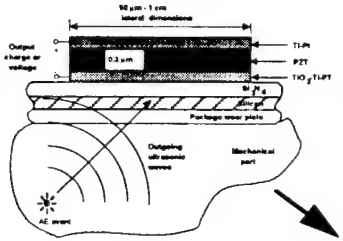

Discrete Sensor Fabrication

Testing

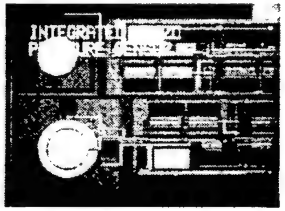

Piezo Materials Synthesis

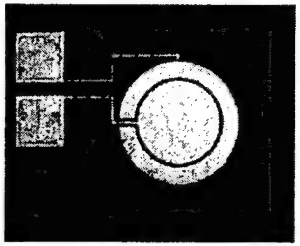

Integrated Circuits

Process Design

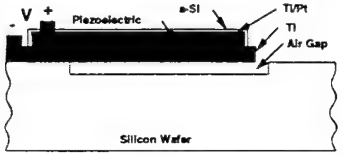

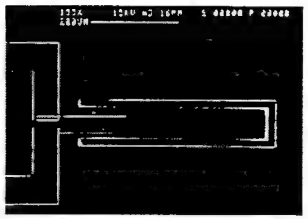

MEMS

Piezoelectric Thin Film Processing

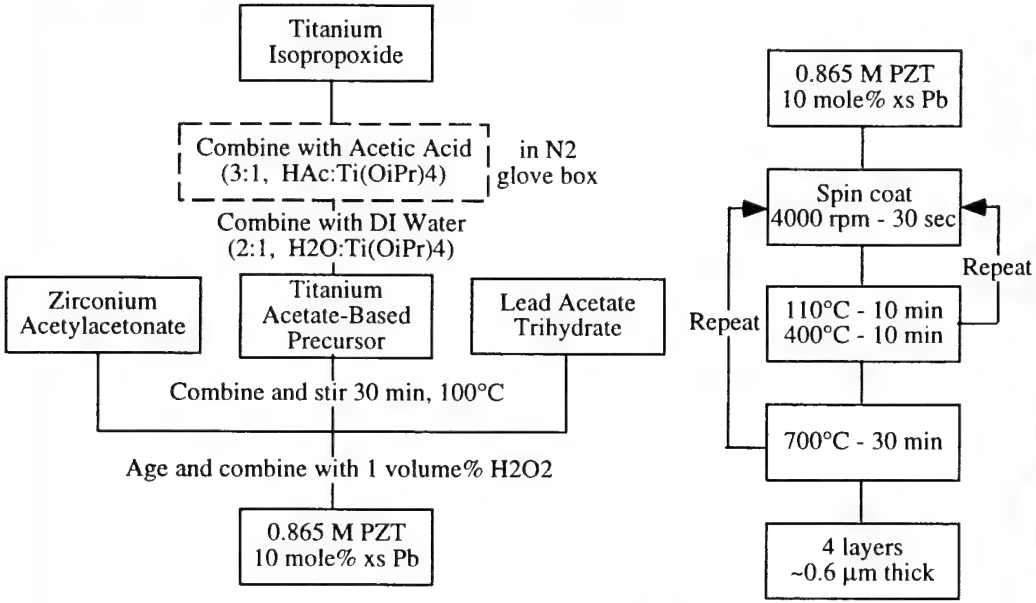

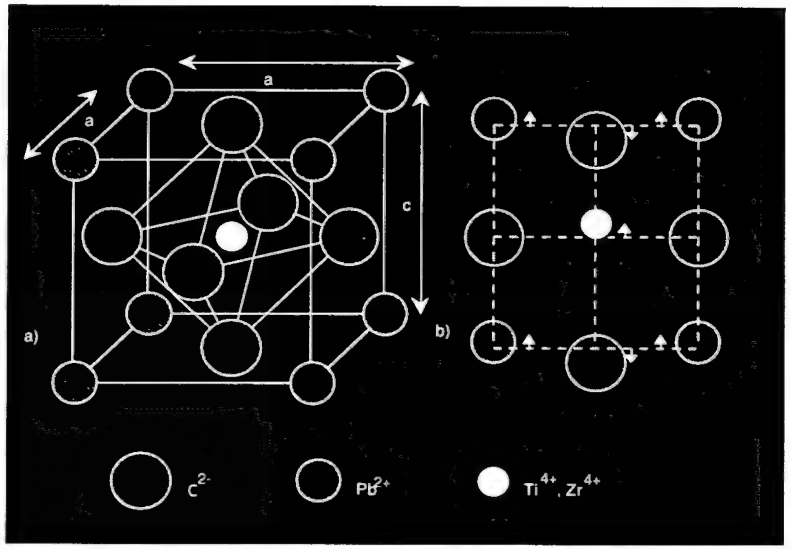

Solution Aging*	Dielectric Constant	Loss Tangent	Remanent Polarization ($\mu C/cm^2$)	Coercive (kV/c
6 days (20°C)	835	0.040	24.13	54.9
10 days (20°C)	726	0.048	21.32	61.2
14 days (20°C)	898	0.048	27.96	57.4
2 days (60°C)	959	0.039	21.39	40.7
2 days (60°C) then frozen for 1 week	948	0.049	27.18	38.0

*includes time before and after addition of H_2O_2

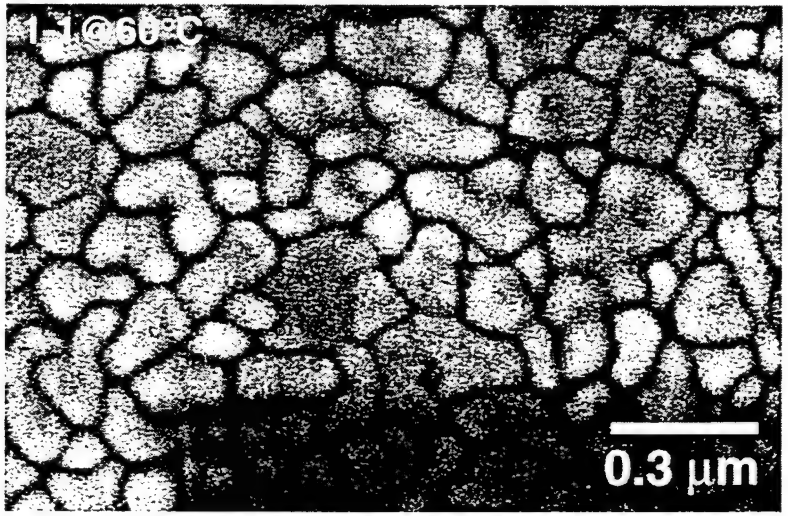

AE Microsensor Needs

- Mechanical components in many naval helicopters nearing design limit of number of stress cycles.
- Parts becoming fatigued and microcracks may develop. Growth of microcracks under further loading results in component failure.
- Development of microcracks accompanied by acoustic AE events.
- If AE events can be detected, fatigued parts can be removed from service before catastrophic failure.
- AE sensors can detect these emissions.
- Arrays of AE sensors mounted on critical parts would significantly increase likelihood of detection of microcrack generation and growth.
- Existing AE sensors lack sufficient bandwidth, and are too large, fragile, and expensive.
- AE microsensors based on MEMS technology offer a potential solution.

AE Microsensor Design Goals

- Small size so that arrays of sensors are feasible. 5-10 mm and dia. 2-7 mm thick.
- Bandwidth: 50 kHz to 10 MHz.
- Sensitivity: 10^6 [V/unit strain] (prior to post-sensor amplification)
- Minimum detectable strain: 10^{-10}
- Power requirements (on-board charge amplifier): < 5 V at 1 mA (< 5 mW)
- Two-wire interconnect (ground and combined dc power-signal line)
- Temperature range: -50 to +100 C

AE Microsensor Design

- Voltage output (D = 0) Charge Output (E = 0)

  $D = \varepsilon E + d T$; $E = \frac{V}{t} = -\frac{d}{\varepsilon} T$ $D = \varepsilon E + e S$; $D = \frac{Q}{A} = e S$

- AE sensor parameters: $d = 3 \times 10^{-10}$ [m/V] ; $t = 1\ \mu m$
  $e \approx 10$ [coul./m^2] ; $\varepsilon \approx 1000\ \varepsilon_o$; $A = 1\ mm^2$; $Y = 5 \times 10$ [N/m^2]

- $\frac{V}{T} = 3 \times 10^{-8}$ [V-m^2/N] $\frac{Q}{S} = 10^{-5}$ [coul. per unit strain]

- Commercial AE sensors have $\frac{V}{T} = 3 \times 10^{-4}$ [V-m^2/N]
  (1 cm thickness)

- Conclusion - significant amplification needed for thin film AE sensor

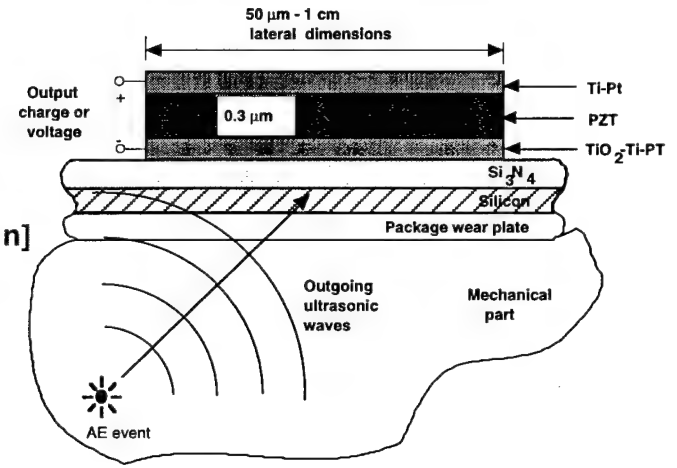

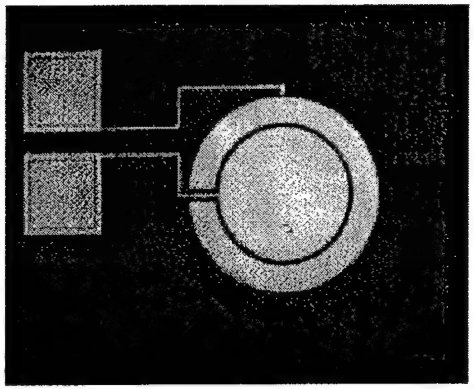

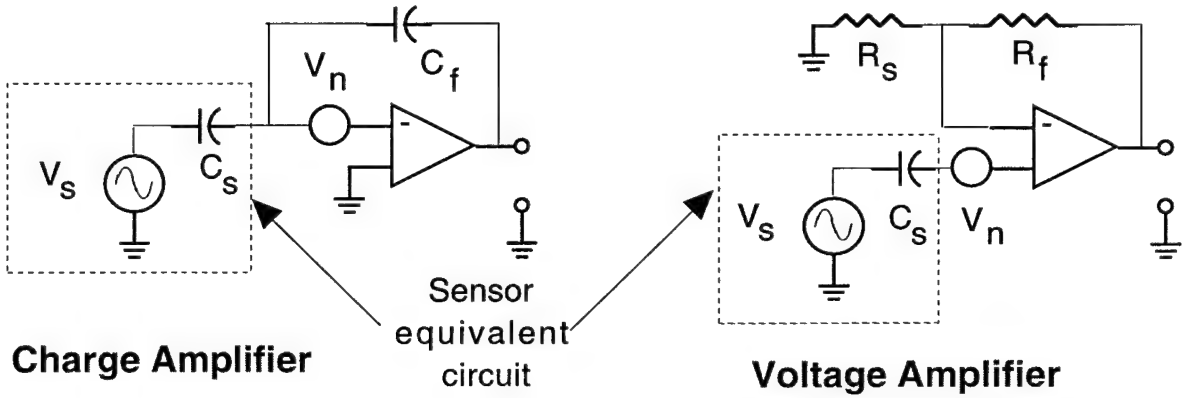

Integrated CMOS Amplifier

Successfully tested as a charge amplifier using off-chip components. Power = 1 mW (5 V at 200 μA). 100 MHz open loop unity gain frequency.

Die with CMOS op amp. Die dimensions are 2 mm by 2mm.

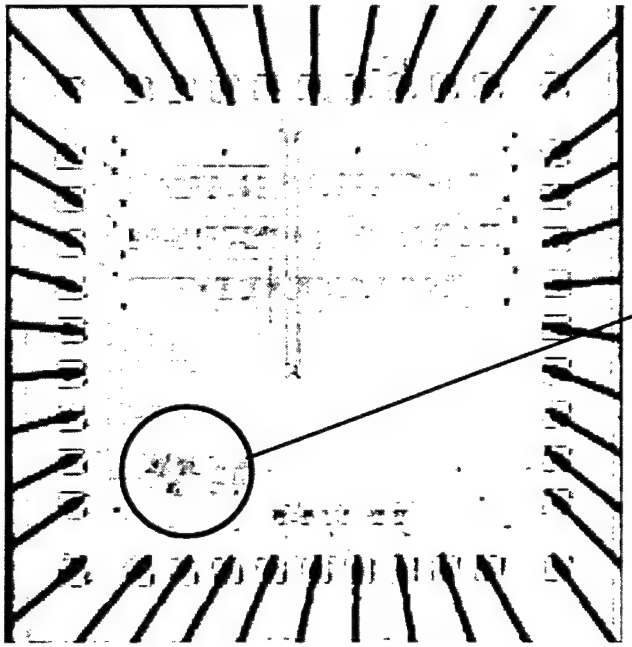

Magnified view showing op amp.

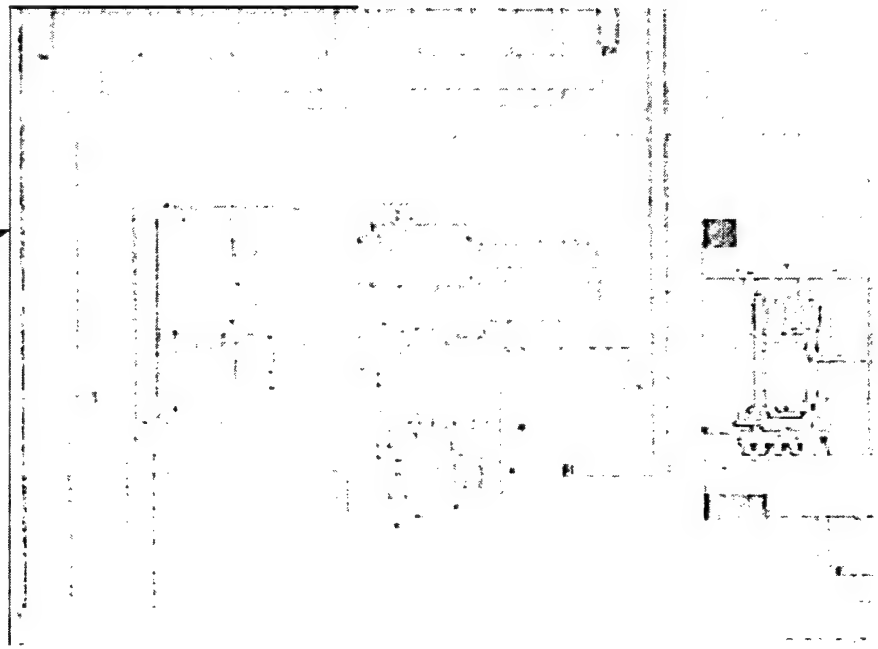

Charge Amplifier Characteristics

- PZT thin films for AE microsensors fabricated on Si wafer
- Miniature charge amplifier developed.
- AE sensors fabricated with integral charge amplifiers.
- Characterization of AE sensors in progress.
- Microsensors used in fatigue experiments.
- Integrated CMOS op amp successfully tested. Basis of integrated charge amp
- Fabrication of an improved integrated CMOS charge amplifier is underway.

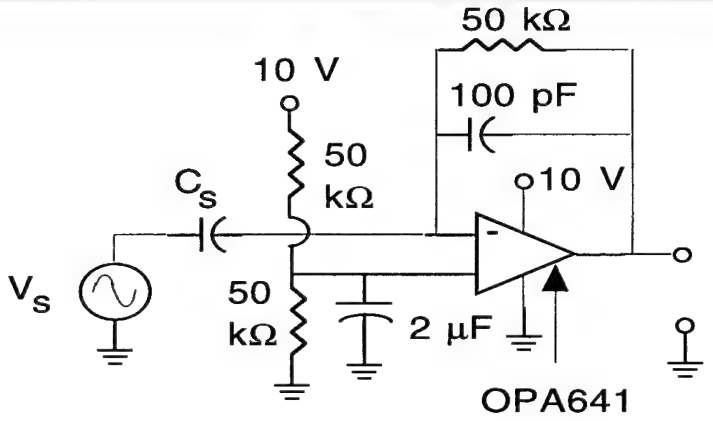

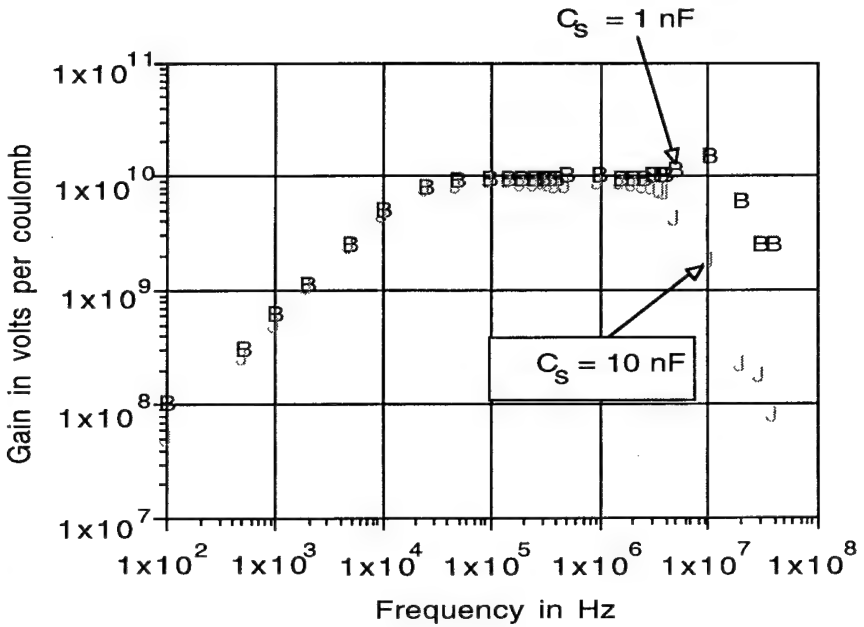

AE Microsensor Packaging

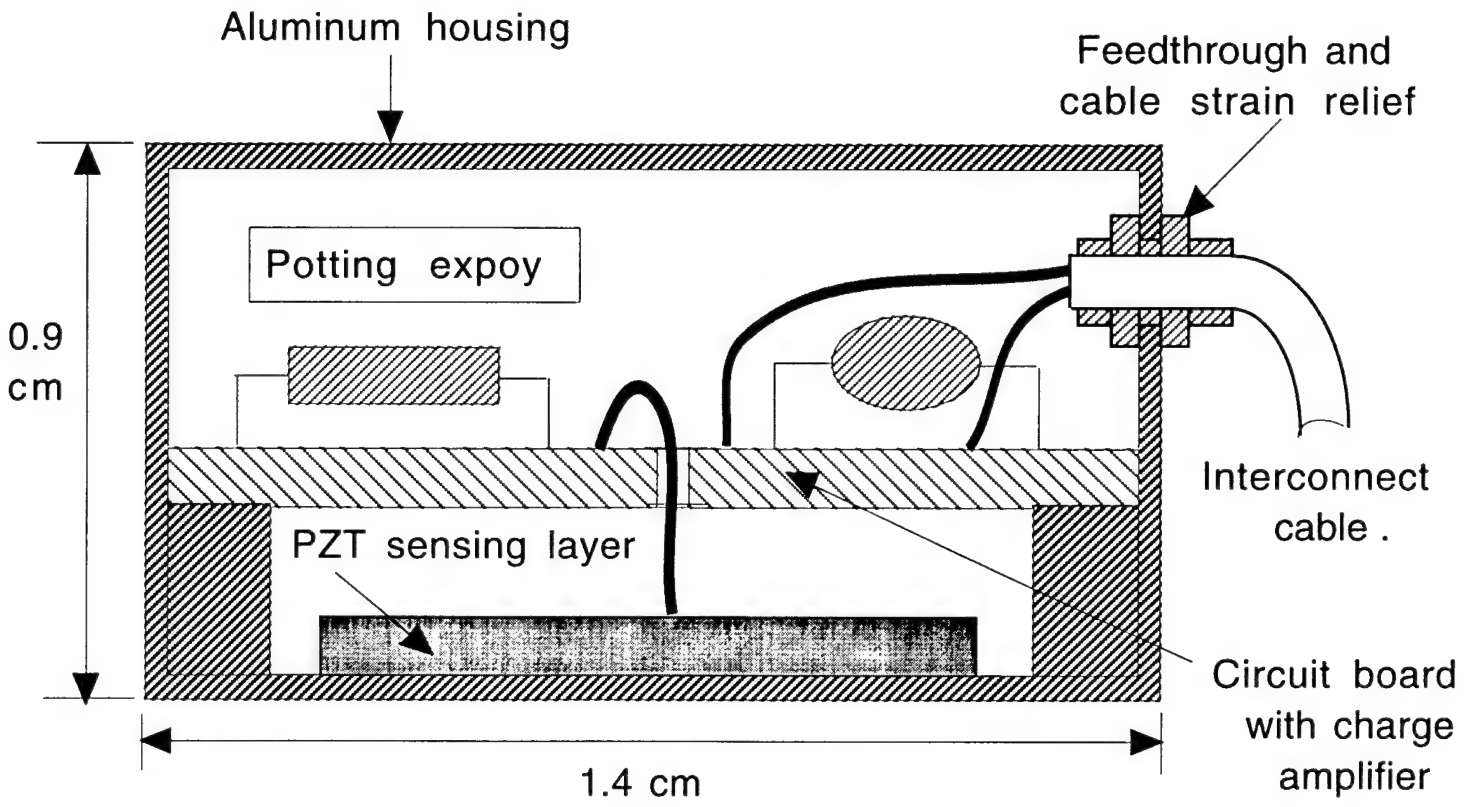

- 1.4 cm diameter by 0.9 cm height set by amplifier surface mount components on circuit board.

AE Microsensor Results

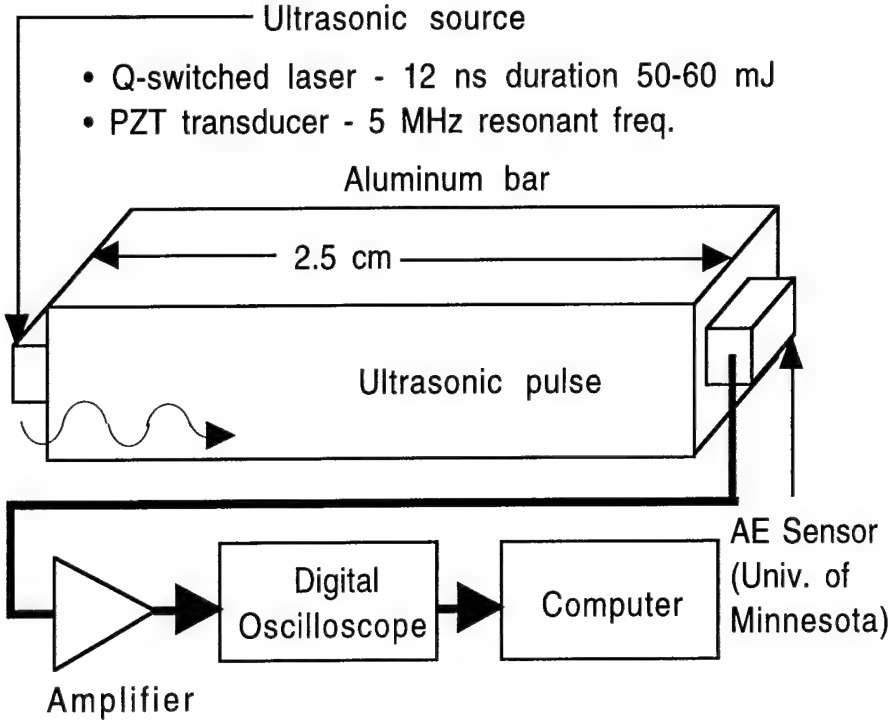

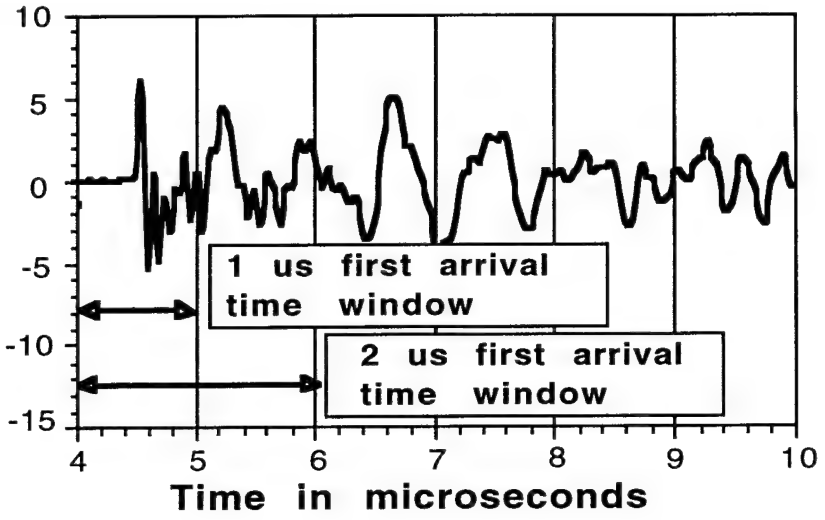

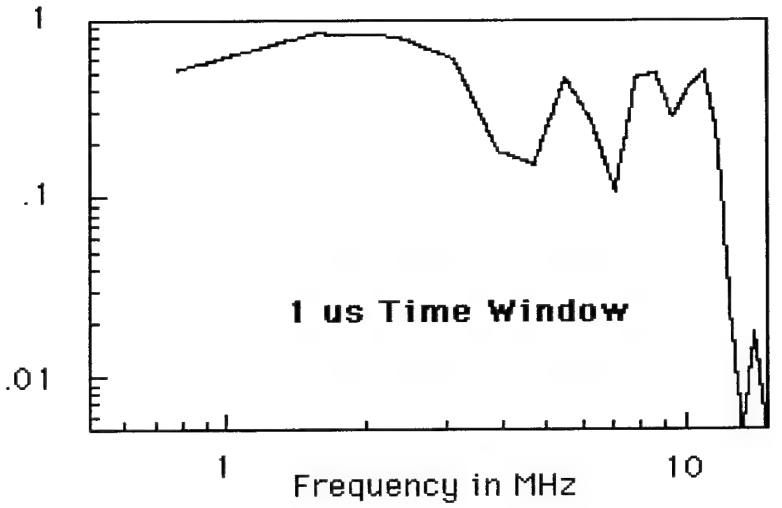

Testing in collaboration with Dr. Sridhar Krishnaswamy
Northwestern University

AE Microsensor Results in Fatigue Test

U. of MN AE sensor response to crack growth in 4330 stainless steel sample.

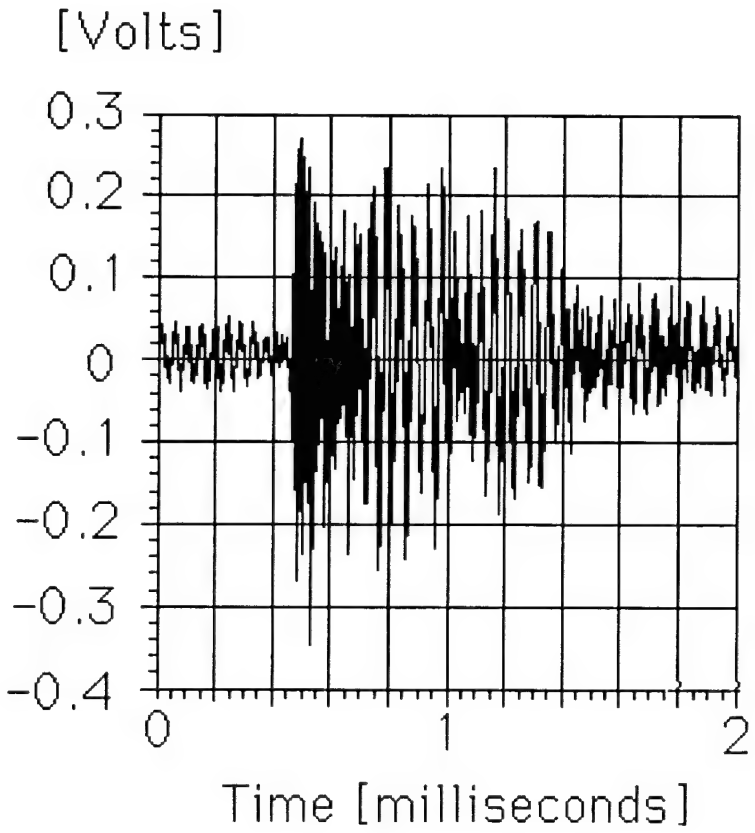

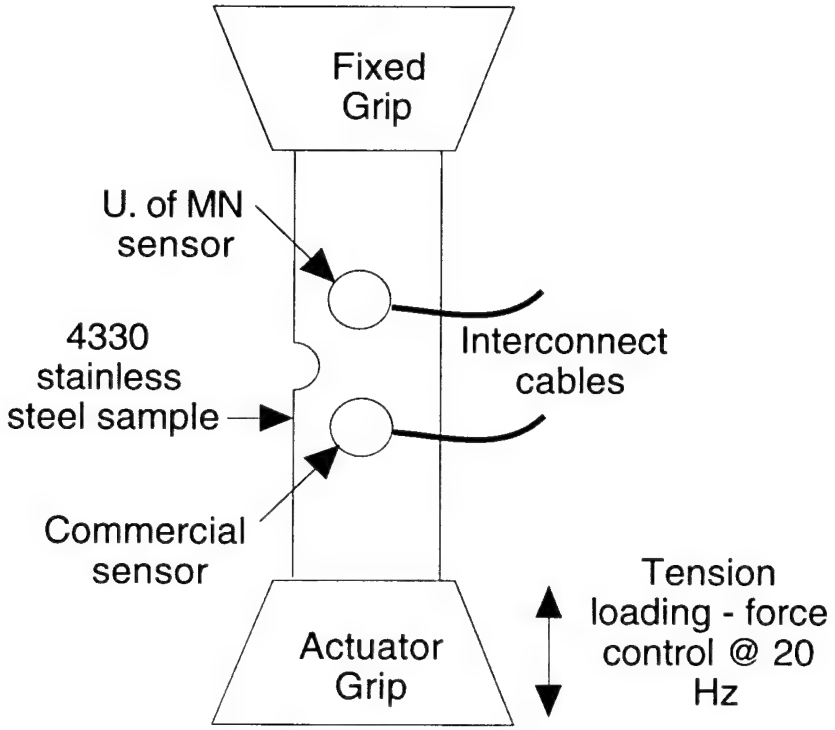

Experiments carried out at Georgia Tech

AE Microsensor Summary

- AE microsensor designed, fabricated, and tested.
- Integration with a charge amplifier built into the sensor package demonstrated.
- Initial test results indicate bandwidth approaching 10 MHz.
- Characterization of AE microsensors demonstrated in fatigue testing experiment.
- Functional integrated CMOS-based charge amplifiers demonstrated.

Multi-University Center for Integrated Diagnostics

Key Microelectronics Technologies

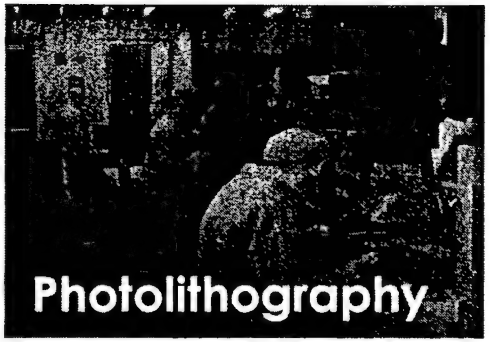

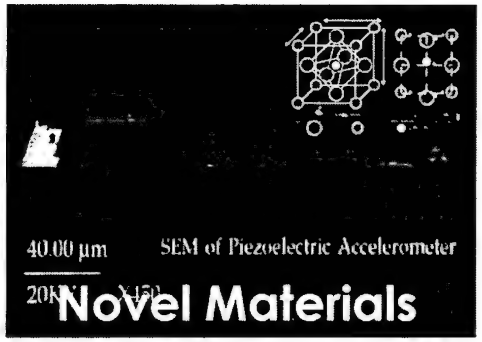

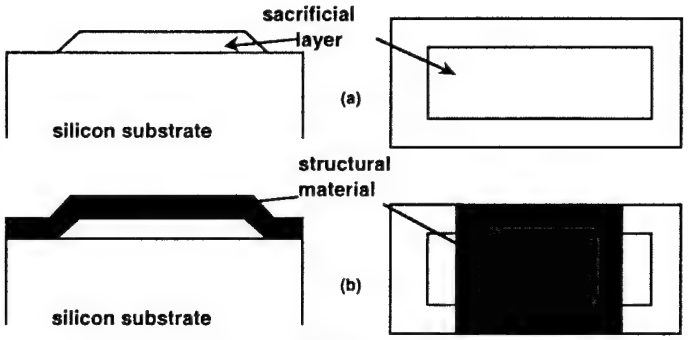

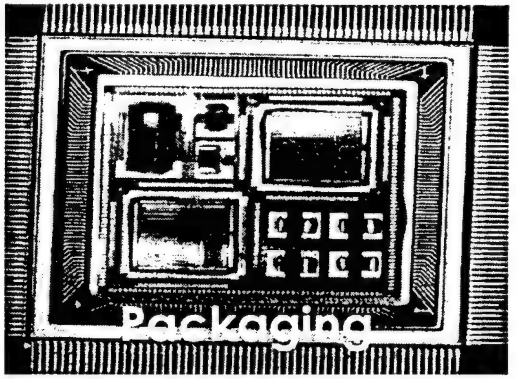

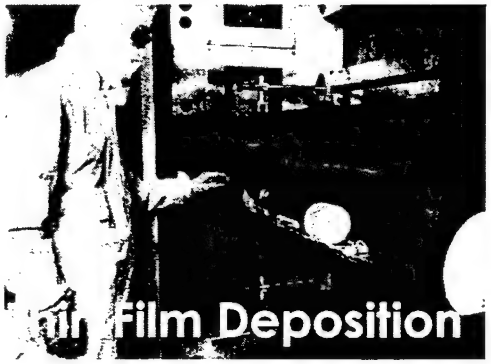

Solid-State Microsensing

Vibration Microsensor Fabrication

1. Etch silicon wafer by RIE and fill it with PSG by LPCVD.

2. Deposit Low stress Si_3N_4 and polysilicon by LPCVD.

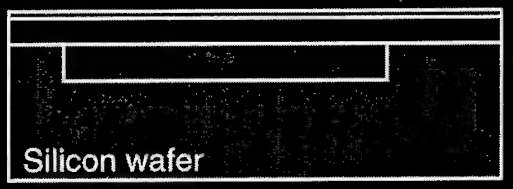

3. Deposit PZT thin film by MOD and top electrode by sputtering.

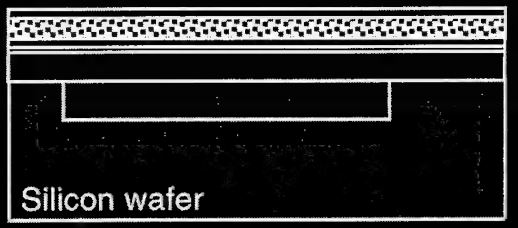

4. Patterning top electrode & PZT and bottom electrode by ion milling and deposit encapsulation layer.

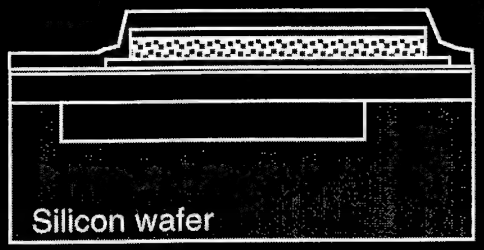

5. Etching holes through PSG by RIE to etch PSG and patterning the beam structure.

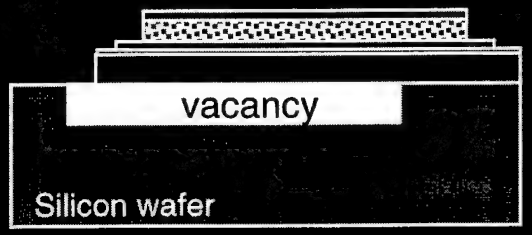

(Side view)

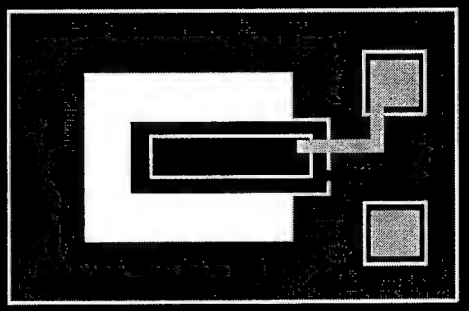

(Top view)

Vibration Monitors

Key Aspects

- PZT thin films deposited on silicon nitride cantilever microbeams
- Solid-state surface micromachining
- Compatibility with AE microsensors and CMOS electronics
- Frequency response set by microbeam dimensions
- Low power
- Very low weight

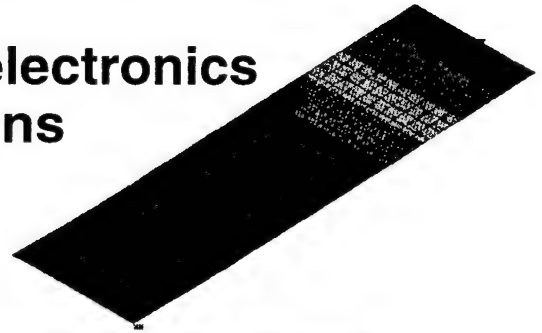

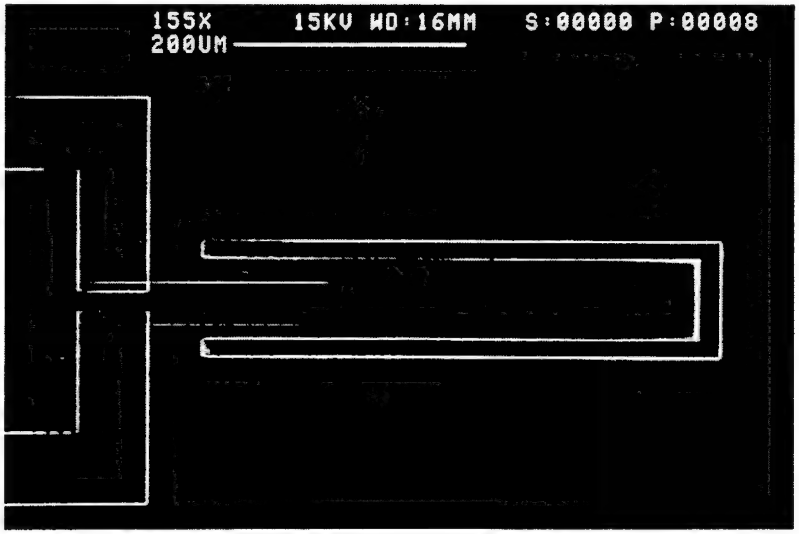

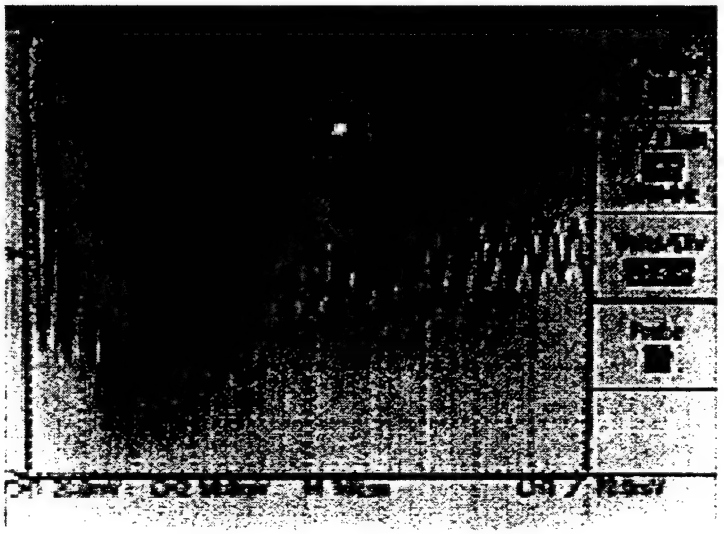

Future Plans: Microsensors

- Continued fatigue testing of integrated microsensors (with additional functionality including improved charge amplifiers and telemetry).
- "Coupon" integration of components.
- Variable temperature testing
- Testing of coupon system on a helicopter.
- Integration of MEMS with thin film batteries.

Signal Processing

Fault Monitoring using Acoustic Emissions

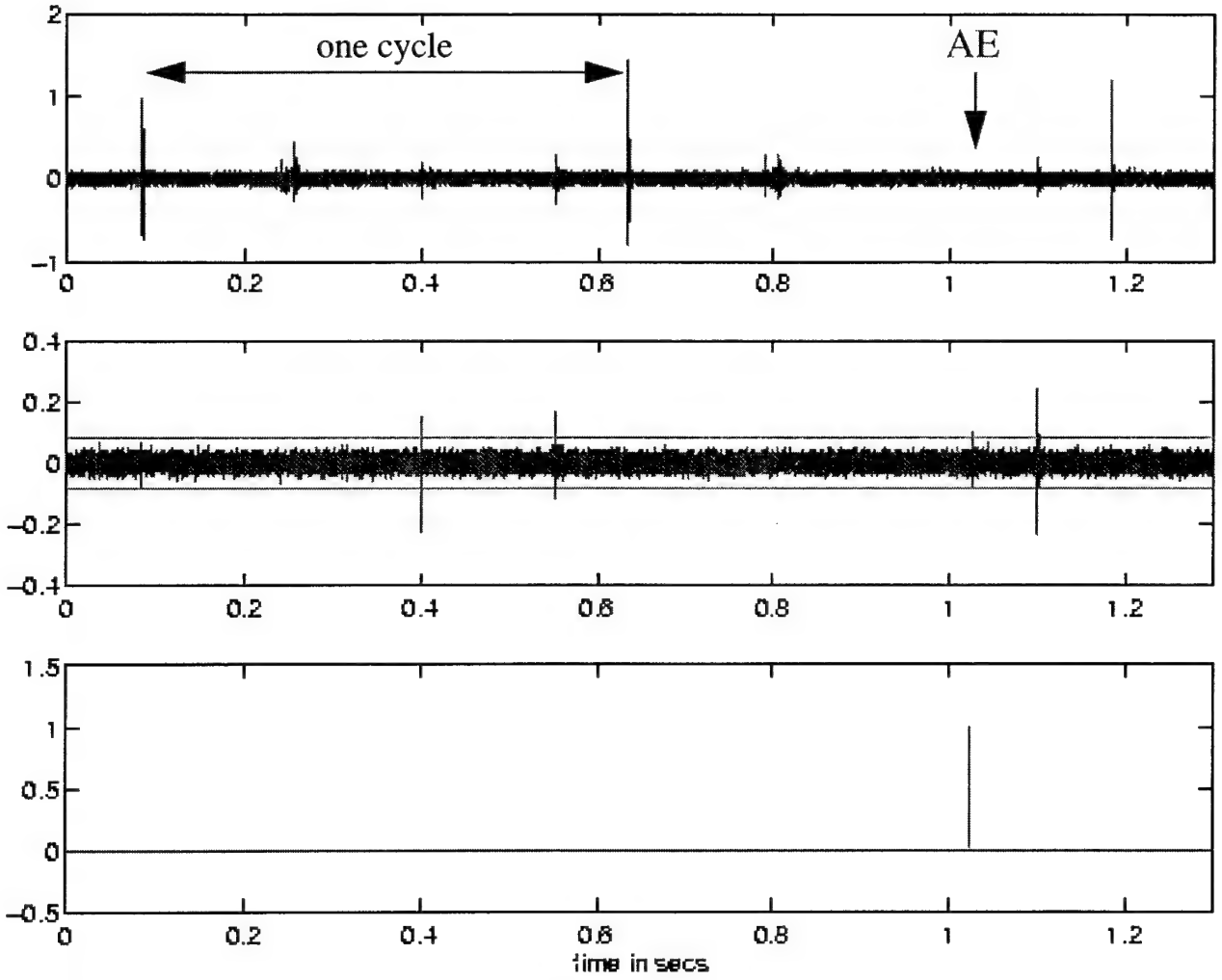

Data recorded at a sensor.

AE transients

+ Fretting transients
+ EM transients
+ other transients
+ background noise

Output of an eigenfilter bank channel.

Acoustic emission event detected at output of neural network.

Block Diagram of Processing System

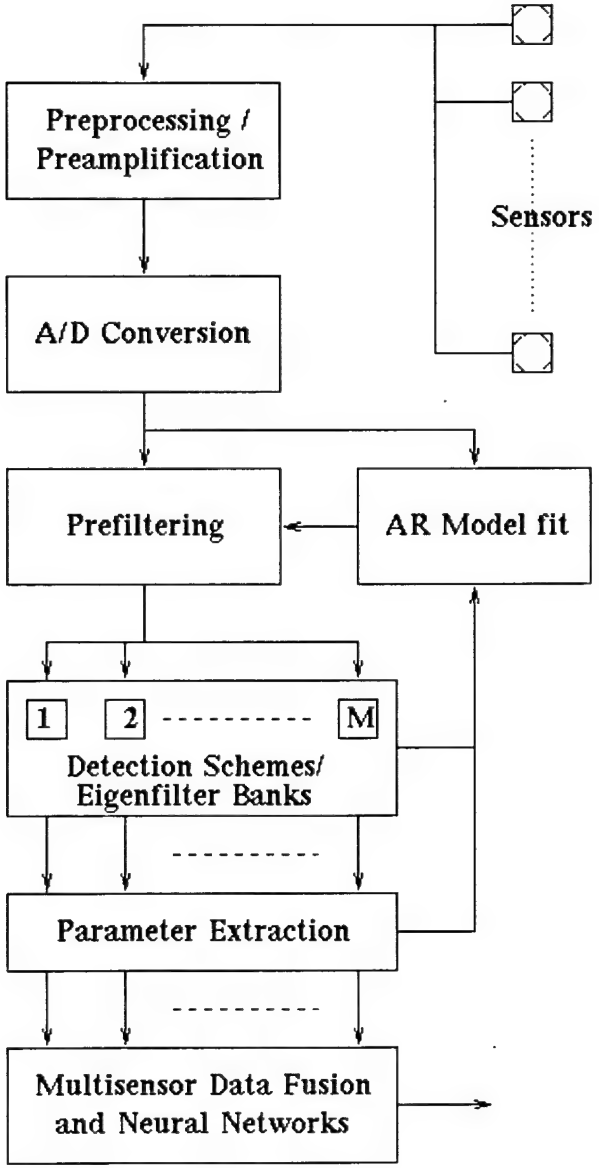

Preprocessing/Preamplification
Includes 50 kHz high pass filter.

Prefiltering
Whitening of pseudo-stationary background noise.

Eigenfilter Banks and Transient Detection
Decomposes time series into subbands that optimally concentrate the signal energy.

Parameter Extraction
Extraction of various parameters from the recorded transients (includes channel and crack signature characterization).

Multisensor Data Fusion and Signal Detection
Reliable detection of crack occurrence and propagation using neural networks trained on extracted parameters.

Study Plan

- **To study the characteristics of noise**
  - Is there significant vibration energy above the audible range?
  - Is there any other component of noise (other than vibration noise) that needs to be contended with?
- **To study the characteristics of crack formation/propagation AE signals**
  - What do the characteristics of AE signals depend upon? Material? Geometry?
  - What are the characteristics of signals generated by the rubbing of crack faces (micro-fretting) ?
- **To study propagation effects on the crack signal in a component**
  - How do the characteristics of the signal change as the wave propagates through the material?
  - Are there different types of modes? Is it important to distinguish between these different modes?
- **To design detection schemes**
  - What are the major issues involved in designing a reliable detector?
  - Is vibration noise reduction the major issue in designing the detector?
  - Can we differentiate between different kinds of cracks using the data measured at different sensors?

AE Source/Channel Characterization

Partial Listing of Available Acoustic Emission Data :

- Tantalum Nitride on sapphire, Micro-mechanical tester (U of M, Mat. Sci.)
- Iron on Silicon, Micro-mechanical tester (U of M, Mat. Sci.)
- Tantalum Nitride on 4340 Steel, Micro-mechanical tester (U of M, Mat. Sci.)
- 4340 Steel, Instron Servo-hydraulic Tester (U of M, Mat. Sci.)
- Fatigue test data of 4130 Steel and PH-13H Mo Stainless Steel (Georgia Tech),
- Fatigue test data of Aluminum alloy specimen (Northwestern University)

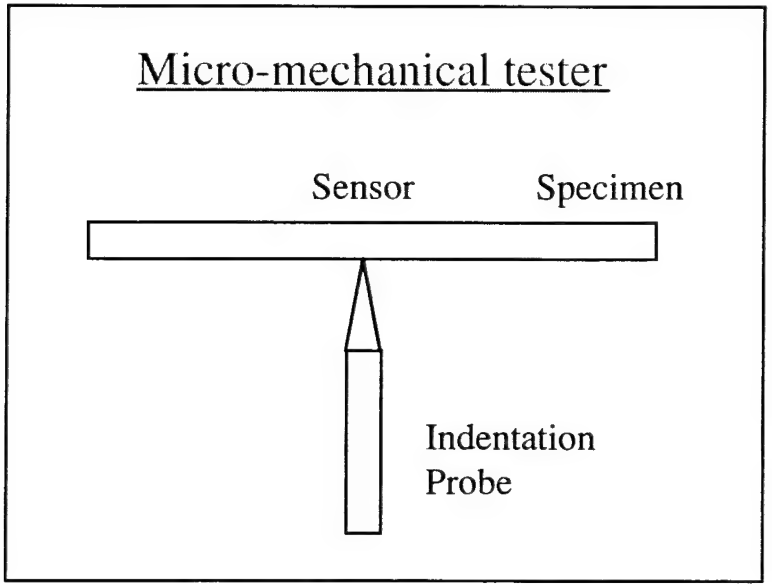

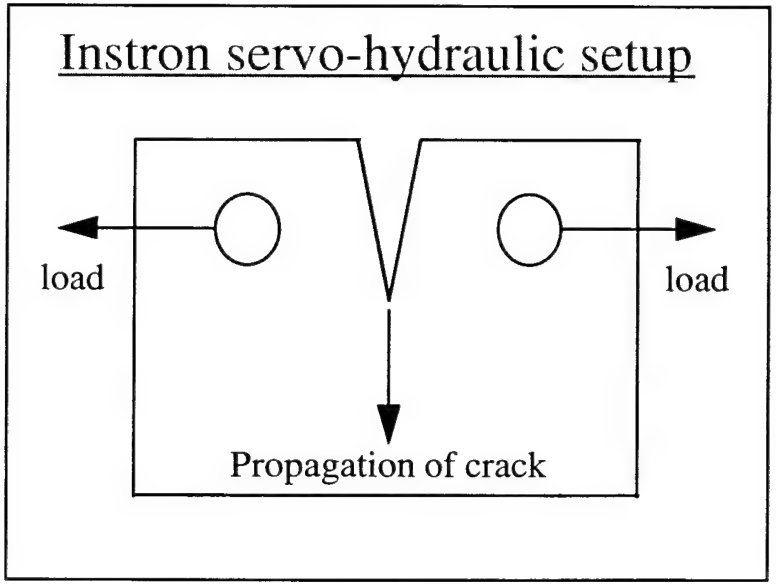

Micro-Mechanical Tester Setup

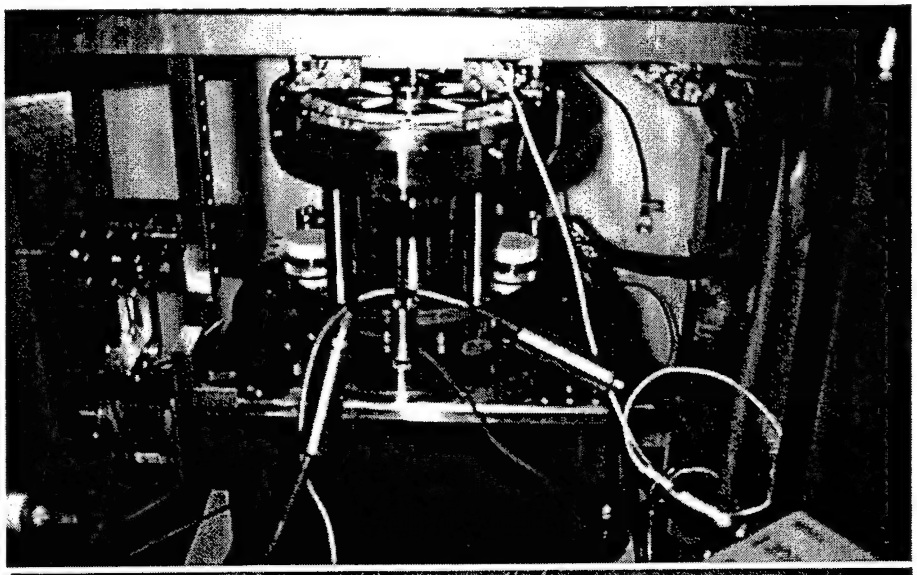

The Micro-mechanical test bed.

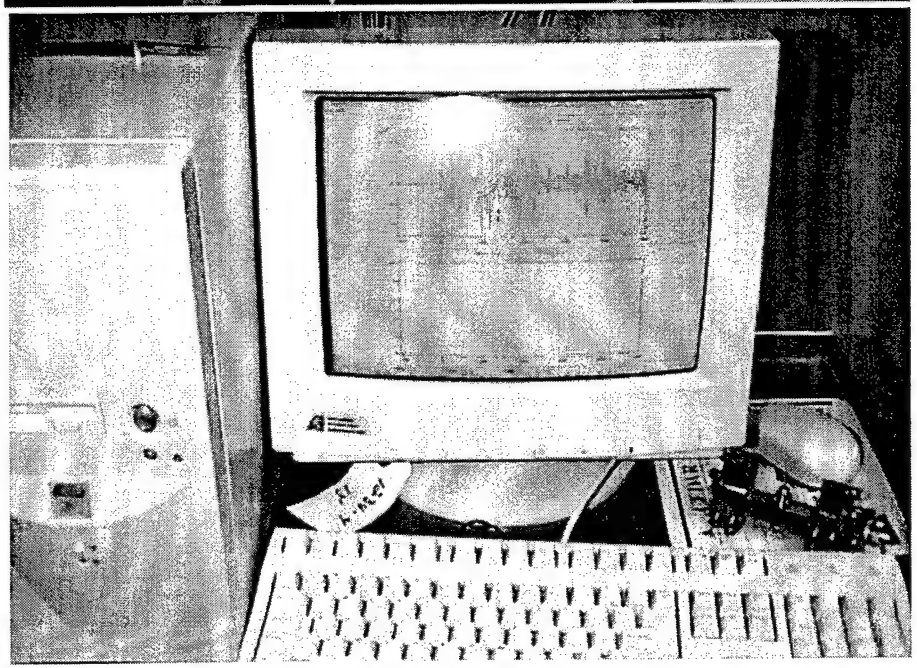

Data acquisition and on-line analysis system.

AE Source/Channel Characterization

- **How do the characteristics of the AE signal change as the the AE waves propagates through the material ?**
- **Are there different modes of propagation? Is it important to distinguish between these different modes?**

Experimental Setup

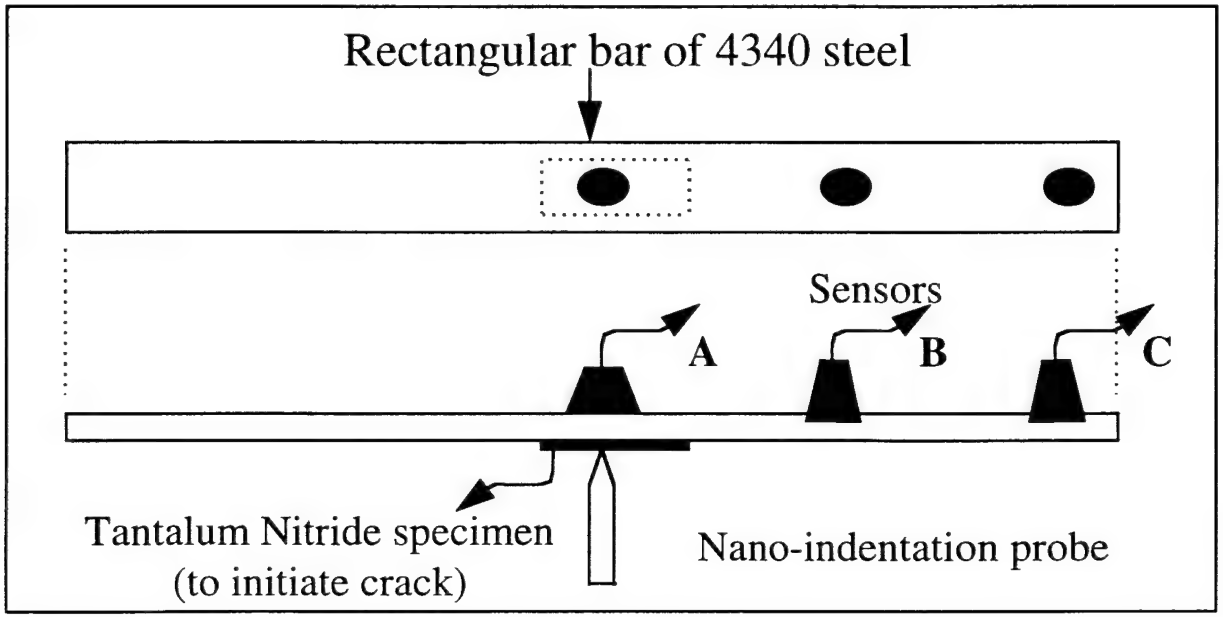

AE Source/Channel Characterization

Time series plot

Time-frequency plot

Sensor A

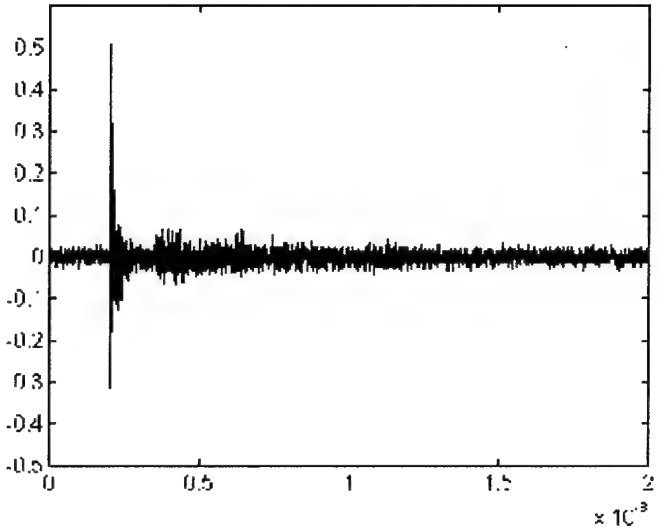

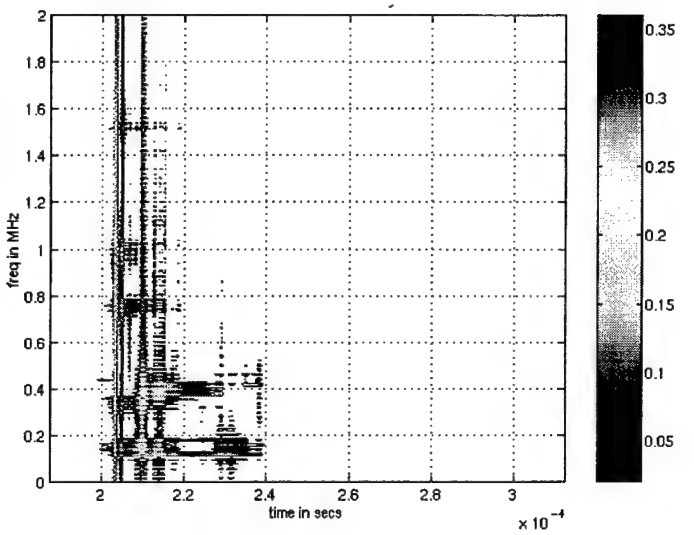

Sensor B

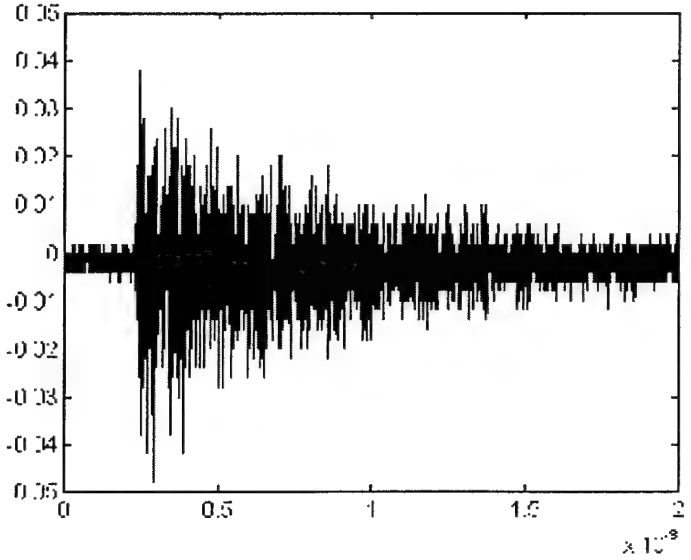

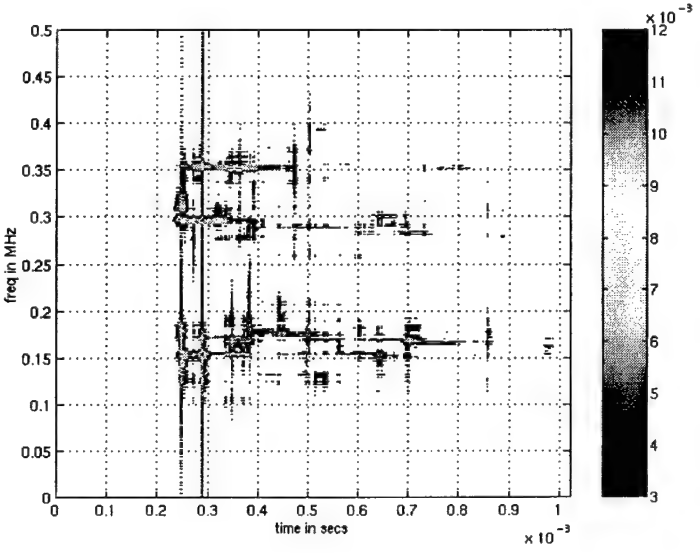

AE Source/Channel Characterization

- The AE source is of very short duration and exhibits broad spectral bands. Its spectral characteristics vary depending on the material of the specimen. The AE source exhibits energy from as low as 60 kHz to as high as 1.2 MHz.

- The channel can be characterized as a linear, lossy, dispersive waveguide of finite dimensions.
  - The loss in energy with distance increases as the frequency increases.
  - The channel has distinctive resonant frequency bands.
  - The propagation effects are complex and exhibit a variety of modes and multipath characteristics. These effects coupled with the dispersion in the channel increase the duration of the transient signal as the propagation distance increases.

<u>Conclusions drawn from above results about the characteristics of the AE signal measured at the sensors</u>:

- The signal is transient. The starting time of the transient is well predicted by the propagation velocity.
- These transients can be modeled as a sum of decaying sinusoids whose frequency and decay rates depend on the material and geometry of the specimen.

Noise Characterization

Partial Listing of Available Noise data :

- Helicopter vibration noise data - St. Paul Airport
- Helicopter vibration noise data - Cherry Point
- Boeing Test bed data (from Honeywell) for 50%, 75%, 100% and 150% load conditions and a variety of flight scenarios.
- Fretting noise on 4340 steel - U of M, Material Science.

- The energy of the vibration noise is limited almost entirely to the audible range. Hence, vibration noise reduction is not a major factor in designing the detector.

- The noise data also consists of a number of AE-like noise transients (e.g. fretting and electromagnetic transients) that seriously obscure the recognition of a crack formation/propagation AE signal.

- Distinguishing between these noise and AE signal transients, we believe, is the most important problem in providing reliable fault diagnostics using AEs.

Signal + Noise Characterization

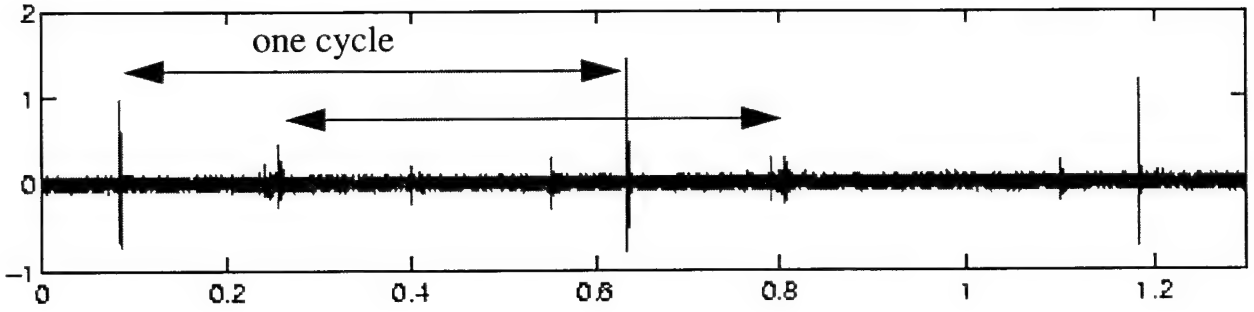

time in sec

- Some noise transients are periodic and occur at approximately the same time index in every cycle. A major fraction of fretting transients fall under this category.

- Electromagnetic transients, in general, occur at the approximately the same time instant at all the sensors.

- Mechanical fretting/electromagnetic transients have been observed to decay slower/faster than AE signals respectively.

- The time of occurrence of the AE signal in a cycle might be correlated to the time of occurrence over the previous cycles. Also, a high degree of correlation may exist between the actual AE events over neighboring cycles.

Eigenfilter Detection

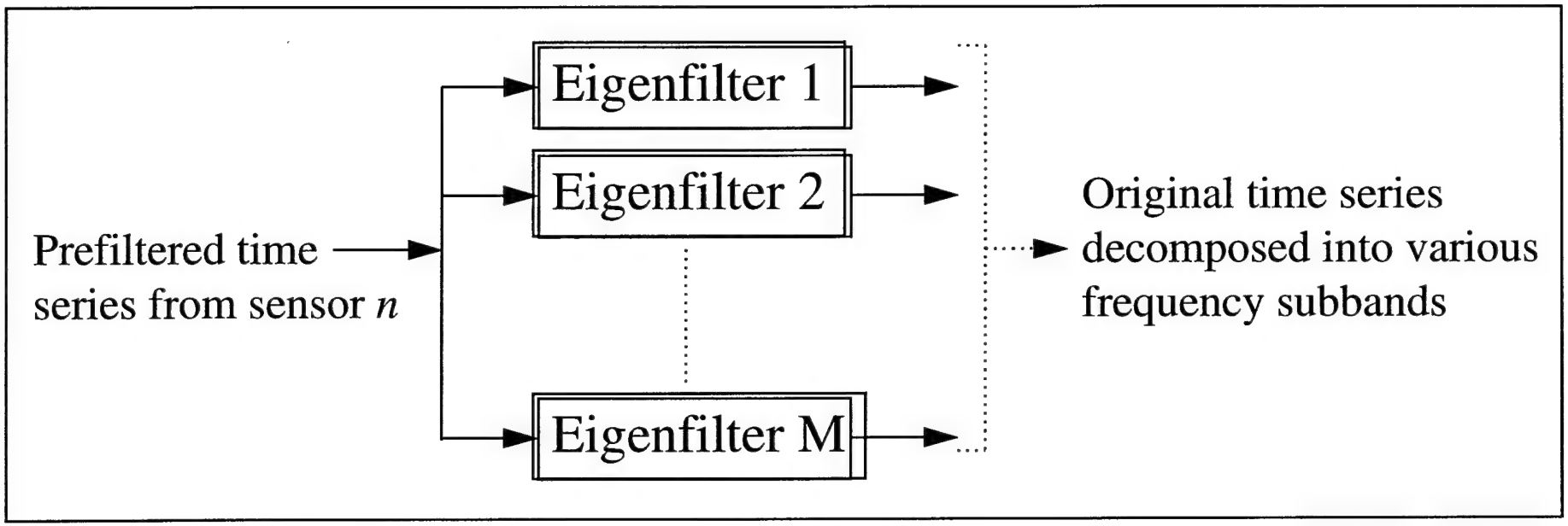

The eigenfilters maximally concentrate the energy of the transients within the specified frequency subband for a given range of decay rates.

The eigenfilters can be obtained by a generalized eigendecomposition,

$$\max_{\mathbf{w}} \frac{\mathbf{w}^T\mathbf{A}\mathbf{w}}{\mathbf{w}^T\mathbf{B}\mathbf{w}}$$

where A and B represent the signal and the signal complement space respectively.

Eigenfilter Detection

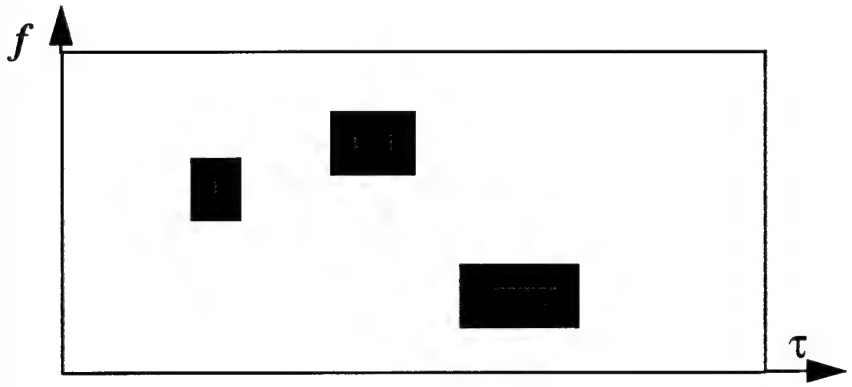

Subspace visualization of eigenfilter bank channels

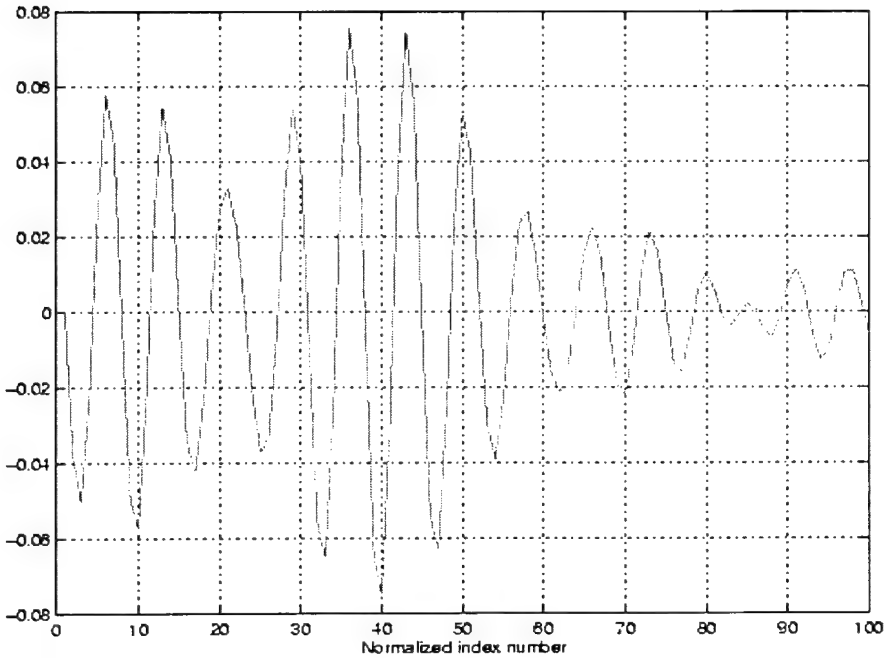

An eigenvector

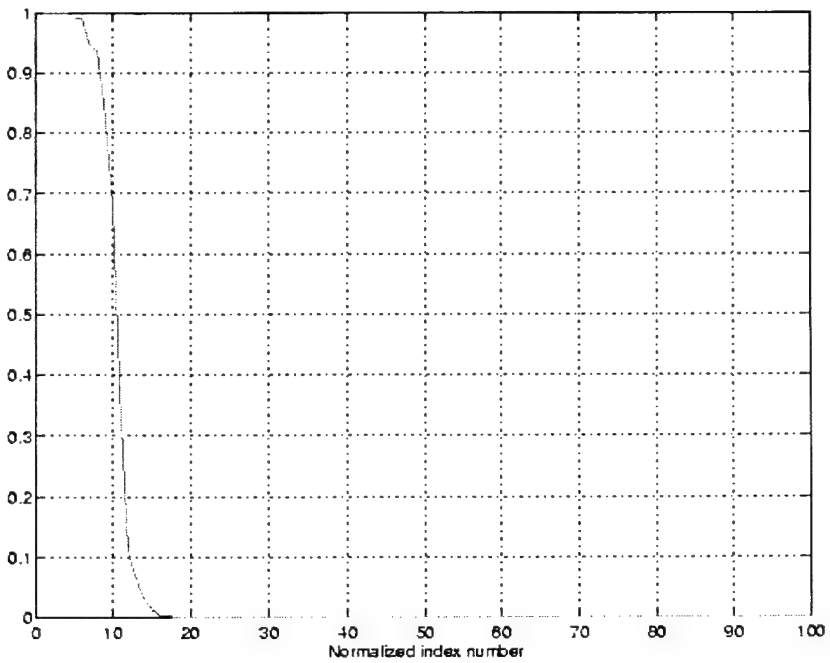

Eigenvalues of a signal subspace

Crack Signature Estimation

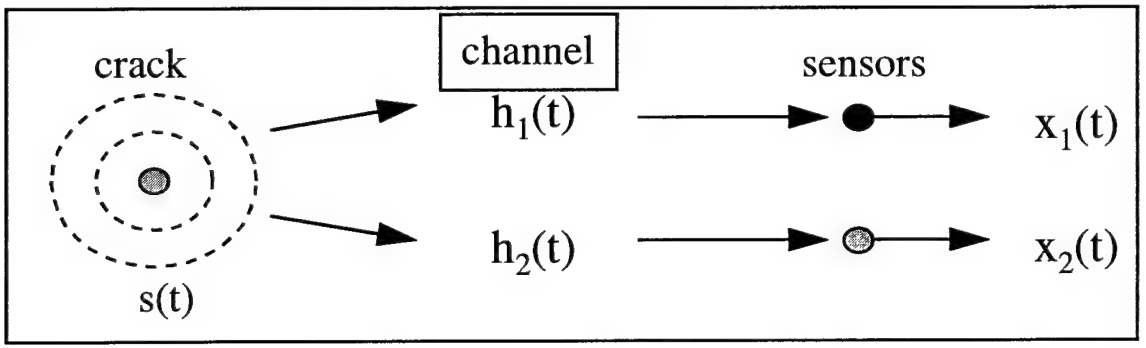

- Estimation is blind.
- Channel responses are estimated as intermediate step.
- Channel response estimates could possibly be used for crack localization.

Magnitude Spectrum of :

- crack signature estimated using blind equalization
- smoothed spectral estimate of data measured closest to crack.

(Three channel Honeywell Boeing test bed data was used)

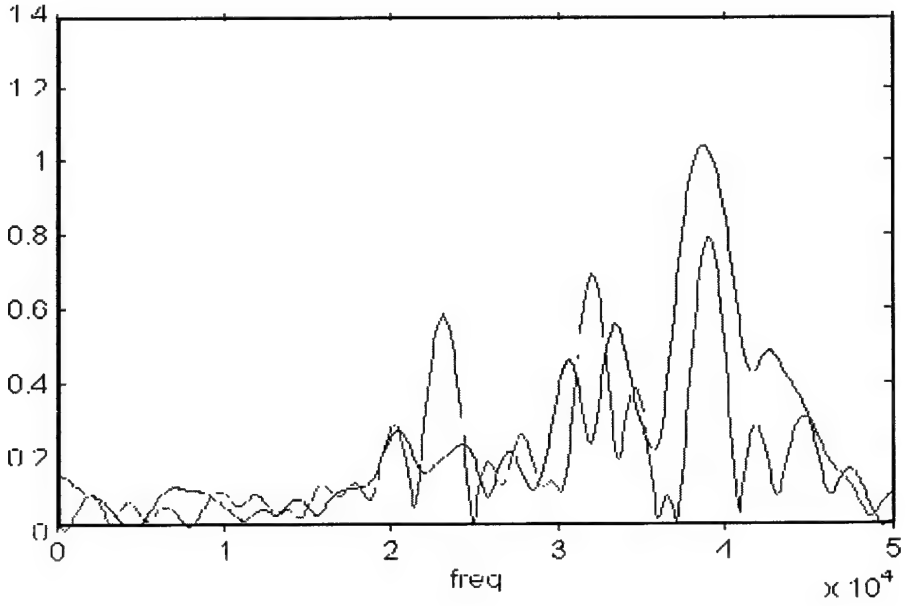

Neural Network Based Detection - Input Data Model

		Near Sensor	Far Sensor
AE Signal	A	U (3,5)	U (0.4,0.6)
- high frequency	f	N (0.75π,0.0167π)	N (0.75π,0.167π)
component	α	U (0.02,0.025)	U (0.02,0.025)
AE Signal	A	U (3,5)	U (2.7,4.5)
- low frequency	f	N (0.45π,0.0167π)	N (0.45π,0.0167π)
component	α	U (0.01,0.014)	U (0.01,0.014)
	A	U (5,10)	U (4.5,9.1)
Fretting transient	f	N (0.45π,0.0167π)	N (0.45π,0.0167π)
	α	U (0.011,0.014)	U (0.011,0.014)
	A	U (3,13)	U (3,13)
Electromagnetic transient	f	U (0,π)	U (0,π)
	α	U (0.03,0.052)	U (0.03,0.052)
SNR (peak of transient)		10-20 dB	10-20 dB

A - amplitude
f - frequency
α - decay rate

U - Uniform distn.
N - Normal distn.

- All three classes of transients are a sum of decaying sinusoids whose frequency bands overlap. All the parameters are subject to a random jitter.
- Both AE and fretting transients decay with distance. This decay increases as as frequency increases. This characteristic does not apply to electromagnetic transients.

Neural Network - Input Data Scatter Plot

2-D plot

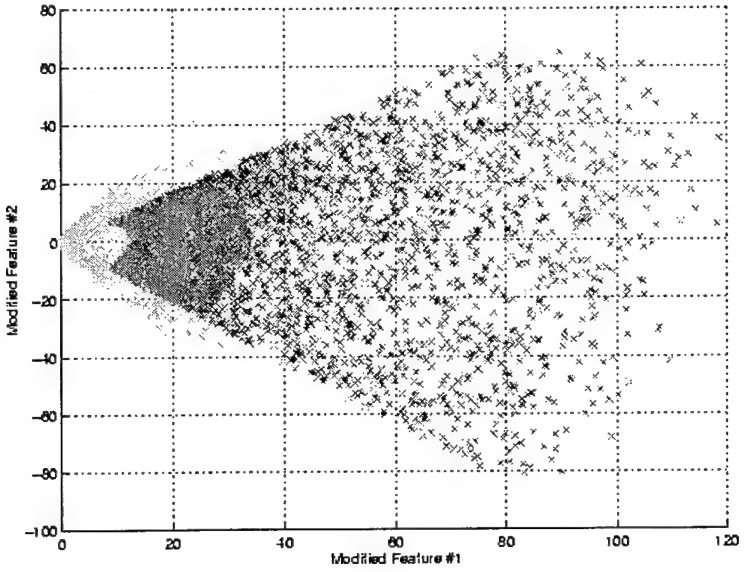

x AE
x Fretting
x EM

3-D plot

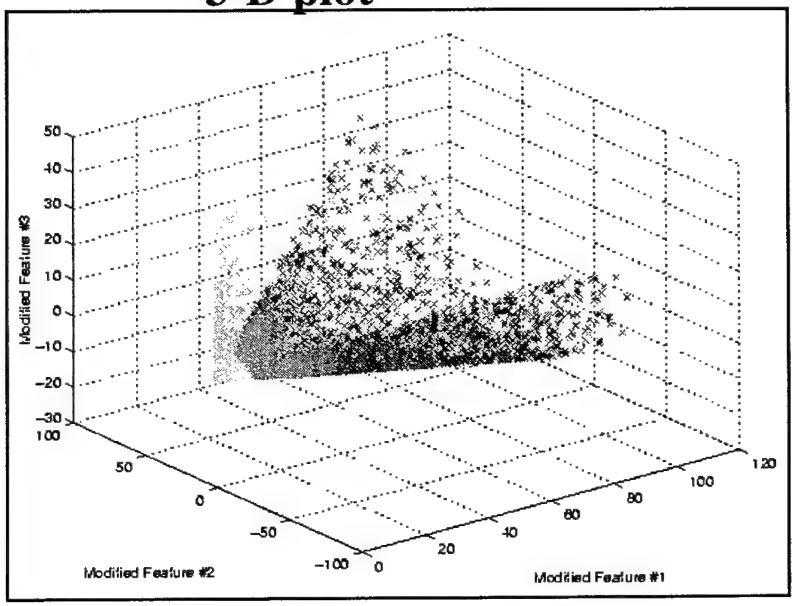

Scatter plots shown above with data comprising of the PSD of the detected transients projected along two and three most dominant directions respectively. The eigenspread of the space is shown in the figure to the right.

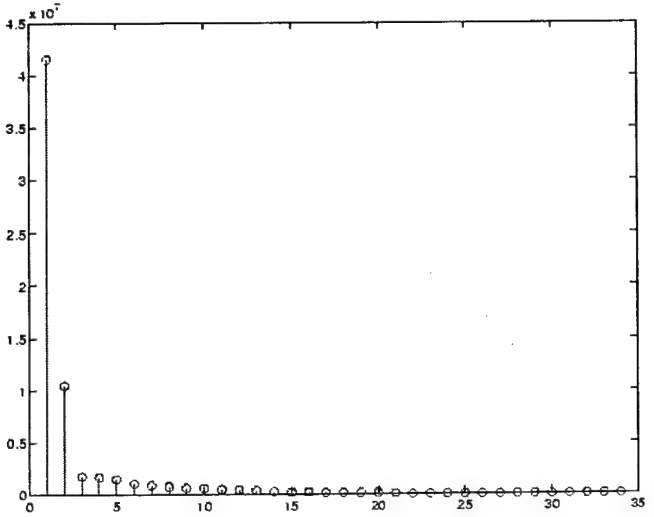

From the scatter plots the need for a non-linear detector to differentiate AE data from noise data is apparent. Hence, we used a neural network trained by back-propagation algorithm.

Neural Network - Output Data Scatter Plot

2-D plot

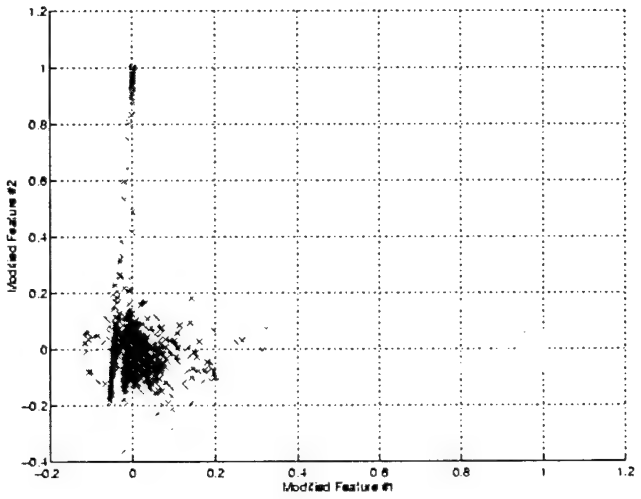

3-D plot

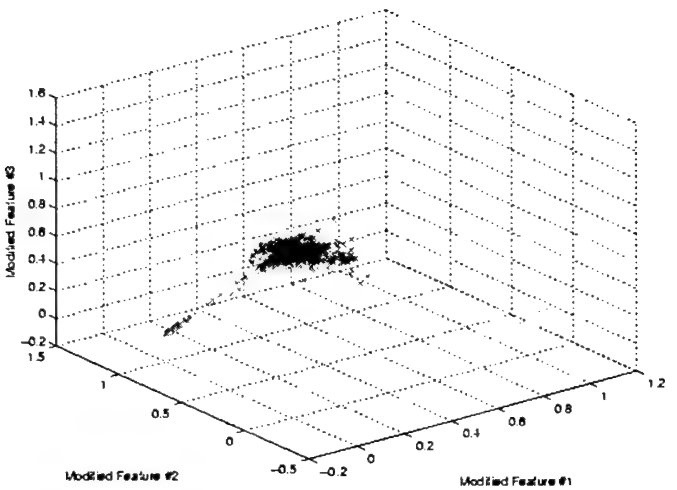

The three clusters are well separated. This separation can be further improved by feeding this output to another neural network.

Neural Network Detector Performance

Data sets used for training	200,000
Probability of false alarm	$< 2.7 \times 10^{-7}$
Probability of miss	2.7×10^{-7}

Future Work Signal Processing

Data Analysis - Refinement of noise and signal model

- in-flight experiment (Honeywell)
- micro/macro fretting data from multiple sensors.

Refinement of detection/estimation schemes

- alternative detection schemes.
- neural network architectures and multisensor data fusion.
- crack localization.

Non-AE condition-based maintenance

- signal processing for condition monitoring with multiple micro-accelerometer data.

Telemetry and Sensor Interface Electronics

Fatigue/Failure Monitor

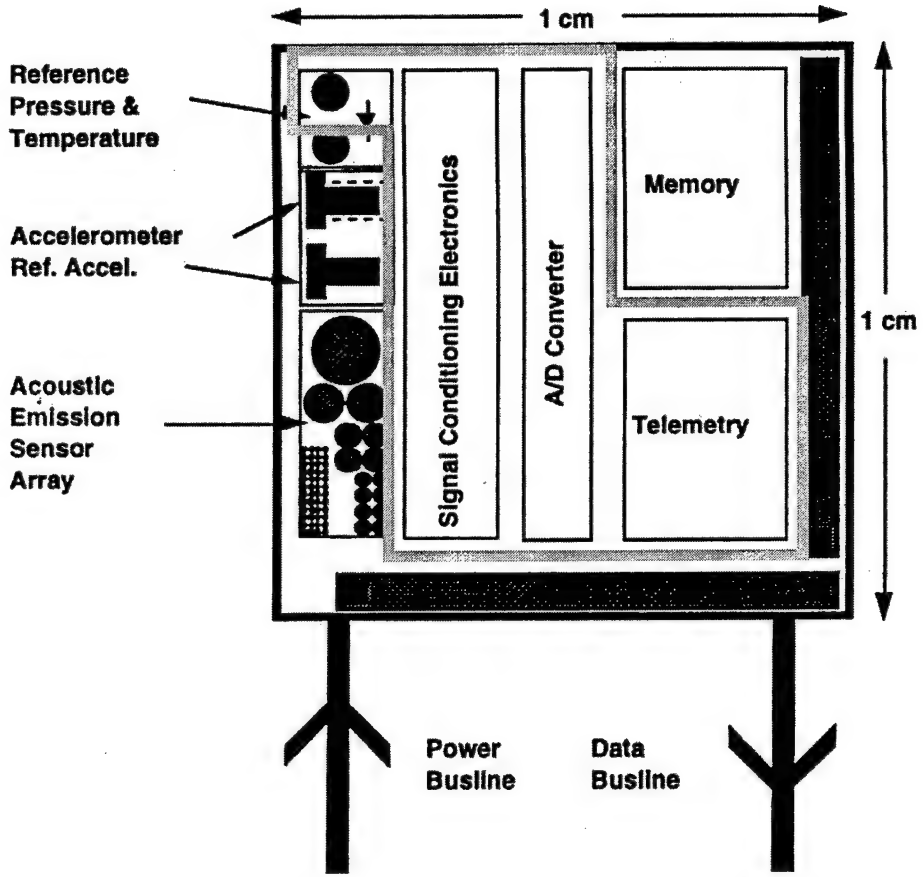

Temperature Sensor

- **Sensor basics**
  - **Use bipolar (weak inversion) exponential characteristics**
  - **Generate proportional to absolute temperature signal (PTAT)**
  - **Compare PTAT signal with reference signal**
- **Two approaches**
  - **Parasitic vertical bipolar in CMOS**
  - **CMOS operating in weak inversion**
- **Status**
  - **Early versions of both approaches designed and tested**

Our Switched-Capacitor Realization

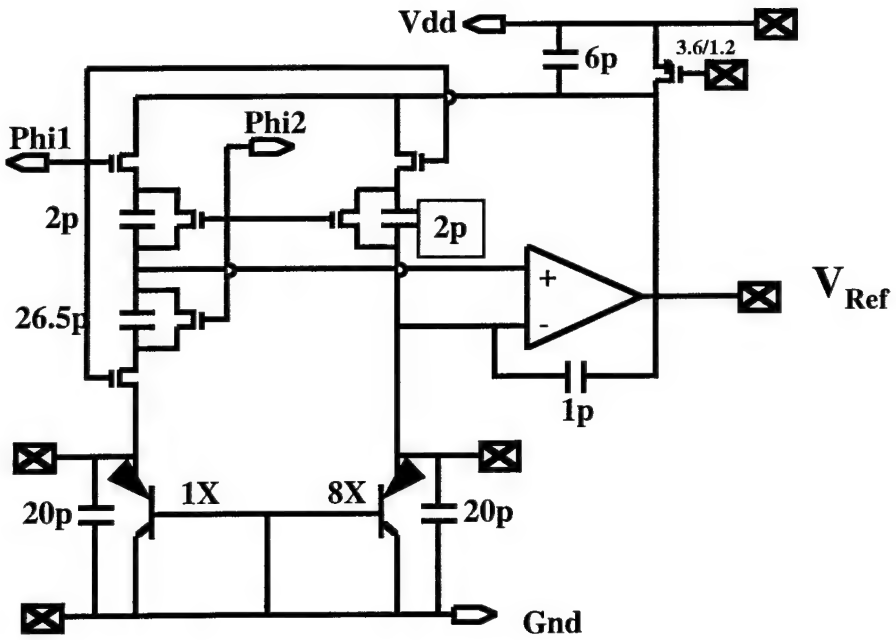

- **Significantly lower area at micro power levels**

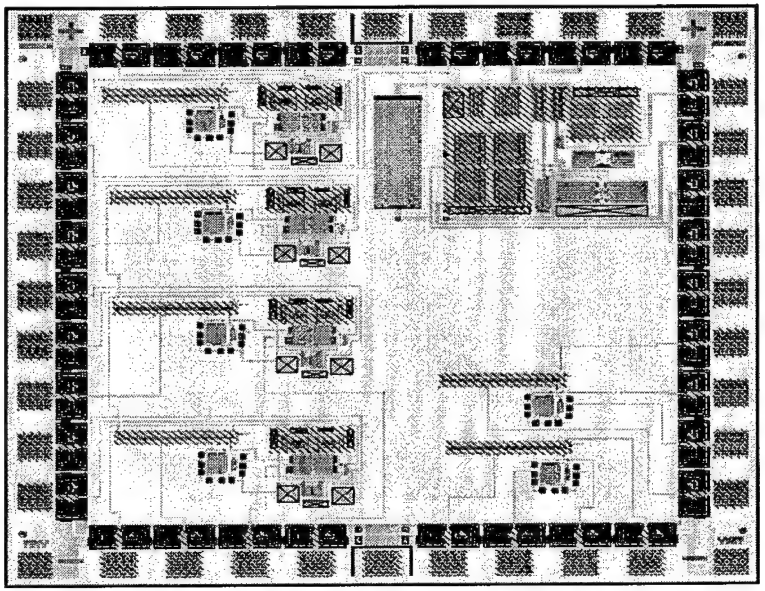

Weak Inversion PTAT Cell

- **Sensor design**

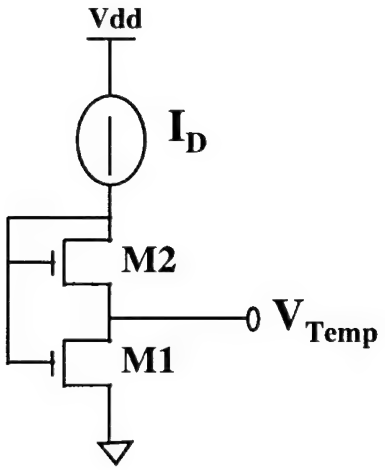

$$V_{Temp} = \frac{kT}{q} \ln\left(1 + \frac{S_2}{S_1}\right)$$

- **Measurement results**

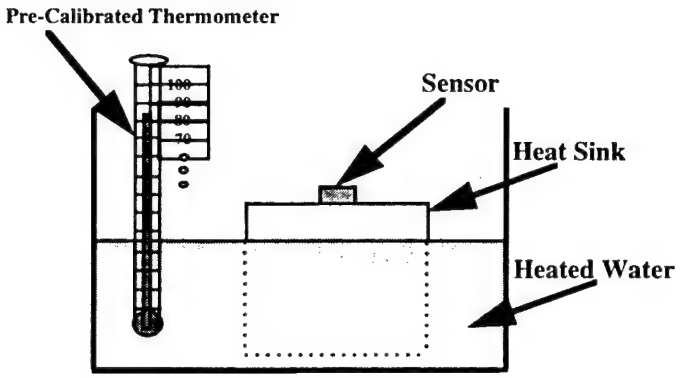

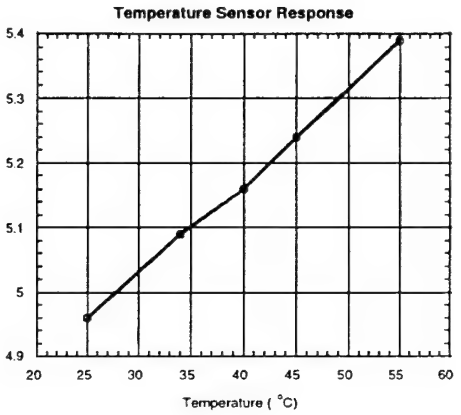

Acoustic Emission

- **Acoustic emission (AE) sensor**
  - **Piezoelectric sensor converters AE signal into charge**
  - **Voltage across sensor amplified by charge amplifier**
  - **Output of charge amplifier quantized by A/D converter**
- **Charge amplifier**
  - **Preferred over voltage amplifier**
    - **PZT has high permitivity => small output voltage**
  - **Modified to remove DC offset and flicker noise**
- **Status**
  - **Preliminary charge amplifier designed and tested**

Modified Charge Amplifier

- **Circuit design**

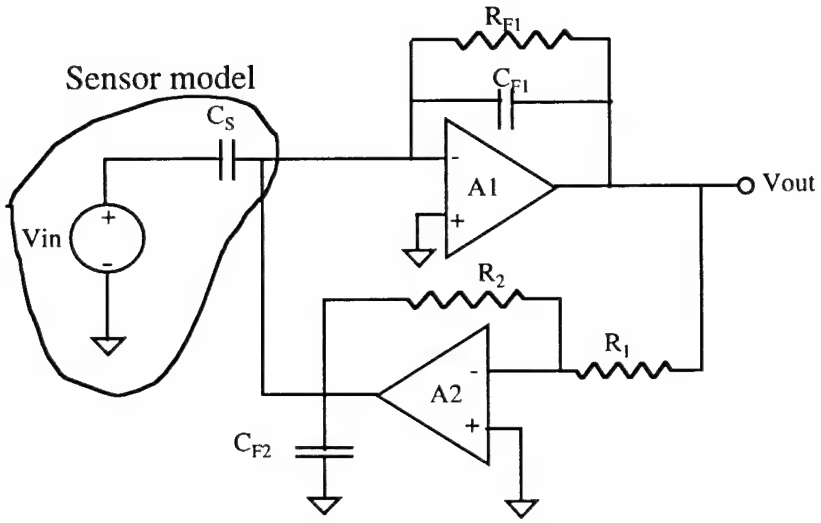

- **Measured results**
  - **Frequency response**

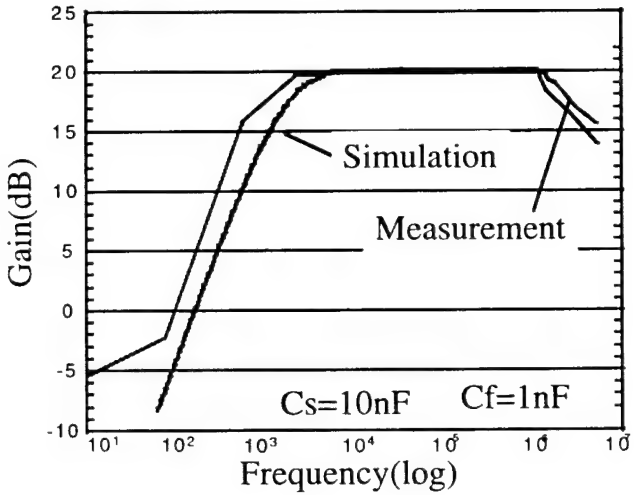

A/D Converters

- **Design choices**
  - **Data rate: 1 - 2MHz @ 10 bits**
  - **Viable designs: Sigma-delta and pipelined**

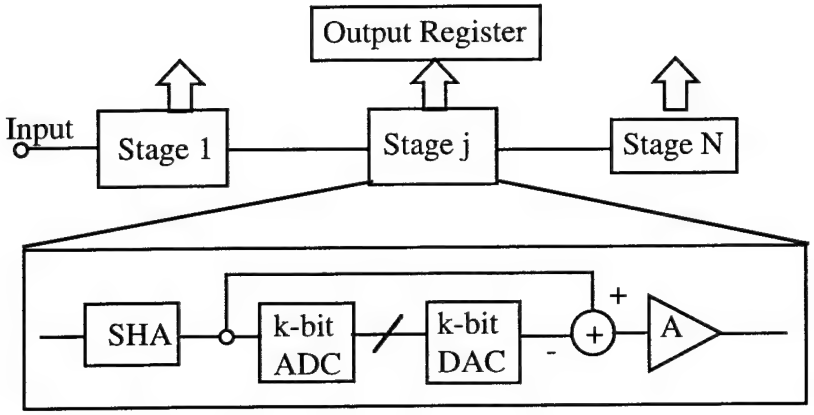

Pipelined Architecture

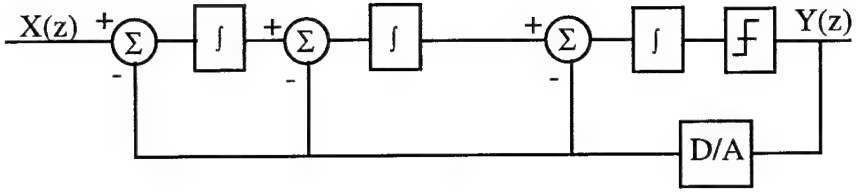

Sigma-delta Architecture

Telemetry

- **Transceiver block diagram**

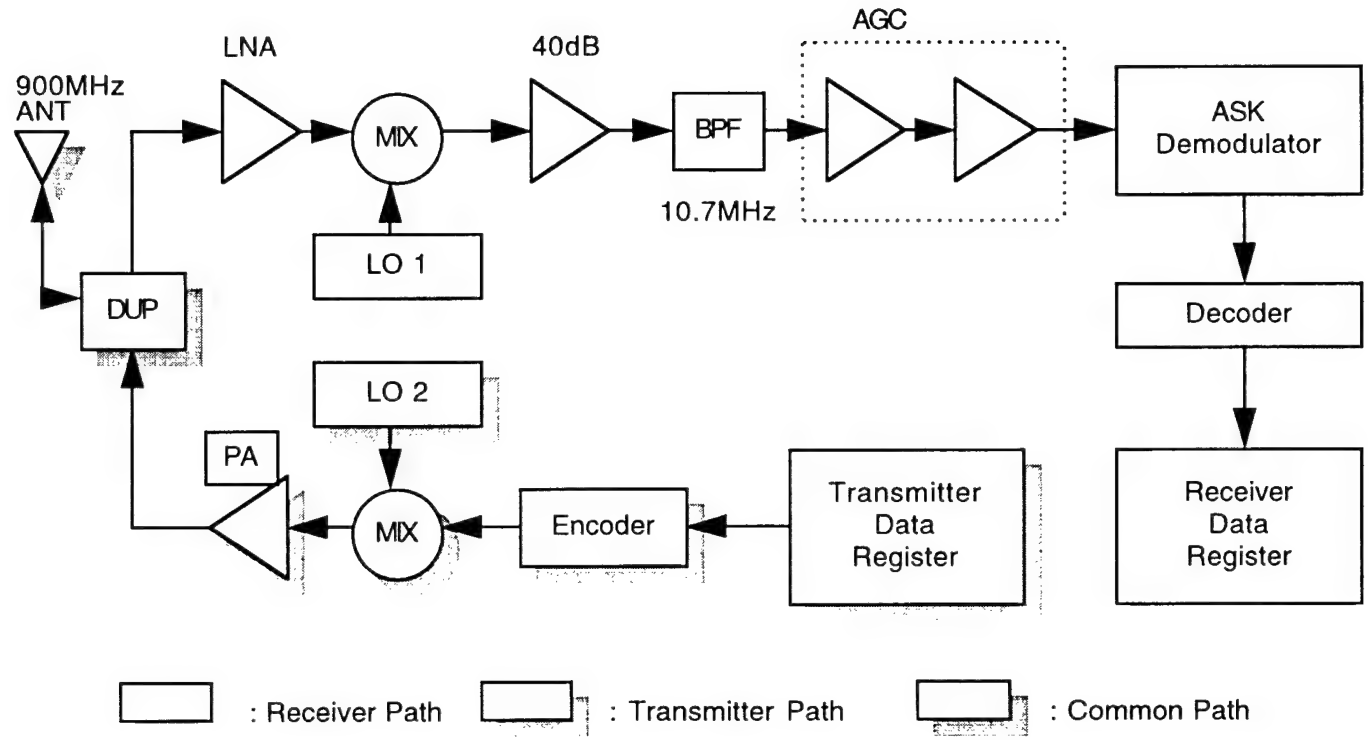

Telemetry

- **Current modulation scheme (ASK for low power)**
  - **To be modified (FSK, PSK)**
- **Status**

	Block Level	Current Status	Future Work
01	Antenna	Study & Prototype Design	Design & Test
02	CMOS LNA	Off-chip inductor LNA : Done	On-chip inductor LNA Design
03	Mixer	Design & Test : Done	Conversion Gain : Improve
04	Oscillator	Design & Test : Done	LC Tank & SAW Resonator
05	AGC	Dynamic Range :40dB	redesign & Limiter Design
06	ASK Demodulator	Design & test	Test & Re-Design
07	Power Amplifier	Low gain & Lower efficient	Re-Design and Test
08	Tx Modulator	Design & poor work	Design & Test

Oscillator Design

- **Oscillator circuit**

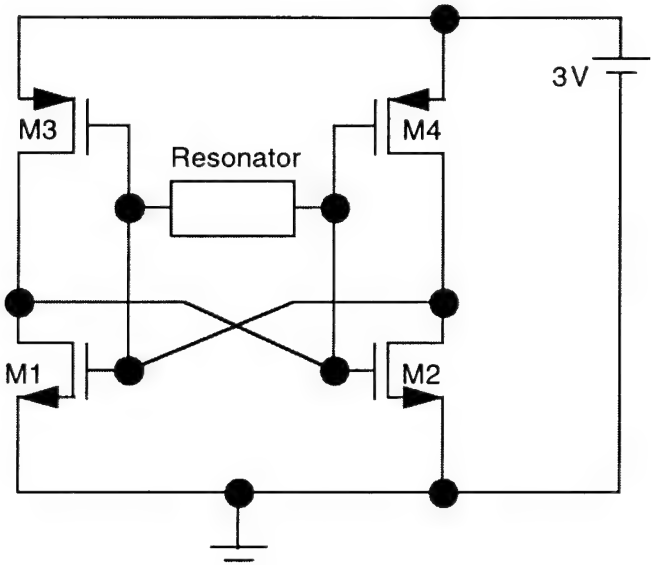

Resonator : Ceramic Resonator (864MHz)
Since it was available only for the test.

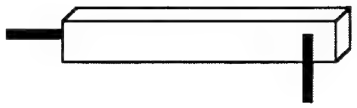

- **Measurement results**

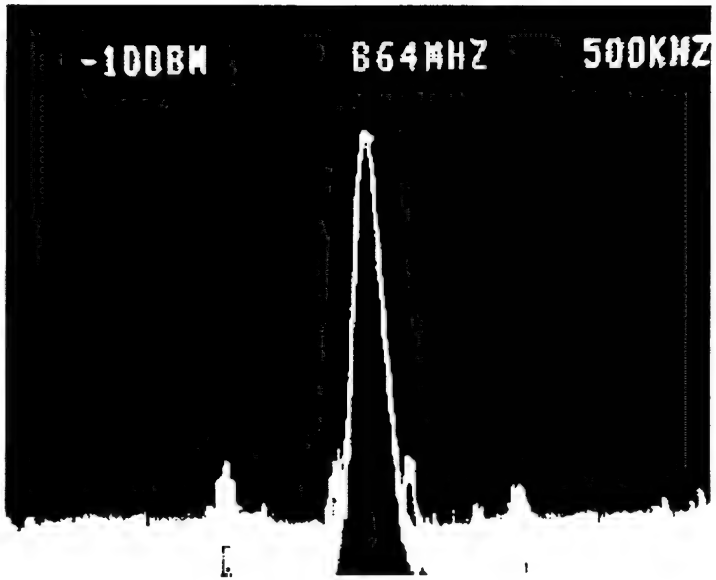

Front-end Integration Test Setup

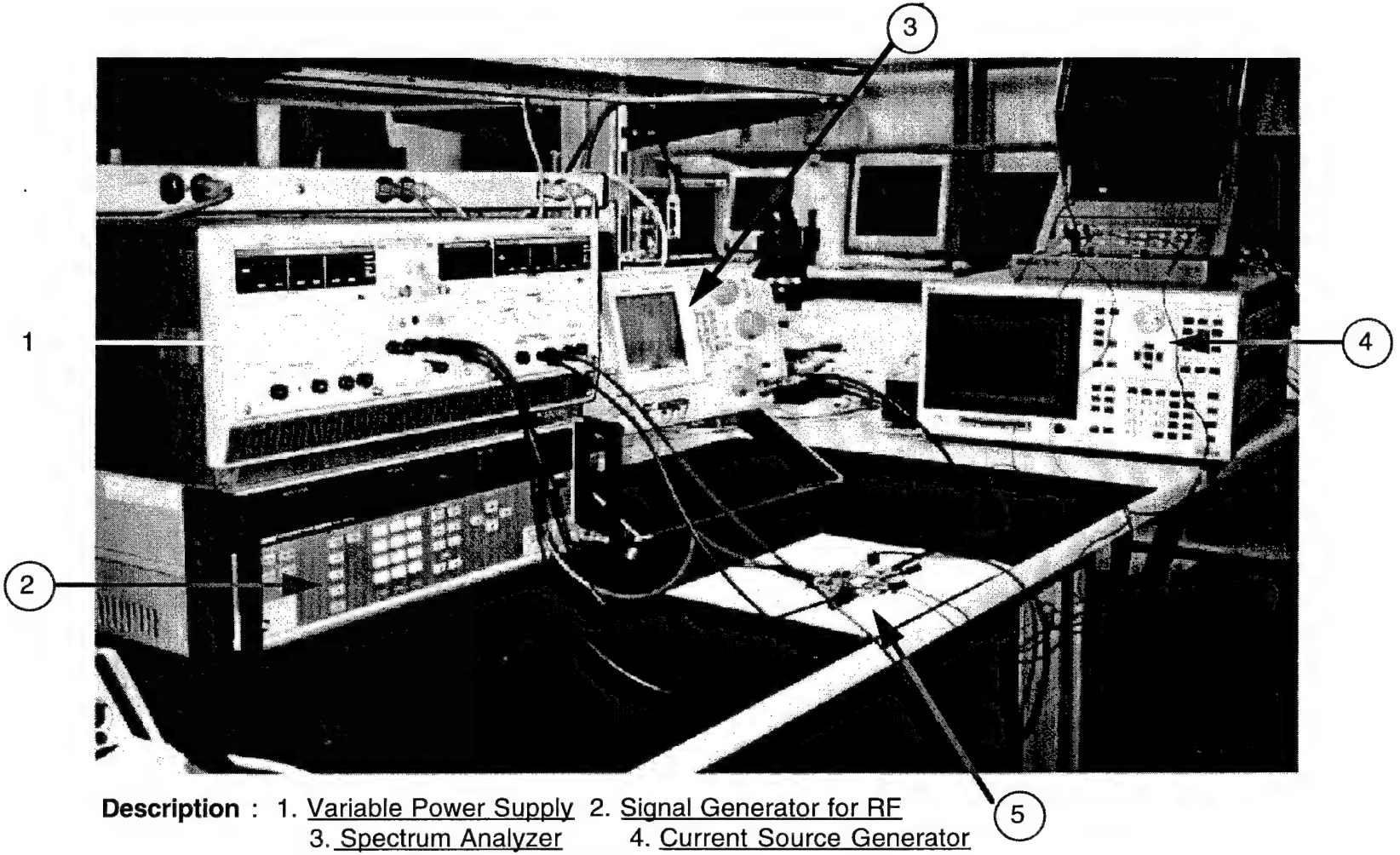

Description : 1. Variable Power Supply 2. Signal Generator for RF
3. Spectrum Analyzer 4. Current Source Generator
5. Test Board with Chipset

Test Board and Chipset

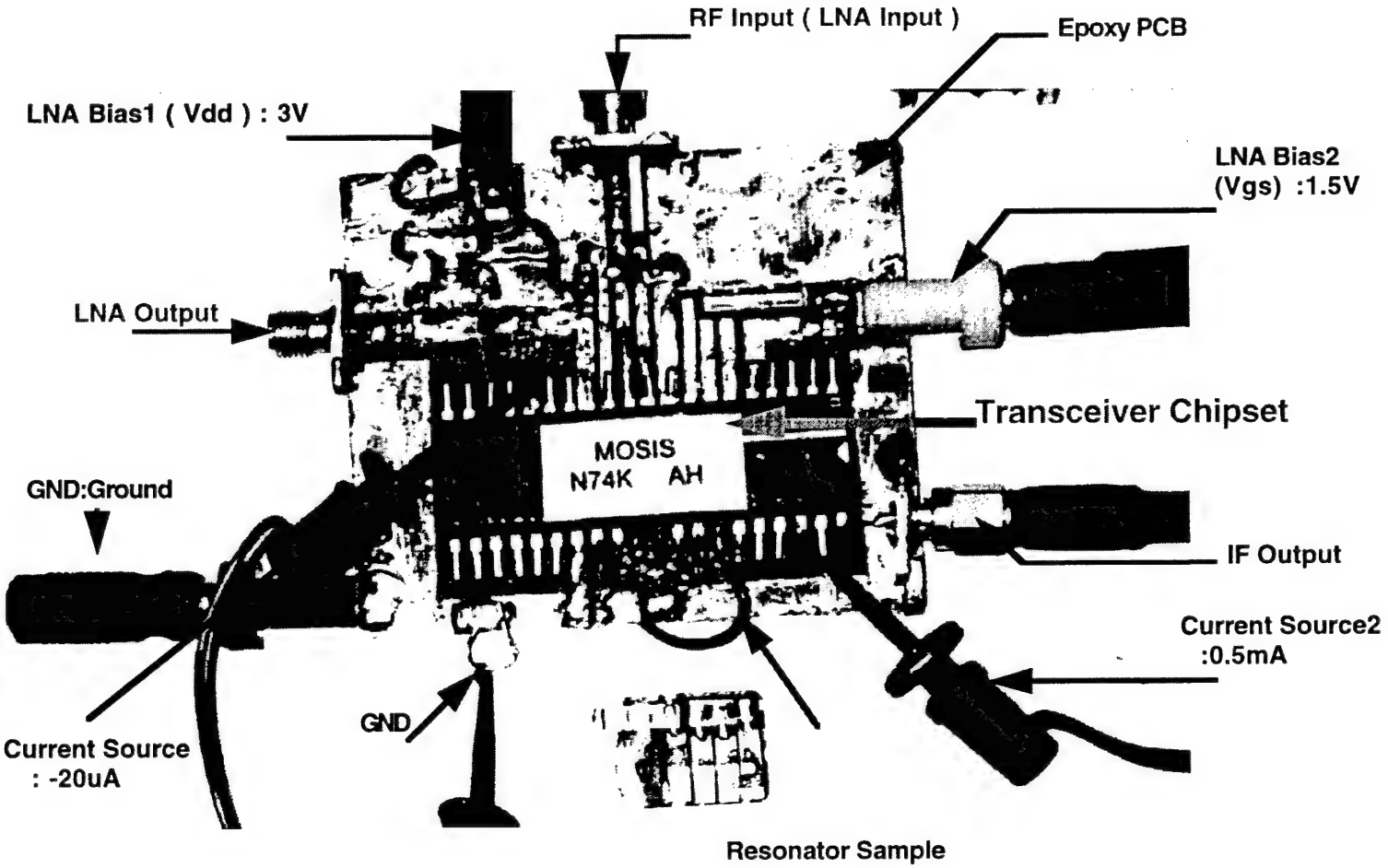

Front-End Test Result

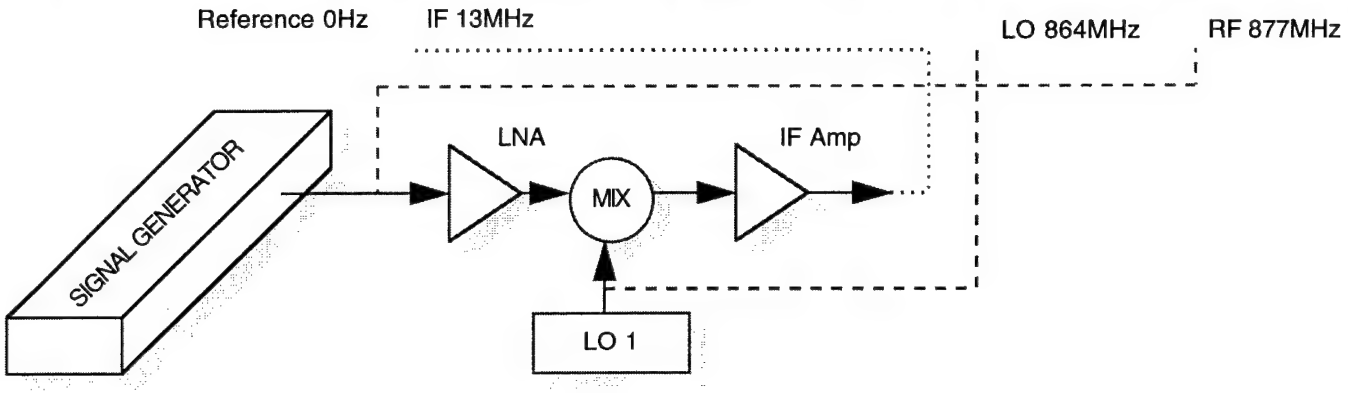

Future Work

- **Temperature sensor**
  - Design incremental A/D converter
  - Integrate and test system performance
- **Acoustic emission electronics**
  - Modify charge amplifier for improved performance
  - Design and fabricate high-speed A/D converter
- **Telemetry**
  - Modify design to accommodate new modulation scheme
  - Evaluate and design miniature antenna design
- **Overall integration**
  - Single chip implementation

Summary

- Piezoelectric materials have been developed for AE sensing and vibration monitoring.
- AE microsensors have been used in fatigue testing
- Signal processing methods have been used to understand both noise sources and AE transients associated with material fatigue and cracking.
- Microsensor interface electronics have been developed for the sensors used in this work.
- A general-purpose telemetry system has been developed to interface with MEMS.

Future Work

- Single-chip integration of microsensors (AE + vibration + temperature) and interface electronics.
- Improvement and development of additional microsensor interface electronics (A/D)
- Refinement of detection/estimation schemes including crack localization.
- Development of signal processing methods for vibration signatures in rotating machinery.
- Application of neural network methods.
- Development of a self-contained monitoring system (MEMS + electronics + telemetry + thin film batteries + signal processing = warning)

Failure Characterization and Prediction Methodology

Structural Fatigue Tasking

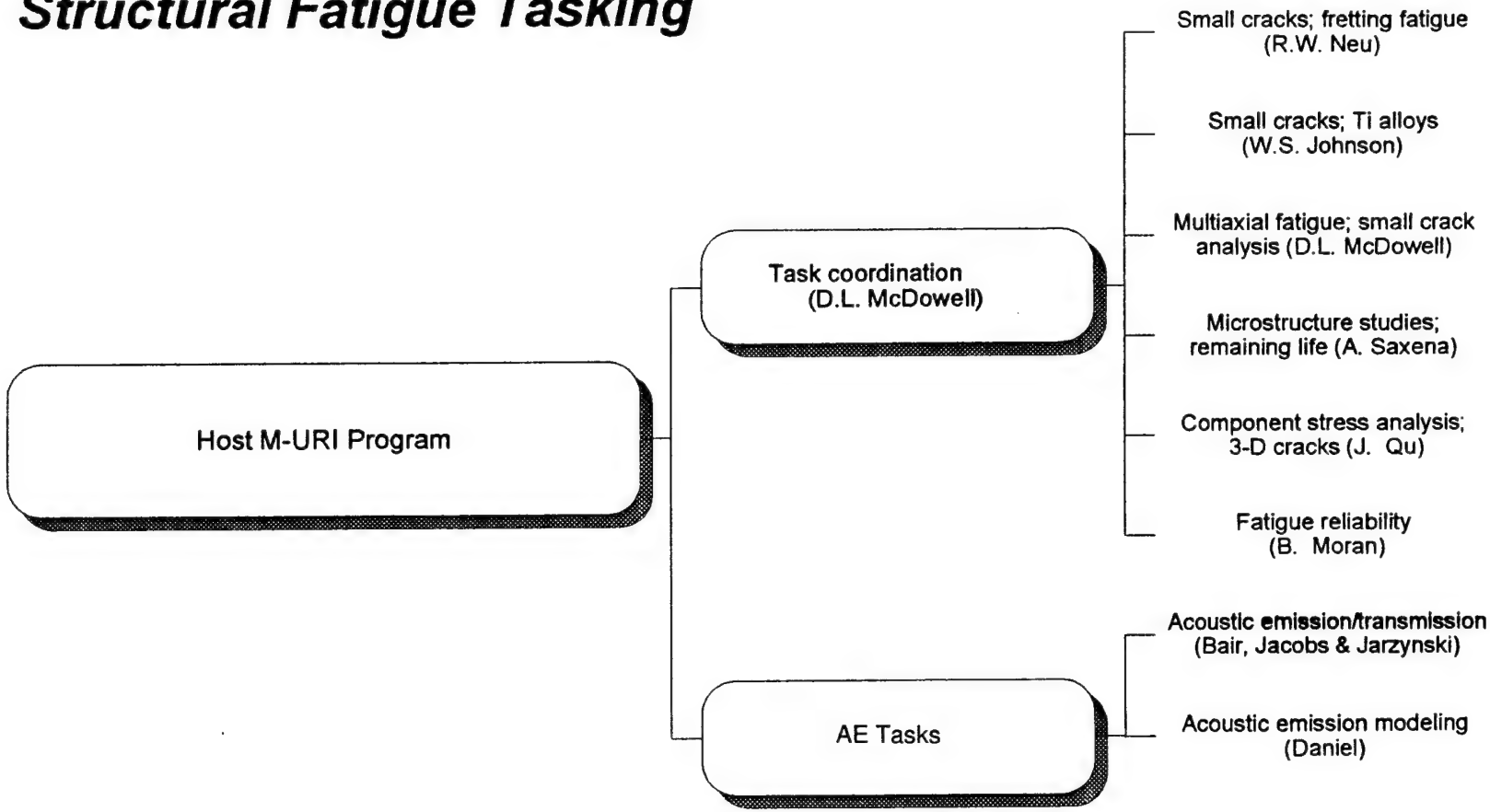

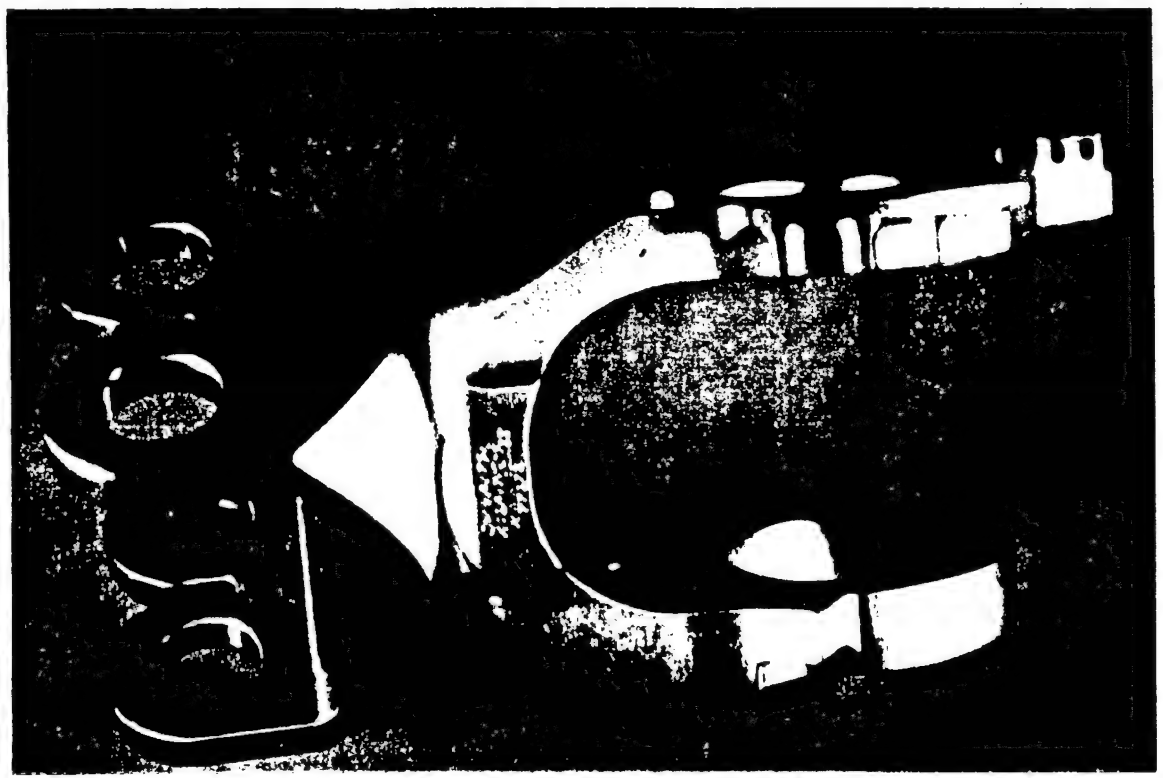

Retired Helicopter Connecting link

Damage is observed on pinhole surface and edge.

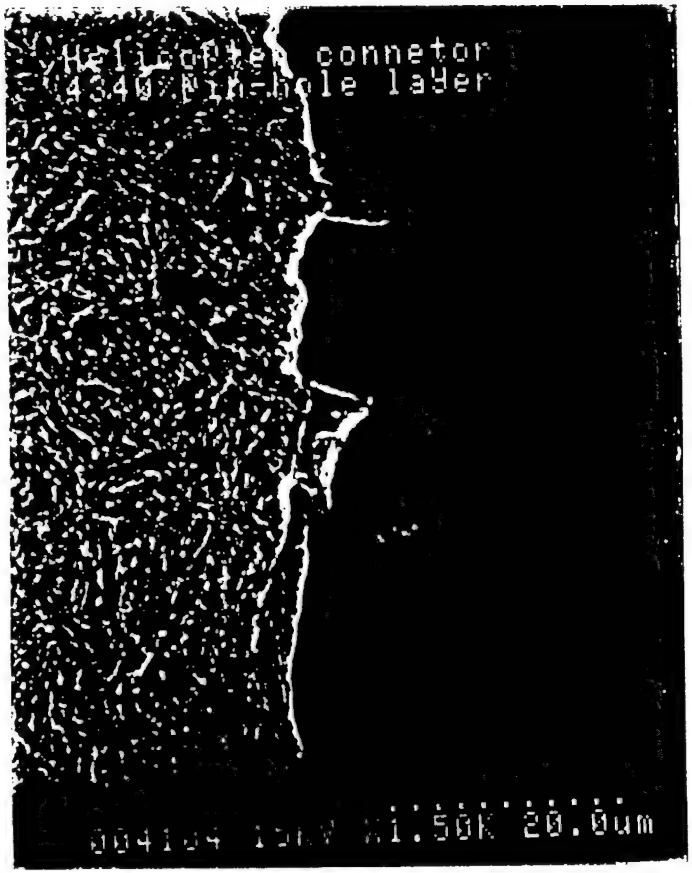

Sectioned Pinhole Region

Damage is limited in the coating layer, component may have been retired prematurely.

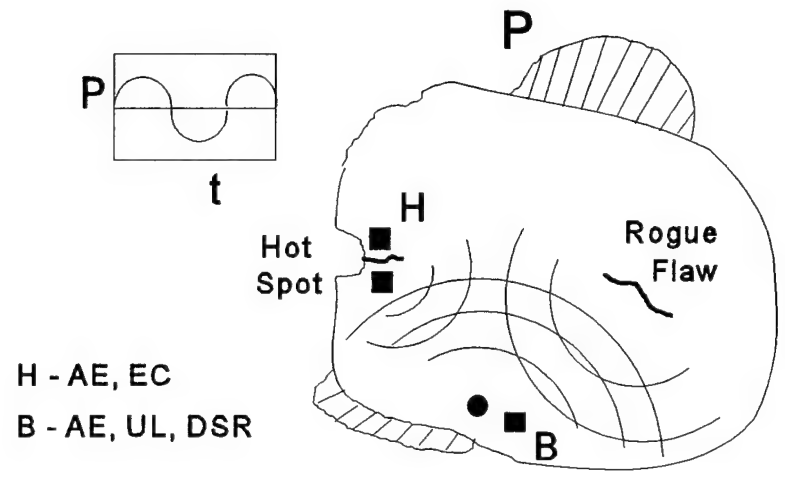

Hot Spots Versus 'Rogue' Flaws:

hot spot monitored using focused micro sensors (H)

rogue flaw detected using broad area scanning detection (B) methods

Legend: acoustic emission (AE)
eddy current (EC)
active ultrasound (UL)
changes of dynamical system/component response (DSR)

Stress and Flaw Analysis of Structural Components

Objectives

- Calculate the "Driving" force (SIF) for crack growth.
- develop a computational algorithm to compute the 3-D crack-front parameters under complex state of stresses.
- Develop a simulation and visualization program for the growth of 3-D cracks.

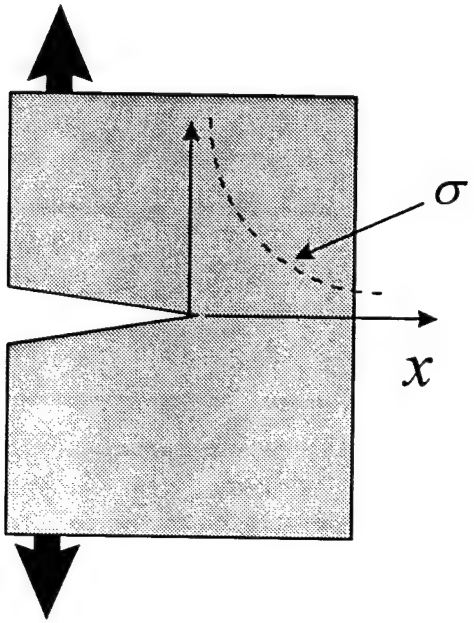

$$\sigma = \frac{K}{\sqrt{2\pi x}}$$

Fracture Criterion

There is a critical value so that fracture occurs when

$$K \geq K_c$$

Calculation of Driving Force

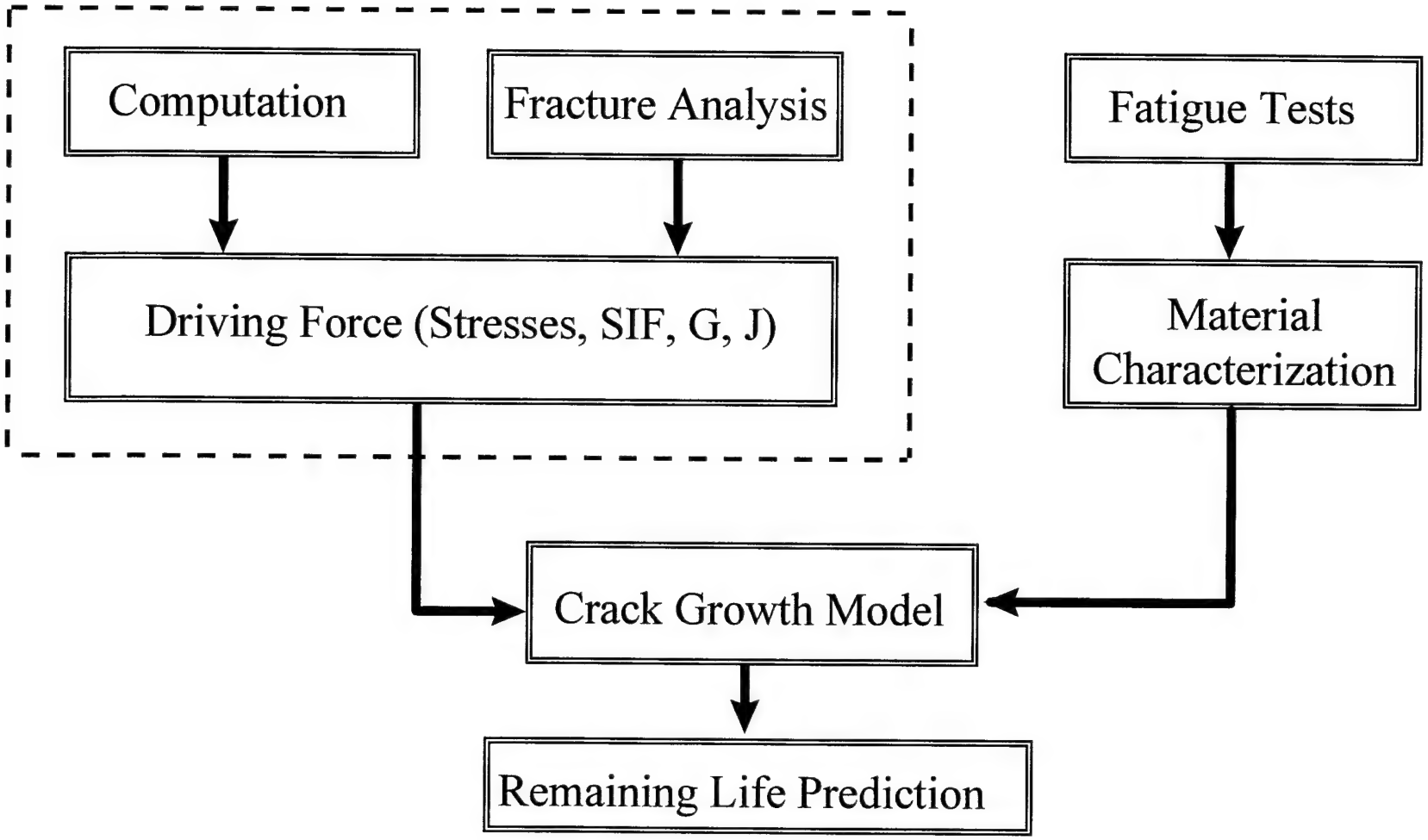

Stress Analysis of the Rotor Hub

Challenges

- Complex 3-D geometry
- Difficult to identify "hot spots"
- Cannot "see" the stress inside the component

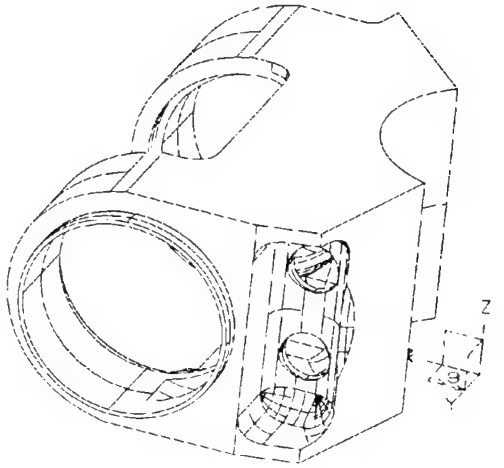

Solution

Developed a 3-D FEM model for stress analysis and a computer visualization program that has

- Cutting plane to view any cross-section,
- Sequencer to enable automatic 3-D scan to find the hot spots,
- Position interrogation to locate a specific point in the component.

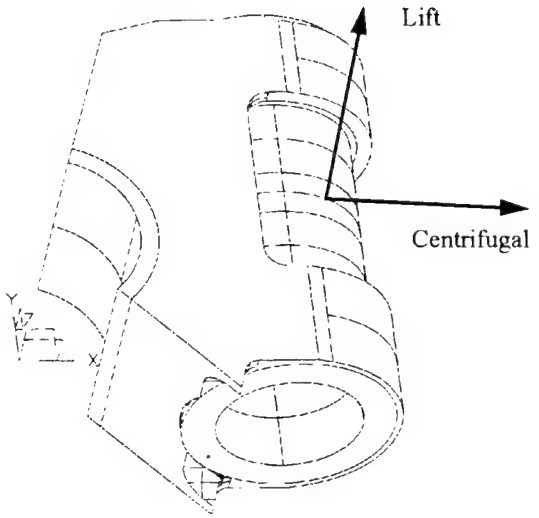

Field Quantity : Max Prin Stress

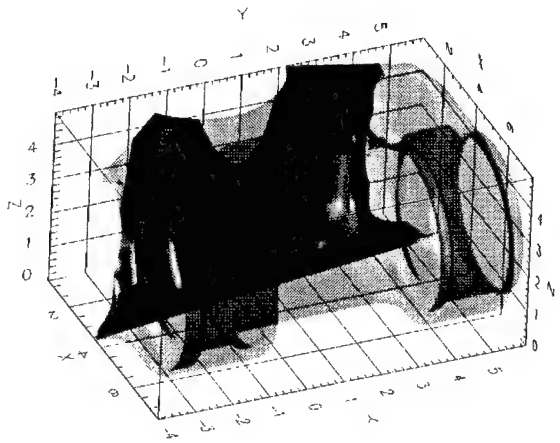

Normal: [0.9710, 0.1470, 0.1900] Point: [2.2520, 3.7760, 0.9810]
Max Max Prin Stress Value : Current Plane 0.6524, Entire Body 0.6866

Field Quantity : Max Prin Stress

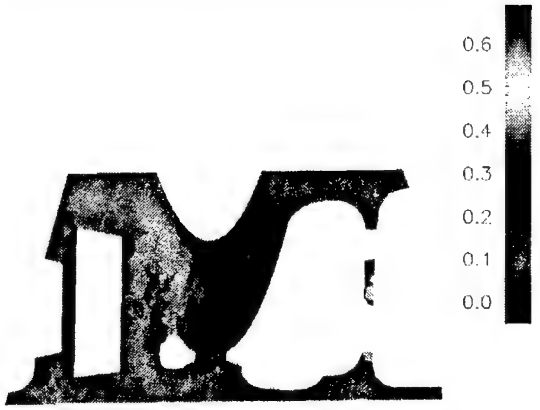

Normal: [0.9710, 0.1470, 0.1900] Point: [2.2520, 3.7760, 0.9810]
Max Max Prin Stress Value : Current Plane 0.6524, Entire Body 0.6866

Conclusions

- The visualization program is a powerful tool for interpreting the stress analysis results.
- Predicted failure sites are all located near through holes in the rotor hub.
- Several of the predicted failure sites coincided with actual failure sites recorded at Cherry Point.

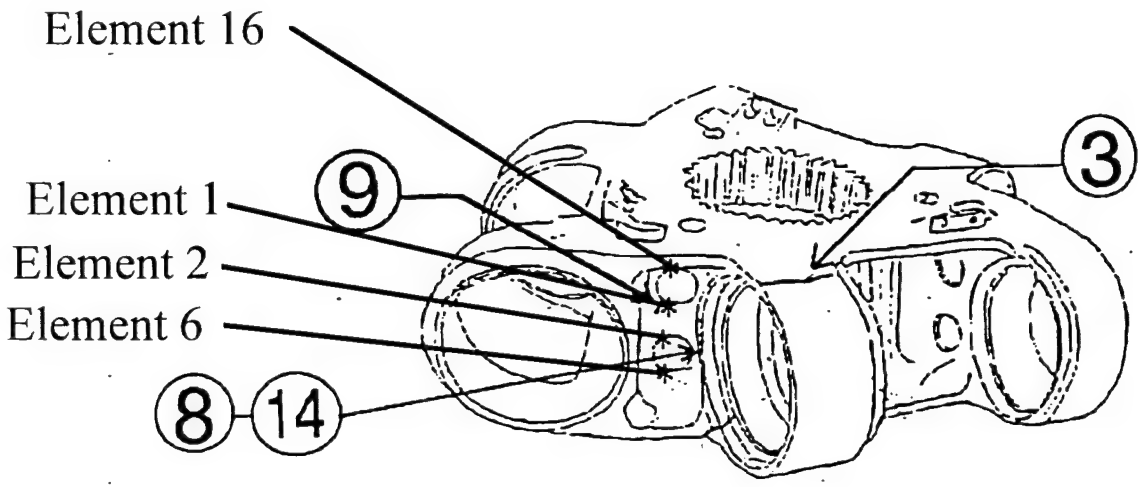

Why are Small Cracks Important?

- Small crack growth can account for 50-90% of the total life, particularly under HCF
- LEFM concepts applied to small crack growth result in an overestimation of life
- Small cracks inherently grow under mixed mode/multiaxial conditions even under completely reversed loading conditions

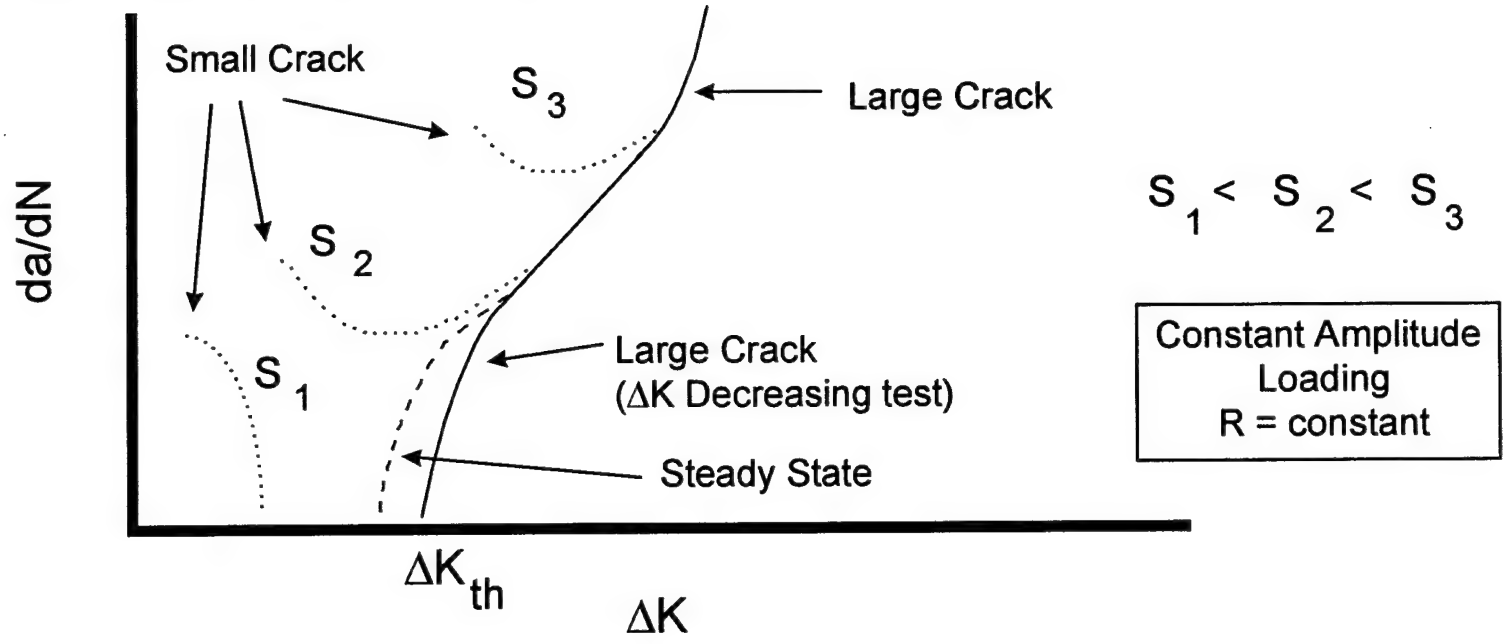

Features of Small Fatigue Crack Growth

- Highly dependent on material microstructure
- Nucleation preferentially occurs along slip systems in surface grains
- Small cracks propagate through or around slip barriers
- Fatigue crack propagation is linked to the cyclic slip ahead of crack tip

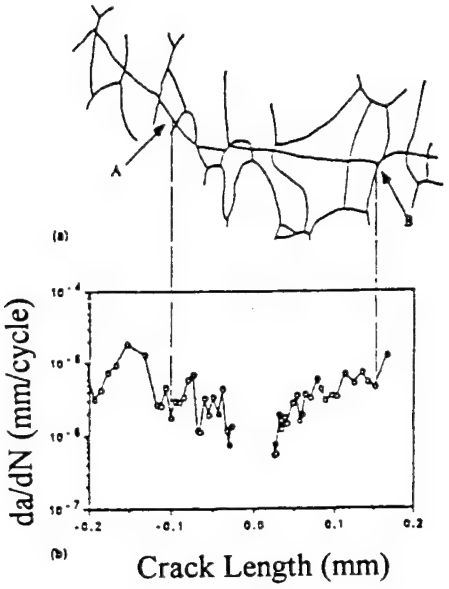

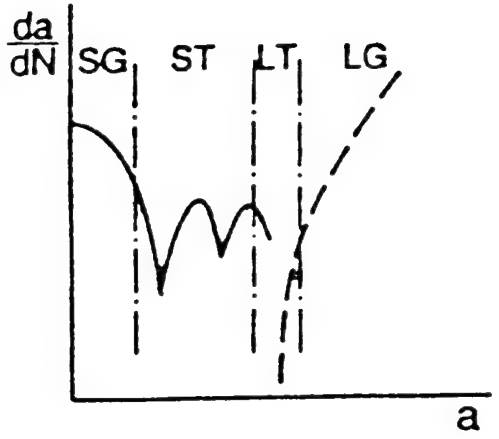

Small Fatigue Cracks in Steels

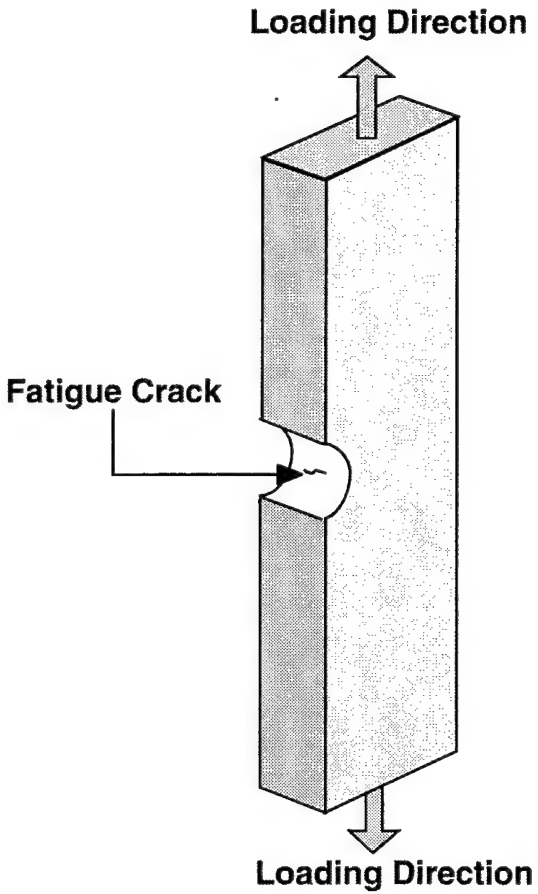

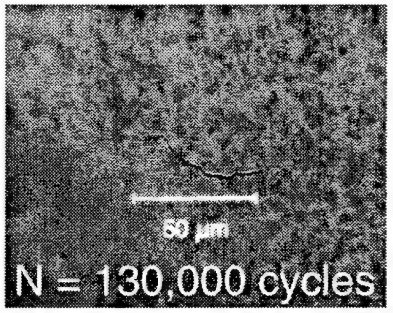

N < 110,000
No Crack found

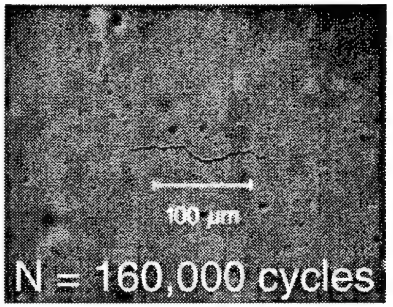

Growth to 100 µm:
70 - 90% of total life

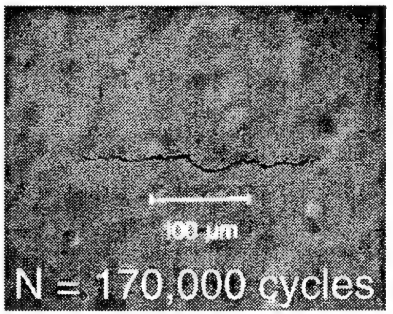

N = 220,000
Complete Fracture

Critical Data for Evaluating Small Fatigue Crack Growth Models

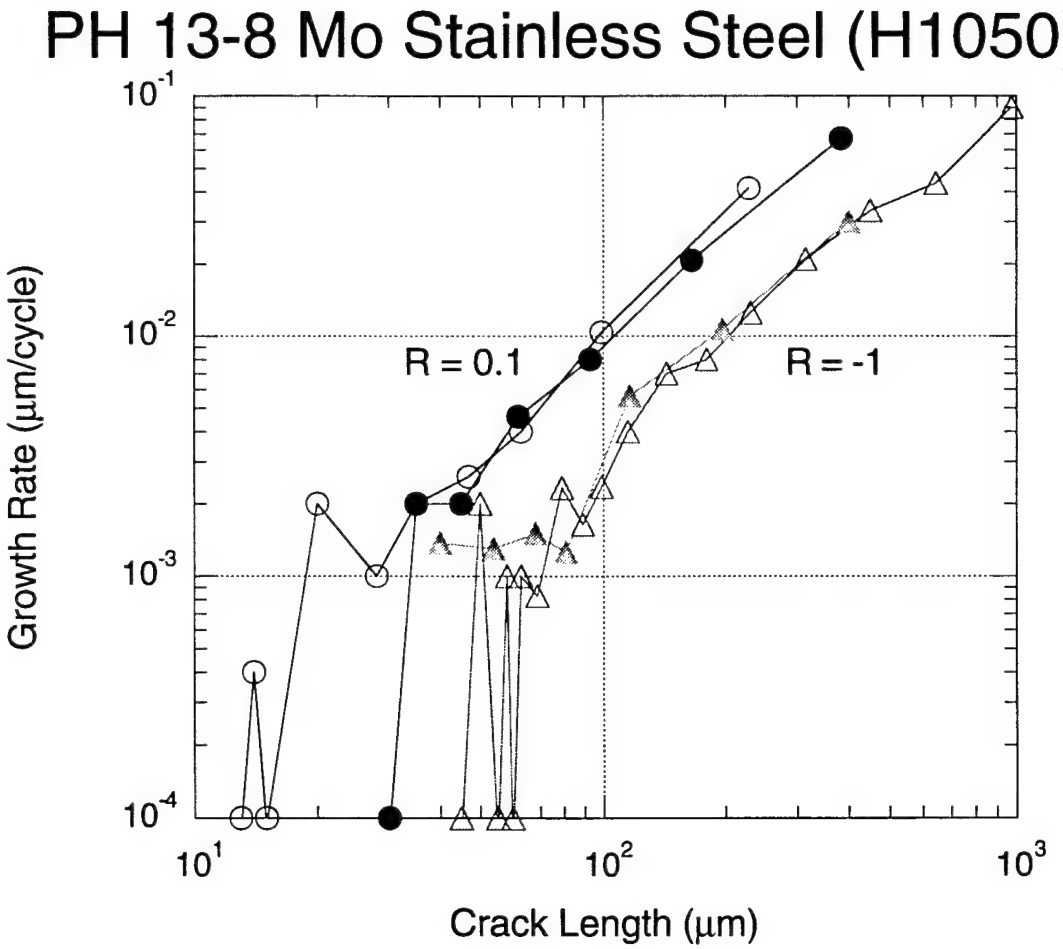

Correlation of Small Fatigue Crack Growth Models

Plasticity-induced Crack Closure Model (Newman, 1981)

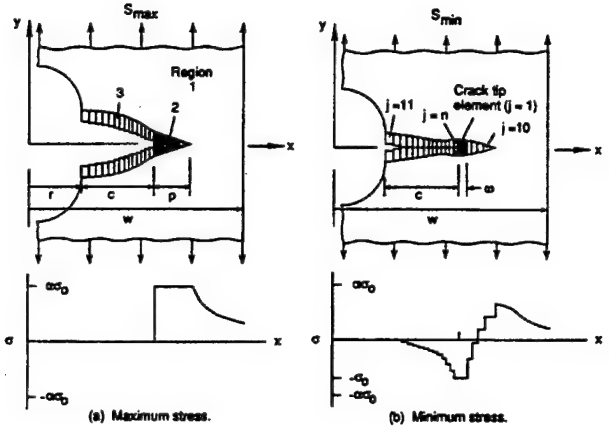

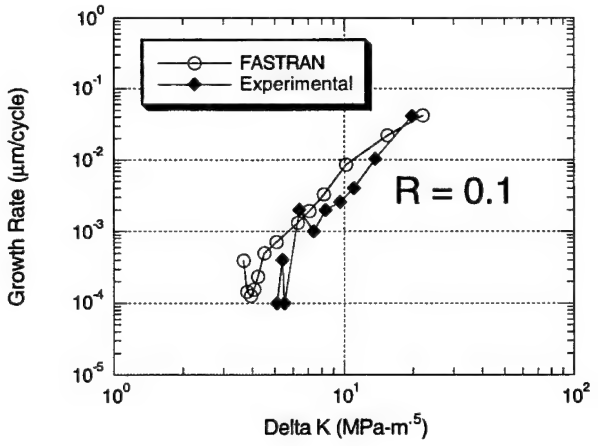

Sequential Barrier Model (Wang, 1996)

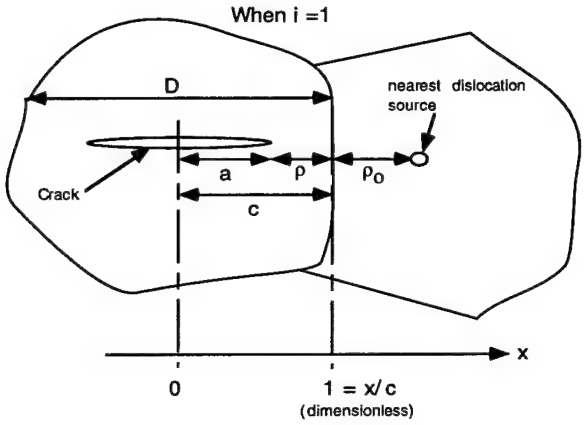

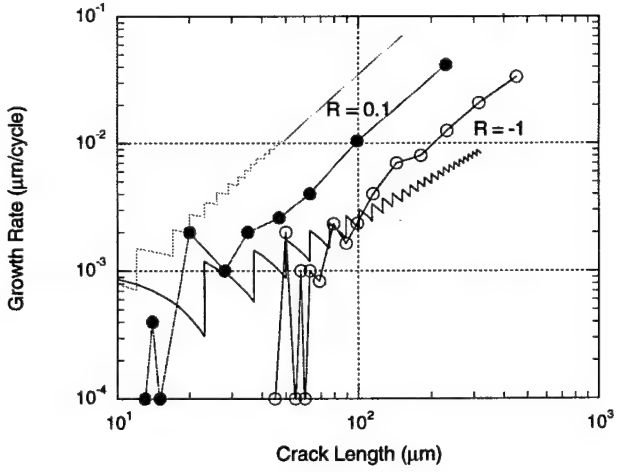

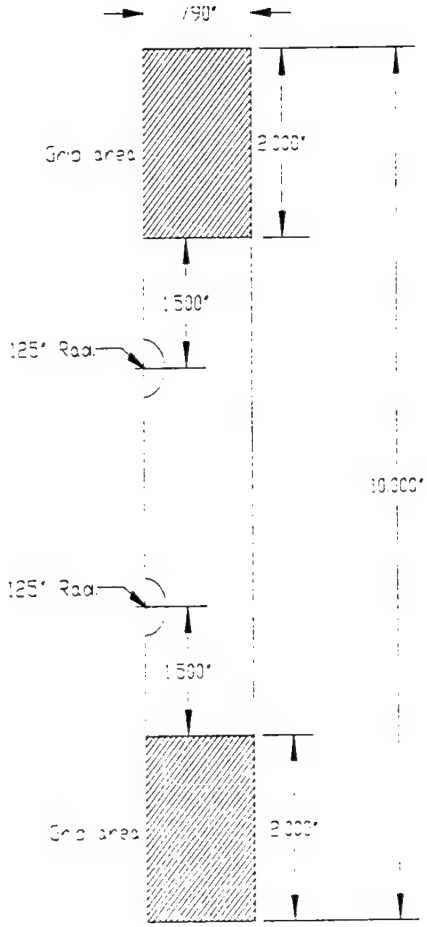

$K_t = 3.62$

Thickness: .131 inches

Polishing:

Notches were mechanically polished -

400	grit
1200	grit
6 μm	diamond paste
3 μm	diamond paste
.25 μm	diamond paste

Monitoring:

Cracks were monitored using replicant method.

Background: Material Microstructure

α grain size: ~ 5 μm

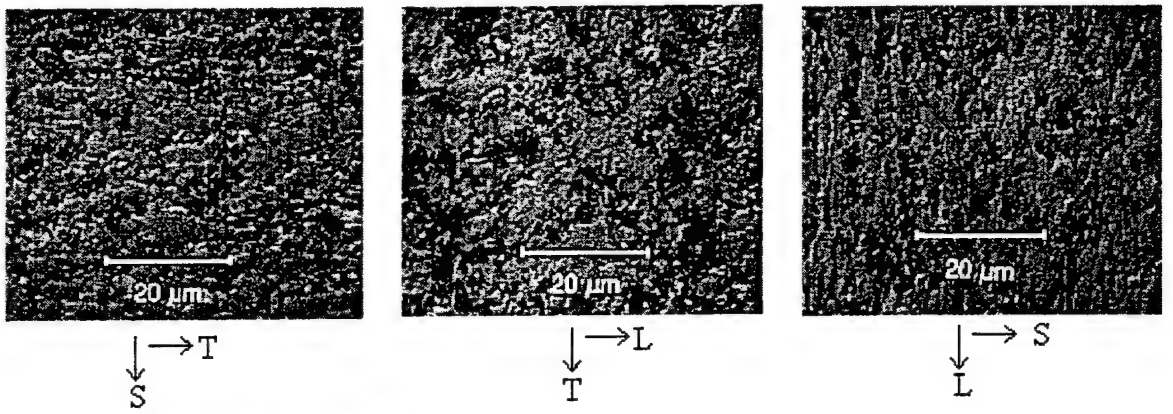

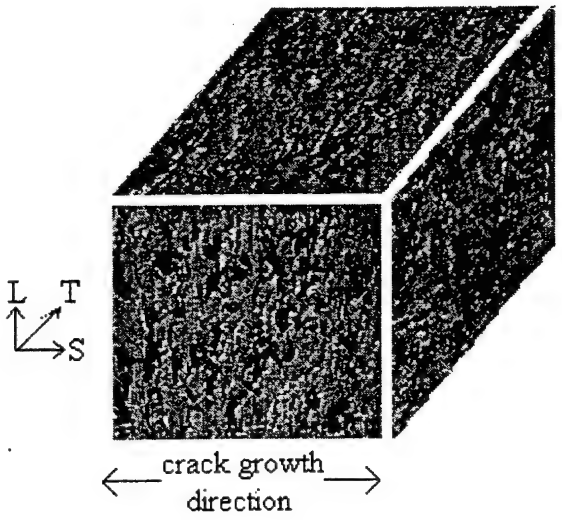

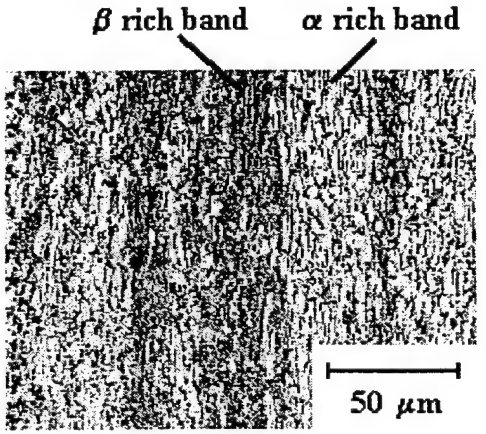

Modeling: Application of Wang and Navarro de los Rios Models

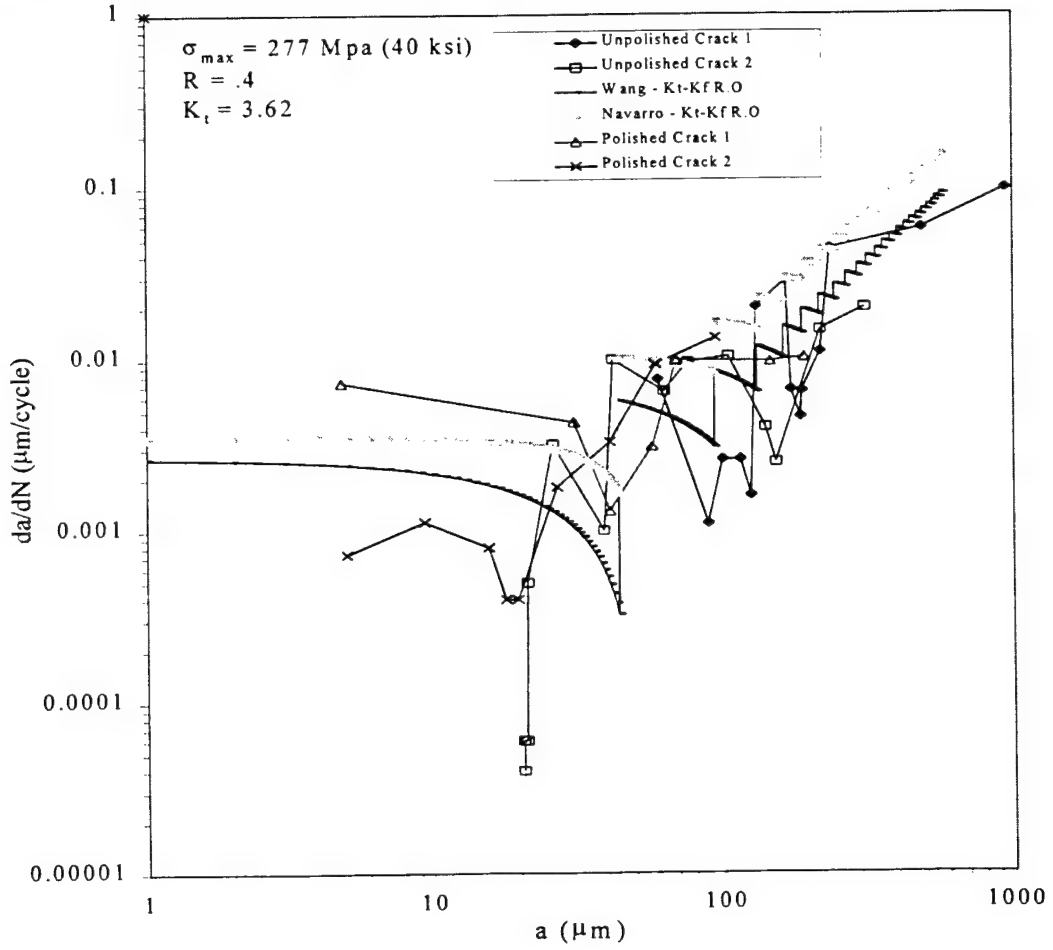

What is Multiaxial Fatigue?

Macro level

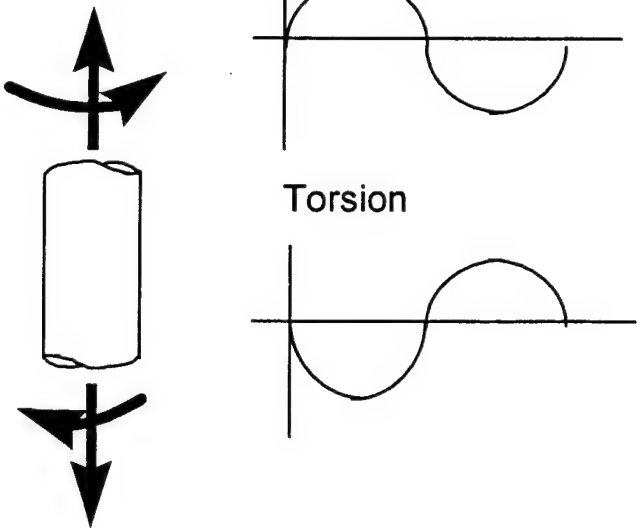

Micro level

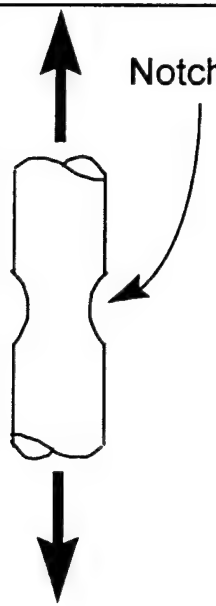

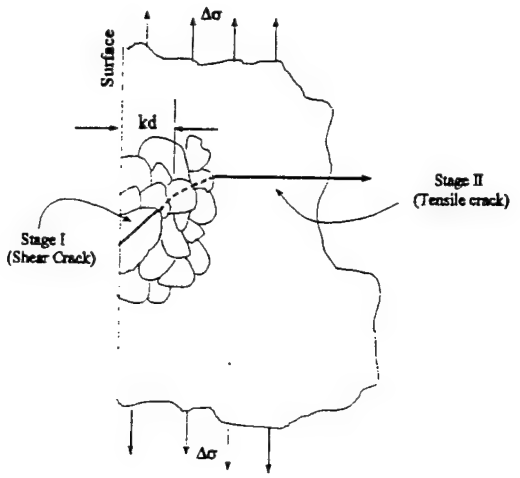

Stress-State Dependence of Small Crack Growth

1045 Steel (Socie, 1993)

Tension

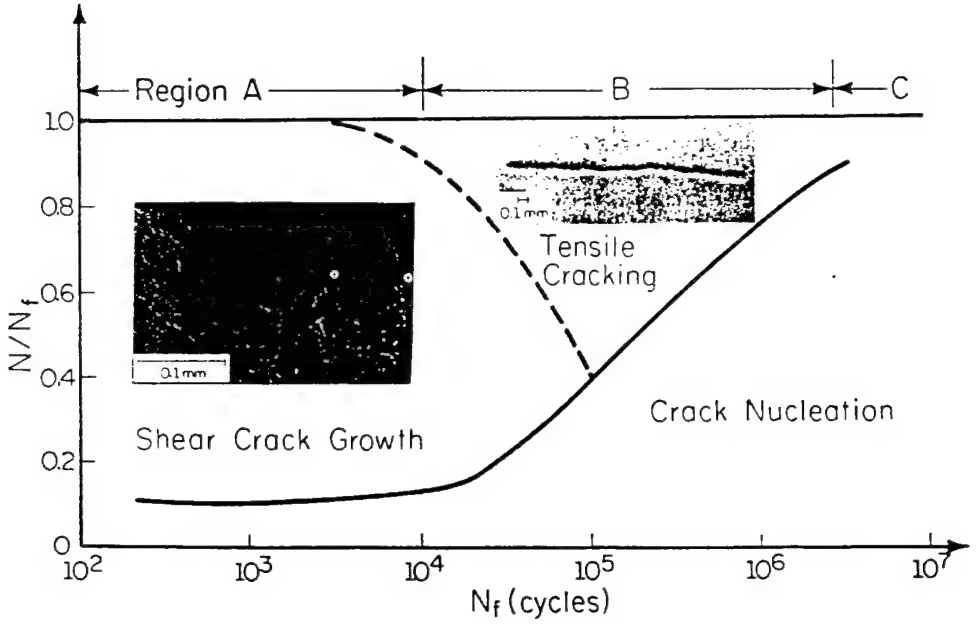

Torsion

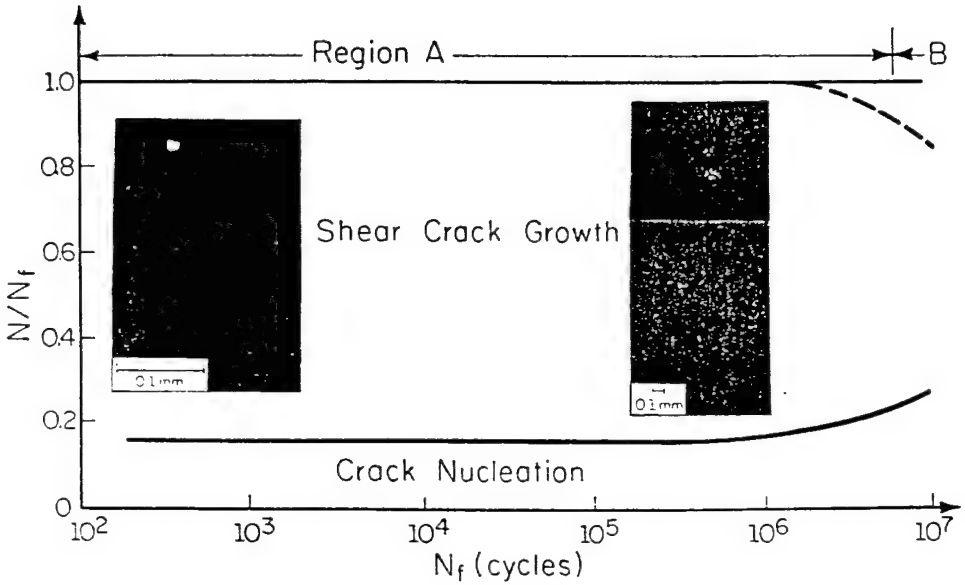

Stress-State Dependence of Small Crack Growth

Multiaxial Stress State - Sequential Loading

Torsion ⟶ *Tension* (o)

Tension ⟶ *Torsion* (Δ)

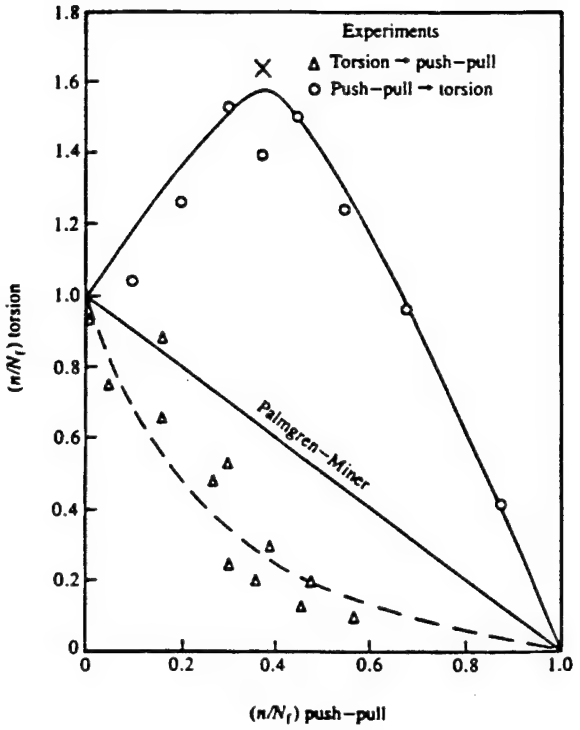

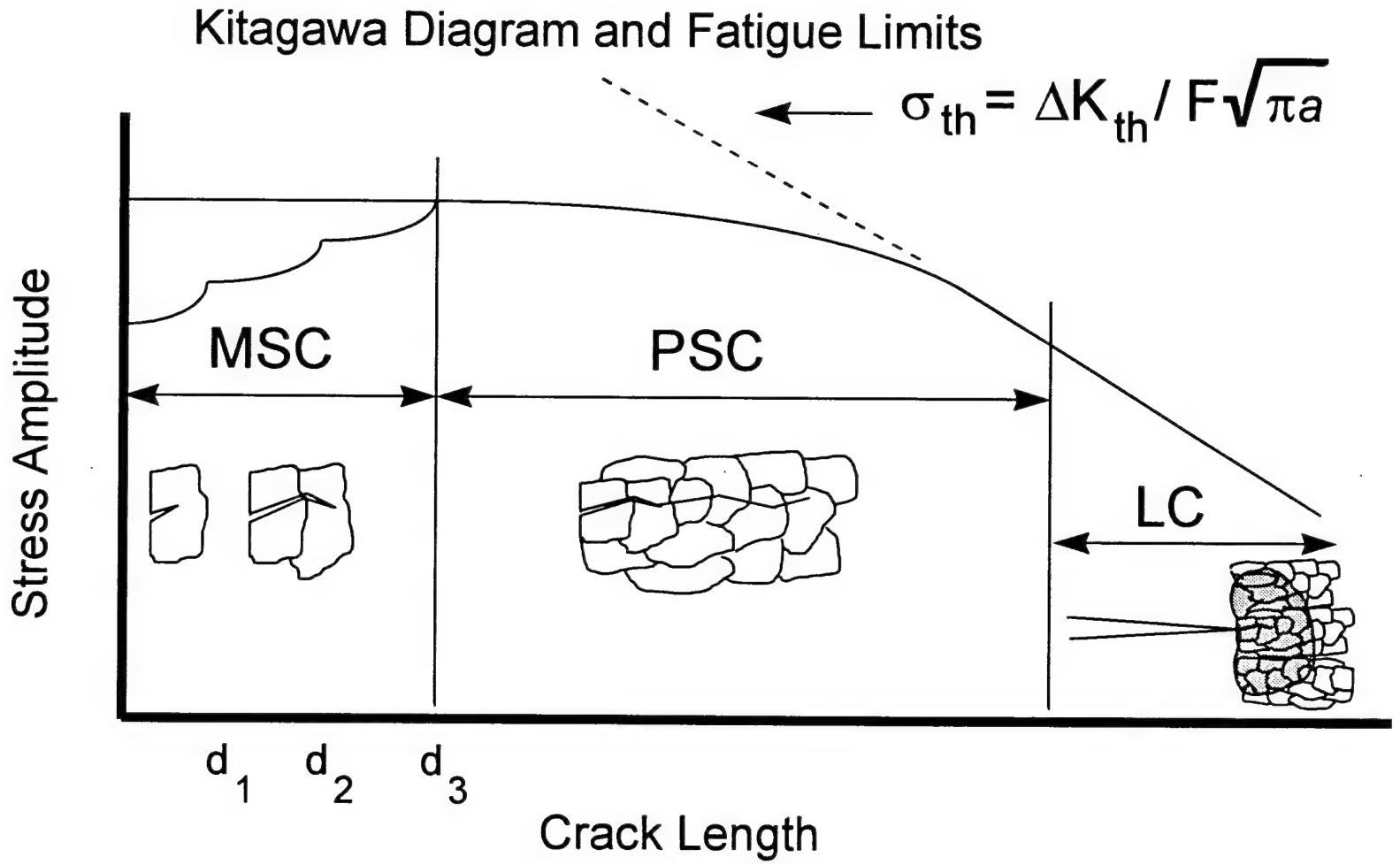
Kitagawa Diagram and Fatigue Limits
$\sigma_{th} = \Delta K_{th} / F\sqrt{\pi a}$
Stress Amplitude
MSC
PSC
LC
d_1
d_2
d_3
Crack Length

Multiple Stage Small Crack Multiaxial Fatigue Growth Law

$$\left(\frac{da}{dN}\right)_{I} = D_{aN}\,\psi\,A\,\psi^{B}\left(1 - \frac{a}{d}\right) \quad (MSC,\ Regime\ I)$$

$$\left(\frac{da}{dN}\right)_{II} = D_{aN}\,\psi\left\langle \psi^{r}\left(\frac{a}{kd}\right) - D\right\rangle \quad (Transition,\ Regime\ II)$$

$$\left(\frac{da}{dN}\right)_{III} = D_{aN}\,\psi\left\langle \psi^{r}\left(\frac{a}{kd}\right) - D\left(\frac{a}{kd}\right)^{1-Mr}\right\rangle \quad (PSC,\ Regime\ III)$$

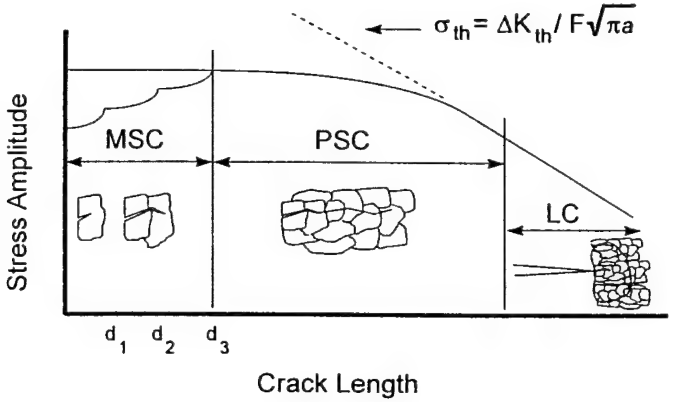

Transition to either EPFM or LEFM relations in Regime III

$$\left(\frac{da}{dN}\right) = \max\left(\left(\frac{da}{dN}\right)_{III}, \left(\frac{da}{dN}\right)_{FM}\right) \quad (\ for\ a > kd\ )$$

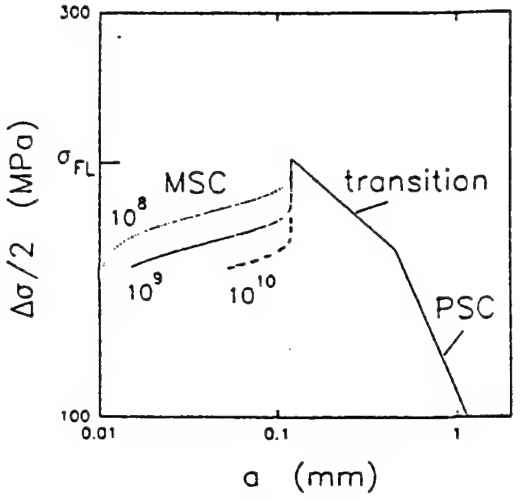

Multiple Stage Small Crack Multiaxial Fatigue Growth Law

$$\frac{da}{dN} = D_{aN}\left[R_e C_e(\Psi_e)^M + (1 - R_e)C_p(\Psi_p)^m\right]\left(\frac{a}{kd}\right)^{m_v}$$

McDowell & Berard (1992) proposed a generalized CTD based growth law for combined stress state propagation

$$\Psi_e = (1 + \mu\rho)\,(\beta_e(R_n)\,R_n + 1)\left(\frac{\Delta\tau_n}{2}\frac{\Delta\gamma^e{}_{max}}{2}\right) \qquad \Psi_p = (1 + \mu\rho)\,(\beta_p(R_n)\,R_n + 1)\left(\frac{\Delta\tau_n}{2}\frac{\Delta\gamma^p{}_{max}}{2}\right)$$

$$\Psi = R_e C_e(\Psi_e)^M + (1 - R_e)C_p(\Psi_p)^m$$

$$\beta_e = \left[4\left(\frac{\tau_f'}{\sigma_f'}\right)^2 - 1\right](R_n)^{j_e} \quad , \quad \beta_p = \left[\frac{4}{3}\frac{K_o'(\gamma_f')^{(1+n_o)}}{K'(\varepsilon_f')^{(1+n)}} - 1\right](R_n)^{j_p}$$

β_e and β_p reflect the effects of local mode mixity (primary and secondary slip) of the cyclic crack tip displacement

Correlations with Growth Law
1045 Steel

Tension

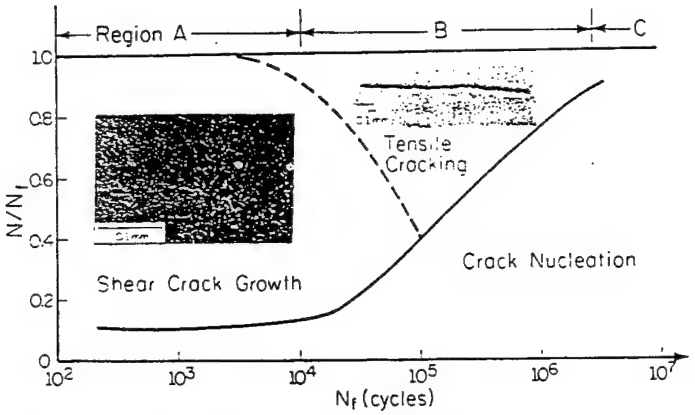

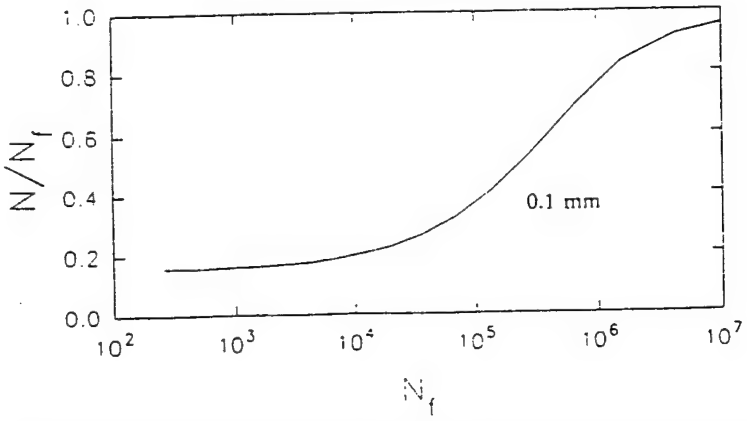

Torsion

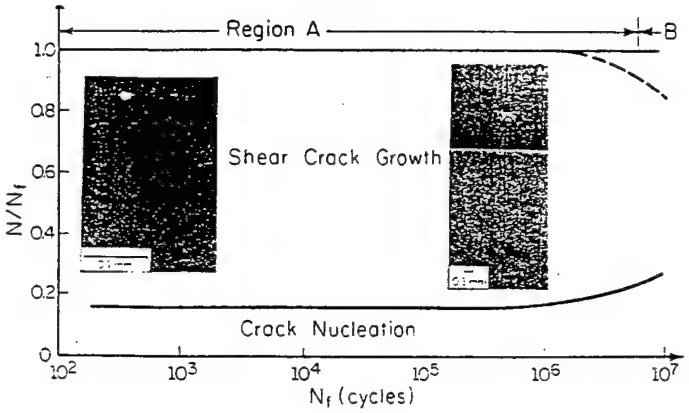

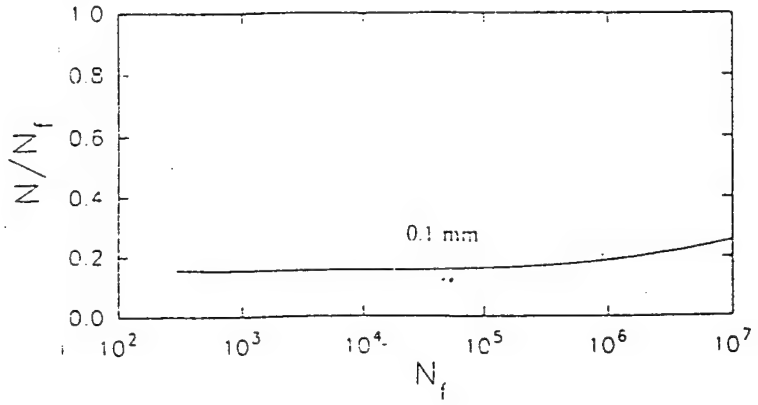

Correlations with Growth Law

Multiaxial Stress State Sequence

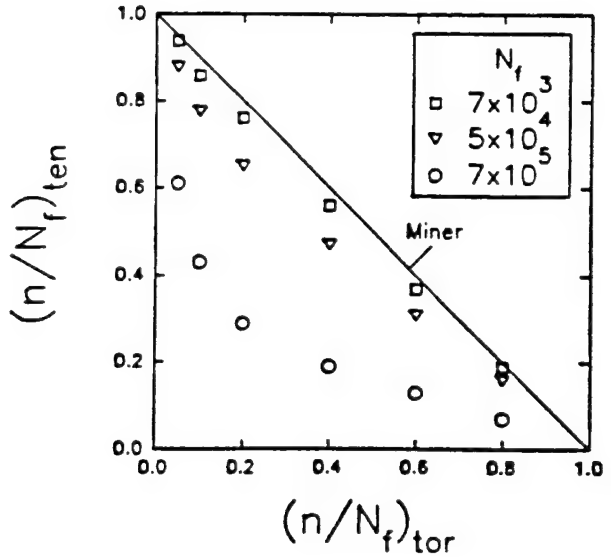

da/dN vs. ΔK_J

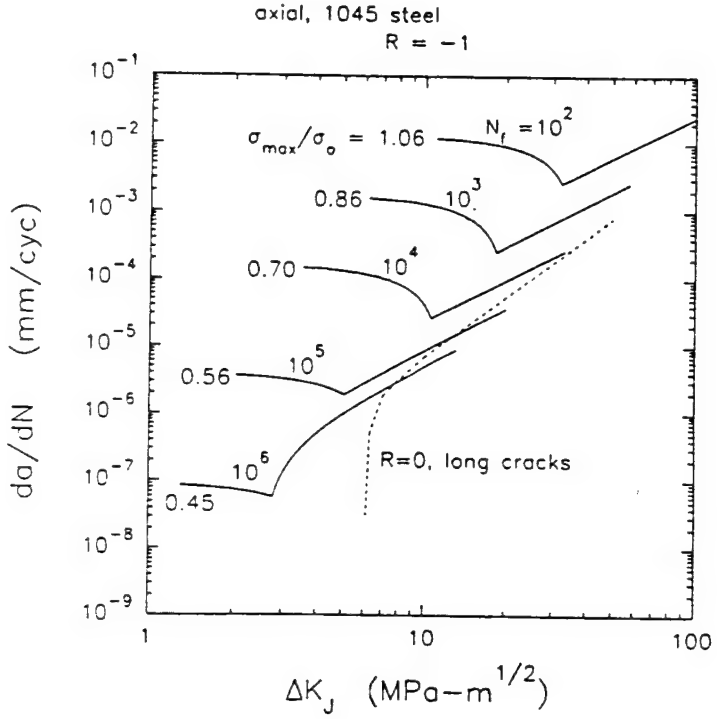

Crystal Plasticity and Finite Element Analysis

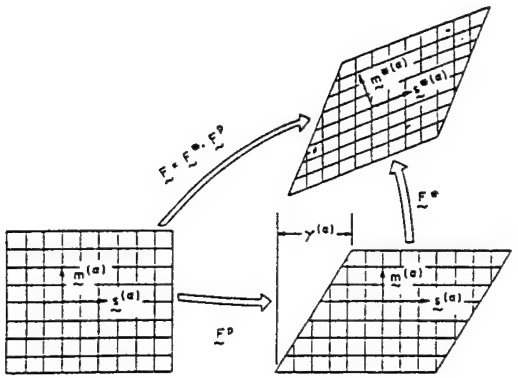

Planar Double Slip

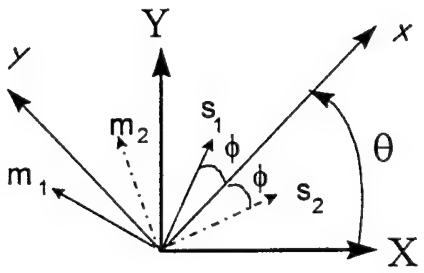

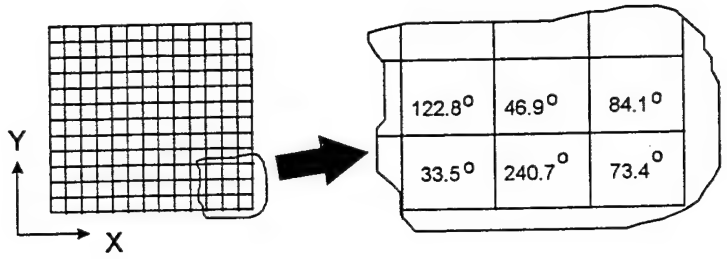

Cyclic Tension

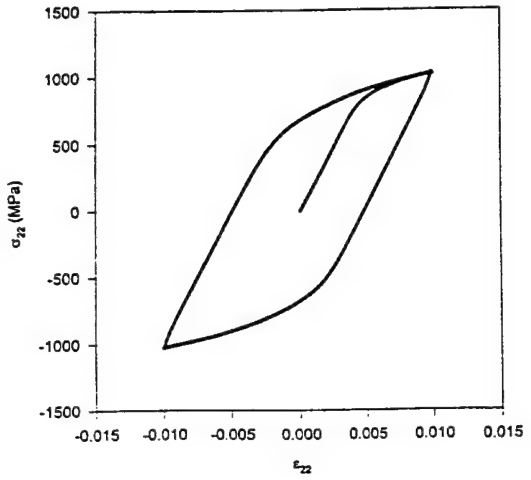

FEA: Micromechanical Distribution Effects

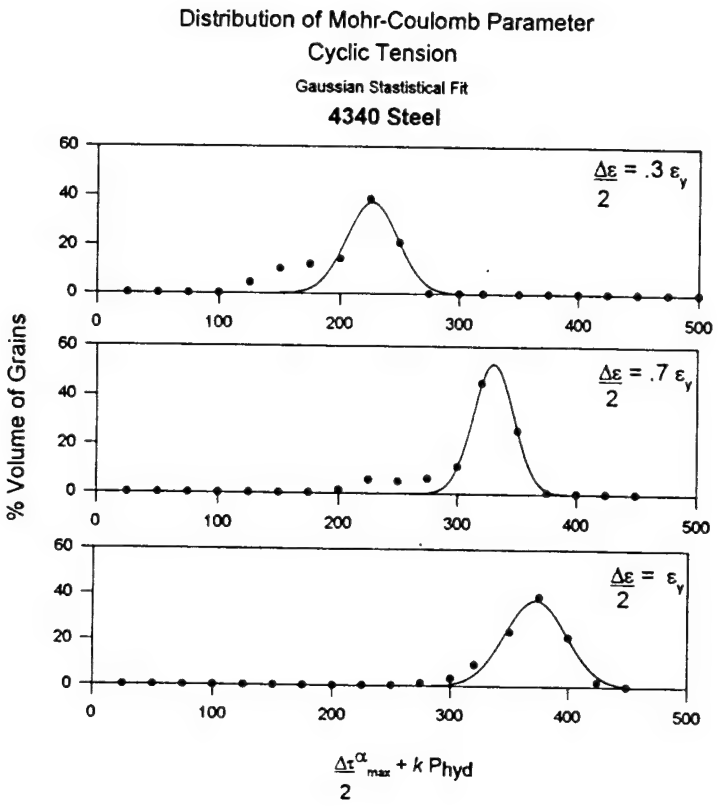

$\varepsilon_y = .6\%$

ABAQUS

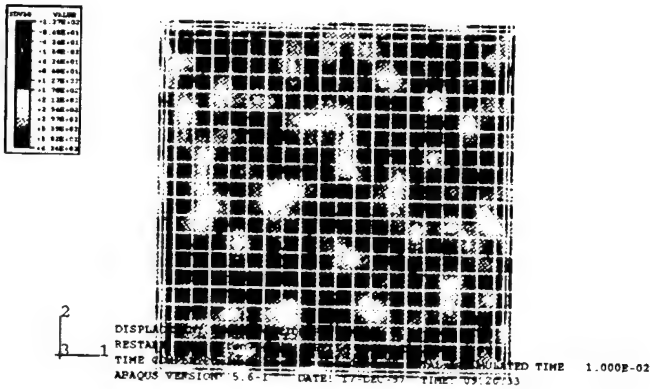

FEA: Micromechanical Distribution Effects

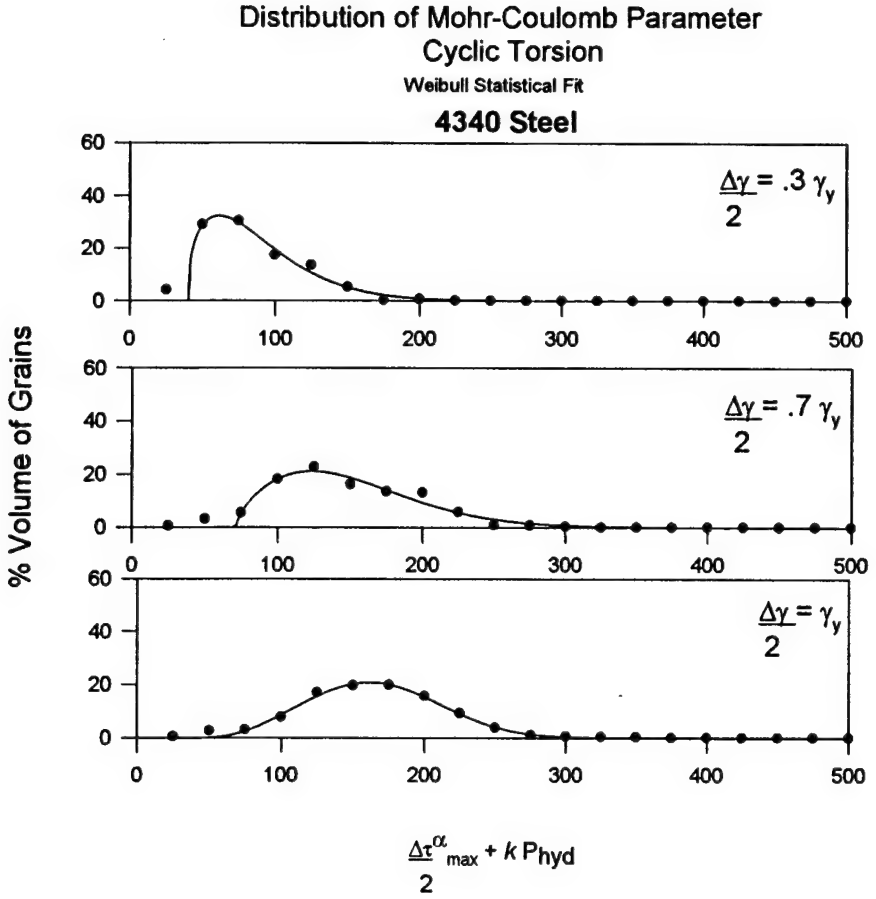

$\gamma_y = .42\%$

ABAQUS

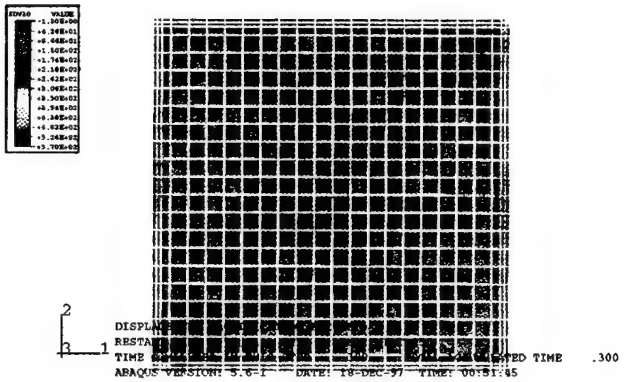

FEA: Small Cracks in Microstructures

ABAQUS

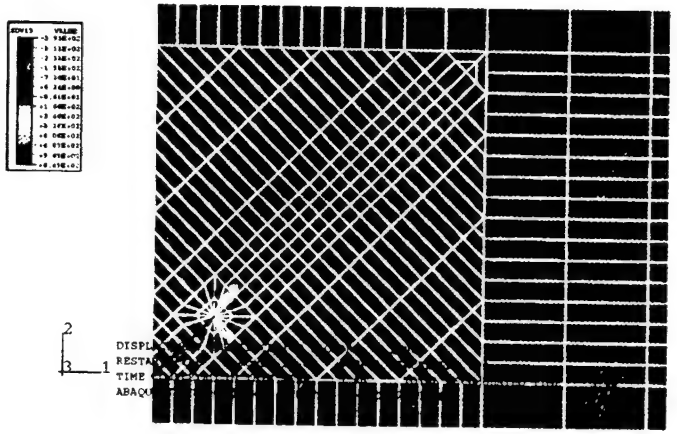

ABAQUS

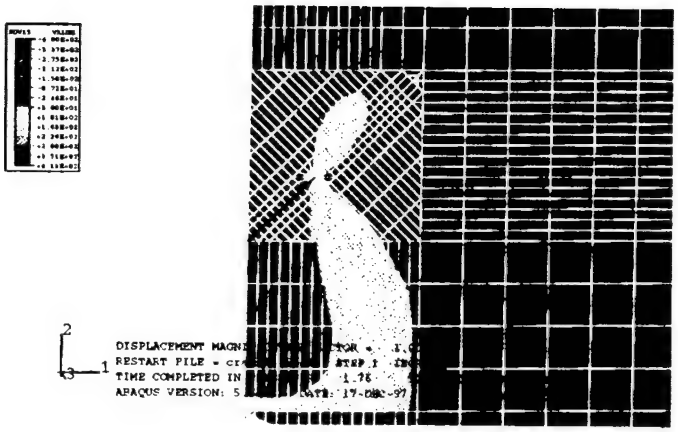

FEA: Small Cracks in Microstructures

Crack oriented at 0°, a/d = .9375, First Half Cycle in Shear

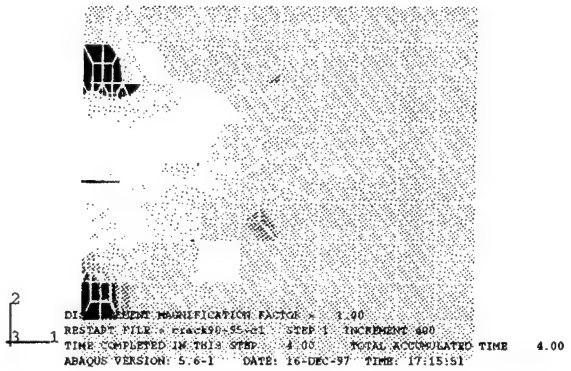

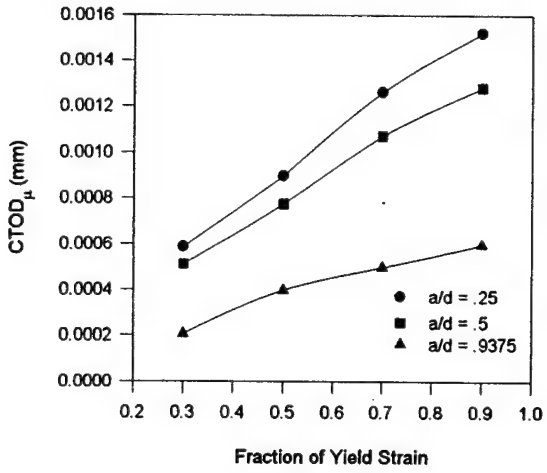

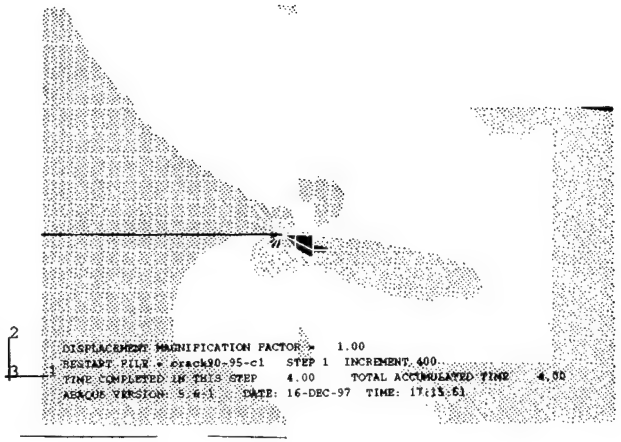

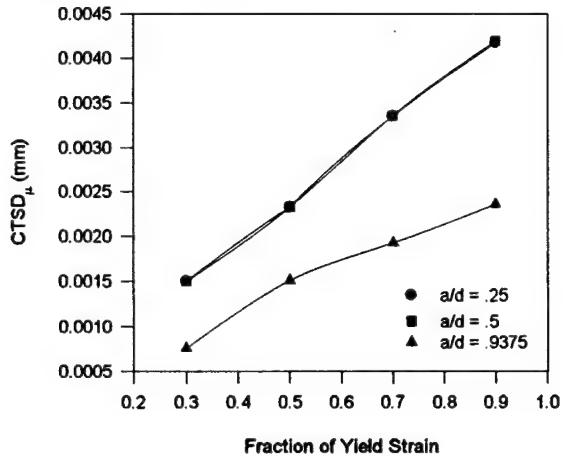

Fretting Fatigue

Problem Statement

Combined fretting and fatigue leads to rapid nucleation and subsequent growth of fatigue cracks

Common Occurrences

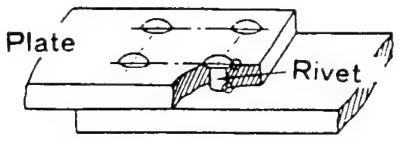

Riveted Joint

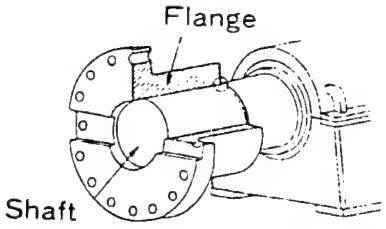

Shrink Fitted Shaft Coupling

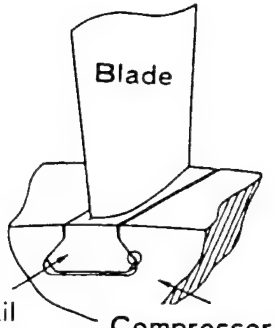

Compressor Rotor

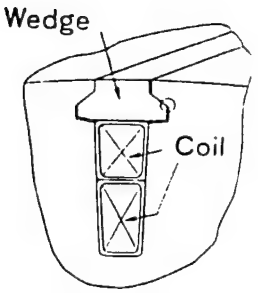

Turbine Genera

Research Objectives

- to characterize fretting fatigue crack nucleation and early crack growth and elucidate the stages of the fretting fatigue process using both destructive and non-destructive methods
- to develop the next generation life prediction models for fretting fatigue crack nucleation and early crack growth

Experimental Approach

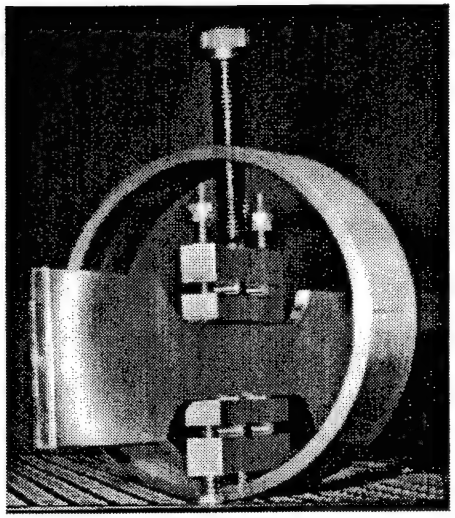

Experimental Parameters:

Control:

bulk fatigue loading
relative slip
normal pressure distribution

Measure:

frictional force

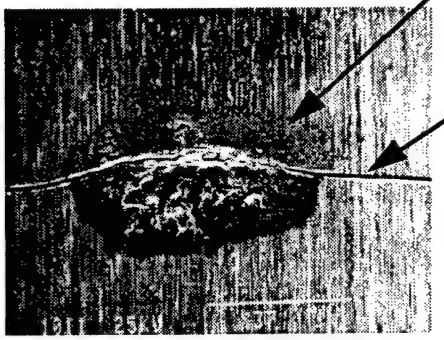

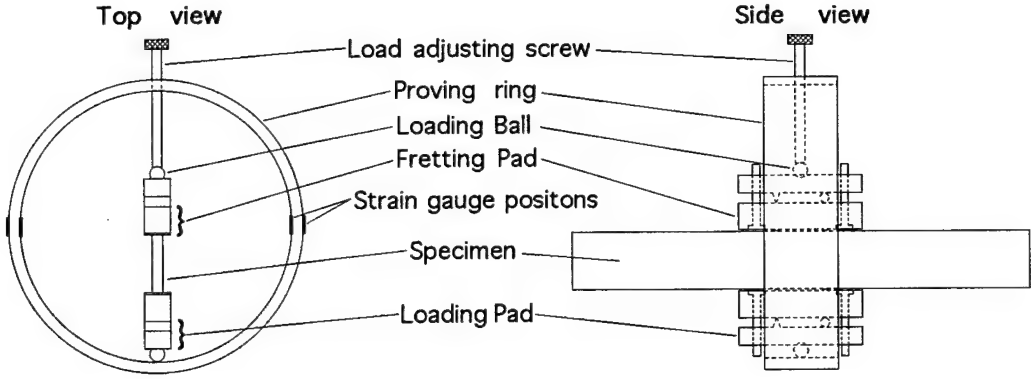

Monitoring of Damage Evolution:

In Situ:

acoustic emission
electric potential difference
hysteresis of frictional force and displacement

Interrupted Tests:

SEM
confocal scanning laser microscope
nanoindenter

Life Prediction Approach

State of the Art

Fretting Fatigue Crack Nucleation

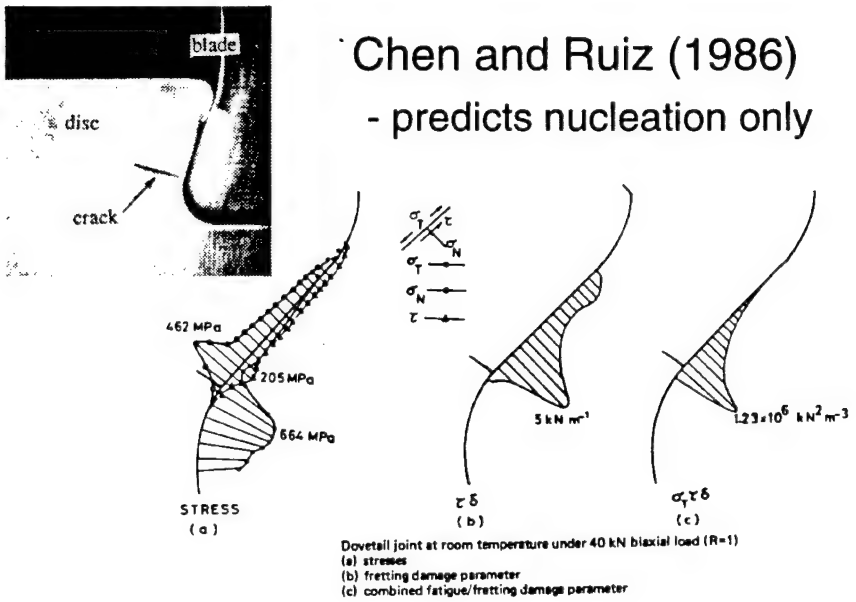

Dovetail joint at room temperature under 40 kN biaxial load (R=1)
(a) stresses
(b) fretting damage parameter
(c) combined fatigue/fretting damage parameter

Chen and Ruiz (1986)

- predicts nucleation only

Fretting Fatigue Crack Growth

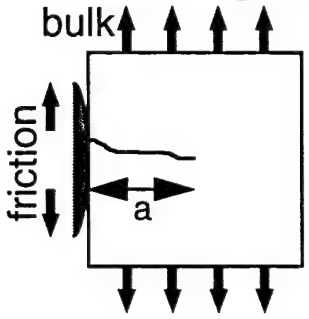

Fracture Mechanics

$$\frac{da}{dN} = f\left(\Delta K_{bulk} + \Delta K_{friction} - \Delta K_{redistrib}, K_{mean}\right)$$

- based on continuum description

Next Generation

Multiaxial Fatigue Criteria Based on Critical Plane Approaches

- potential to predict both nucleation and direction of early crack growth

LINK

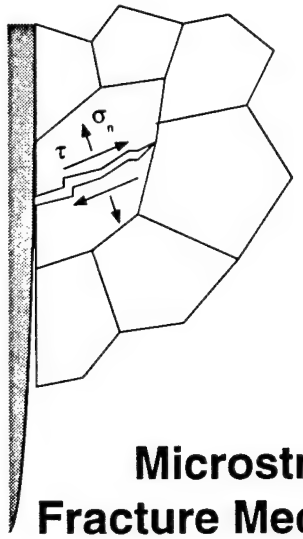

Microstructural Fracture Mechanics

- potential to use length scale appropriate for describing early crack growth where continuum description breaksdown

Test Results

PH 13-8 Mo Stainless Steel (H1050)
[MIL Handbook Data (H1000)]

- □ Fatigue Tests, R=0.1, MIL Handbook, 1994
- ■ Fatigue Limit, R=0.1, Patel, 1997
- ○ Fatigue Tests, R=-1.0, MIL Handbook, 1994
- ● Fatigue Limit, R=-1.0, Patel, 1997
- △ Fretting Fatigue, R=0.1
- ◇ Fretting Fatigue, R=-1.0

Fretting fatigue failures can occur at stress levels well below the fatigue limit

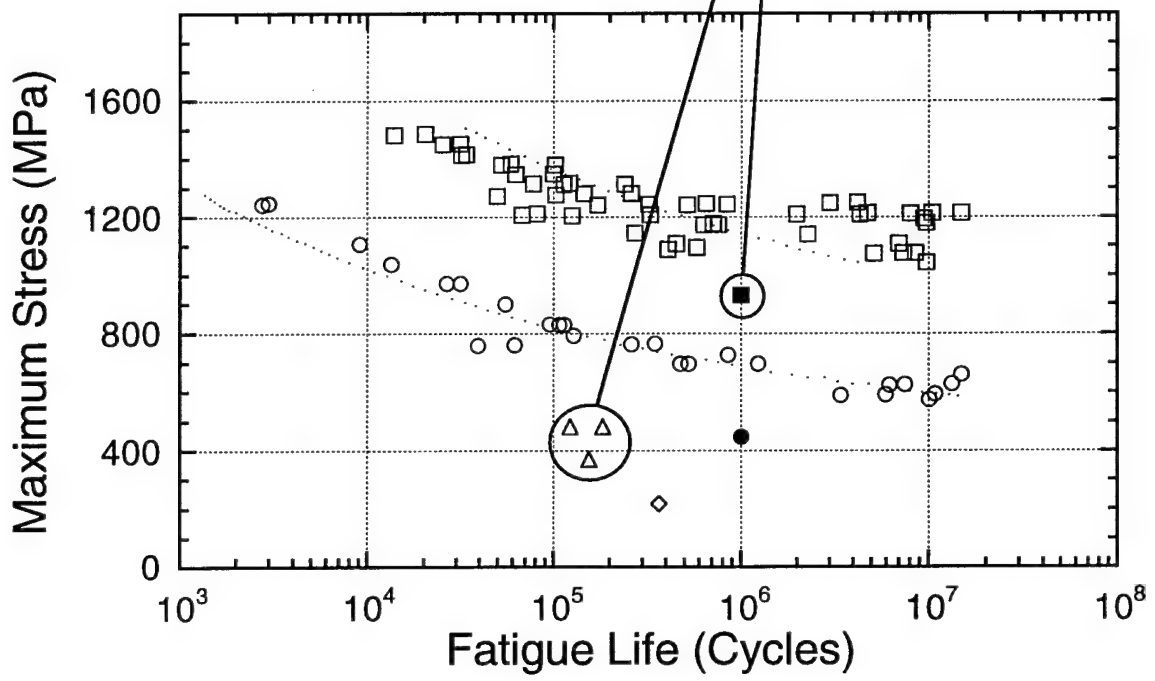

Stages of Fretting Fatigue

PH 13-8 Mo Stainless Steel
Flat Pad Contact Pressure: 30 MPa
Pad Span: 16.5 mm
Stress Ratio: 0.1
Stress Amplitude: 217 MPa

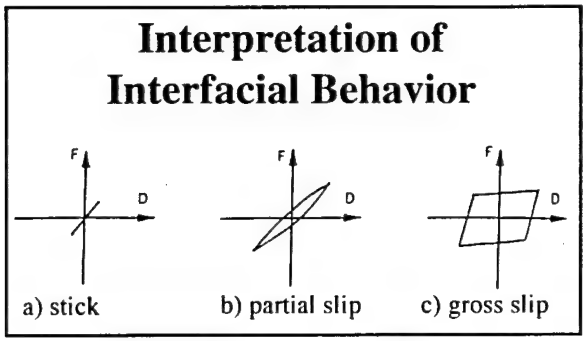

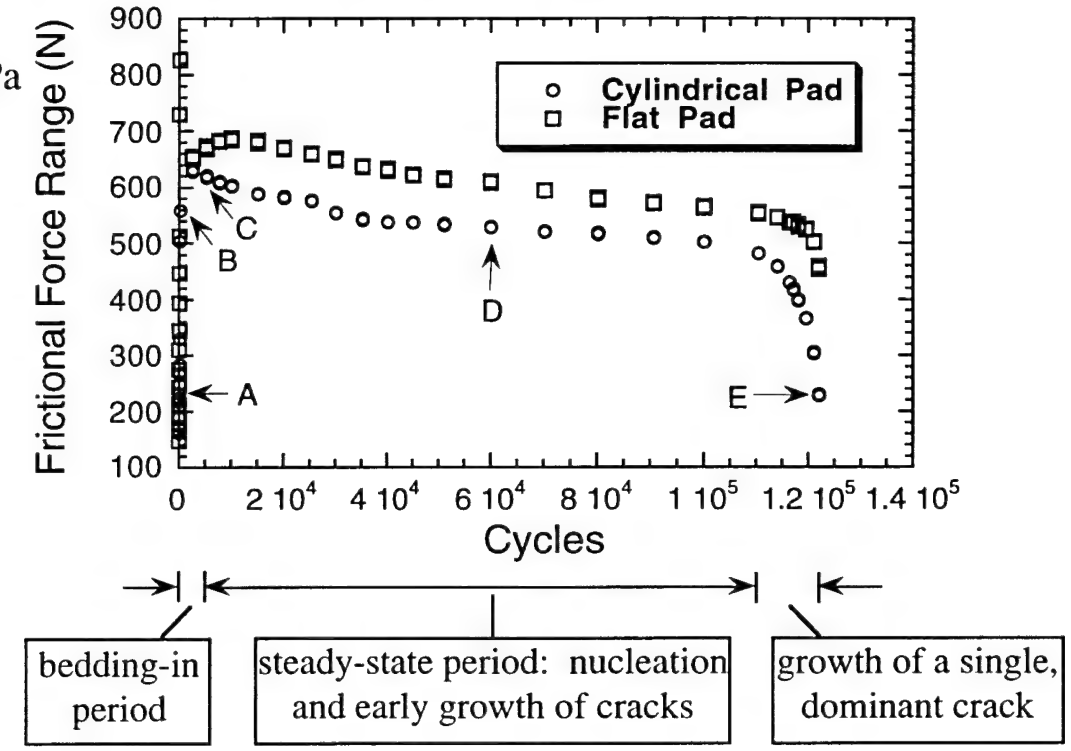

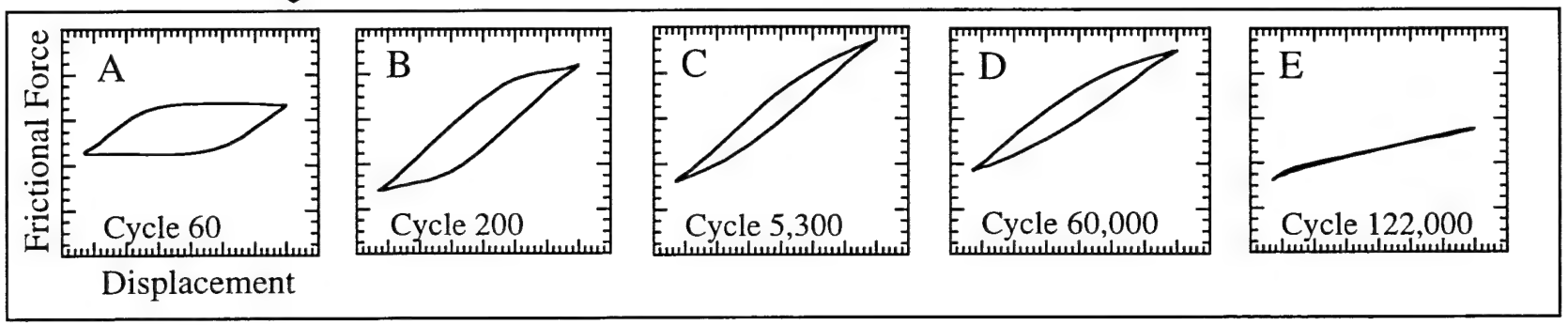

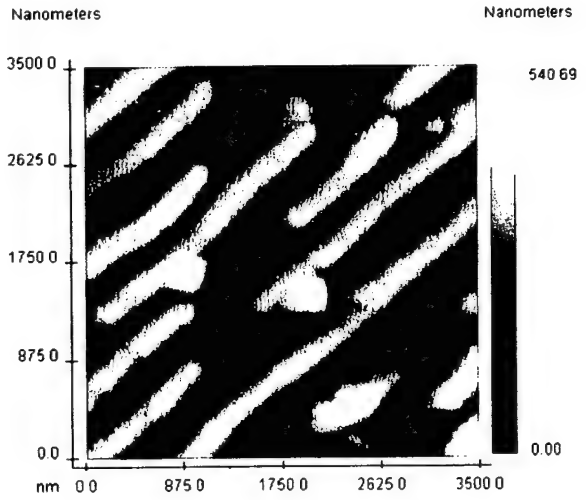
Nanometers
Nanometers
3500 0
2625 0
1750 0
875 0
0.0
nm 0 0
875 0
1750 0
2625 0
3500 0
540 69
0.00

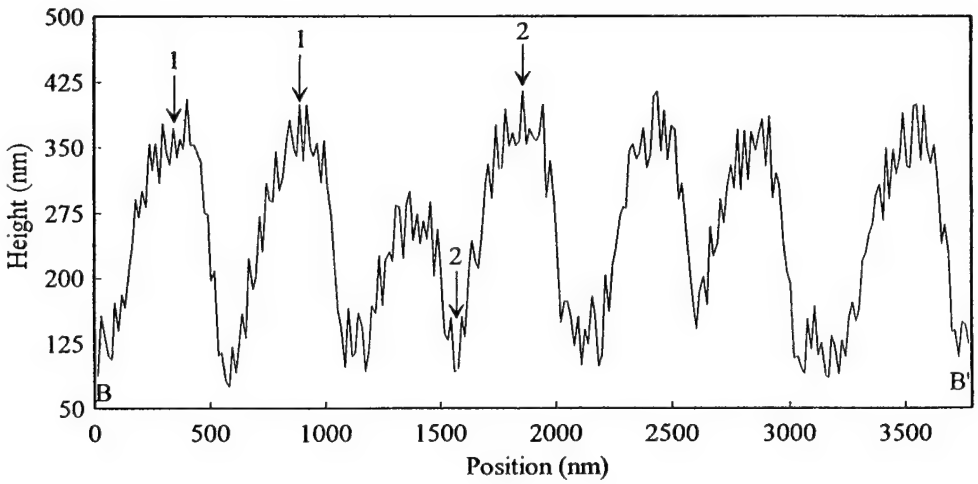
Height (nm)
Position (nm)
500
425
350
275
200
125
50
0
500
1000
1500
2000
2500
3000
3500
1
1
2
2
B
B'

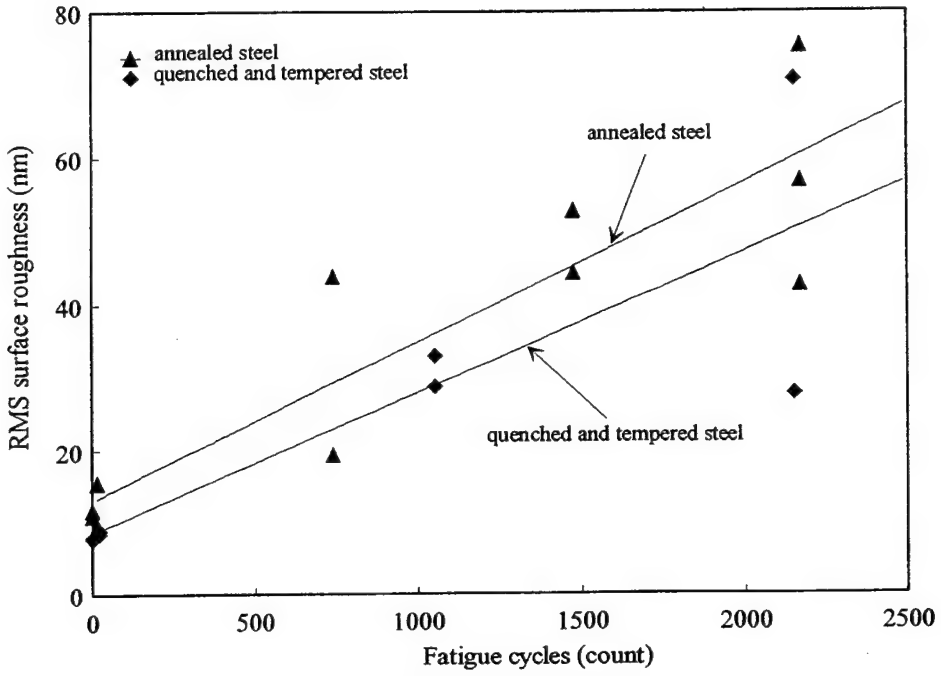
RMS surface roughness (nm)
Fatigue cycles (count)
annealed steel
quenched and tempered steel
annealed steel
quenched and tempered steel
80
60
40
20
0
0
500
1000
1500
2000
2500

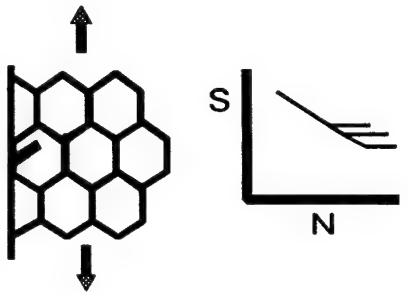
S
N

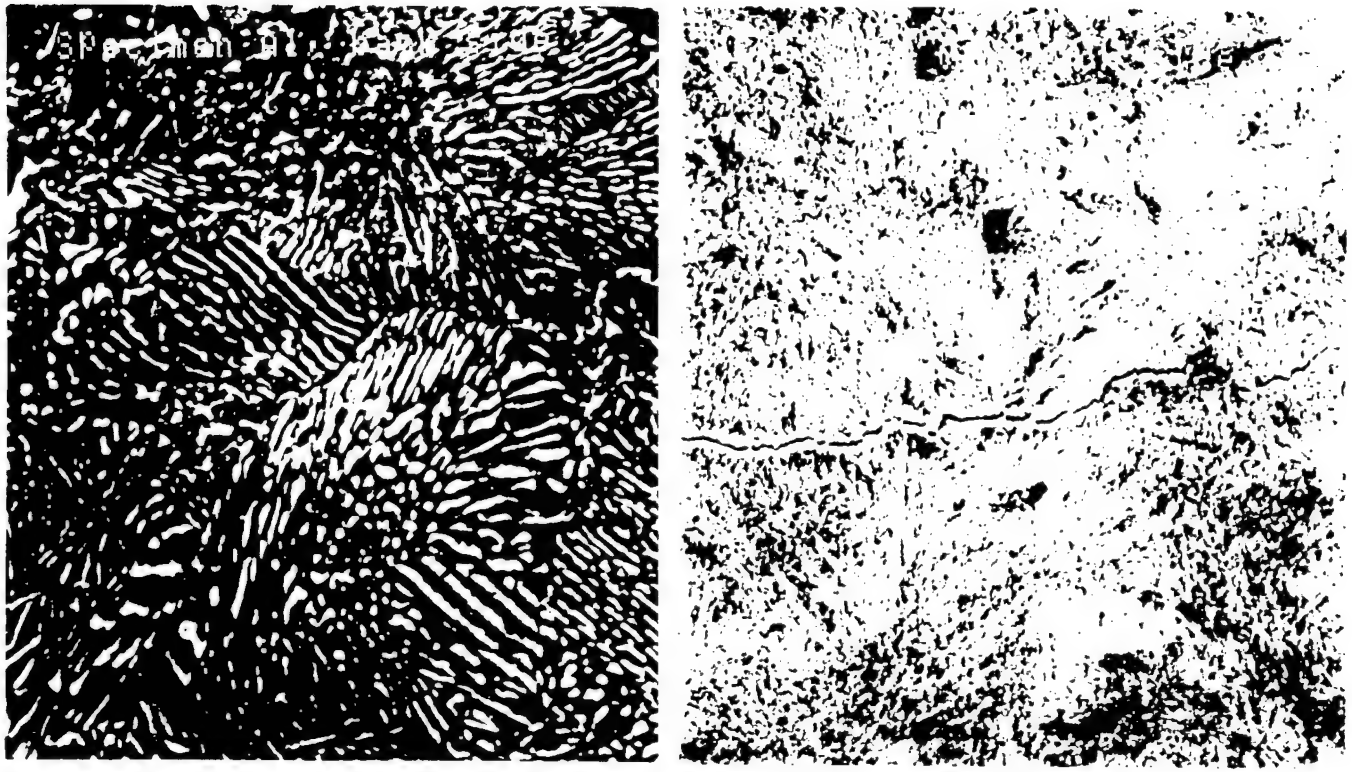
15 μm

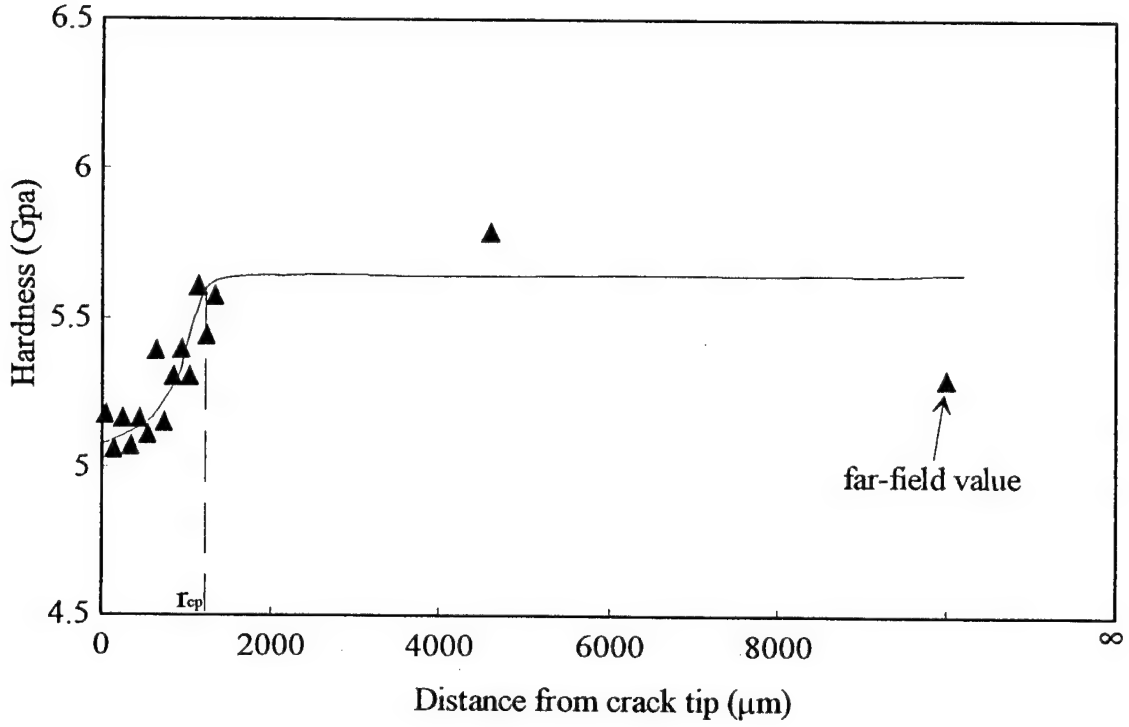
6.5
6
5.5
5
4.5
Hardness (Gpa)
r_{cp}
far-field value
0
2000
4000
6000
8000
∞
Distance from crack tip (μm)

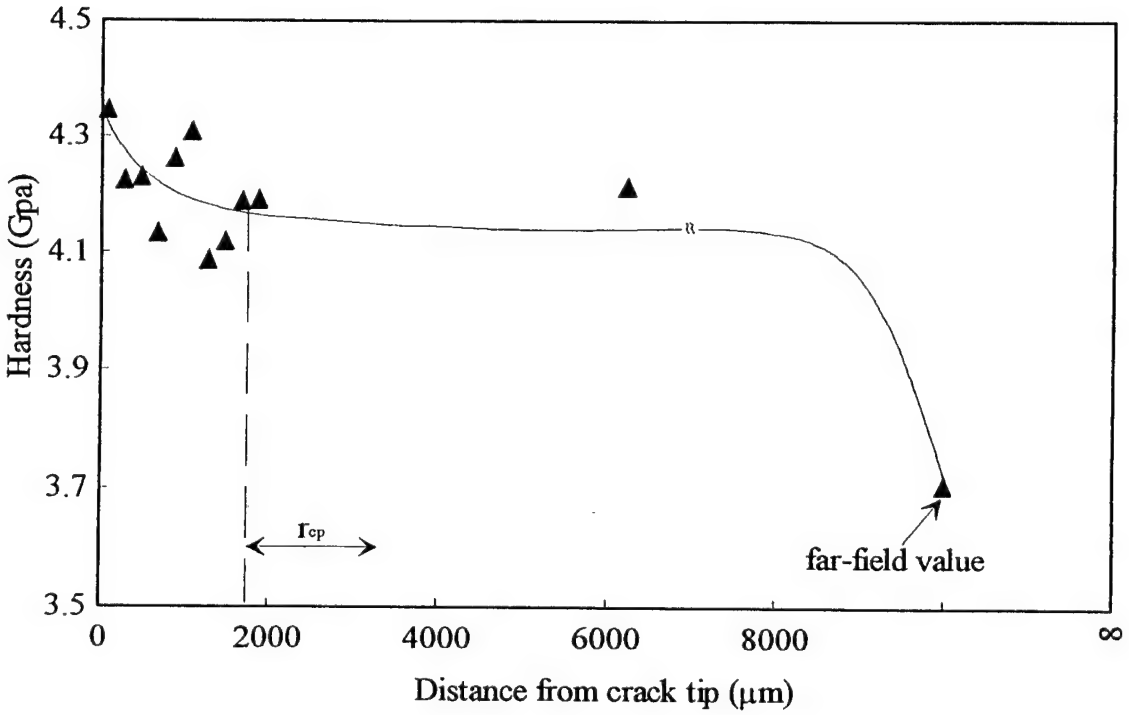
4.5
4.3
4.1
3.9
3.7
3.5
Hardness (Gpa)
r_{cp}
far-field value
0
2000
4000
6000
8000
∞
Distance from crack tip (μm)

Study of Acoustic Emission and Transmission from Incipient Fatigue Failure

(a) Fracture Characterization

G.W.Woodruff School of Mechanical Engineering
Georgia Institute of Technology

Co-PIs: Scott Bair, Laurence Jacobs, Jacek Jarzynski
Graduate Students: Zhiqiang Shi, Maxim Koutsak, Brad Beadle

Objectives:

- Develop passive acoustic emission (AE), and active ultrasonic transmission techniques that can quantitatively locate and characterize small cracks in complex engineering components.

Accomplishments:

- Realized an understanding of the acoustic source characteristics of a crack propagation event, successfully discriminating these source signals from ambient environmental noise.
- A unique feature of this investigation is the ability to experimentally capture and characterize complete acoustic waveforms in real time.

Experimental Setup

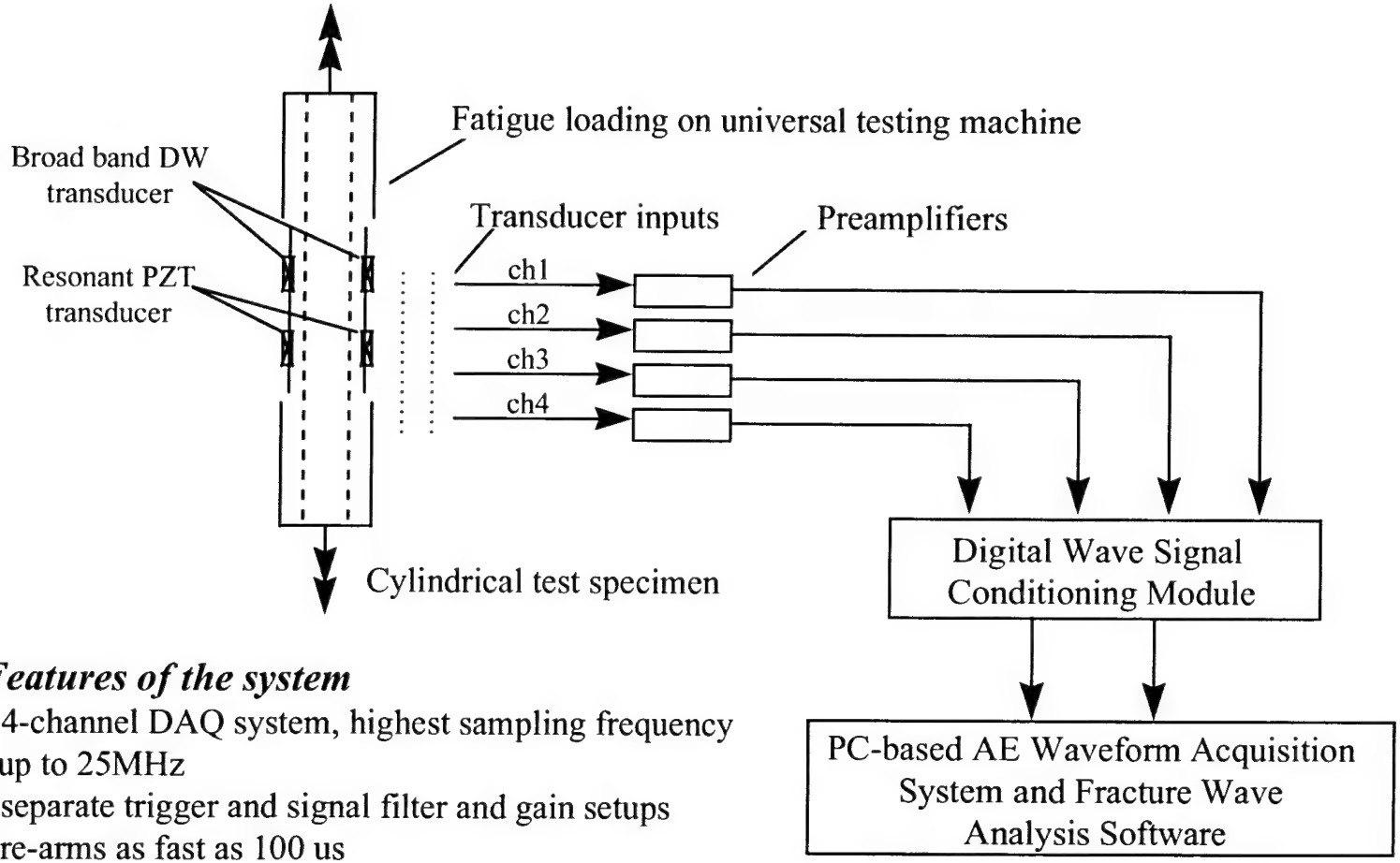

Features of the system

- 4-channel DAQ system, highest sampling frequency up to 25MHz
- separate trigger and signal filter and gain setups
- re-arms as fast as 100 us

Results - AE signals from distributed cracks in smooth specimens

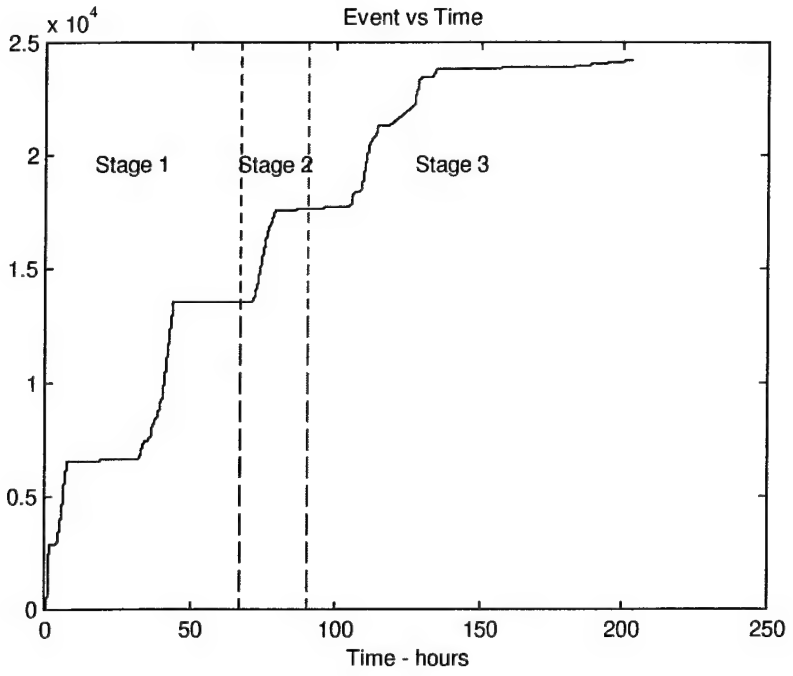

Cumulative AE events

Three regimes of crack growth were identified with acoustic signals and confirmed by the surface replicates:

1) uniform growth and distribution of small sub-grain sized cracks;
2) growth of these micro-cracks across grain boundaries;
3) coalescence of these cracks into localized cracks.

Results - AE signals from distributed cracks in smooth specimens

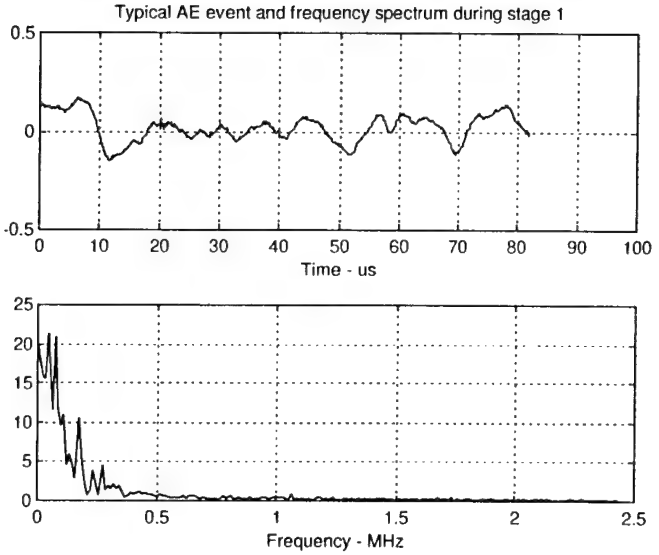

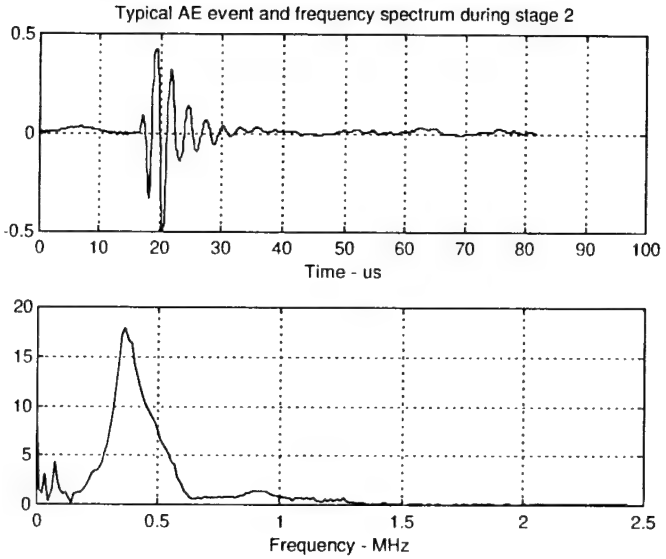

Stage 1
AE signal from uniform growth and distribution of sub-grain sized cracks

Stage 2
AE signal from growth of micro-cracks across grain boundaries

Results - AE signals from distributed cracks in smooth specimens

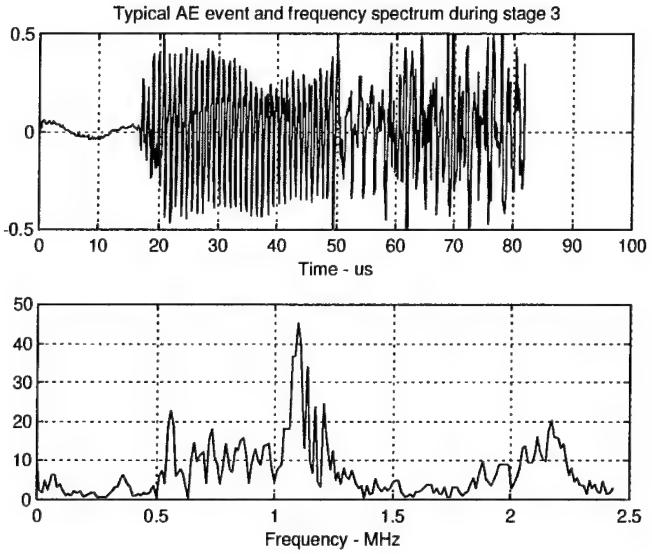

Stage 3
AE signal from coalescence of cracks into localized cracks

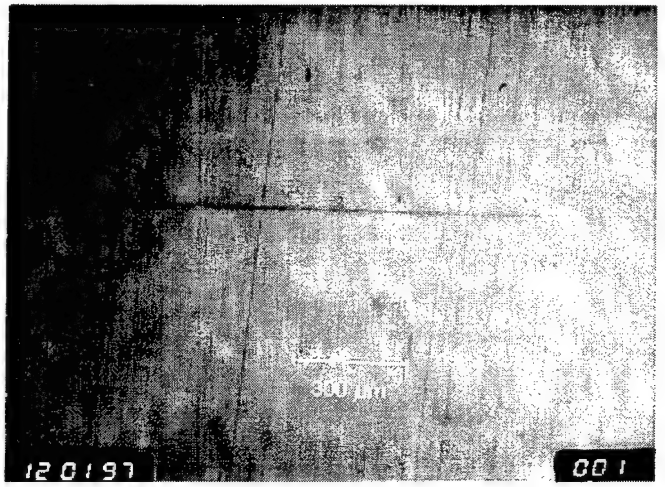

A typical surface replicate from stage 2

Results - AE signals from fretting fatigue test

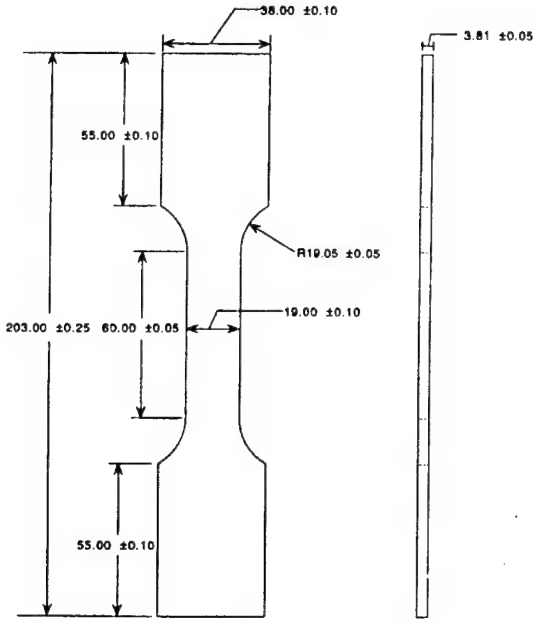

Geometry of specimen

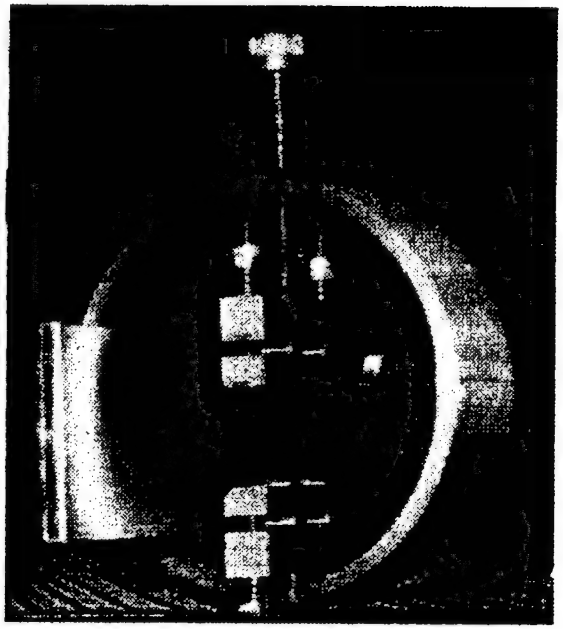

Fretting loading appratus

Results - AE signals from fretting fatigue test

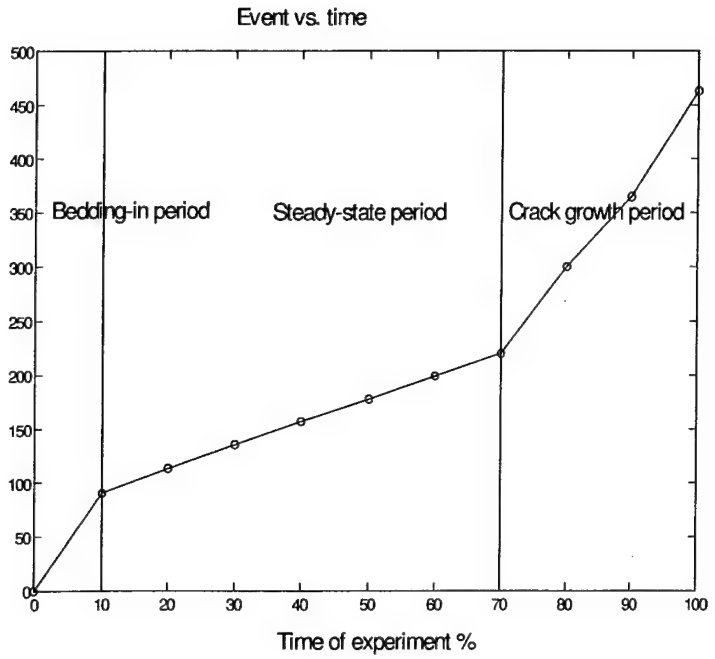

Cumulative AE events

Three distinctive regimes of crack growth were identified based on the acoustic emission signals and friction force measurements:

1) bedding-in period;
2) steady-state period: nucleation and early growth of cracks;
3) growth of a single dominant crack.

Results - measurements of friction force for fretting fatigue test

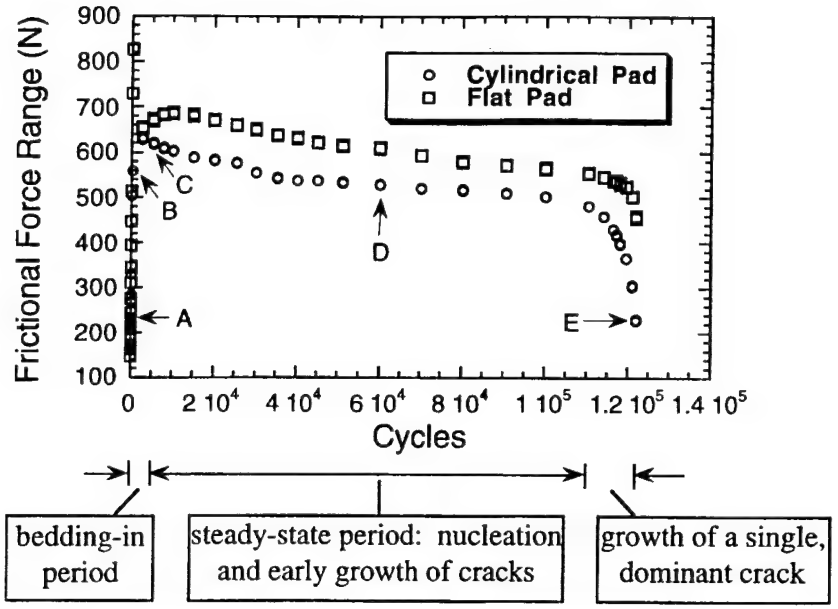

Results - AE signals from fretting fatigue test

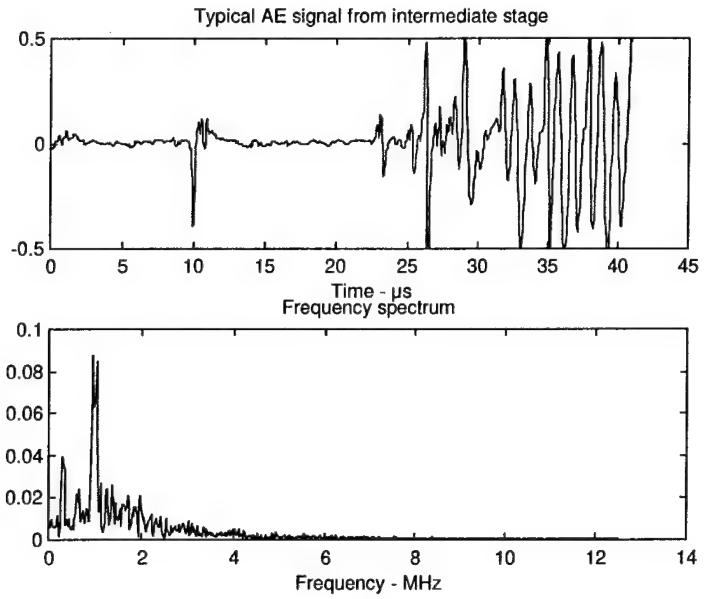

Typical fretting AE signal during steady-state period

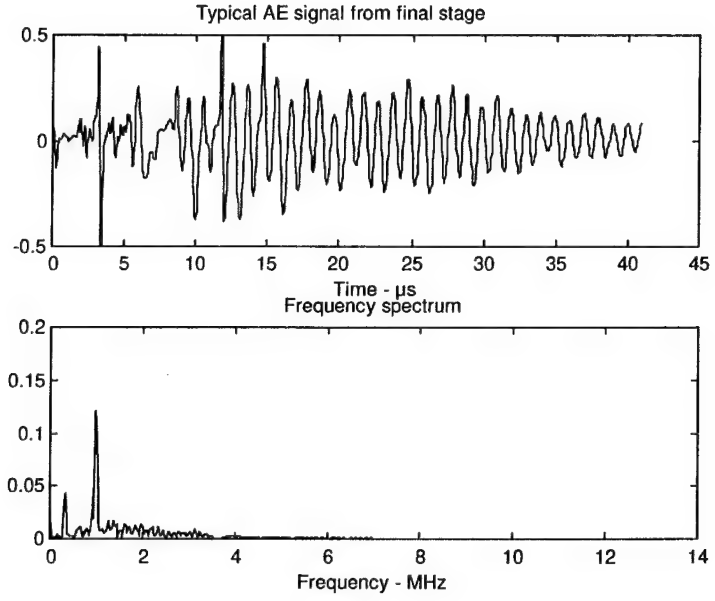

Typical fretting AE signal from growth of a single dominant crack

Study of Acoustic Emission and Transmission from Incipient Fatigue Failure

(b) New Sensors

G.W.Woodruff School of Mechanical Engineering
Georgia Institute of Technology

Co-PIs: Scott Bair, Laurence Jacobs, Jacek Jarzynski
Graduate Students: Zhiqiang Shi, Maxim Koutsak, Brad Beadle

Objectives:

- To develop new receiving transducers with improved discrimination against noise and reverberation:
  (1) an array of piezoactive ceramic elements;
  (2) an optical fiber sensor designed to measure tangential (in-plane) surface strains .

Accomplishments:

- Two transducer arrays have been developed and tested, an array with PZT-plastic composites, and an array with miniature (2×2mm) PZT elements.
- An optical fiber sensor has been assembled and tested. The minimum detectable displacement is estimated to be 5× 10-14 meters per $\sqrt{Hz}$.

Optical Fiber Receiving Array

Responds to strain in the plane of the sample surface, therefore discriminates against environmental noise which produces mainly out-of-plane surface vibrations. The sensor can be designed for frequencies in the range 200 - 700 KHz, with a bandwidth of ~ 50KHz.

Advantages: High sensitivity, and immunity to electromagnetic noise.

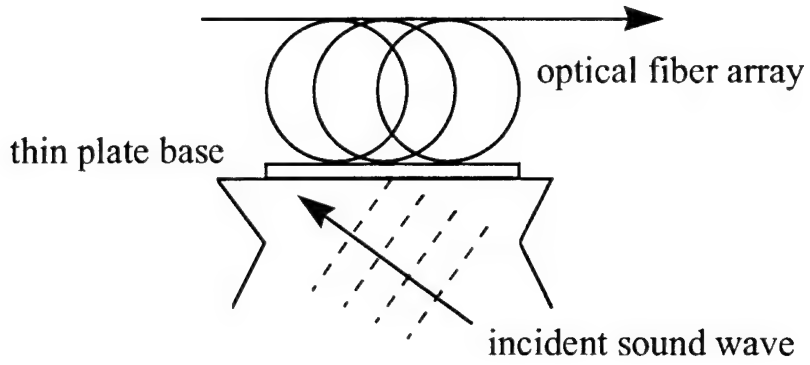

Results - tests of new sensors

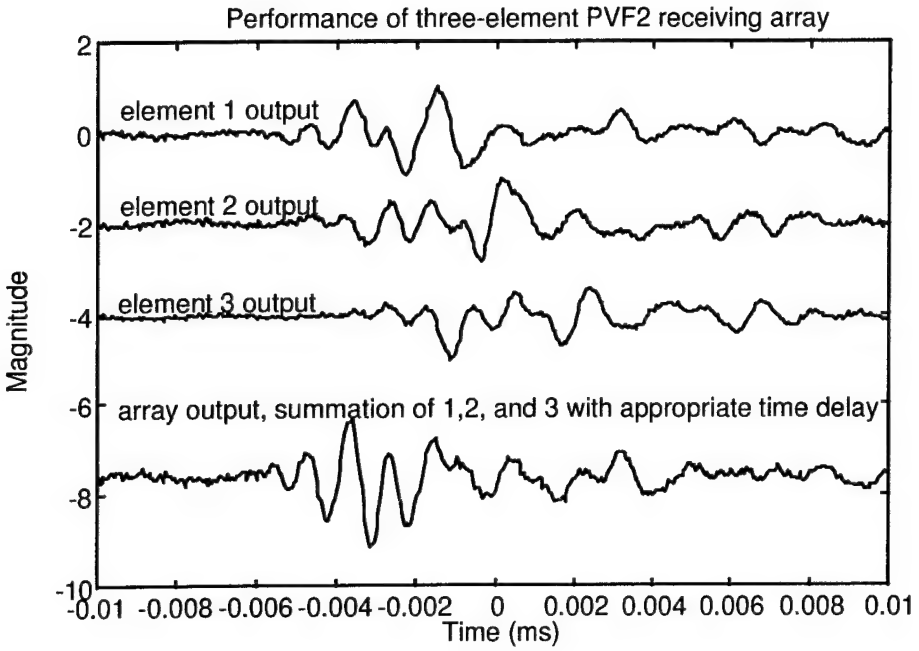

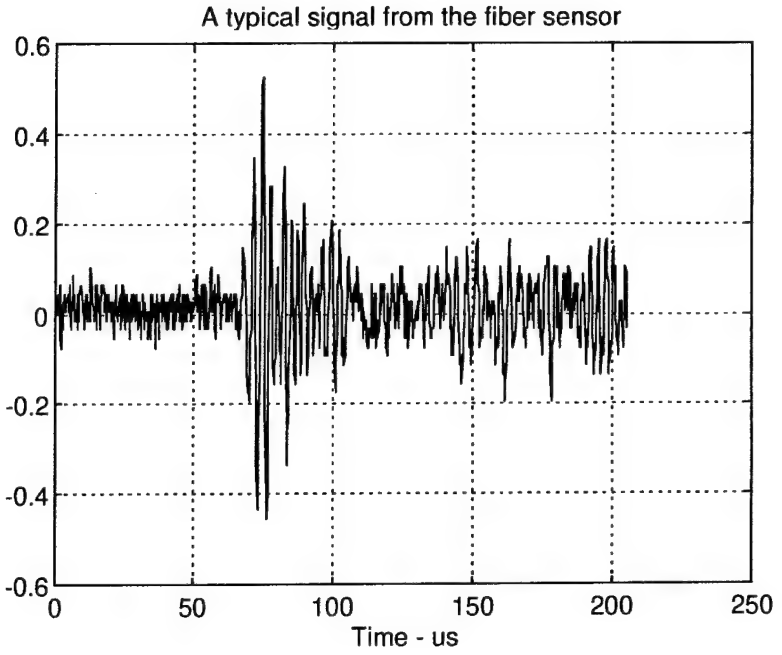

Signals from an array transducer

A typical signal from the fiber sensor

MULTIUNIVERSITY CENTER FOR INTEGRATED DIAGNOSTICS

Acoustic Emission Modeling for Integrated Diagnostics

Professor I. M. Daniel
Northwestern University

Specimen Geometry and Test Setup

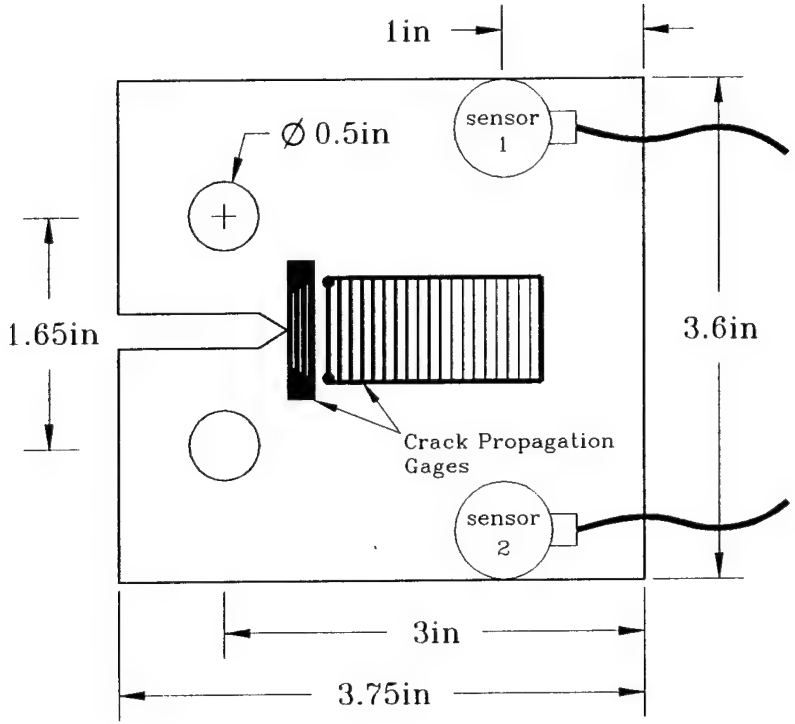

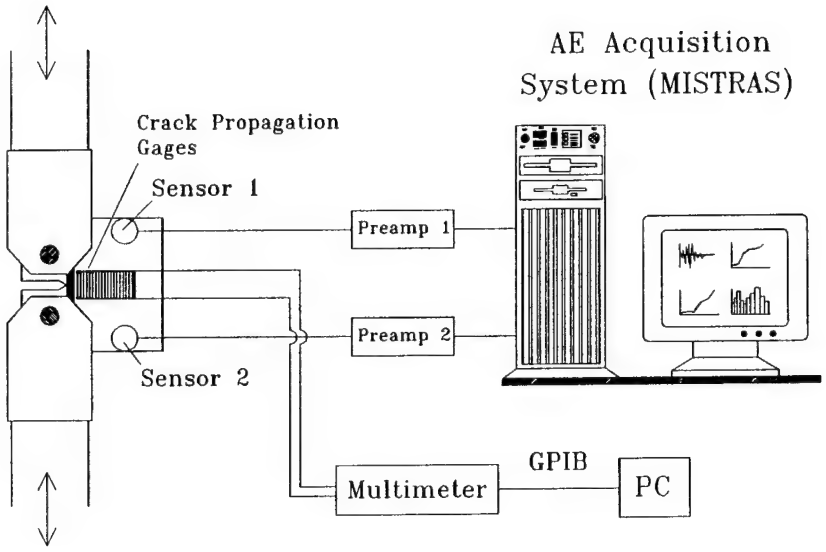

Test Materials: 2024-T3 Aluminum
4340 Steel

Crack Length and AE Counts vs. Cycles

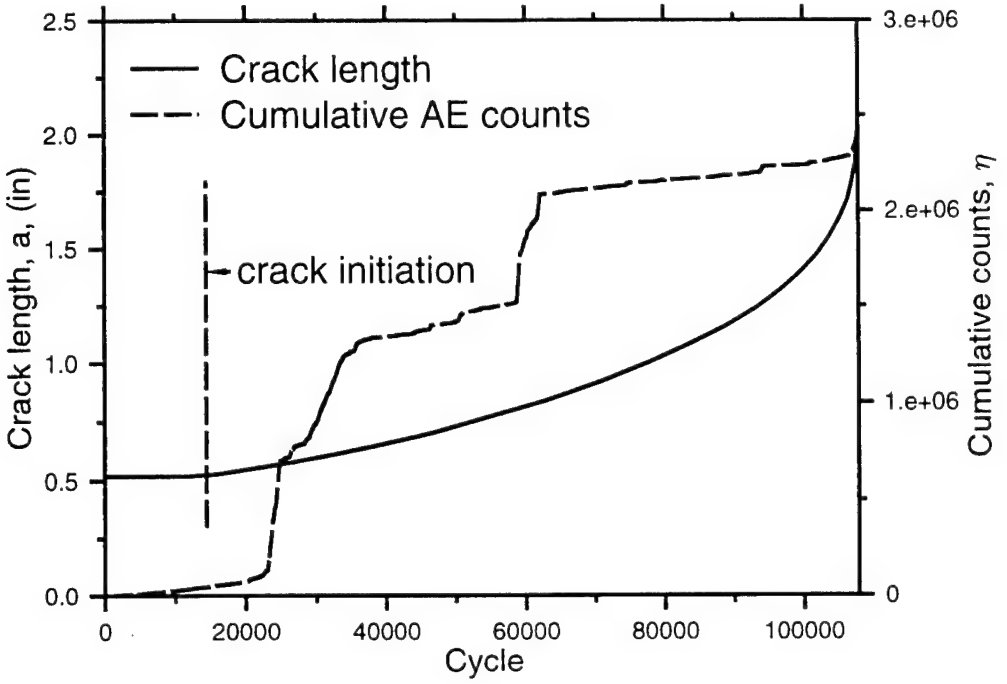

Loading Phase Distribution of AE Counts

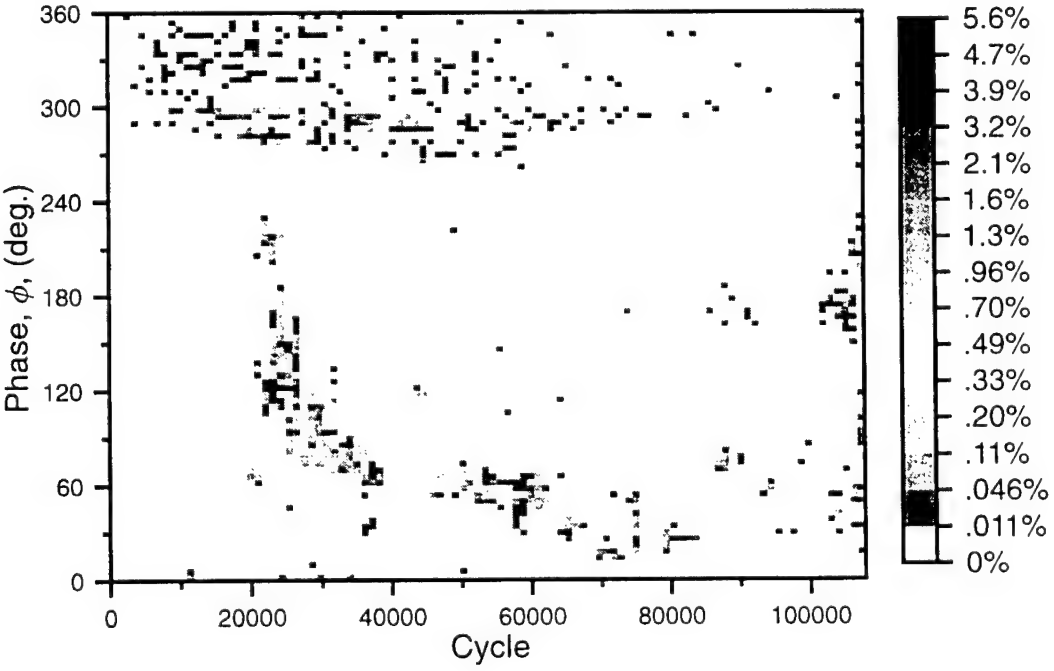

Correspondence of AE Signal Groups and Crack Propagation

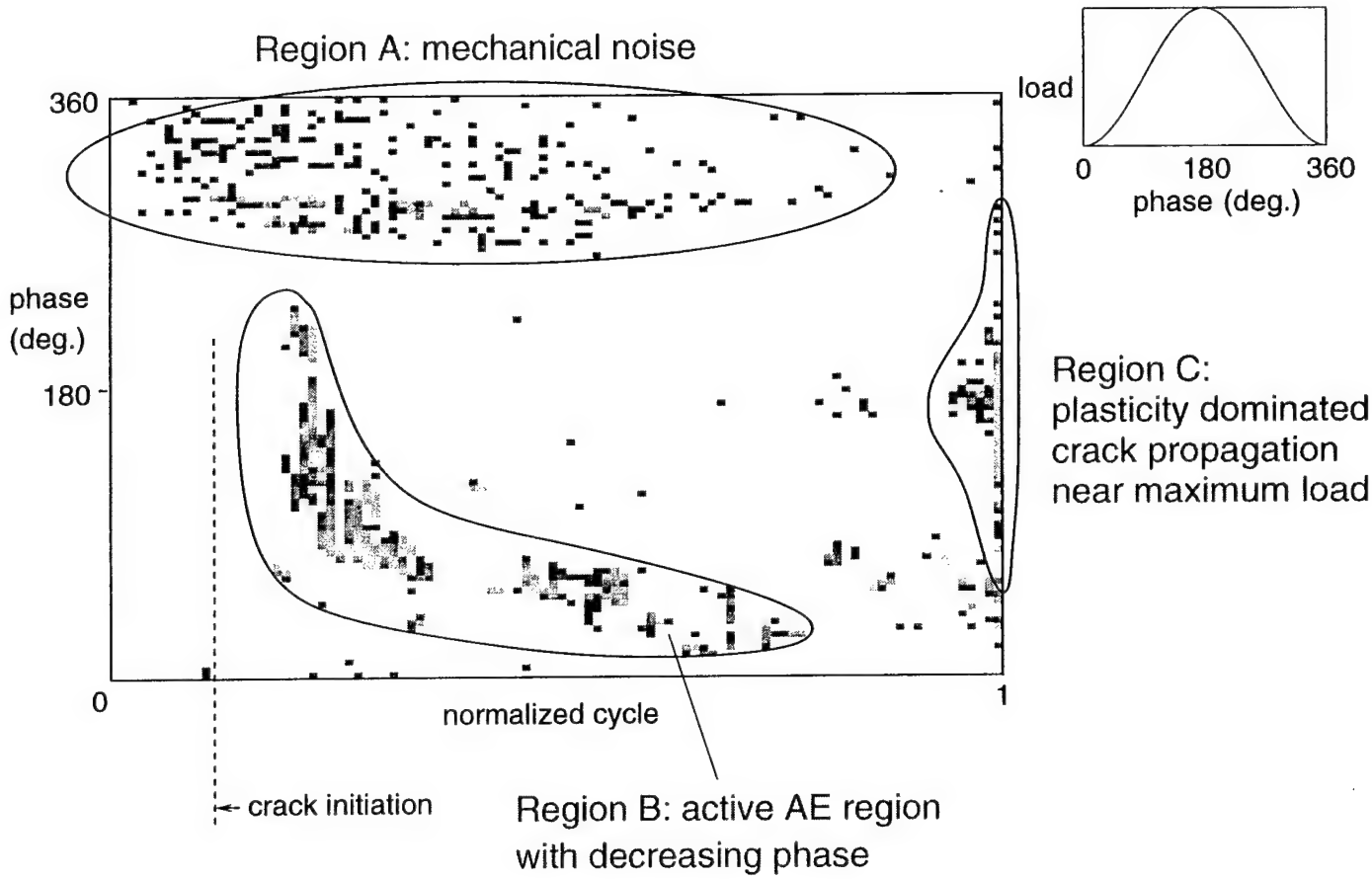

Relevance

This research applies to components whose failure results from initiation and propagation of a major crack at a known stress concentration.

Acoustic emission activity related to the loading part of a cycle (Group B) is related to actual crack propagation.

The pattern of AE activity in this group of signals, including amplitude, duration and loading phase distributions and waveform characteristics, can serve to characterize the "age" of the component and its remaining life.

Sources of Uncertainty

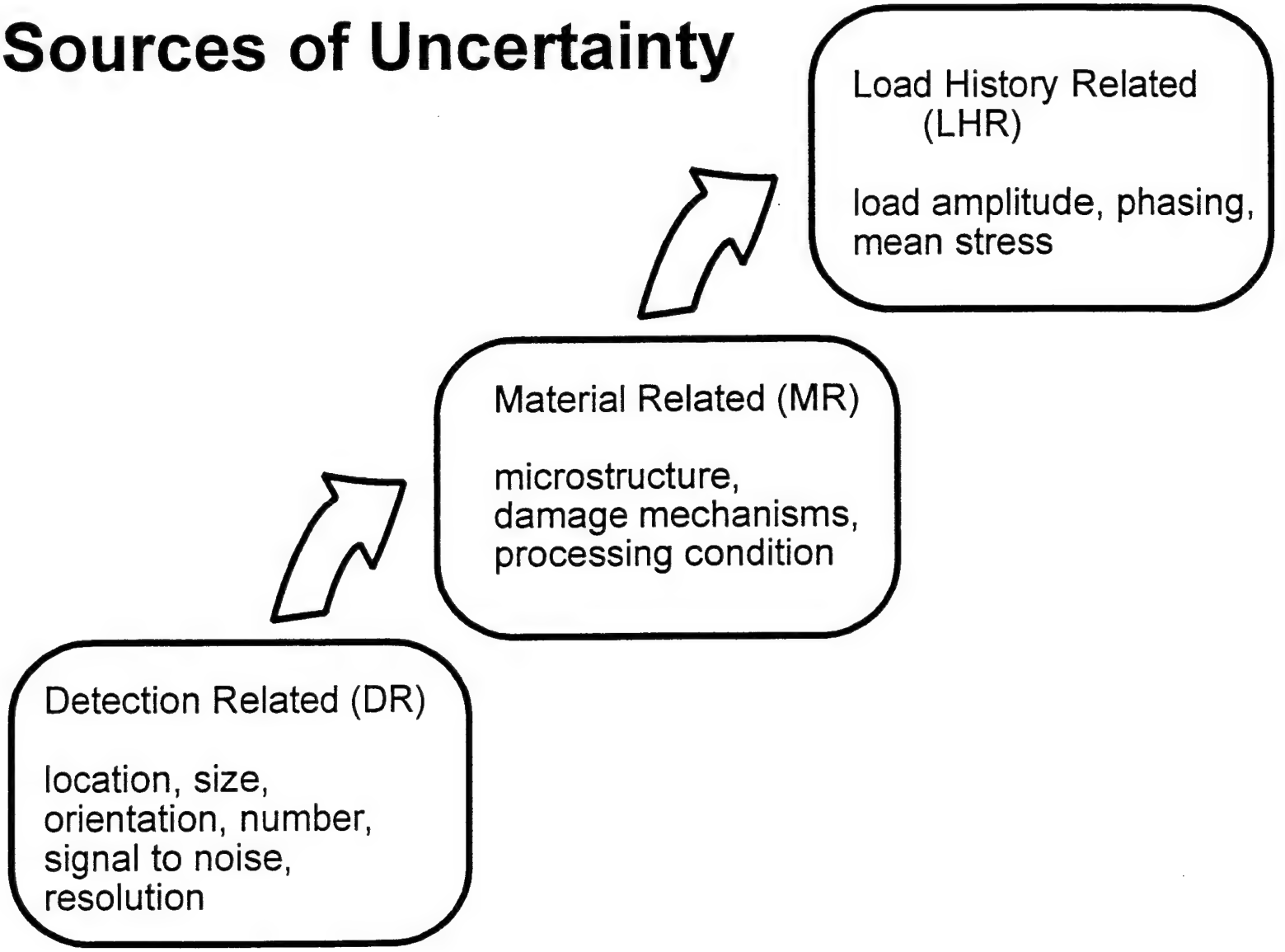

FATIGUE RELIABILITY

P.I. Prof. Brian Moran - Northwestern University
Res. Prof. Dr. Yonglin Xu
Res. Assistant: Ali Zulfiqar

Sources of Uncertainty

- Crack Growth Law
- Initial Crack Length
- Probability of Detection
- Load

Determine

- Failure Probability, P_f
- Inspection Intervals

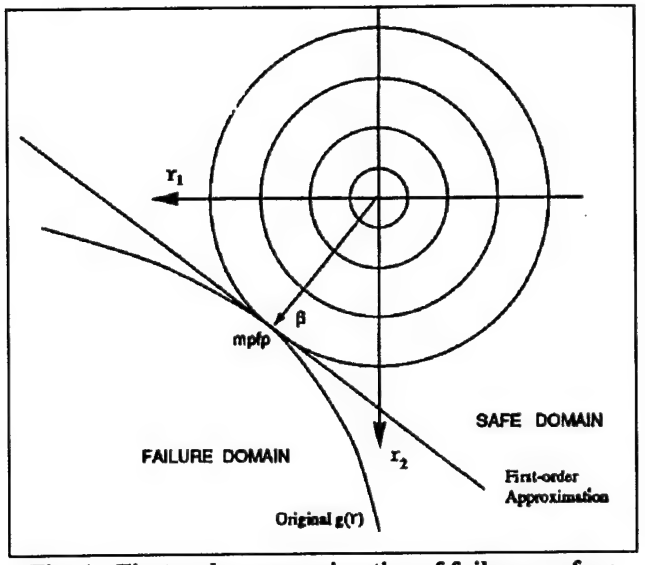

Fig. 1 First order approximation of failure surface

$$P_{nd}(\boldsymbol{r}, N) = \prod_{i=1}^{I} \left\{1 - POD\left[a(\boldsymbol{r}, N_i)\right]\right\},$$

where $POD[a(\boldsymbol{r},N_i)]$ is the probability of detection for the inspection method, and $a(\boldsymbol{r},N_i)$ is the crack length upon the i^{th} inspection for the realization $\boldsymbol{r}$. The probability of failure is therefore given by

$$P_f(N) = \int_{\Omega_f^r} f_R(\boldsymbol{r}) P_{nd}(\boldsymbol{r}, N)\, d\boldsymbol{r},$$

where Ω_f^r includes all $\boldsymbol{r}$ such that $g \leq 0$.

Monte Carlo Simulation: Not feasible for highly reliable systems (requires millions of 3D crack growth simulations)

FORM: Inaccurate when limit state(failure) surface exhibits high curvature

New Method: Limit State Surface Element Method (LSSE)

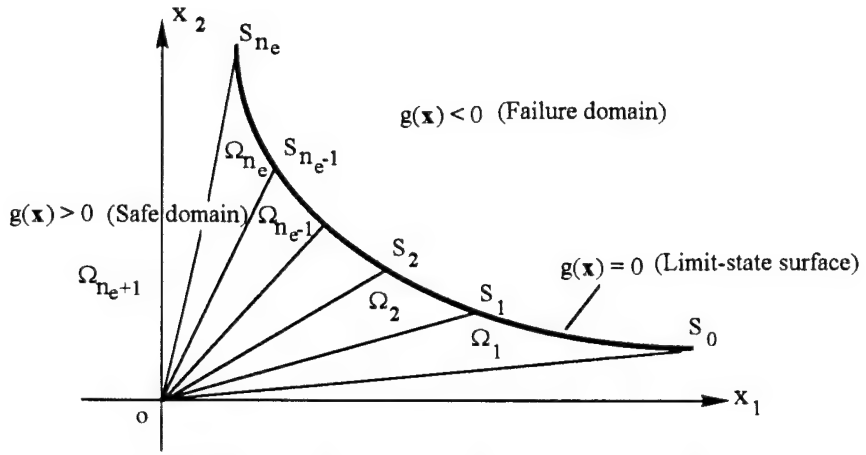

Fig. 2 Discretization of limit-state surface

$$P_{nd}(\boldsymbol{r}, N) = \prod_{i=1}^{I} \left\{1 - POD\left[a(\boldsymbol{r}, N_i)\right]\right\},$$

where $POD[a(\boldsymbol{r},N_i)]$ is the probability of detection for the insp method, and $a(\boldsymbol{r},N_i)$ is the crack length upon the i^{th} inspection realization $\boldsymbol{r}$. The probability of failure is therefore given by

$$P_f(N) = \int_{\Omega_f^r} f_R(\boldsymbol{r}) P_{nd}(\boldsymbol{r}, N)\, d\boldsymbol{r},$$

where Ω_f^r includes all $\boldsymbol{r}$ such that $g \leq 0$.

Table: Reliability for Elliptic Safe Domain

a/b	1	2	3	4	5
p_r	0.3933	0.5899	0.6490	0.6657	0.6722
a/b	6	7	8	9	10
p_r	0.6756	0.6775	0.6787	0.6795	0.6801
a/b	11	12	13	14	15
p_r	0.6806	0.6809	0.6811	0.6813	0.6826

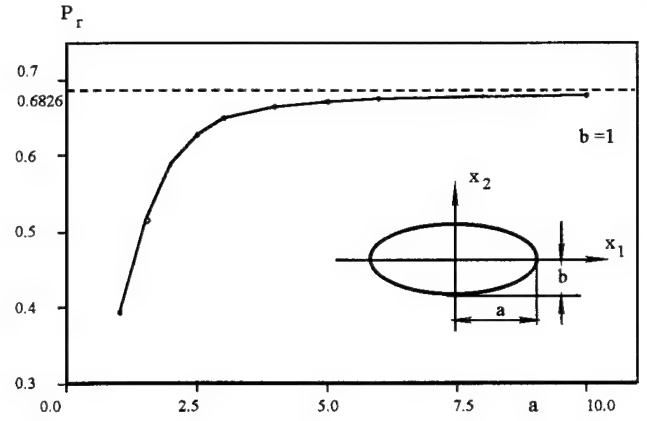

Fig. 3 Reliability for elliptic domain

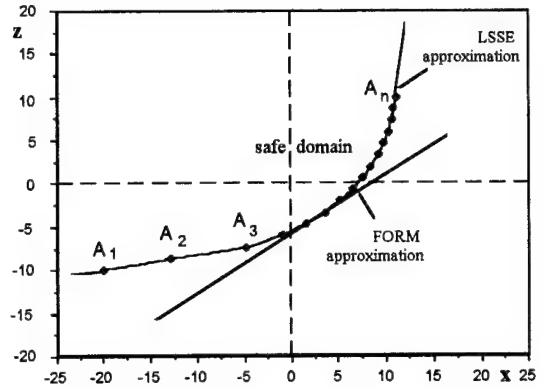

Fig. 4 Limit-state surface approximated by the FORM method

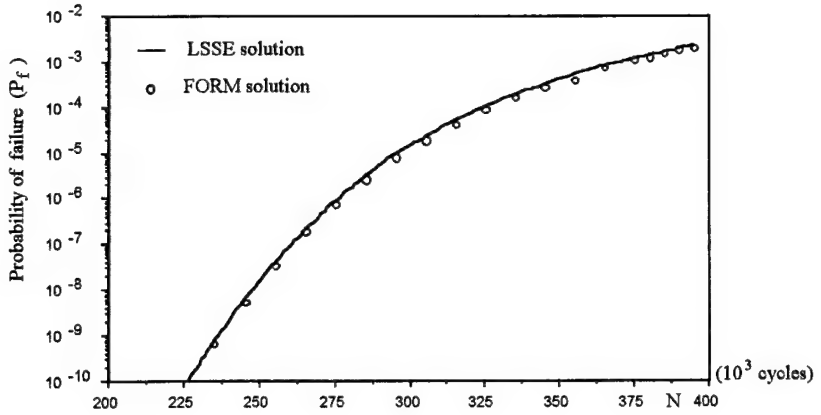

Fig. 5 Probability of failure for edge crack under tensile loading

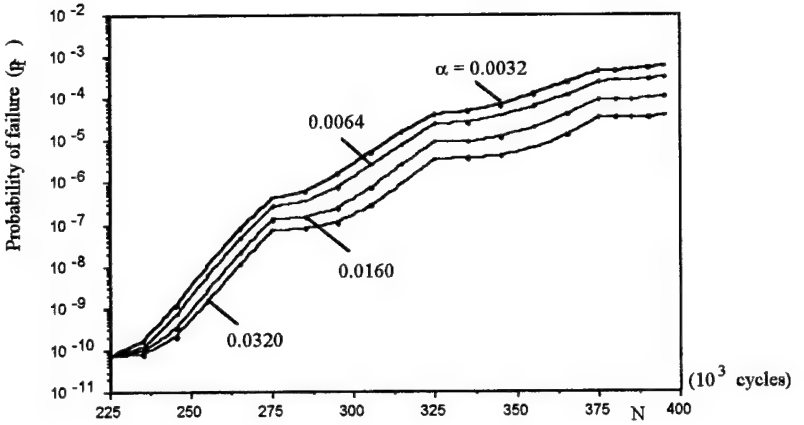

Fig. 6 Probability of failure with inspections

Domain Integral Formulation for Stress Intensity Factor Computation along non-planar Cracks in 3D

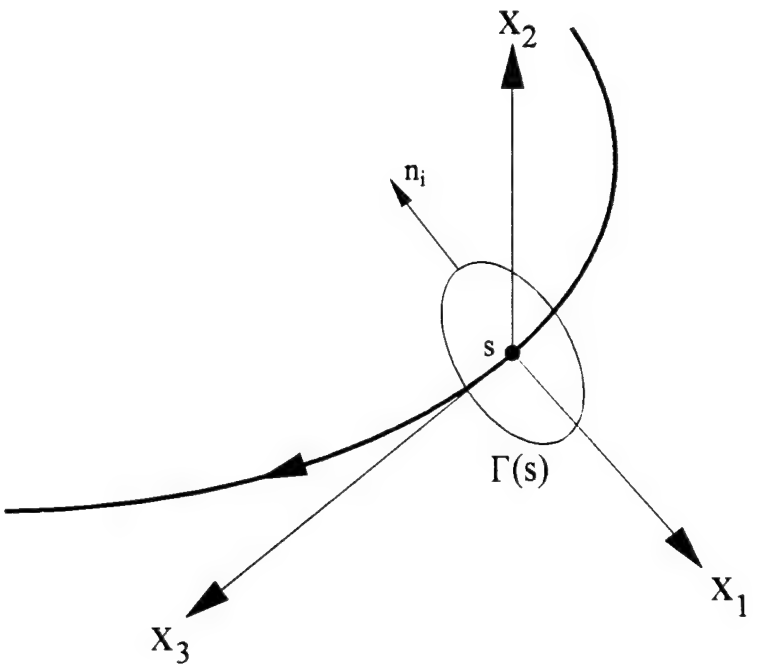

Fig. 7 General curvilinear crack front

Interaction Energy Formulation

$$I(s) = \lim_{\Gamma \to 0} \xi_l(s) \int_{\Gamma(s)} P_{lj} n_j d\Gamma$$

$$I(s) = \frac{2(1-\nu^2)}{E}[K_I K_I^{aux} + K_{II} K_{II}^{aux}] + \frac{1}{\mu} K_{III} K_{III}^{aux}$$

$$\bar{I} = -\int_V [tr(\mathrm{P} \cdot \bar{\nabla} \mathrm{q}) + (\bar{\nabla} \cdot \mathrm{P}^T) \cdot \mathrm{q}] dV$$
$$+ \int_{C^+ + C^-} (\mathrm{q} \cdot \mathrm{P} \cdot \mathrm{m}) d\Gamma + \int_{S^+ + S^-} (\mathrm{q} \cdot \mathrm{P} \cdot \mathrm{m}) d\Gamma$$

due to curvature of crack front

$$(\bar{\nabla} \cdot \mathrm{P}^T) = \boldsymbol{\sigma} : (\boldsymbol{\varepsilon}^{aux} \bar{\nabla} - \bar{\nabla} \mathrm{u}^{aux} \bar{\nabla}) - (\bar{\nabla} \mathrm{u}) \cdot (\bar{\nabla} \cdot \boldsymbol{\sigma}^{aux}) \neq 0$$

Curved Crack Problem

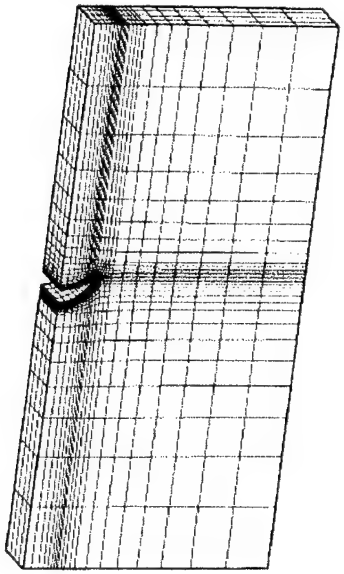

$\frac{G^{FEM}}{G^{analytical}}$	$\frac{K_I^{FEM}}{\sigma\sqrt{(\pi R\alpha)}}$	$\frac{K_{II}^{FEM}}{\sigma\sqrt{(\pi R\alpha)}}$	$\frac{G^{FEM}}{\frac{1-\upsilon^2}{E}(K_I^2-K_{II}^2)}$
0.998	0.53	0.59	0.996

Future Work

- Simulation of Crack Growth in 3D
- Assessment of Crack Growth Laws (mixed mode small and large cracks).
- Robust Tools for Engineering Life Cycle Design

ALGORITHMS FOR REMAINING LIFE PREDICTION

typical fracture mechanics-based methodology

Step 1

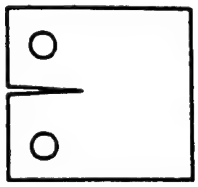

Fracture Toughness and Crack Growth Specimens

Tensile Specimens

J_{IC} (or K_{IC})

$\frac{da}{dN} = C\,\Delta K^{n1}$,

$\varepsilon = \sigma/E + D\sigma^{m}$, $\Delta\varepsilon = K'\,\Delta\sigma^{n'}$

Step 2

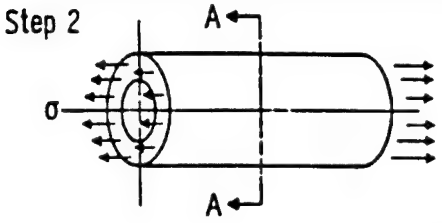

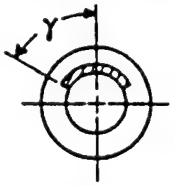

Sect. A-A

$\Delta K = f_1(\Delta\sigma, a, t)$

$J = f_2(\sigma, a, t, \sigma_{YS}, D, m)$

$C = \gamma R$

Cracked Component

Step 3

$J_{IC} = f_2(\ldots a_f \ldots)$

$N_f = \int_{a_0}^{a_f} \frac{dN}{[f_1(\Delta\sigma, a, t)]^n}$

$= \int_{c_0}^{c_f} \frac{dN}{[f_2(\Delta\sigma, c, R)]^{n_1}}$

a_0 —— Initial Crack Depth

c_0 -- Initial Half Crack Length

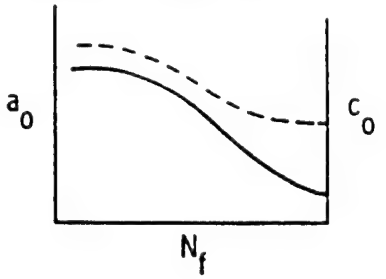

Accomplishments

visualization methodology to determine hot spots in components

robust engineering model developed for growth of small cracks under multiaxial loading conditions

prediction methods for microstructure dependence examined for steels and Ti alloy, along with novel computational micromechanics models for fatigue

fretting fatigue models under development

microstructure level changes associated with fatigue examined

connections made to progressive AE counts and signal shapes for small and long cracks in notched and smooth specimens

Elements of Structural Fatigue Task
Prognostics within an Integrated System - Years 4-5

Find the hotspots

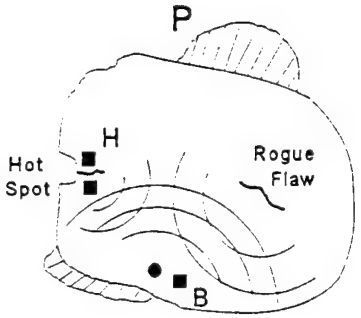

Link fatigue degradation to characteristic sensor signatures

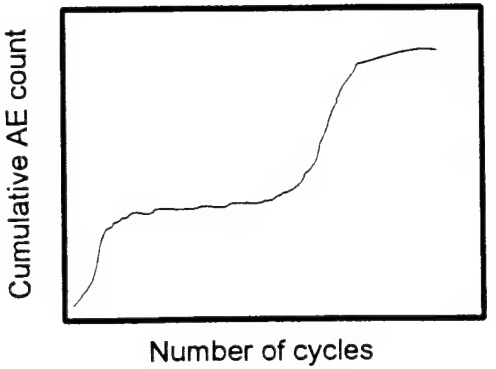

Quantify and model fatigue damage

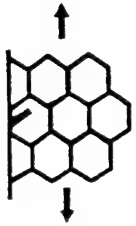

$$\frac{da}{dN} = f(a, \text{history, microstructure})$$

Build up a prognostics capability with multiple models for multisite, multispectral signals, including bounds on remaining life

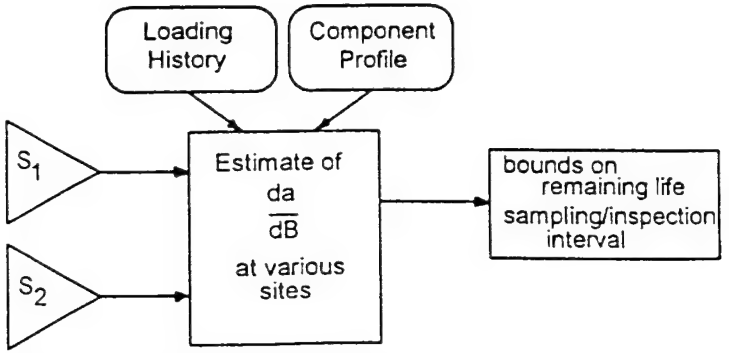

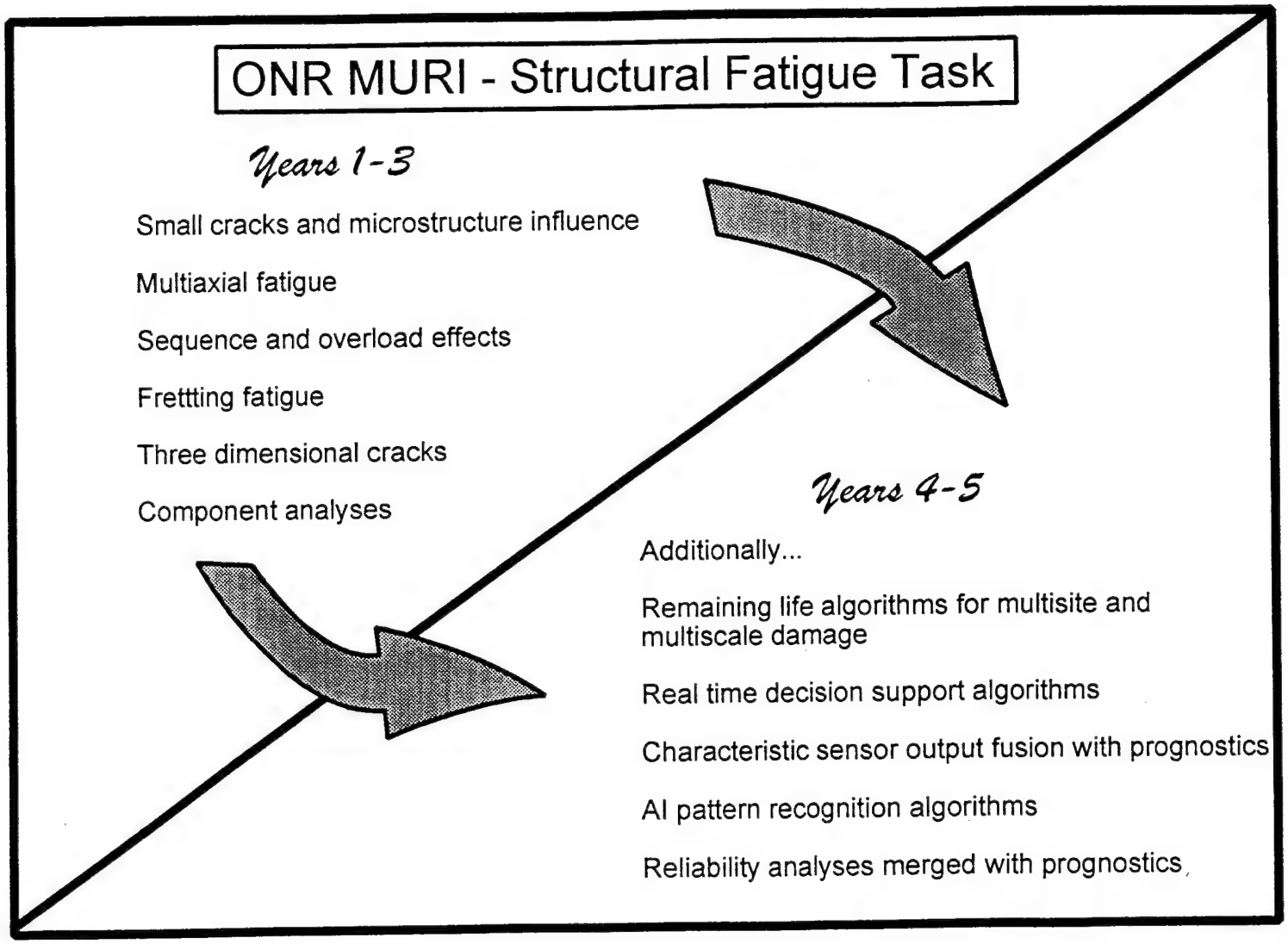
ONR MURI - Structural Fatigue Task
Years 1-3
Small cracks and microstructure influence
Multiaxial fatigue
Sequence and overload effects
Frettting fatigue
Three dimensional cracks
Component analyses
Years 4-5
Additionally...
Remaining life algorithms for multisite and multiscale damage
Real time decision support algorithms
Characteristic sensor output fusion with prognostics
AI pattern recognition algorithms
Reliability analyses merged with prognostics

MULTIUNIVERSITY CENTER FOR INTEGRATED DIAGNOSTICS

Nondestructive Evaluation

Failure Detection and Identification

- ## Crack Detection in Annular Structures by Ultrasonic Guided Waves

Y. Berthelot, Woodruff School of Mechanical Engineering, Georgia Tech
L. Jacobs, Woodruff School of Mechanical Engineering, Georgia Tech
J. Qu, Woodruff School of Mechanical Engineering, Georgia Tech

- ## Laser-Based Ultrasonics for Integrated Diagnostics

J. D. Achenbach, Center for Quality Engineering and Failure Prevention
Northwestern University
A. Kromine, Center for Quality Engineering and Failure Prevention
Northwestern University
P. Fomitchov, Center for Quality Engineering and Failure Prevention
Northwestern University
S. Krishnaswamy, Center for Quality Engineering and Failure Prevention
Northwestern University

Crack Detection in Annular Structures by Ultrasonic Guided Waves

Y. Berthelot, L. Jacobs, J. Qu

Woodruff School of Mechanical Engineering
Georgia Institute of Technology
Atlanta GA 30332-0405

e-mail: yves.berthelot@me.gatech.edu

NEED

- Catastrophic failures of mechanical systems are often caused by cracks.
- There are numerous annular components in naval mechanical systems.
- Radial cracks often are found on the inner walls of such annular components.
- Visual and traditional NDE techniques are not effective in detecting such cracks.
- Detecting and characterizing such radial cracks provides critical information in determining the remaining life and structural integrity of a mechanical system.

MISSION

Provide an efficient diagnostic/prognostic capability for detecting cracks in annular structures.

GOAL: The goal is to develop a robust nondestructive method using ultrasonic guided waves to detect and localize radial cracks in annular components of mechanical structures.

APPROACH: Ultrasonic guided waves

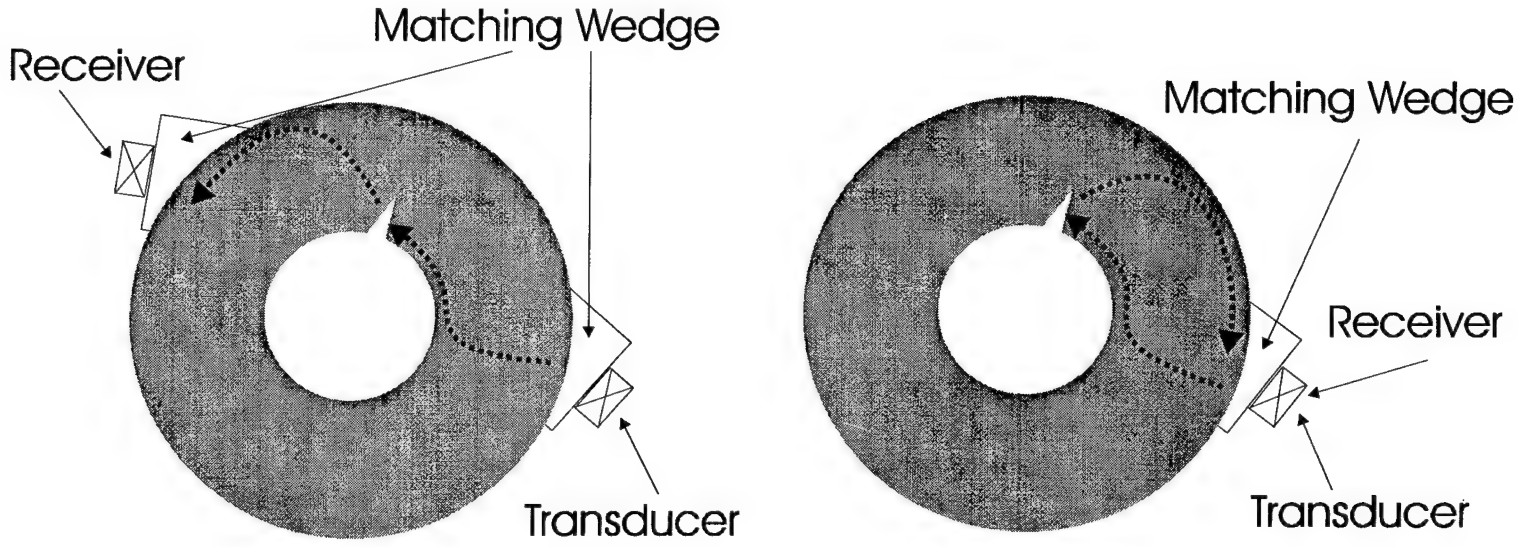

Transmission

Pulse-echo

CRACK DETECTION USING GUIDED WAVES

Uniqueness and Advantages

- Can quickly inspect a large annular component.
- Can inspect a large annular component with only one (or two) transducers by controlling the modal content of the signals.
- Can inspect locations that are not accessible for placing transducers.

Challenges

- Waves are dispersive and the dispersion relationships are very complex.
- Waveforms are sum of many propagating modes.
- Controlled generation of desired modes (frequency, wedge angle, position, etc).

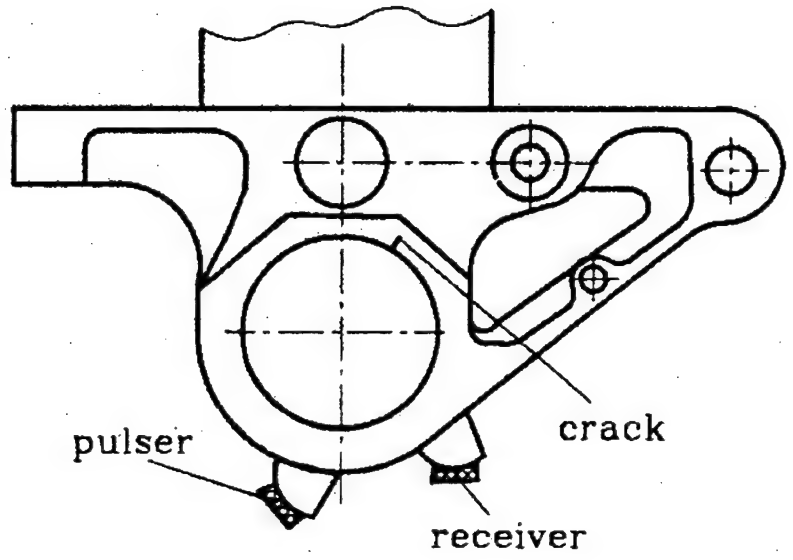

INTEGRATION

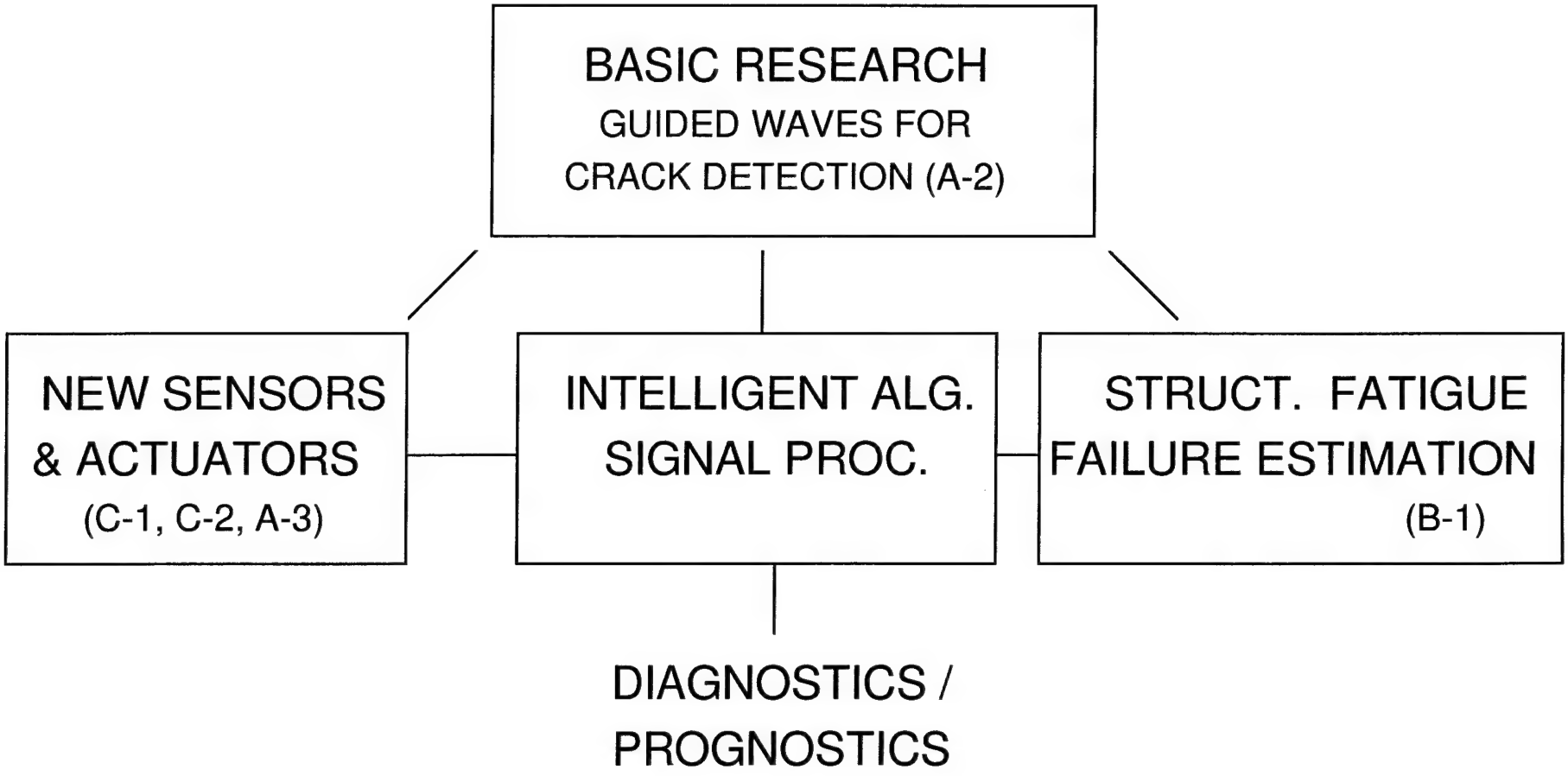

RESULTS (analytical and numerical)

- developed numerical algorithm for the evaluation of the dispersion curves in thick annular structures.
- implemented the modal expansion method.
- computed the displacement profiles across the wall thickness for the first 10 modes.
- FEM modeling of ultrasonic guided waves (a) in an ideal ring, and (b) scattering by cracks. Verified the FEM codes with analytical predictions.

EXAMPLE

FEM Simulation of Guided Waves in Complex Geometries

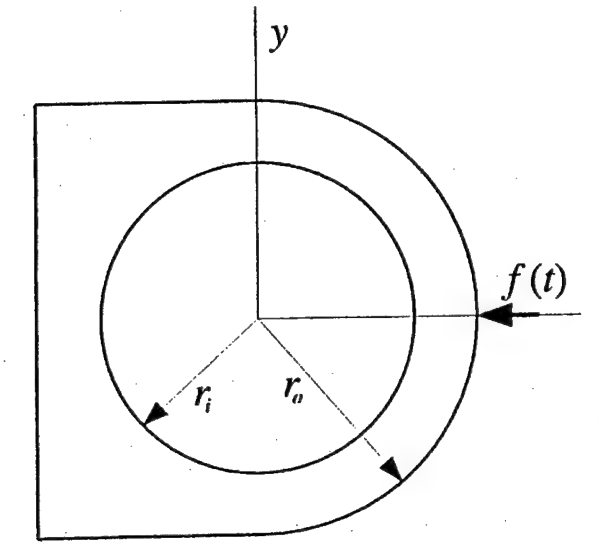

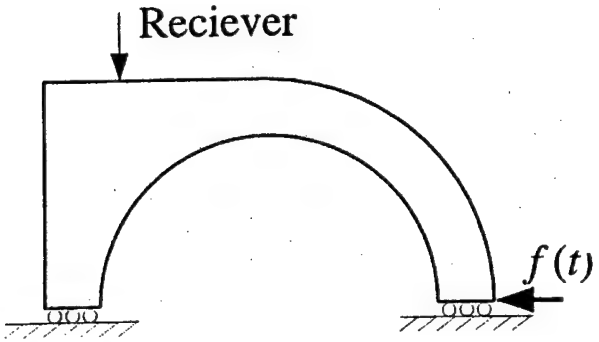

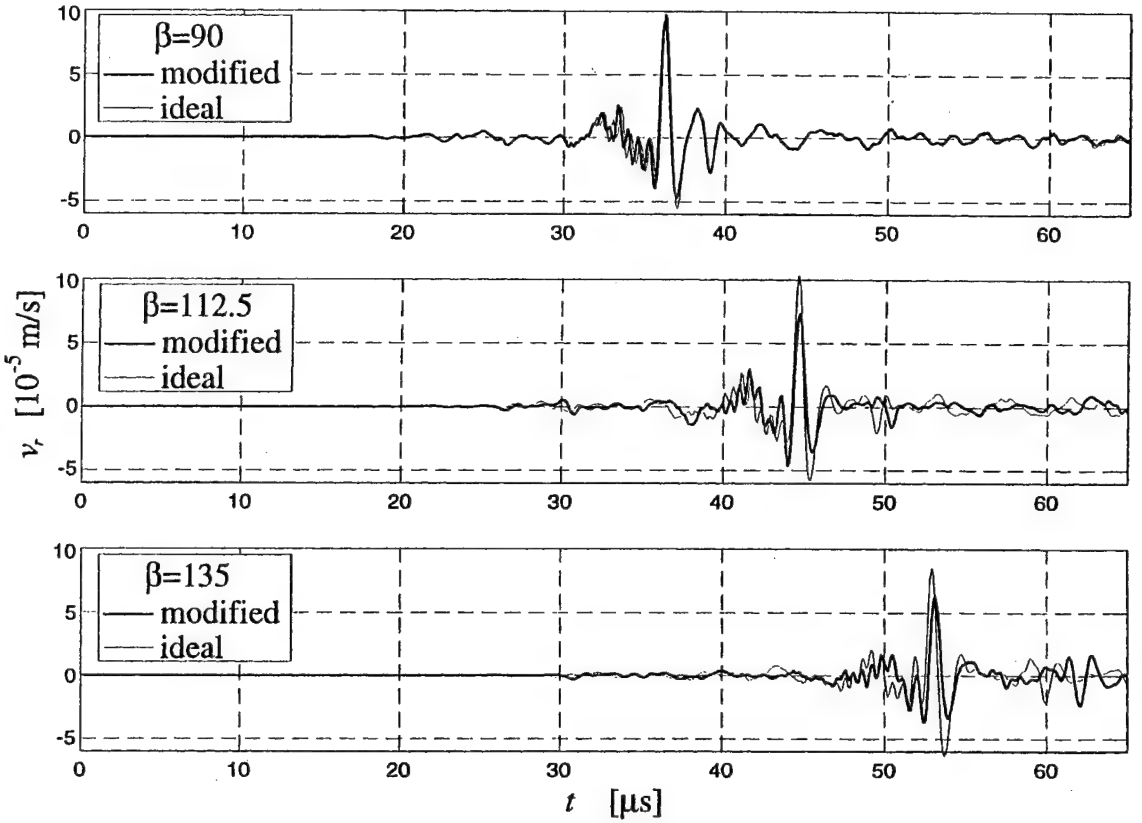

Comparison for modified and ideal ring at different angle, β, between the load and the receiver.

RESULTS (experimental)

- Demonstrated proof-of-concept of crack detection by UGW in thick annular structures.
- Successfully implemented a signal processing technique based on integrating the wavelet transform over a limited bandwidth and over a sliding time window to locate a crack.
- Detected hidden cracks in the pitch-shaft of the H-46.

These results are summarized in the written report.

EXAMPLE

Detection of an inaccessible crack in the pitch-shaft of an H-46

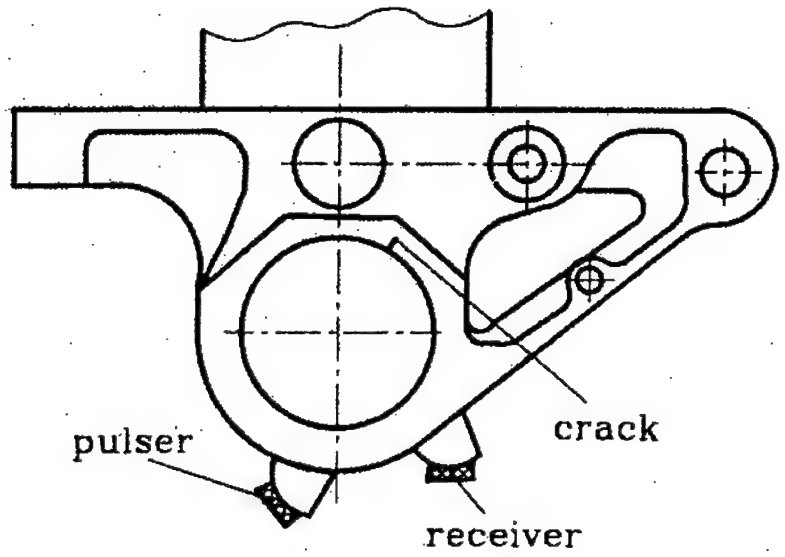

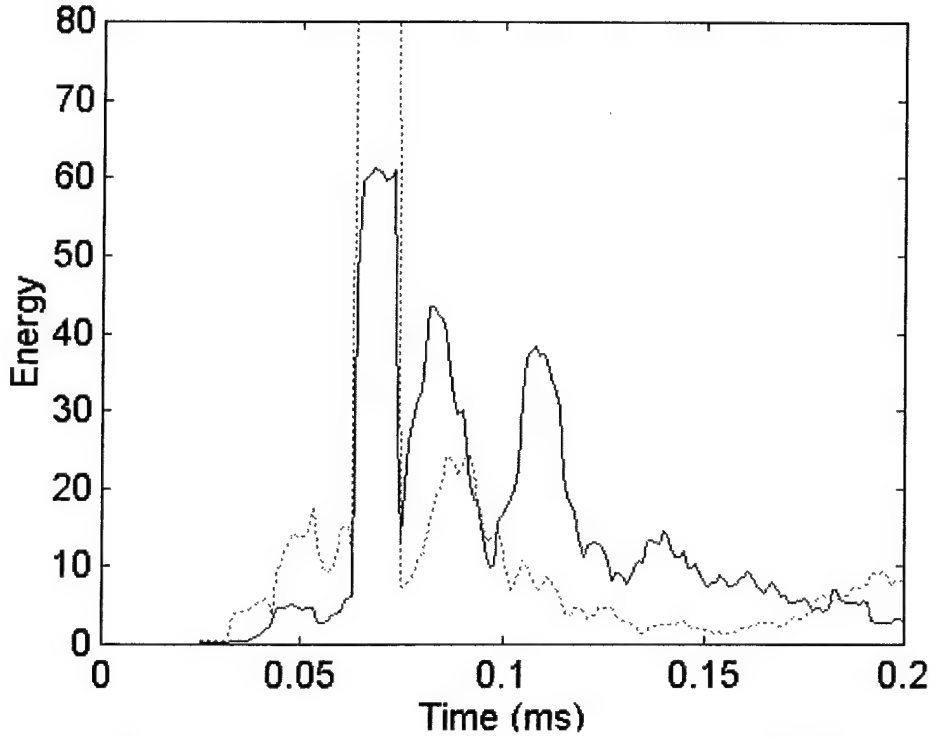

Band-limited / time-windowed energy = square of the wavelet transform, integrated over a band B and over a sliding time window of duration T.

The signal energy in frequency band of 2.0 to 2.5 MHz and time duration of 0.01 ms(solid line: with 3.0mm crack, dot line: without crack).

Laser-Based Ultrasonics for Integrated Diagnostics

J. D. Achenbach, A. Kromine, P. Fomitchov
and S. Krishnaswamy

Center for Quality Engineering and Failure Prevention
Northwestern University
Evanston, IL 60208-3020

e-mail: achenbach@nwu.edu

OBJECTIVE

Develop an ultrasonic technique for the field detection and characterization of flaws in components of complicated structures without disassembling or physically touching the componentry.

APPROACH

Use laser-based ultrasound (LBU) with optical fiber delivery and laser detection.

Combined LBU system

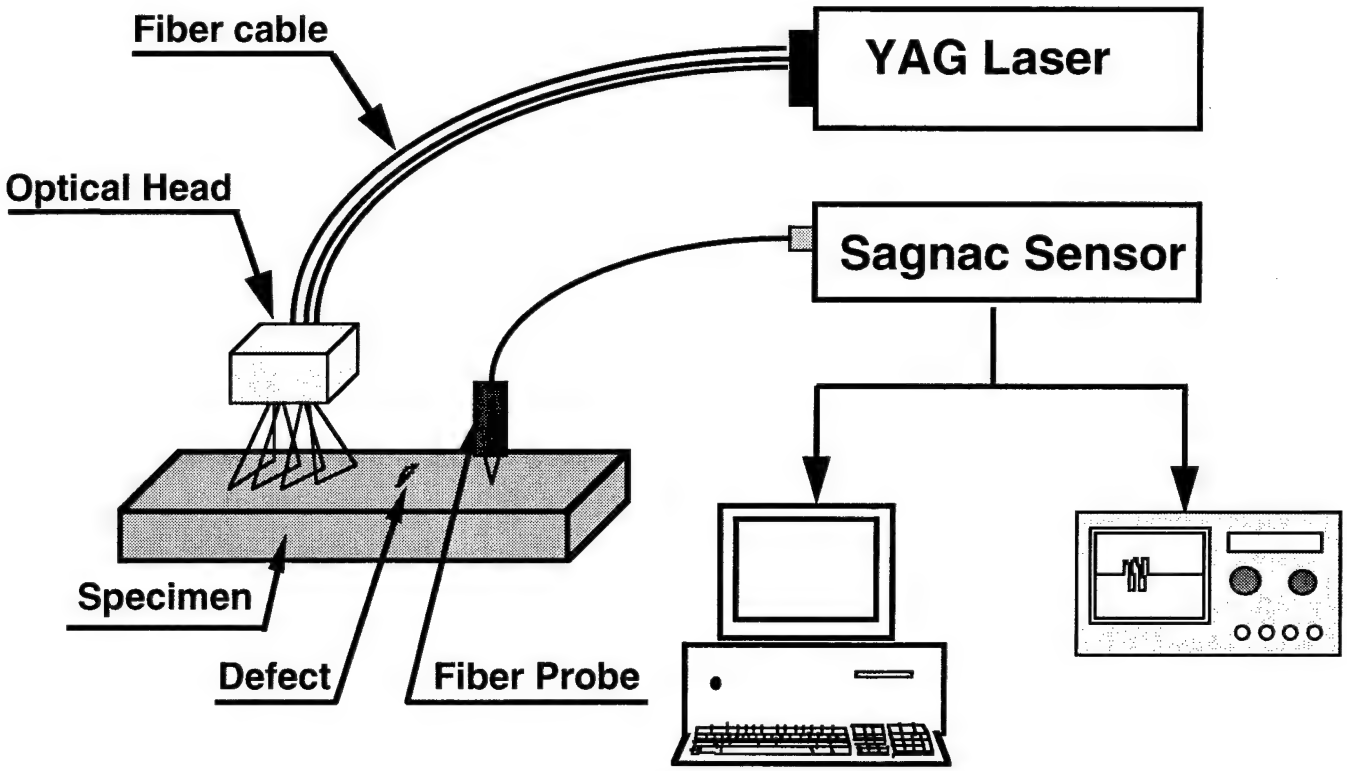

Laser Based Ultrasound Generation

OBJECTIVE: To develop a new robust, non-contact ultrasonic source suitable for field applications

APPROACH: To use fiber optic system for the delivery of laser energy to an inspection place

ADVANTAGES:

- Non-contact ultrasonic generation
- Tunable narrow-band and broad-band generation of ultrasonic waves
- Remote placement of equipment by use of fiber optics
- High efficiency in energy delivery
- Applicable to curved surfaces

Laser Ultrasonic Source for Narrow-band Generation

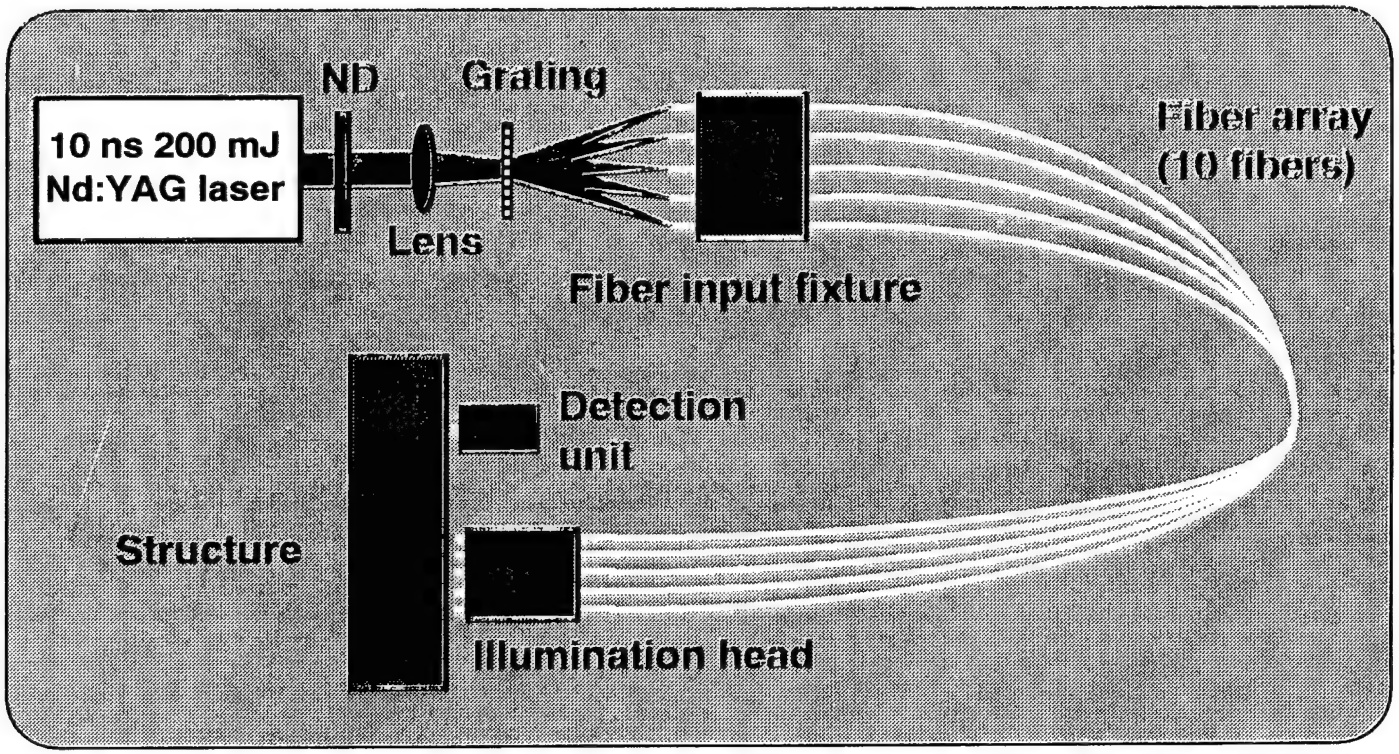

Fiber Coupler Scheme

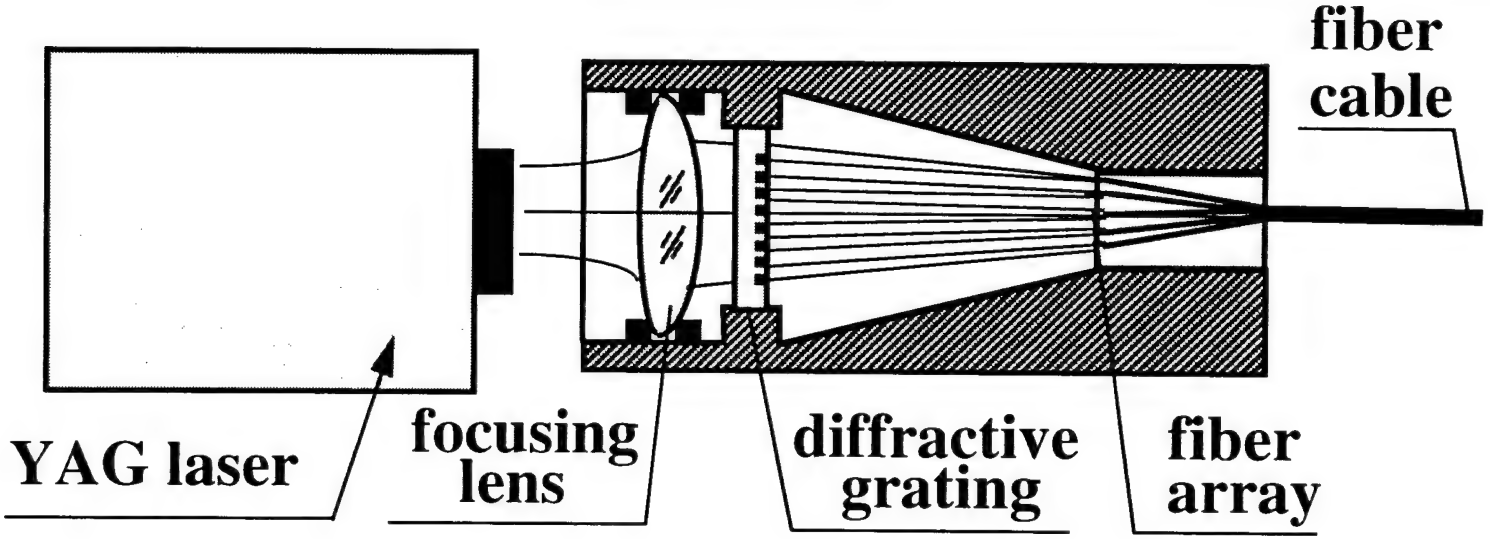

Parameter	Fiber array coupler	Single fiber coupler
Fiber core diameter, μm	**350**	**200 / 550**
Max energy per fiber, mJ	**8**	**5 / 35**
Number of fibers	**10**	**1**
Coupling efficiency	**up to 65%**	**up to 65%**

Illumination head scheme

Optimum generation conditions:

1. Line array spacing:

$$\delta = c / f$$

where **c** - ultrasonic wave speed,
f - frequency of ultrasound

2. Line width:

$$d = \frac{\delta\sqrt{2}}{\pi}$$

For aluminum **c** ~ 2901 m/s, at **f** = 5 MHz :

δ = 0.58 mm , **d** = 0.26 mm

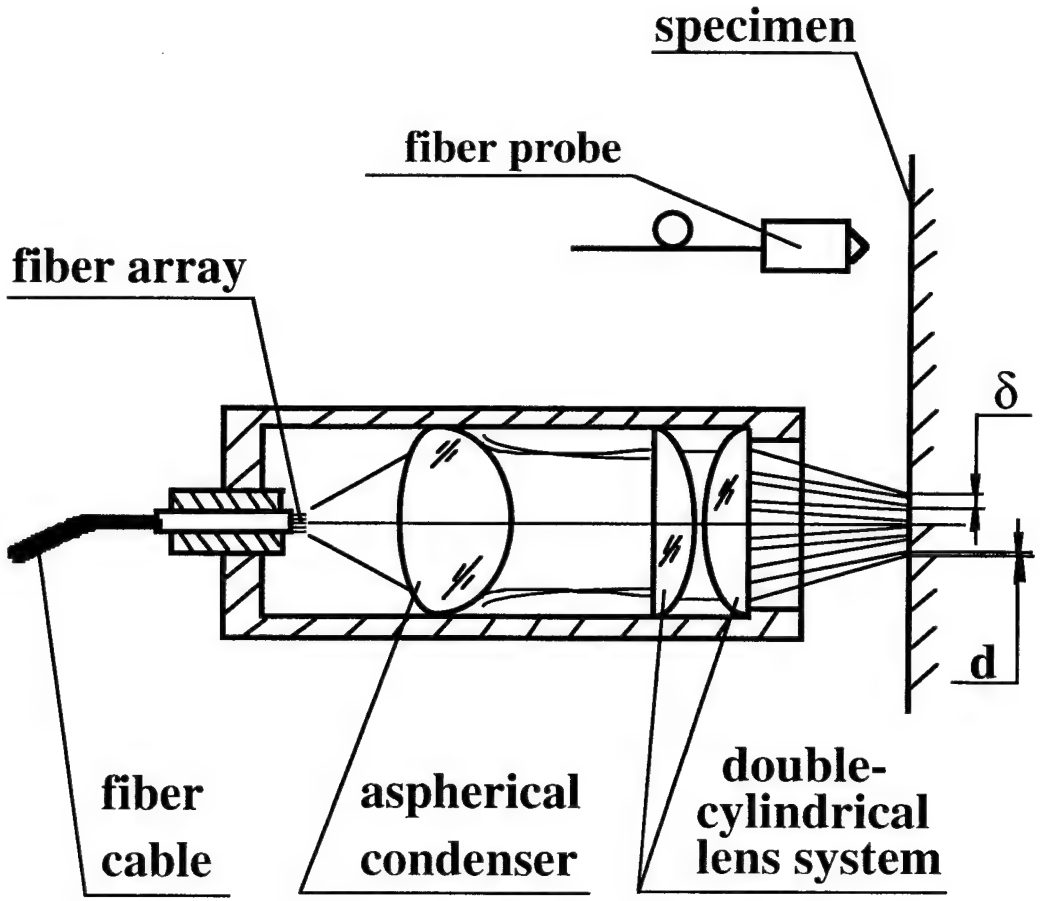

Fiberized Laser Ultrasonic Source

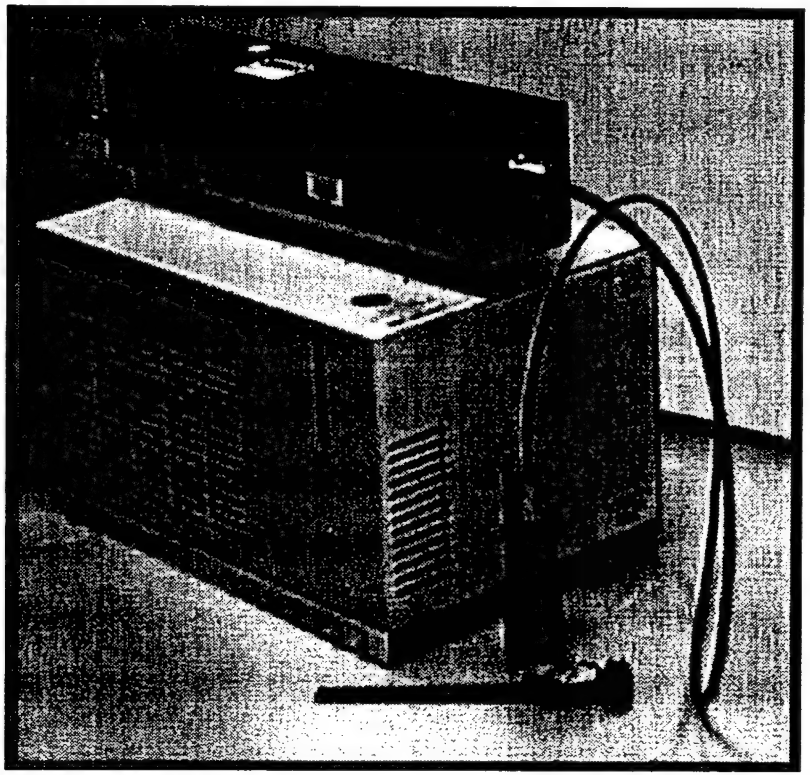

Main parameters

- generation modes:
  tunable narrowband (1-10 MHz),
  short broadband pulses,
- maximum energy : 90mJ,
- repetition rate - up to 30Hz,
- size: 18.5"x 3.6"x 3.7" (head)
  18"x11.4"x 8.3" (power supply)
- total weight: 55 lb..

Laser detection of ultrasonic waves

Objective: To develop a robust, non-contact ultrasonic sensor suitable for laboratory and field applications

Advantages of Sagnac Interferometer:

- Non - contact measurements
- Applicable to curved and rough surfaces
- Point detection
- Absolute measurement of ultrasonic displacement
- Tunable narrow-band detection
- Stable alignment and compact packaging

Schematic of the Sagnac Interferometer

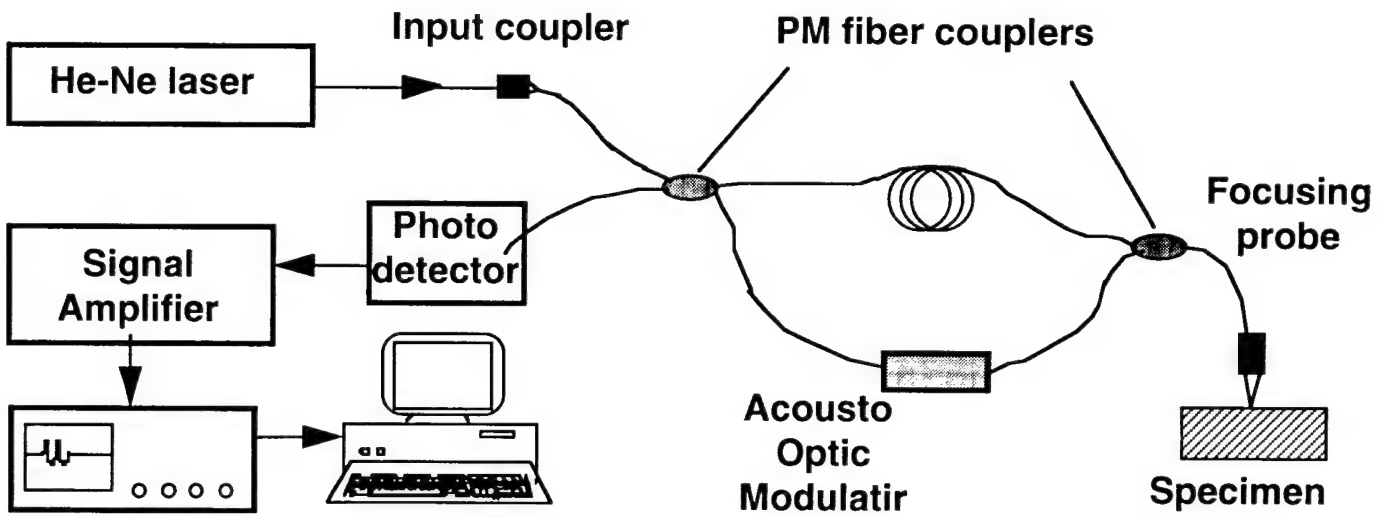

- **Fully fiberized**
- **Precise patc-match**
- **Portable**
- **Point detection / high spatial resoution**
- **AOM: for quadrature point adjustment**

Random Speckle Modulation

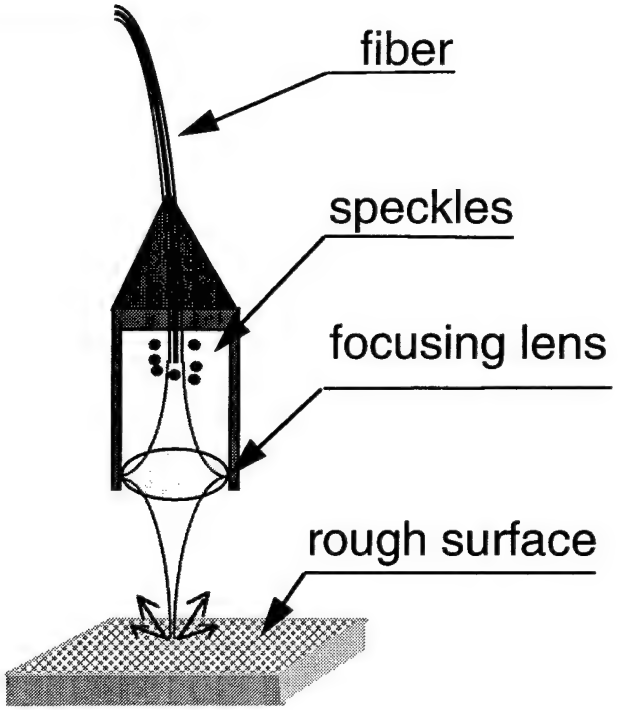

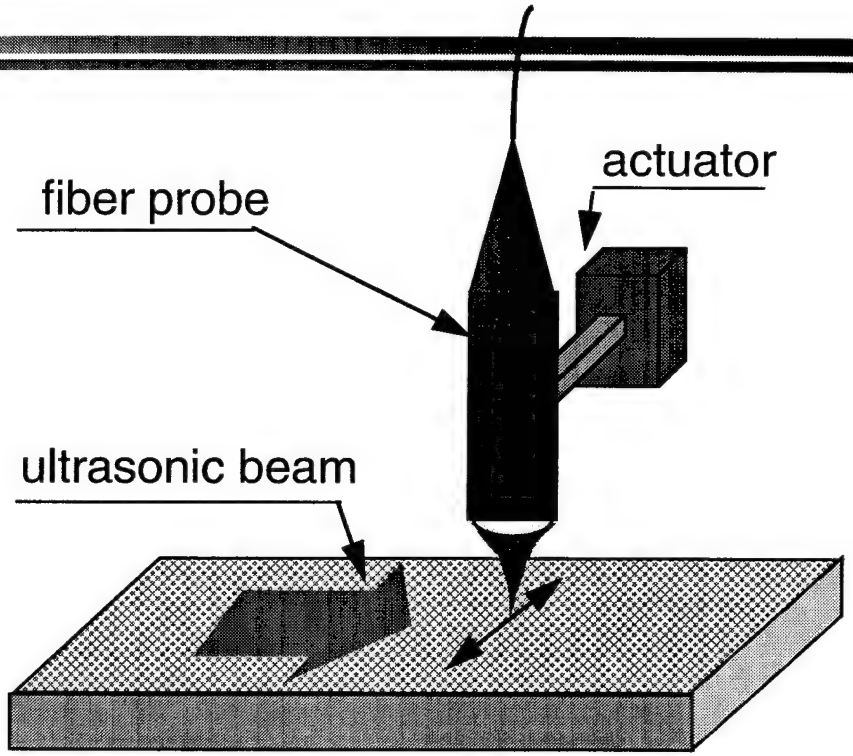

Speckle size: $\sigma \sim 2\,\lambda/NA$

Parameters of fiber probe motion

- transverse jitter amplitude: 0.3-0.5 mm
- jitter frequency: 30 - 100 Hz

MULTIUNIVERSITY CENTER FOR INTEGRATED DIAGNOSTICS

Portable Sagnac Interferometer for Ultrasonic Detection

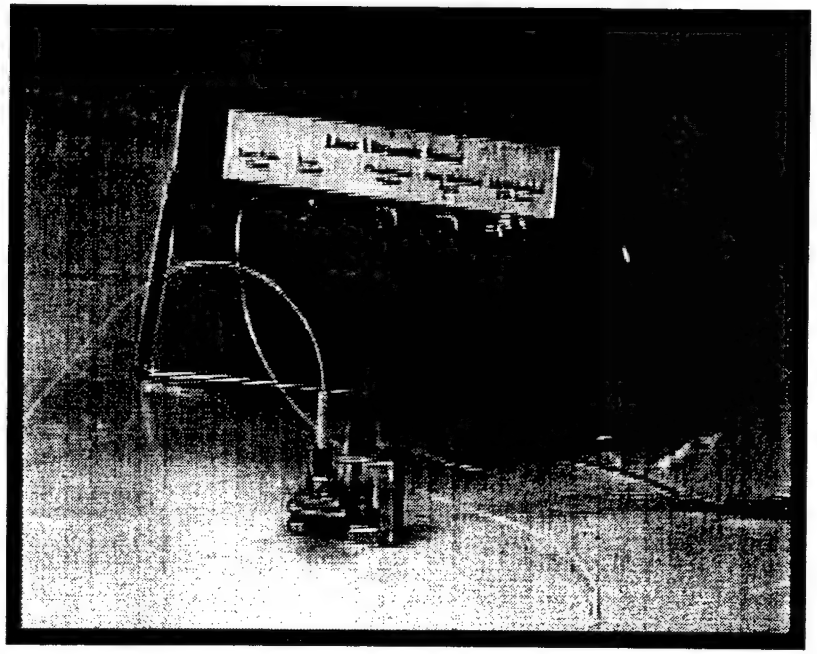

Main parameters

frequency response:
narrowband - 5 +/- 2 MHz,

smallest detectable displacement - 0.2 nm,

can be applied on a rough and curved surface

size:8"x 3"x 11"

weight: 15 lb.

The prototype of a portable LBU System

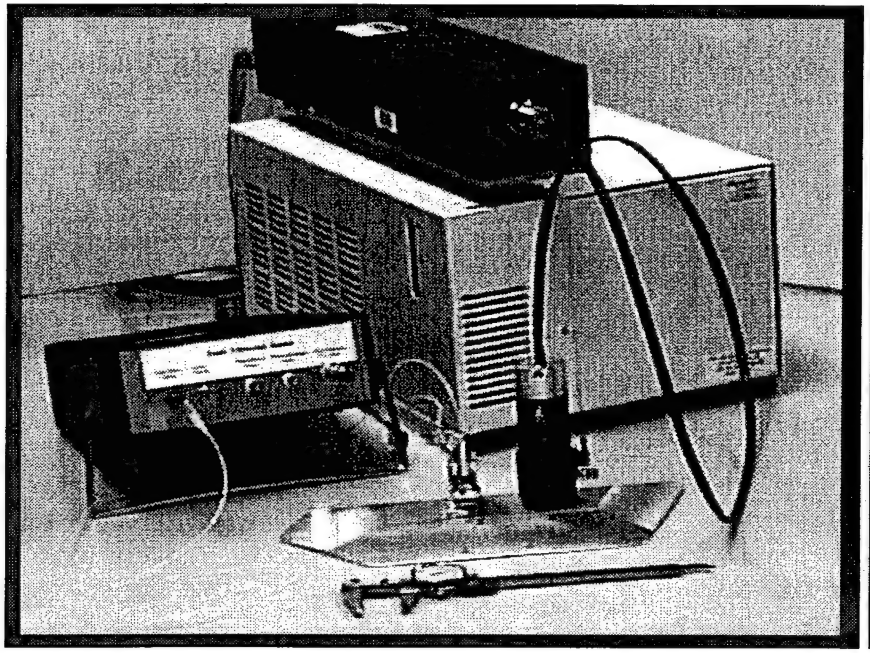

System view

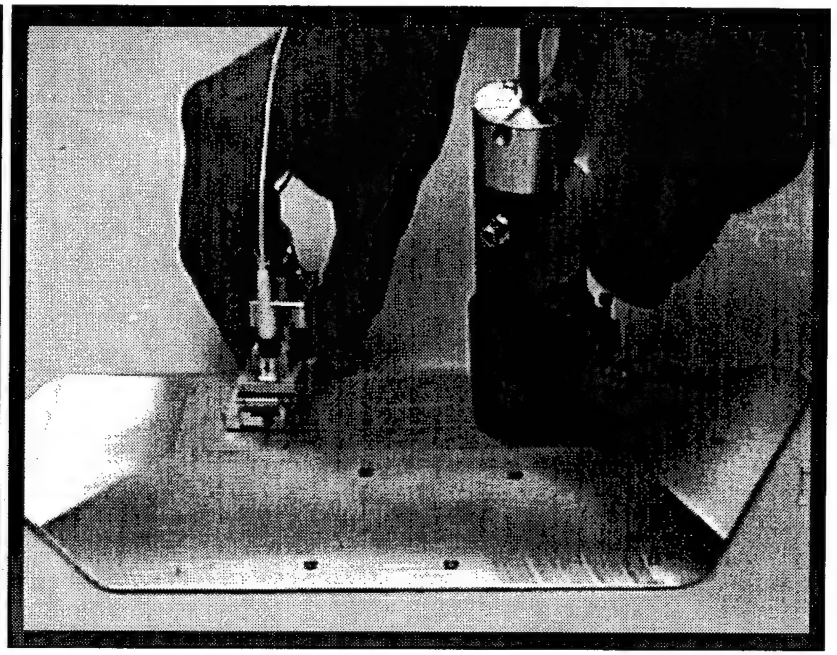

Hand-held probes

Narrow-band ultrasonic generation

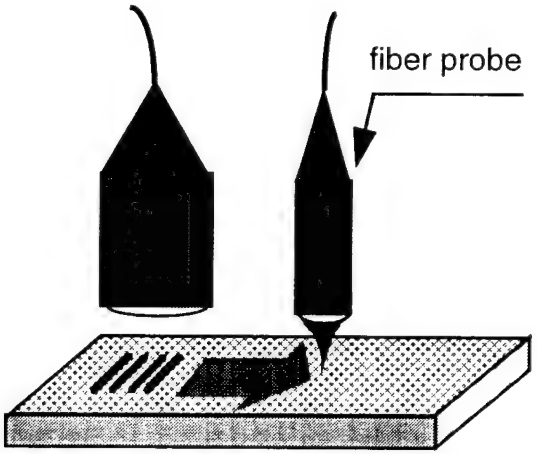

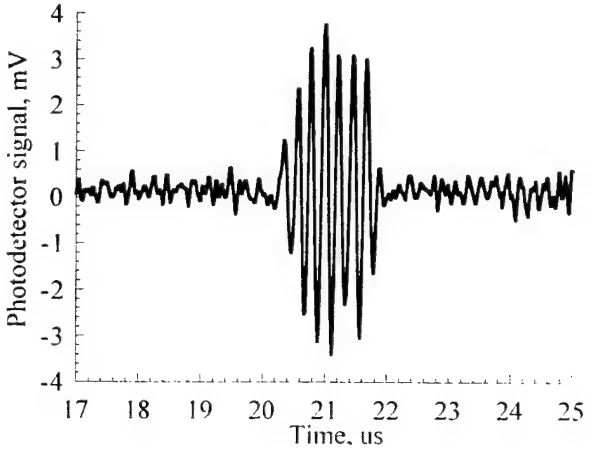

Ultrasonic beam profile

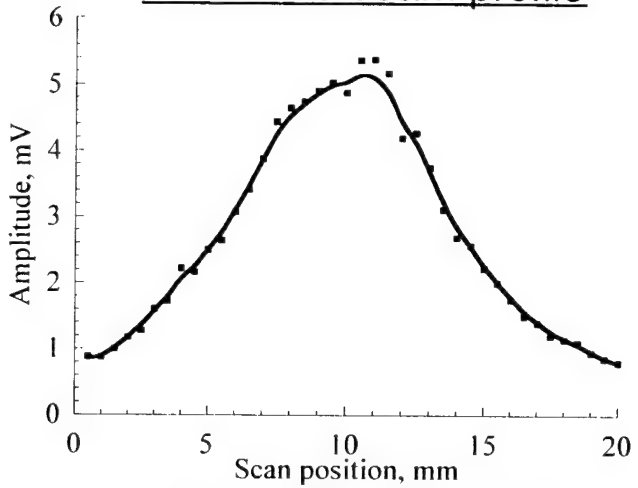

Frequency spectrum

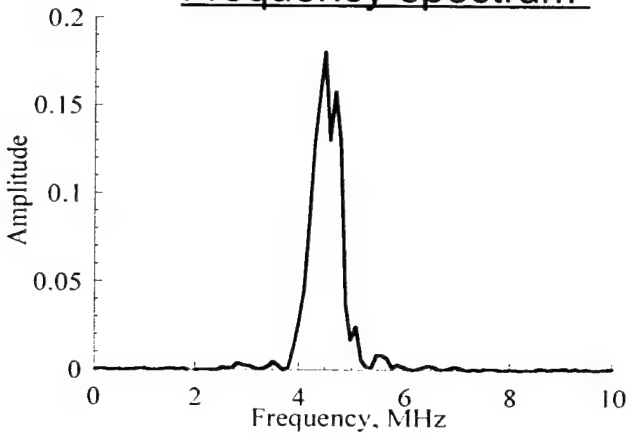

Application on a curved surface

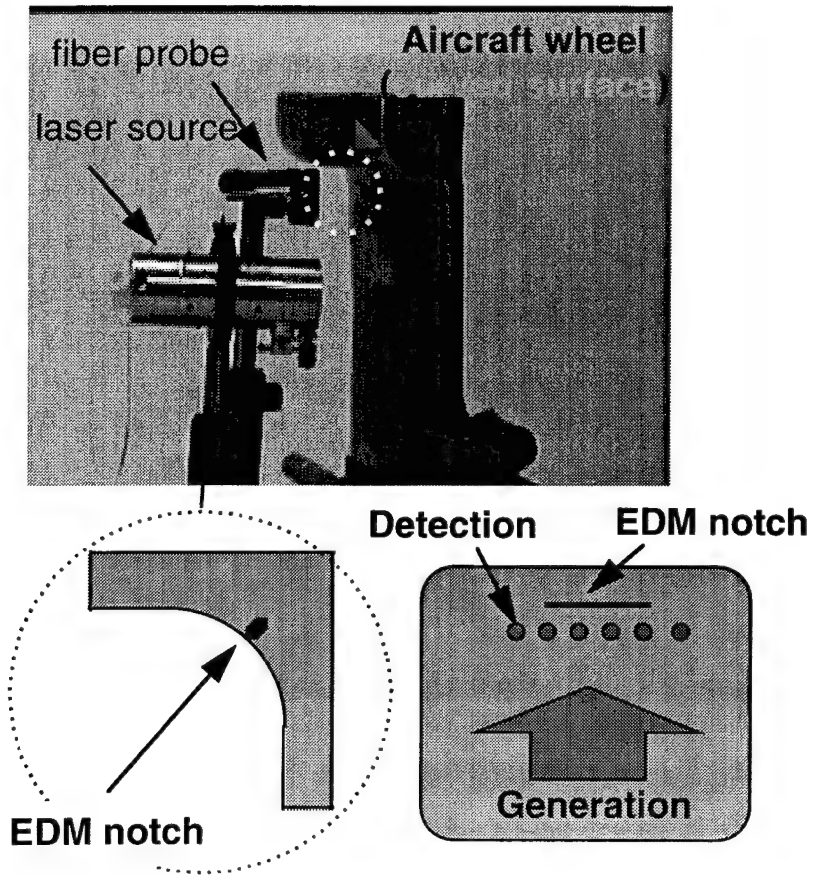

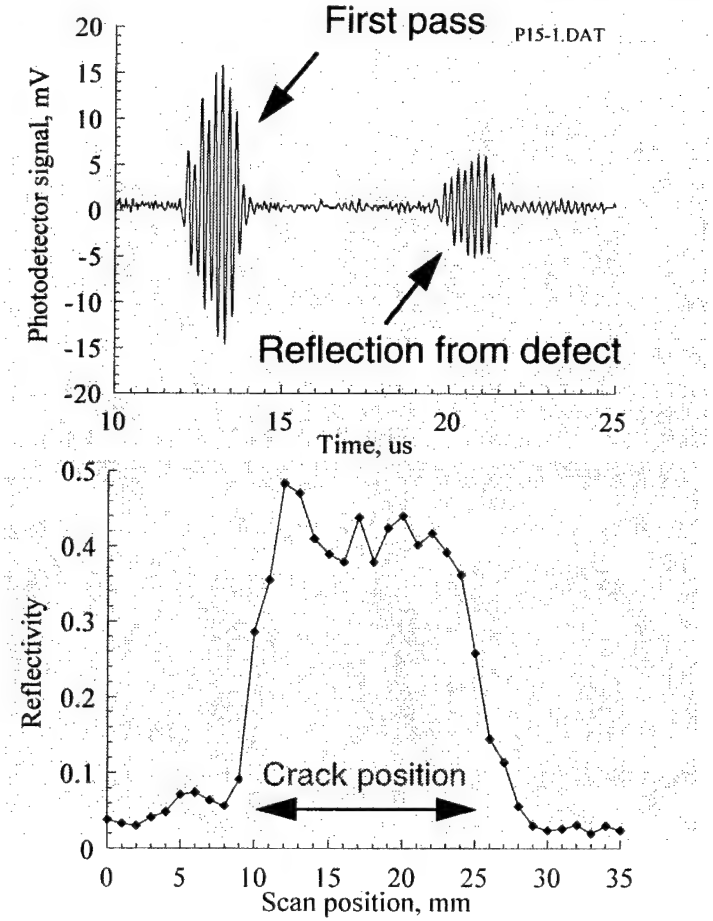

Optical detection of small cracks

Reflections from crack and edge of specimen

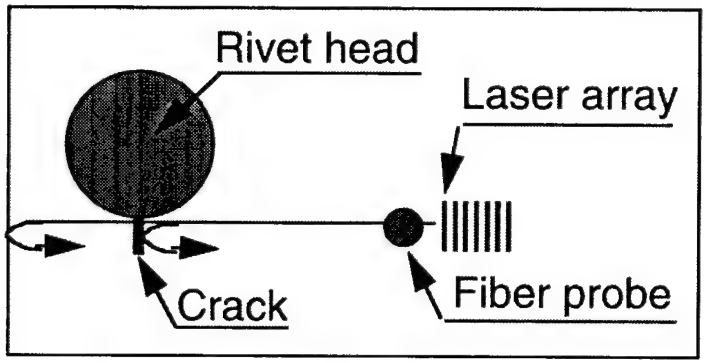

Detected ultrasonic signal

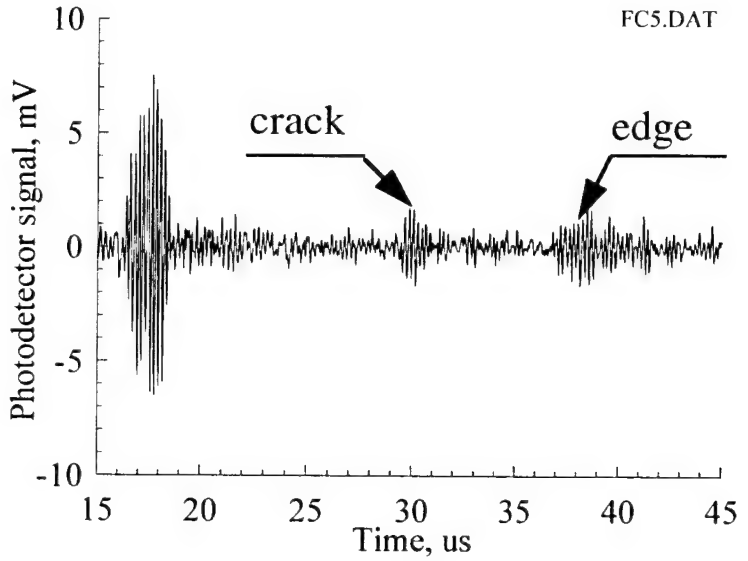

Specimen Information

- two plates riveted together
- fatigue crack from rivet head
- rough surface

Detection of small cracks by LBU

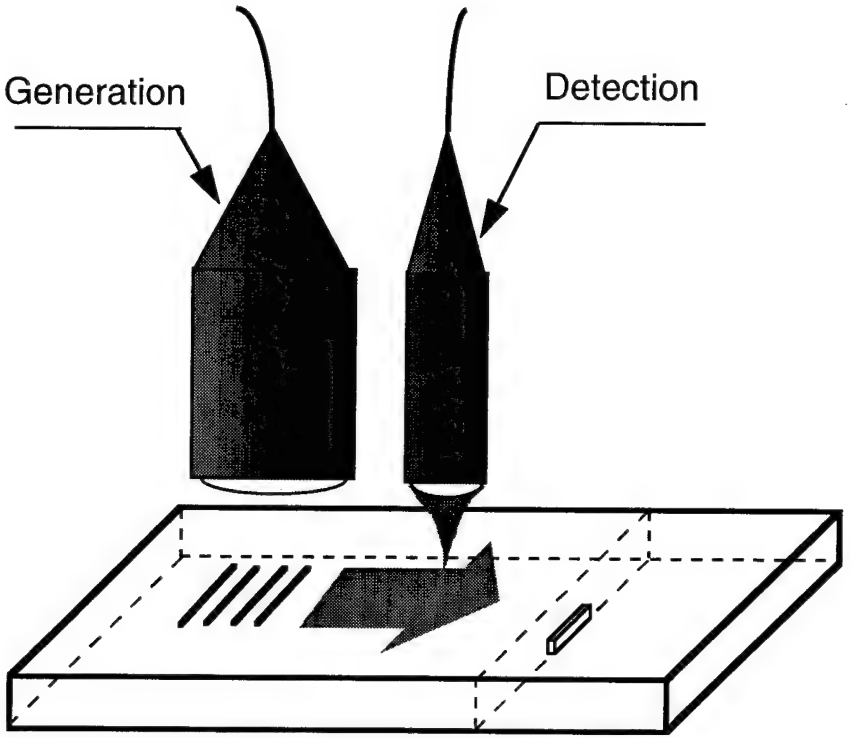

Thickness of plate - 1mm
Depth of notch - 0.5 mm

Crack at blind side

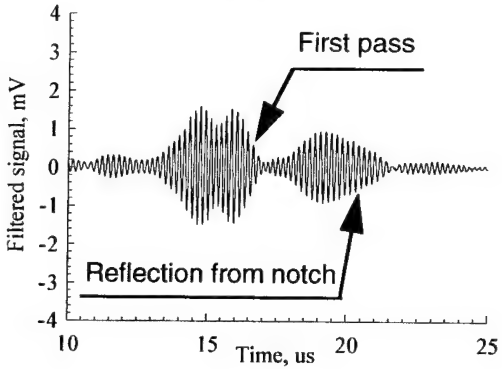

Crack at visible side

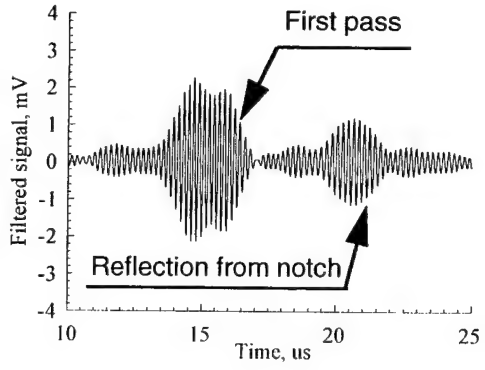

Detection of defect at a bottom of a plate

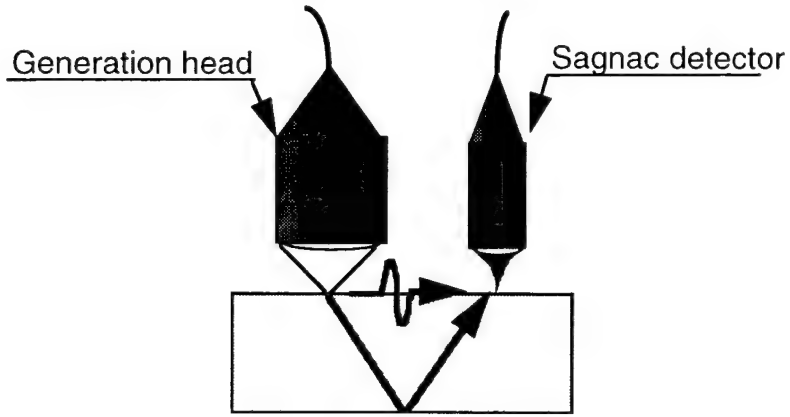

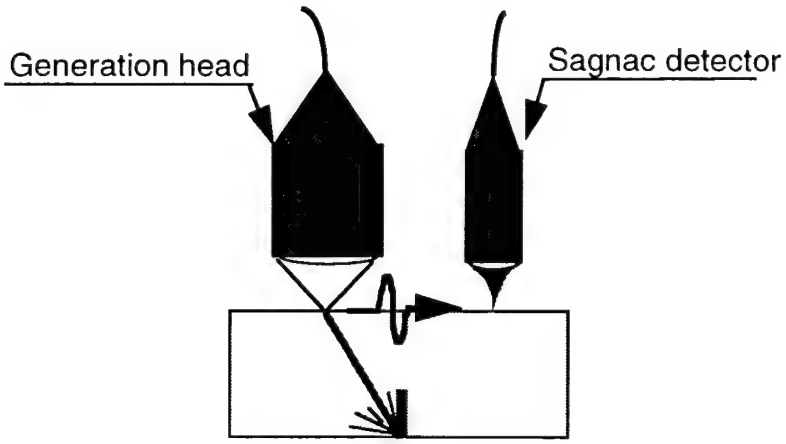

Thickness of specimen - 12 mm
Depth of notch - 1.5 mm

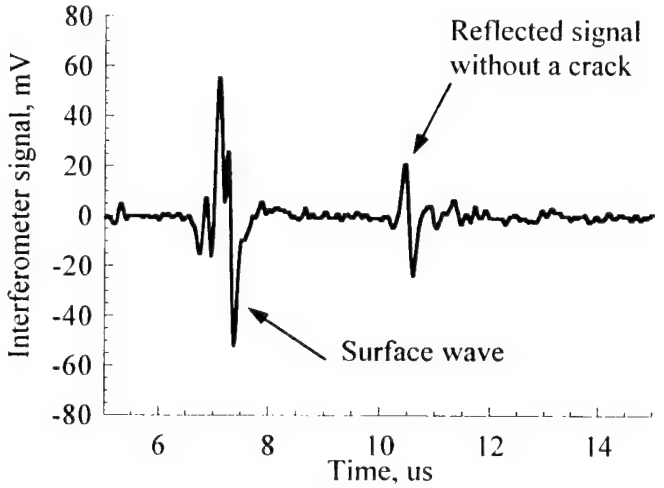

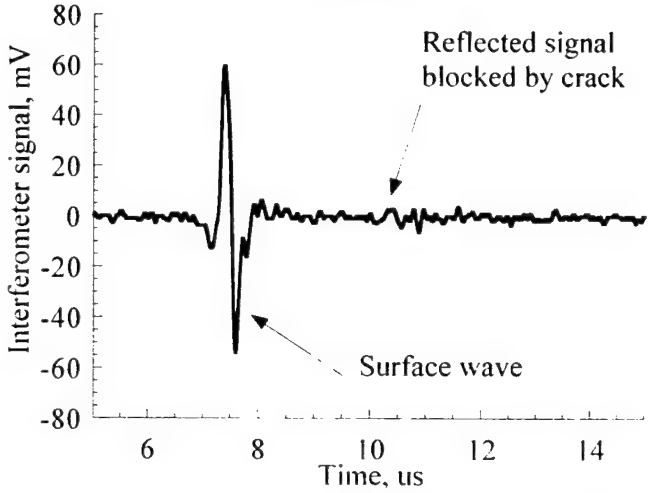

Conclusions:

- ***Generation*: A fiberized laser ultrasonic source for flaw detection has been developed. This device provides both narrowband and broadband generation capability.**
- ***Detection*:A fiberized Sagnac interferometer has been developed. Ultrasonic signals can be detected on rough and curved surfaces.**
- **The combined system is compact and portable, and suitable for field applications.**
- **The system has been used to detect small cracks.**

Plans for Years 4 and 5

- Improve system consistency and reliability
- Design connectorization of fibers of the generation unit for field applications
- Development of time-delay array
- Signal analysis by use of measurement models
- System miniaturization
- Further applications to components with limited access and/or irregular surfaces

MultiUniversity Center for Integrated Diagnostics

Project C-2

Eddy Current Micro-Sensors

S. Ramalingam, Jianhua Xue and Zheng Shi

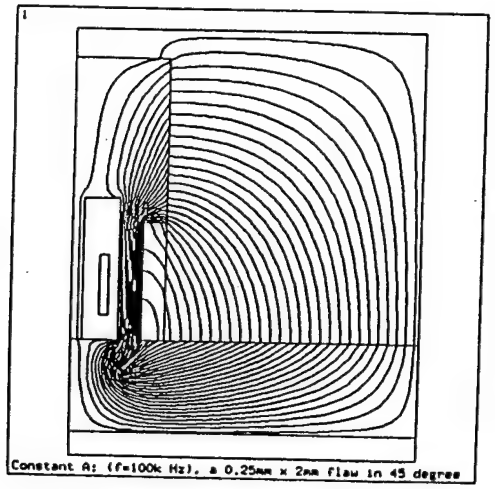

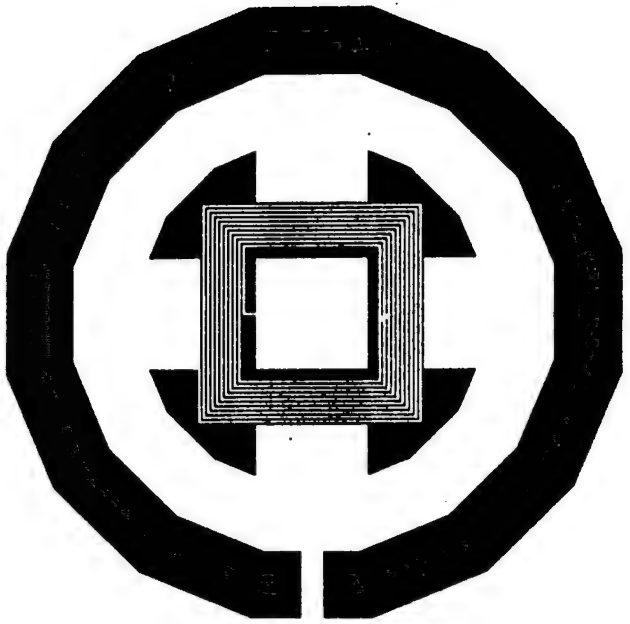

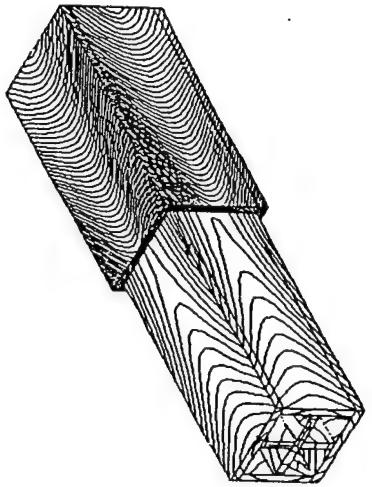

Office of Naval Research

Project C-2: Eddy Current Micro Sensors

- ***Develop and Implement Eddy Current Micro Sensors.***
- ***Need Enhanced Spatial Resolution For Flaw Detection.***
- ***Seeking Spatial Resolution Of 100 μm Or Less.***
- ***For flaw detection In Initiation Phase Of A Critical Component 's Life.***
- ***Develop Procedures To Render Eddy Current Inspection Objective.***
- ***Transition From Flaw Detection To Flaw Imaging.***
- ***Reduce Skill/Training And Time Requirements For Flaw Audit.***
- ***Year 3 Review : Automated, Reliable EC Inspection/Imaging.***
- ***Multi-Axis CNC Or Robotic Inspection.***
- ***Derive Path Control From The CAD Database.***
- ***Reduced Sensitivity to Lift-Off Variation : Automated Flaw Inspection***

From Flaw Sensing to Flaw Imaging (1)

- *Analytical modeling for eddy current signals.*
- *Axisymmetric wire-wound coils and thin film sensors.*
- *Eddy current signals/imaging feasible - flux focusing necessary.*
- *Evaluated flux focusing with a wound-coil model sensor.*
- *Computer- driven X-Y table for eddy current signals (scanning).*
- *Z- modulation display of flaw-induced EC signal Vs position.*
- *Flaw imaging achieved and demonstrated in February 1996.*
- *Proof-of-principle of flux focusing demonstrated.*
- *Spatial resolution achieved unacceptable.*
- *Replace wound coil sensors with Thin Film Micro Sensors.*

From Flaw Sensing to Flaw Imaging (2)

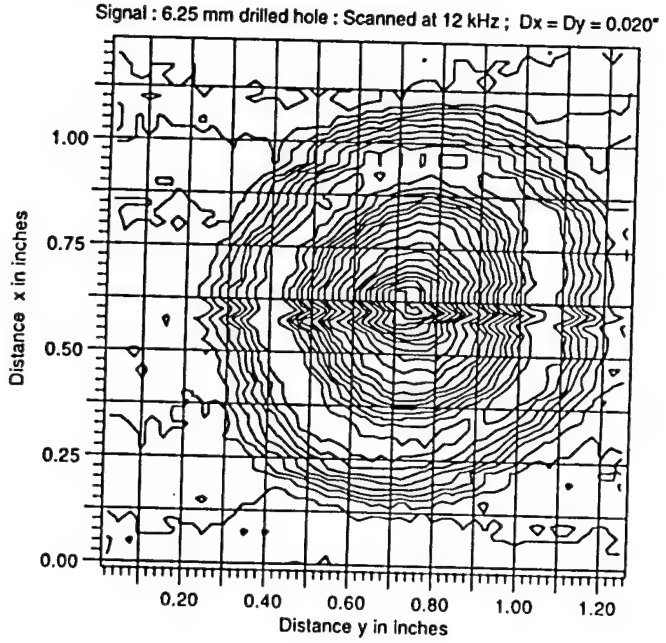

EC Flaw Image - 6.25 mm dia. model flaw

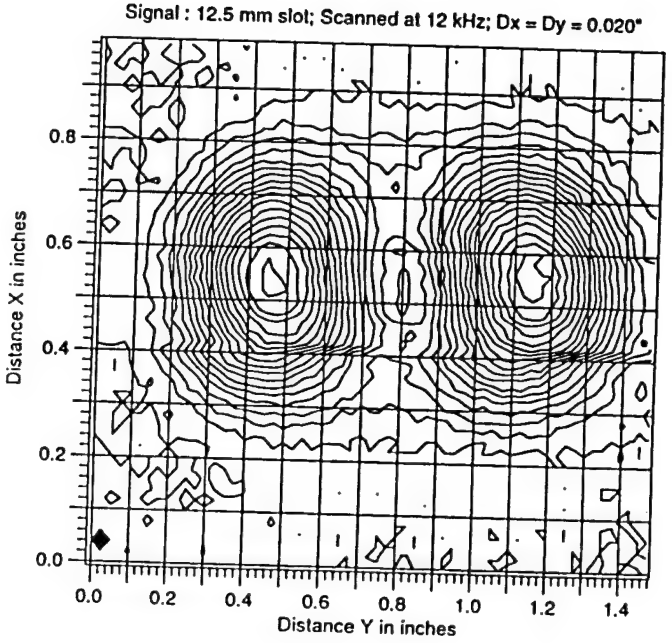

EC Flaw Image - 12.5 mm long slot model flaw

- **Seek spatial resolution improvement with Thin Film Sensors**
- **Flaw detection in initiation stage of fatigue (Resolution ~ 50 μm)**

Model Flaws For Resolution Evaluation

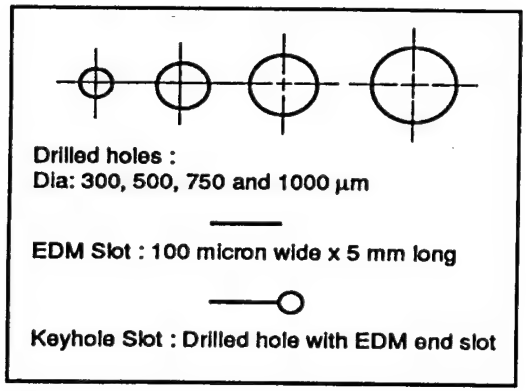

Model Flaws for EC Imaging

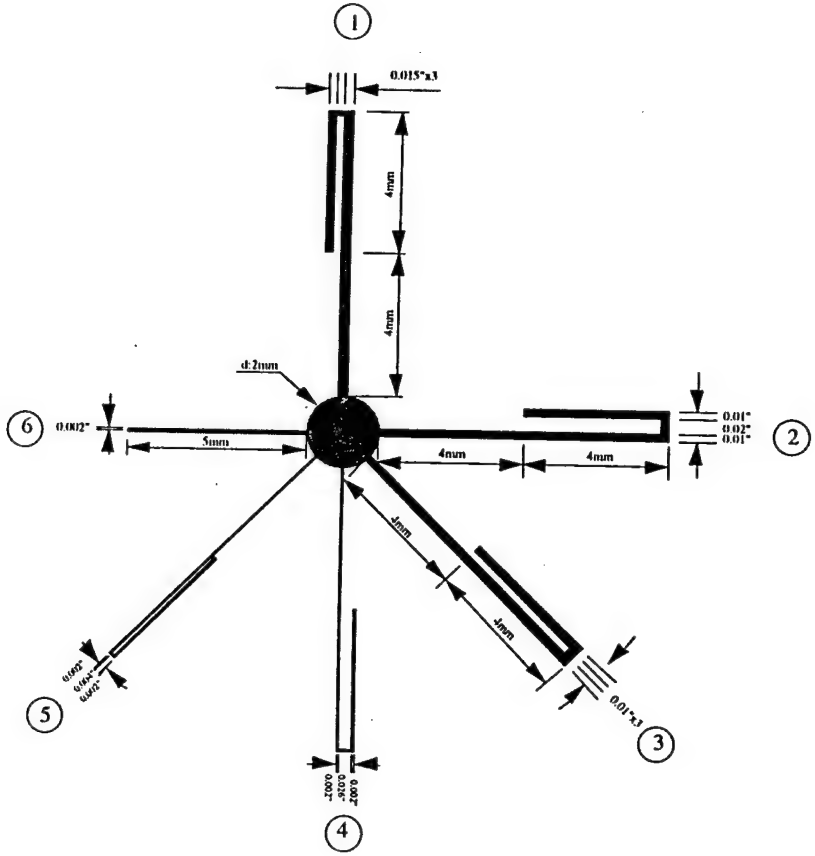

Flaws for ResolutionEvaluation in a Field of Flaws

Eddy Current Micro Sensors in Silicon

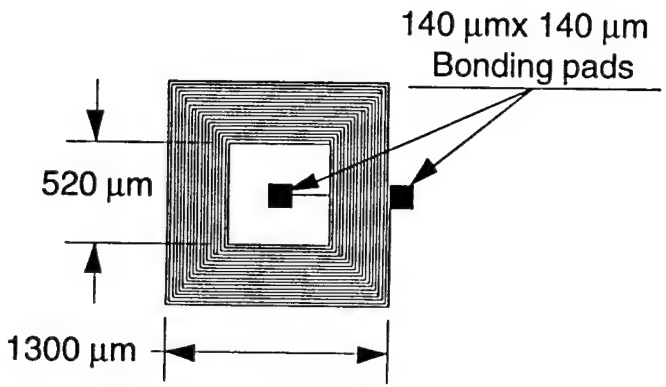

Twenty-turn, single element sensor

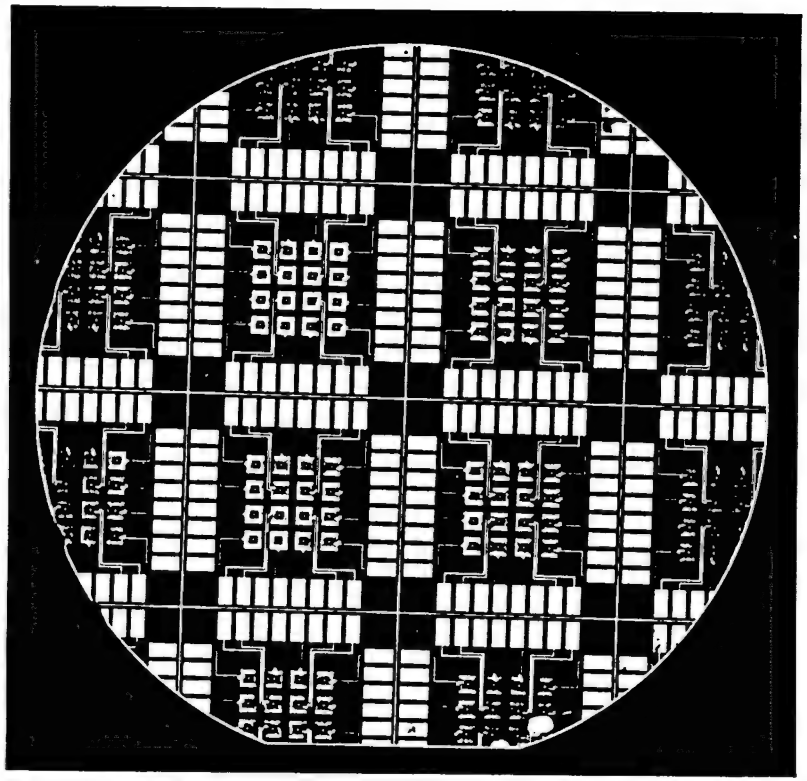

Four x Four sensor array implemented in Si

Single-element Sensor and Imaged Flaws

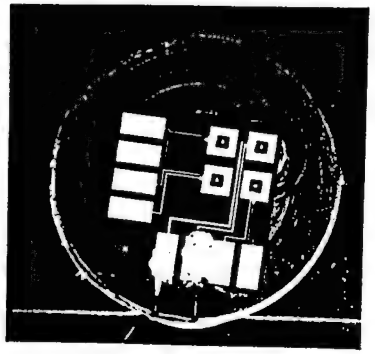

Single element sensor implemented in Silicon

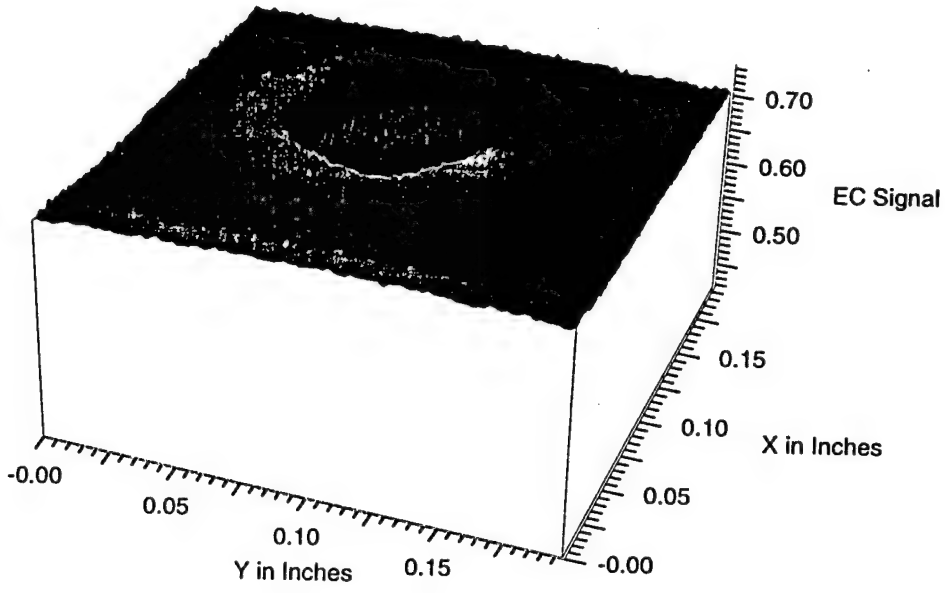

Reconstructed Image: model flaw - 1000 μm dia hole

Digital Model Flaw Images

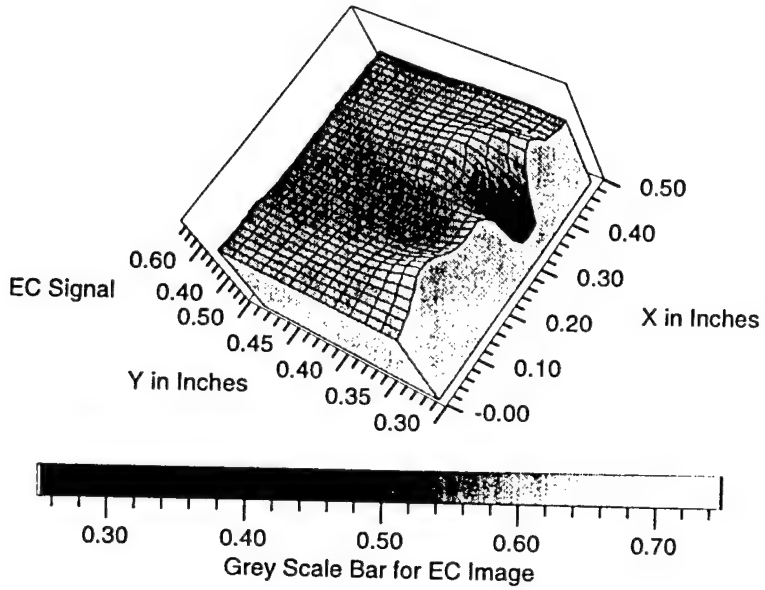

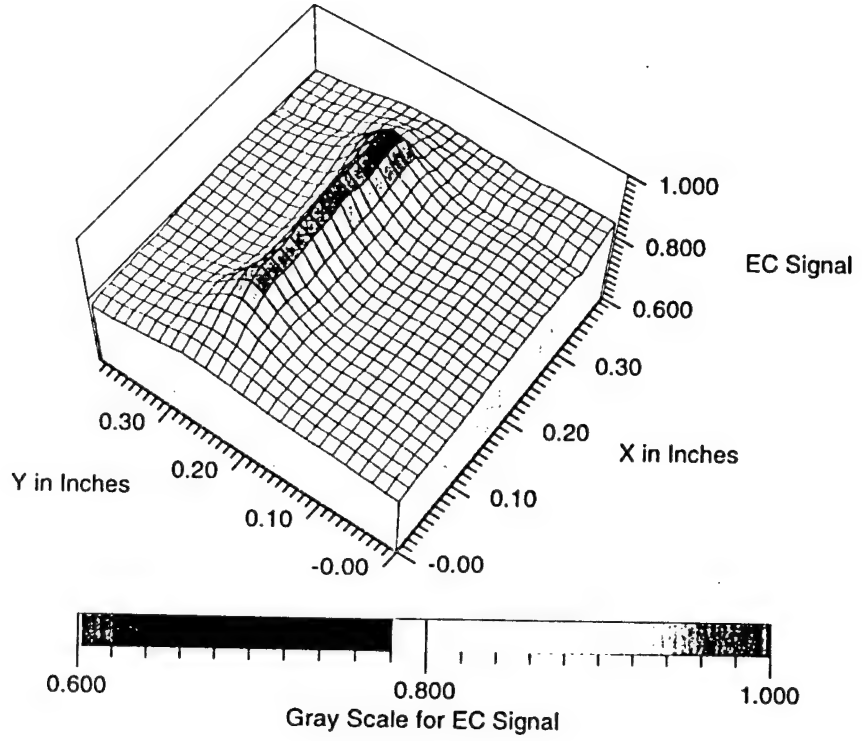

Reconstructed Section of a Model Flaw - Keyhole Flaw

Model Flaw: 100 μm wide EDM Slot - 1300 μm Sq. Sensor

Model Flaw- Resolution Checks

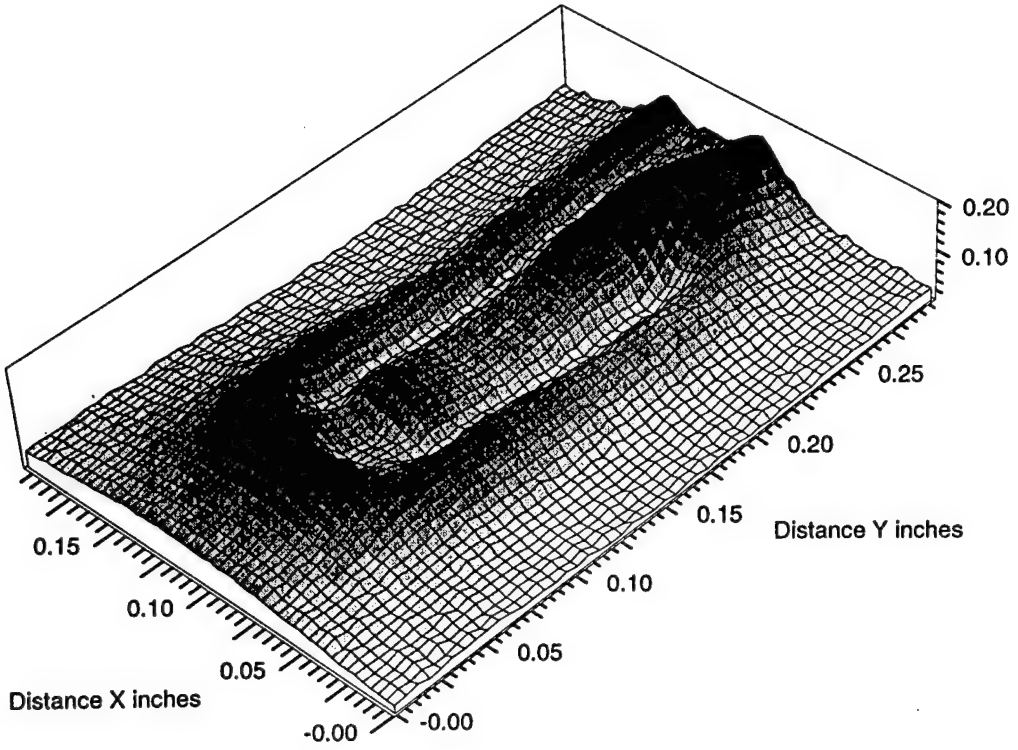

Parallel Slot Flaw: 250 μm/250 μm : 1020 μm Sensor

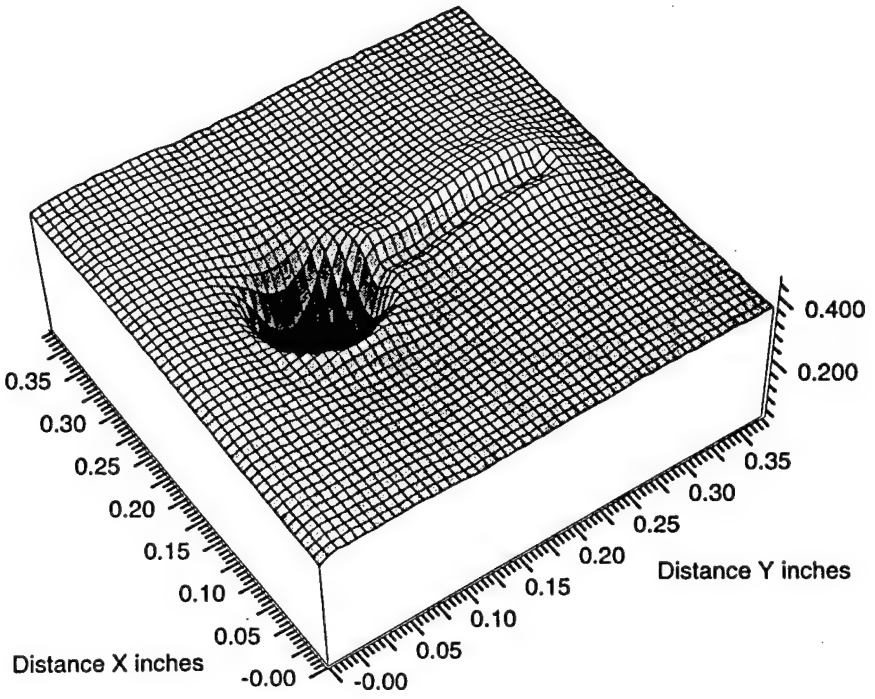

Keyhole Slot Flaw: 100 μmSlot : 320 μm Sensor

Model Flaws In a Field of Cracks

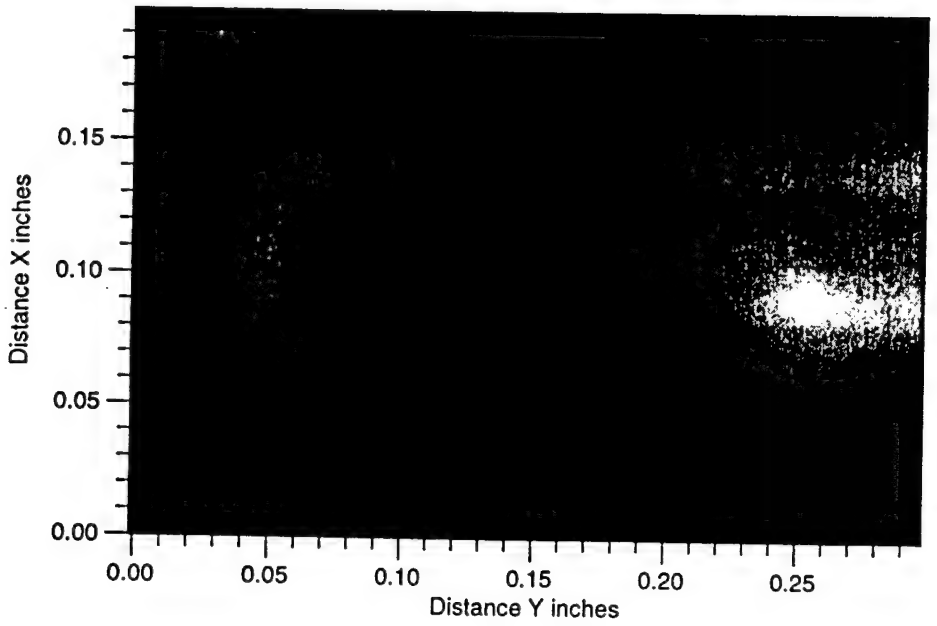

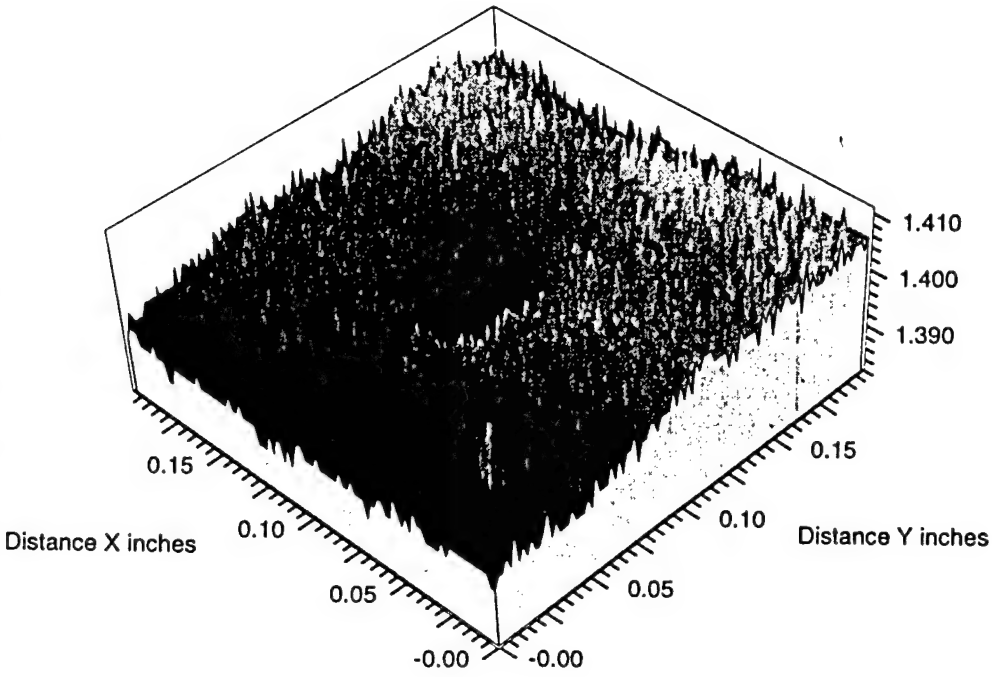

Image of Slot Flaw: 250 μm/250 μm : 1020 μm Sensor

Noisy Image of 330 μm Dia. Hole: 1020 μm Sensor

Model Flaws In a Field of Cracks

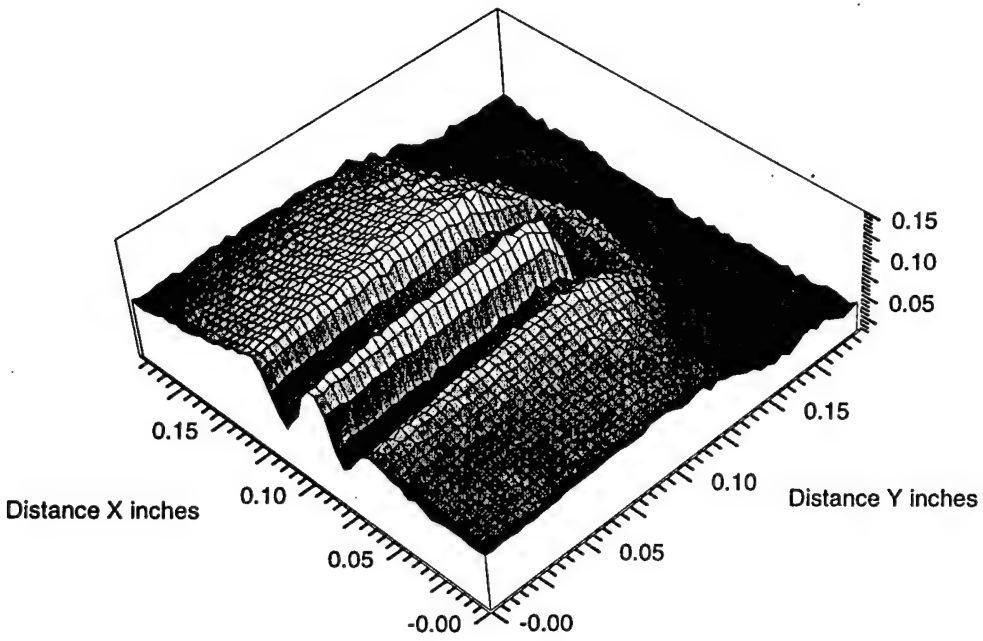

Resolved Slot Flaw: 250 μm/250 μm : 320 μm Sensor

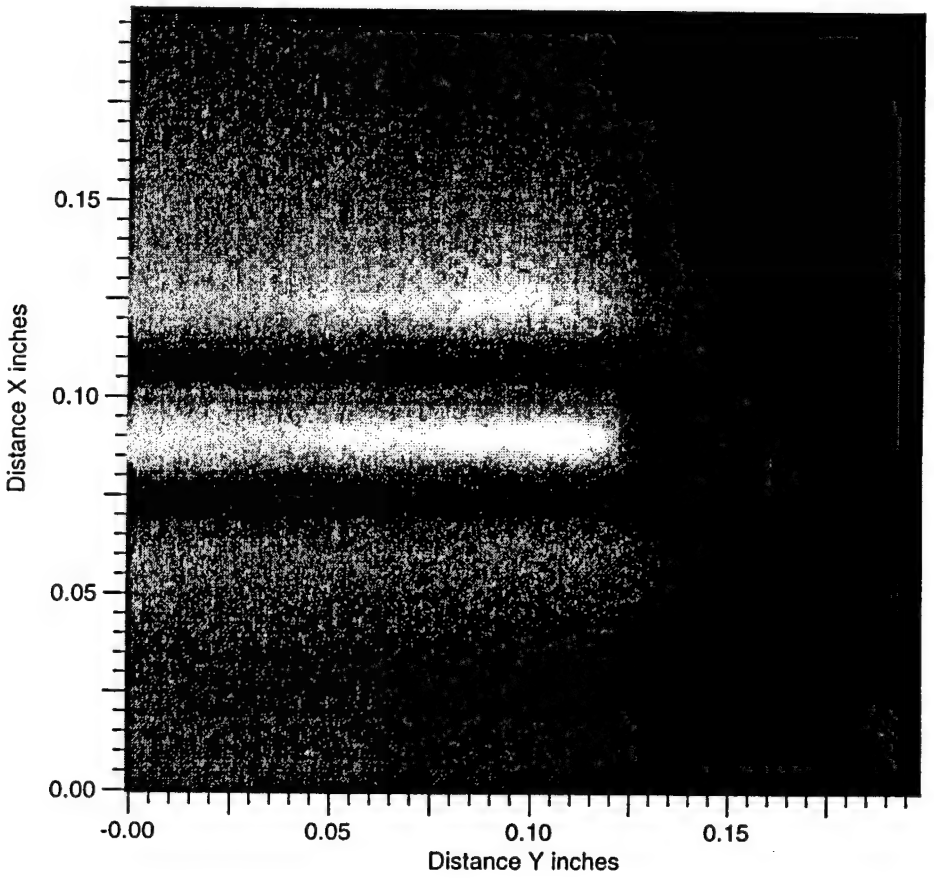

Image of Slot Flaw 250 μm/250 μm : 320 μm Sensor

Model Flaws In a Field of Cracks

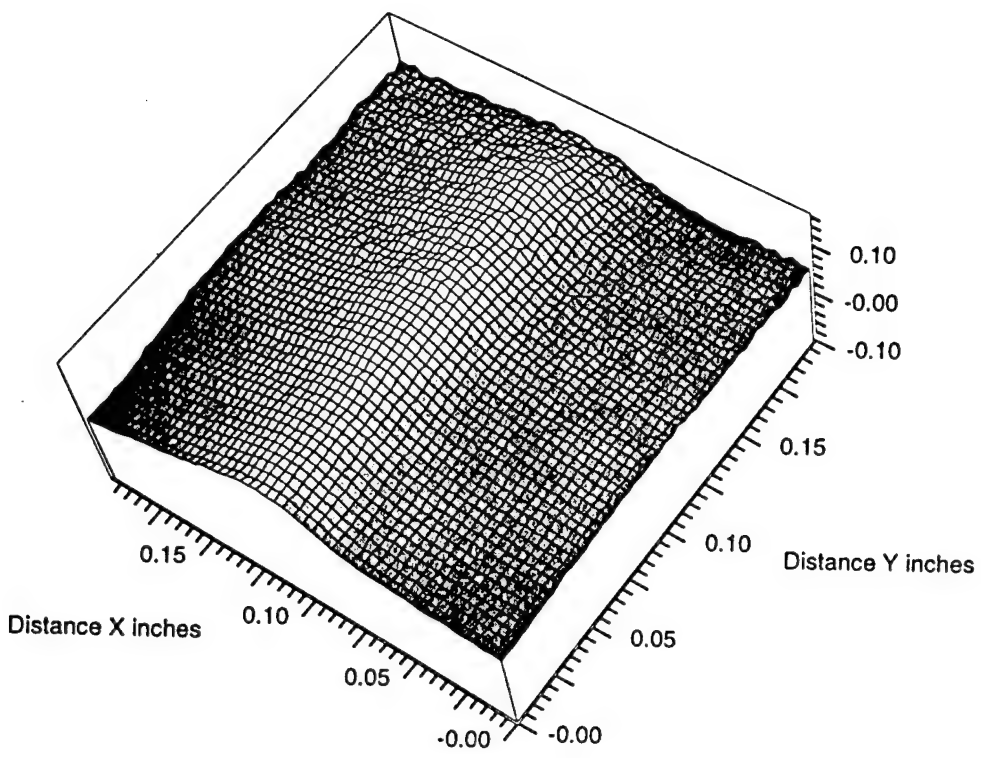

Unresolved Slot Flaws : 320 μm Sensor

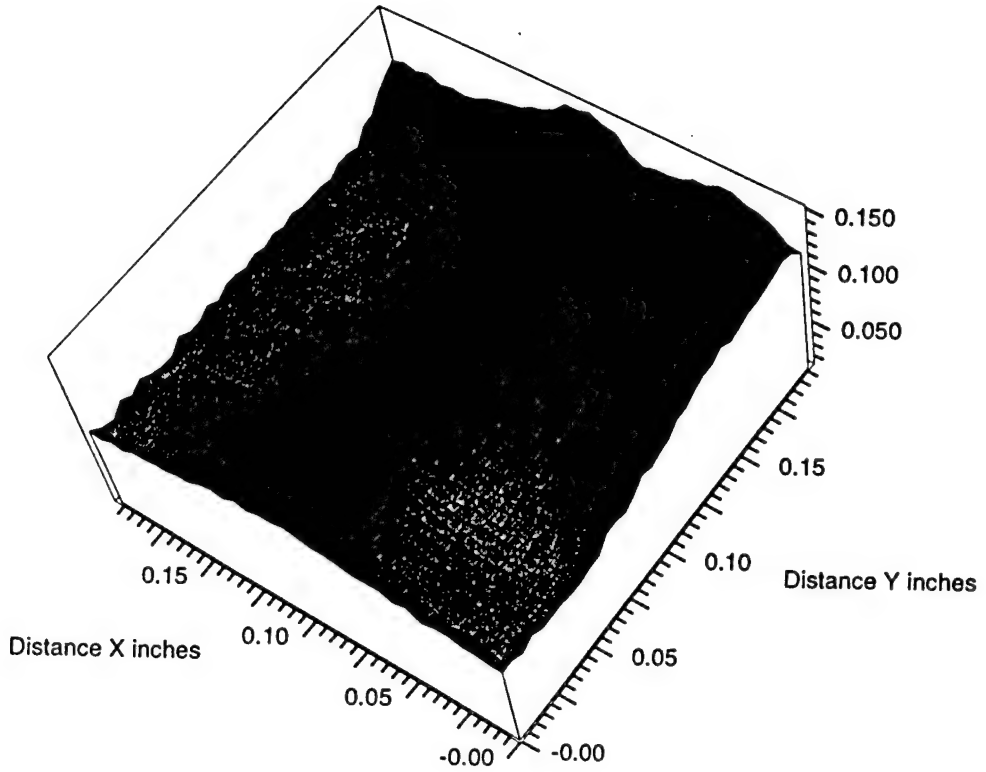

Unresolved Slot Flaws : 320 μm Sensor

Resolution Limit Achieved & Pencil Probe

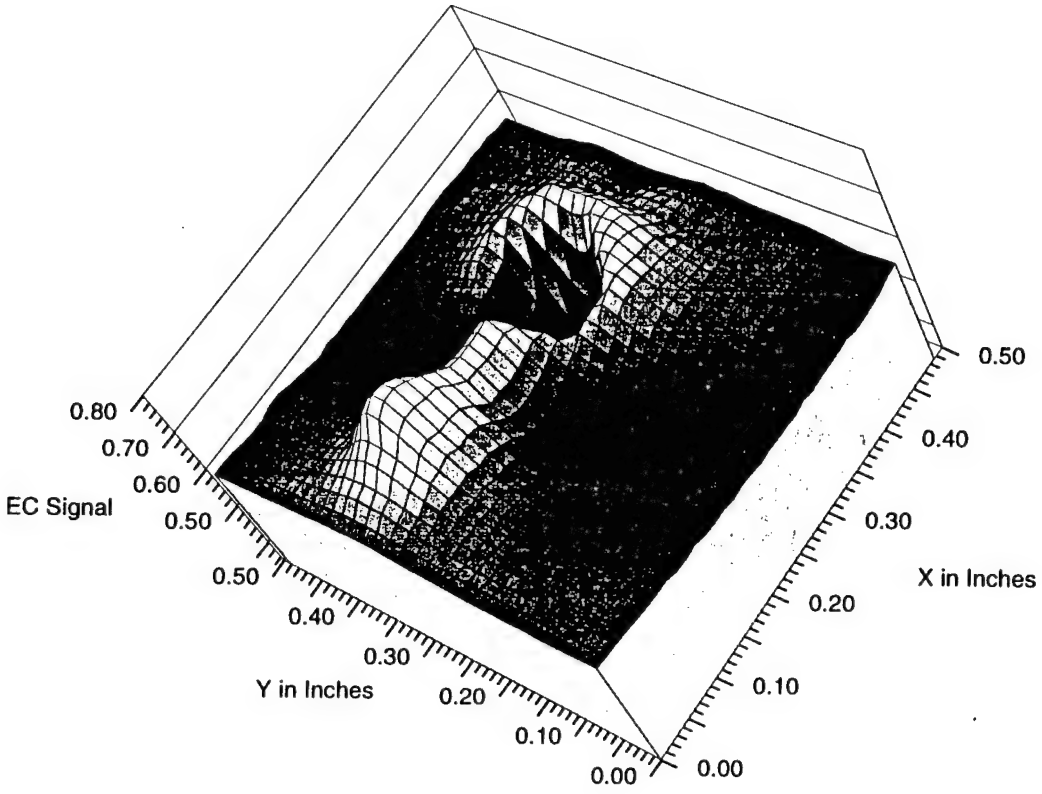

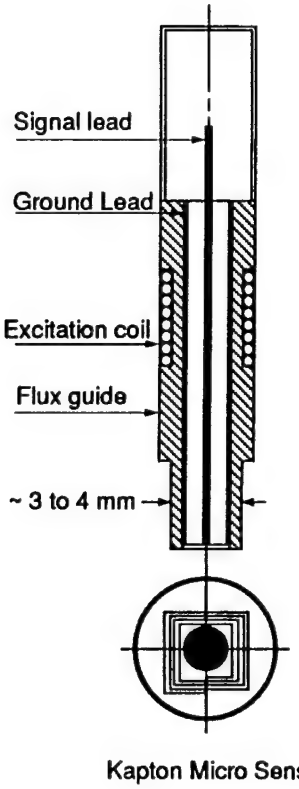

Key-hole Flaw: EDM Slot Not Resolved

'Pencil Probe' : Recommended After 1996 Review

Project Monitor and Principal Investigator

Can We Automate Flaw Detection and Imaging for eventualRobotic/CNC System-based NDT and Inspection ?

Kapton Micro Sensors : Disposable Elements

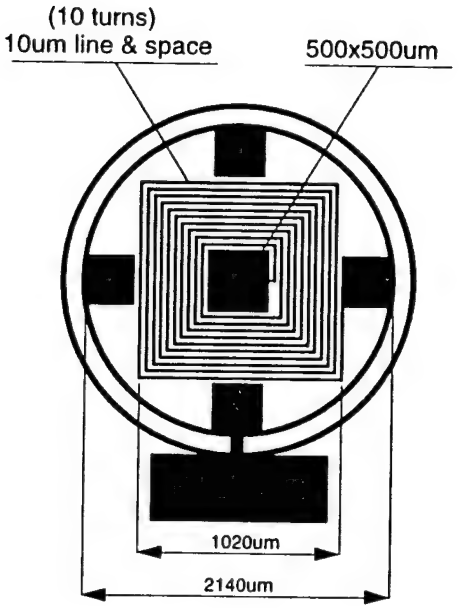

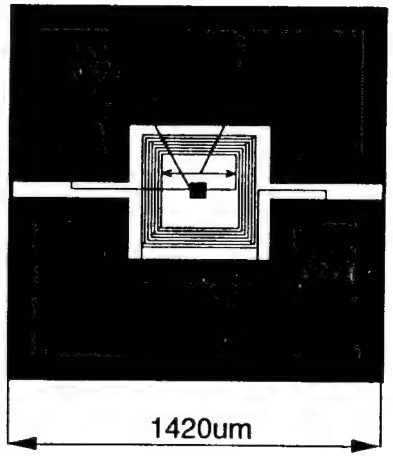

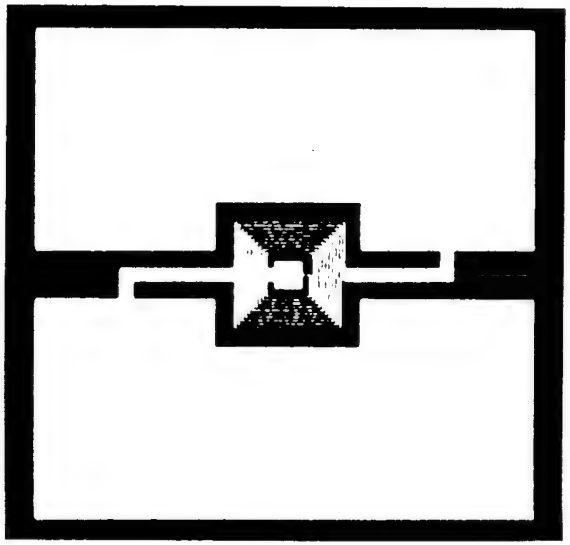

Kapton Sensor Geometries Implemented.

Sensors used in Pencil Probes

Spatial Resolution is a Convolution of Sensor and Flaw Dimension - Design, Build & Evaluate Smaller Sensors

Continuous Motion Scanning

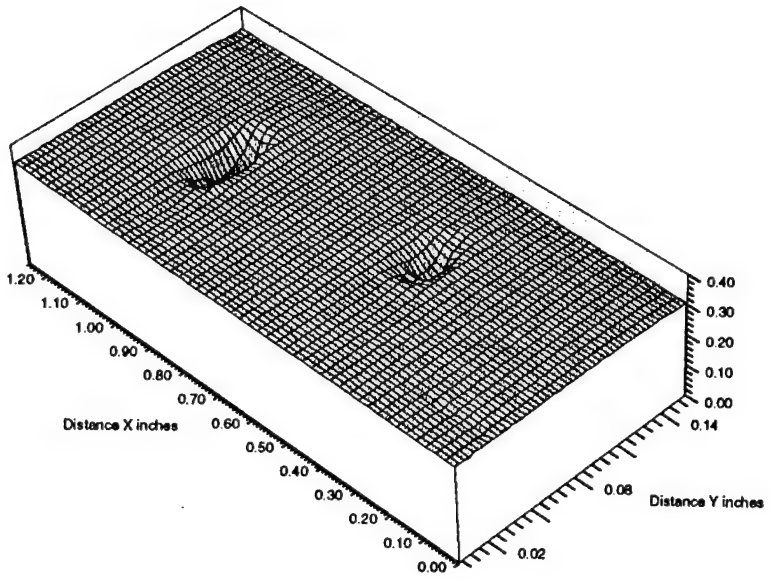

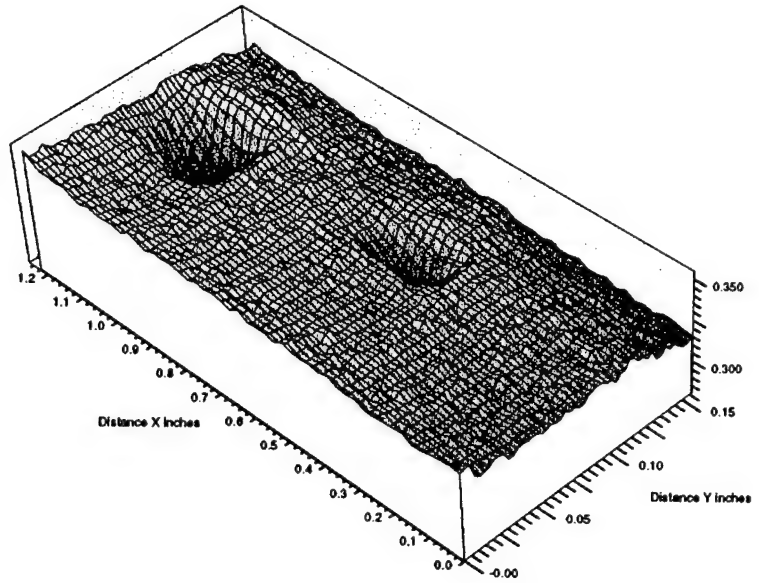

Scanned at 0.635 cm/second

Scanned at 1.905 cm/second

Continuous Motion Scan of a Sample with 1000 μm and 750 μm dia. Model Flaws

Work-in-Progress

- ***Continous scan evaluation in computerized X-Y table***
- ***Continuous scan tests : transition to 3-axis CNC machine***
- ***Path control - derive from Pro-e geometryof test sample***
- ***Cylindrical test sample with model flaw***
- ***X-Y scan with probe motion along Z-axis***
- ***Need improved signal conditioning with a Lock-in Amplifier***
- ***Established methods - no new technology barrier***
- ***Fast scan test - improved micro sensor necessary***
- ***Evaluate rotating field planar sensor- Hoshi sensor***
- ***Implement 2-metal sensor followed by true rotating field sensor***

Work-in-Progress

- ***Continue with automated EC inspection***
- ***Pencil probe with 320 μm x320 μm sensor***
- ***Use three axis system : CNC milling machine.***
- ***Sensor orientation normal to surface.***
- ***Need two more degrees of freedom. Evaluate in year III***
- ***Propose: focus year IV and V effort on automated inspection.***
- ***5 - Axis CNC machine, CMM system or robotic system***
- ***Path control derived from the CAD database (Pro-e)***
- ***Automated derivation of sensor/inspection path.***
- ***Down load for untended inspection of critical components.***
- ***Less expensive flaw imaging under program control than CMM.***
- ***Untended flaw inspection - flaw identification/marking with Ink jets***

Proposed work for Years IV and V

- *Fluxset probes with square loop magnetics.*
- *Sense field flipping : time-shift for saturation.*
- *Forward saturation sooner ; reverse saturation retarded.*
- *Measure time-shift. Leads to precision measurement of fields.*
- *Stand off distances of 5 mm or more.*
- *Reduced sensitivity to stand off variation.*
- *Can detect partially - through - the - thickness flaws.*
- *More significant for non-magnetic materials.*
- *Fluxset probes : evaluate and perfect in years IV and V.*
- *Demonstrate fully automated EC inspection.*
- *Fast Scan And Localized Precision Scan.*
- *Shorter Down-time for Off Line Maintenance.*

Proposed work for Years IV and V

- *Turbine discs; air frame; critical components - hole inspection*
- *Need small diameter pencil probes*
- *Need to eliminate probe sensitivity to flaw orientation*
- *Rotating pencil probes - will need slip rings*
- *Alternate approach - inductive coupling*
- *Needless complexity in signal acquisition gear*
- *Two loop excitation with 90° phase shift*
- *Flaw orientation no longer relevant*
- *Electrically - driven rotating magnetic fields*
- *Probe motion axial - inspection with electrically rotated probe field*
- *Initiate work in year 3; evaluate and perfect in years IV and V*
- *Accommodate probe diameter variation with disposable sensors*

REPORT DOCUMENTATION PAGE

Form Approved
OMB No. 0704-0188

1. AGENCY USE ONLY *(Leave Blank)*	2. REPORT DATE	3. REPORT TYPE AND DATES COVERED
	31 May, 1998	Year 3 Performance: Mar. 1, 1997 - May 31, 1998

4. TITLE AND SUBTITLE

Integrated Diagnostics

5. FUNDING NUMBERS

G N00014-95-1-0539

6. AUTHOR(S)

Richard S. Cowan and Ward O. Winer (eds.)

7. PERFORMING ORGANIZATION NAME(S) AND ADDRESS(ES)

Georgia Institute of Technology
MULTIUNIVERSITY CENTER FOR INTEGRATED DIAGNOSTICS
G. W. Woodruff School of Mechanical Engineering
801 Ferst Drive
Atlanta, GA 30332-0405

8. PERFORMING ORGANIZATION REPORT NUMBER

9. SPONSORING/MONITORING AGENCY NAME(S) AND ADDRESS(ES)

Office of Naval Research
800 N. Quincy Street
Arlington, VA 22217-5660

10. SPONSORING/MONITORING AGENCY REPORT NUMBER

11. SUPPLEMENTARY NOTES

The information conveyed in this report does not necessarily reflect the position or the policy of the Government, and no official endorsement should be inferred.

12a. DISTRIBUTION/AVAILABILITY STATEMENT

12b. DISTRIBUTION CODE

13. ABSTRACT *(Maximum 200 words)*

This document provides a review of basic research being conducted in the area of *Integrated Diagnostics*, a term associated with the technologies and methodologies used to determine how mechanical failures occur, and how they can be detected, predicted and diagnosed in real-time. Objectives, set forth through the Department of Defense Multidisciplinary Research Program of the University Research Initiative (M-URI), are being addressed by faculty and staff from the Georgia Institute of Technology, Northwestern University and the University of Minnesota. This activity is being funded through the Office of Naval Research for a basic period of three years with a potential for two additional years. Third year accomplishments and plans are reported upon.

During this reporting period, experiments based on material, load and vibration information from critical rotorcraft components continued, so as to collect data of relevance in understanding the mechanisms of small crack growth for use in developing fatigue failure models. Such models serve as a guide in the selection and development of sensors to detect faults and pending failures. Effort has been placed on micro-sensor development, and achieving the means to analyze and correlate reliable sensor output for operator use. Organizationally, this activity is being accomplished through (18) projects and sub-tasks, categorized by three thrust areas.

14. SUBJECT TERMS	15. NUMBER OF PAGES
Integrated Diagnostics; Condition-based Maintenance Failure Detection; Failure Prediction; Sensors; Direct Sensing	289
	16. PRICE CODE

17. SECURITY CLASSIFICATION OF REPORT	18. SECURITY CLASSIFICATION OF THIS PAGE	19. SECURITY CLASSIFICATION OF ABSTRACT	20. LIMITATION OF ABSTRACT
Unclassified	Unclassified	Unclassified	SAR